Forest Loss Dynamics and Impacts from Gold Mining in Amazonia

Michelle Kalamandeen

Submitted in accordance with the requirements for the degree of
Doctor of Philosophy

The University of Leeds
School of Geography

January 2019

The candidate confirms that the work submitted is her own, except where work which has formed part of jointly-authored publications has been included. The contribution of the candidate and the other authors to this work has been explicitly indicated below. The candidate confirms that appropriate credit has been given within the thesis where reference has been made to the work of others.

Chapter 2

Kalamandeen, M., Gloor, E., Mitchard, E., Quincey, D., Ziv, G., Spracklen, D., Spracklen, B., Adami, M., Aragão, L. E. O. C. & Galbraith, D., 2018. Pervasive Rise of Small-scale deforestation in Amazonia. Scientific Reports 8: 1600.

MK and DG conceived the study and wrote the manuscript. MK led the data analysis, with support from DG, EG, EM, DQ, GZ, DS and BS. MA and LA advised on the comparisons involving PRODES data. All authors commented on the manuscript.

Chapter 3

Kalamandeen, M., Gloor, E., Mitchard, E., Ziv, G., Spracklen, D., & Galbraith, D., 2019. Forest Loss from Small-scale Gold Mining underestimated across Amazonia. (In preparation).

Chapters 4 and 5

Kalamandeen, M., Gloor, E., Johnson, I., Agard, S., Katow, M., Vanbrooke, A., Ziv, G., Collins-Holder, K., Smartt T., Ashley, D., Phillips, O., & Galbraith, D., 2019. Limited biomass recovery from gold mining in Amazonian forests. (In preparation).

MK and DG conceived the study and wrote the manuscript. MK led the field study and data analysis, with support from DG, EG, IJ, SA, MK, AV, EM, GZ, DS, KCH and TS. All authors commented on the manuscript.

Panapang Tuwepantamaseng	**Young Warrior**
Apagagà	Wake Up
Melenambusaik Uchi	You have arrived
Wakù Kunen!	Congratulations!
Walà Tusé Autàtok Lùppù Nepiatàbusan	However, the remainder of your journey has just started

Patamona Wisdom

Acknowledgments

An important phase of my life is reaching its end. My parents taught me that we should always recognize such moments, and not let them pass without celebrating and thanking those who have walked this journey with us.

To my primary supervisor, David Galbraith, you created the invaluable space for me to do this research and I greatly appreciate the freedom you gave me to find my own path, and the guidance and support you offered when needed. You made sense of the work I was doing, and in your writings and discussions, I found inspiration, and discovered the skills and ideas for development as a researcher. Thank you for guiding me along this new journey.

To my co-supervisor, Manuel Gloor, your mix of candid feedback combined with heart-warming support gave me great confidence as a researcher, and at the same time made me realize what an exciting journey this continues to be. Thank you for guiding me on this intellectual adventure. To Edward Mitchard, Guy Ziv, Dominick Spracklen and Duncan Quincey, thank you for your support, feedback and introducing me to the wonderful world of remote sensing! It is now one of my happy spaces.

A good support system is important to surviving and staying sane during the PhD. I was lucky to have incredible friends such as Adriane Muelbert, Kristina Kare, Fernanda Coelho, Amy Bennett, Sinead D'Silva, Yunxia Wang, Marta Giannichi, Magaly Avellan and Ana Pacheco for their wonderful support and encouragement throughout this process. To Alex Chambers-Ostler, thank you for taking time away from your own journey to always give a lending hand, and for understanding the importance of eating lots of chocolates while climbing hills.

I was lucky to meet some of the nicest people from the Ecology and Global Change cluster: Dr Sarah Batterman, Greta Dargie, Freddie Draper, Ricardo Dal'Agnol Da Silva, Julia Tavares, Lan Qie, Jess Baker, Martin Gilpin, Sophie Faust, Martin Sullivan, Will Barker, Joey Talbot, Bruno Ladvocat, Rakesh Tiwari, Tom Kelly, and Karina Melgaco. Being in your presence gave me the scientific support to carry on and overcome the most difficult moments of PhD life.

To Luca and Sarah Budello– thank you for your support and letting me spend time with Nico building rockets and singing nursery rhymes. These moments gave me perspective of a life outside of my computer. Someday, I will take up the offer to buy Nico for three cows and two camels.

To the friends from the 'other tribes' across the University: William James, Heru Purwandari, Kamla Rathakrishanan, Suad Al Manji, Leandro Patino, James Bell,

Tom Collins, Tom Bone and Nikee Groot thank you for your support and for sharing your passion and curiosity for life. To my Guyanese and "honorary Guyanaese" people who brought the sun through your consistent support and love: Dave and Mina Prashad, Raquel Thomas, Mike McCormack, Merle Mendonca, Osman and Irene Khan, Jewel Liddell, Kerry Anne Cort, Melissa Mitchell, Shellon Nicholas, Odacy Davis, Kaslyn Collins-Holder, Patsy Fredericks, Annalise Bayney and Indranee Roopsind.

I would also like to thank the wonderful staff at the Geography Department - David Ashley, Rachel Gasior and Dave Wilson.

This work would not have been possible without the financial support from the Leeds International Research Scholarship (LIRS), Ecology and Global Change (EGC) cluster and the Guyana Geology and Mines Commission (GGMC). I also wish to thank those who made the fieldwork for this PhD possible such as GGMC Commissioner Noel Dennison, Guyana Forestry Commissioner James Singh, Rickford Vieira, Shenelle Agard, Janice Bollers, Isaac Johnson, Martin Katow, Ashmore Vanbrooke, Rondell DeAndrade, the indigenous communities of Campbelltown and Micobie and the small-scale miners who gave field support. Special thanks for Professor Phil Rees for providing research assistantship along the way.

To Nicholas Twyman, who was very supportive throughout this PhD, a heartfelt thank you for your encouragement.

To my Batman-supporting (though I still think Superman would win in a fight), twin sister, Melina, the "other twin" Saffiyah Yasin, and my brother, Andre, thank you for the laughter and support along this journey. I know you will be very pleased when I start a job with a salary.

To my mom, Rita, who passed two months into this PhD on 25th March 2014, and my dad, Kamal, words can never truly express how grateful I am to you both – for the endless support and encouragement, for the late nights you sat with me while I worked, for the various debates and discussions, and for the willingness to let me have my many crazy adventures – a HUGE thank you. I dedicate this thesis to you both.

The world we live in is complicated. Some problems seem unsolvable, making us feel that any effort is useless. If there is one thing this PhD has taught me is that despite the problems, small beautiful things happen all the time around us to remember why we should keep on insisting.

Abstract

Amazonian rainforests are home to Earth's largest reservoir of biodiversity, providing crucial ecosystem services and storing approximately 17% of all global terrestrial carbon. Today, these forests are experiencing rapid, unprecedented changes due to climate impacts and anthropogenic disturbances. In recent decades, the region has experienced marked variability in deforestation, and after a long period of increase, the deforestation rates in countries like Brazil have sharply declined in recent years. However, little is known about the forest trends and the impact of different drivers in other Amazonian countries. The aim of this thesis, therefore, is to better understand and examine the current dynamics of forest loss across Amazonia and how intensive land uses such as gold mining influence forest loss, nutrient cycling and recovery patterns. Using remote sensing coupled with field observations, this research highlights new spatial patterns in Amazonian forest loss which point to a more complex pattern where new smaller-scale drivers of forest loss are becoming progressively more important (Chapter 2). The expansion of small-scale events were primarily driven by gold mining activities, particularly in northern Amazonia, with underestimation of forest loss occurring at sites driven by a mosaic of small-scale clearings (Chapter 3). Nutrient depletion was found to be the most important factor driving low biomass recovery in previously mined areas, with mercury contamination being of secondary importance (Chapters 4 and 5). Overall, small-scale gold mining can severely impair the forest's ability to recover at abandoned mining pits and tailing ponds while recovery rates of woody biomass on the overburden zone were comparable to other secondary forests across the Neotropics following abandonment of pastures and agriculture (Chapter 5). Gold mining across the Amazon could potentially result in ~90,000 t C yr^{-1} less carbon being accumulated in relation to what would have accumulated under agriculture/pasture. Important conclusions from this work suggests that (1) national deforestation statistics need to include these small-scale events which are currently excluded from important official estimates such as Brazil's PRODES, and (2) active rehabilitation and restoration are required in order to assist the disrupted successional processes at gold mining sites. The results presented here highlight the vulnerability of Amazonian forests to newer, more intense types of land uses such as small-scale gold mining.

Table of Contents

List of Tables

List of Figures

Appendices

Abbreviations

AGB	Aboveground biomass
AGB_{Growth}	Biomass change due to diameter growth
$AGB_{Mortality}$	Biomass change due to mortality
$AGB_{Recuitment}$	Biomass change due to recruitment of new trees
Ag-Tu	Silver thiourea
Al	Aluminium
ASM	Artisanal and small-scale mining
BACI	Before-after-control-impact
Ca	Calcium
CEC	Cation Exchange Capacity
CO_2	Carbon dioxide
DBH	Diameter at breast height
DETER	Real Time System for Detection of Deforestation
ENSO	El Niño Southern Oscillation
FAO	Food and Agricultural Organization
FARC	Fuerzas Armadas Revolucionarias de Colombia
Fe	Iron
FOTO	Fourier Transform Textural Ordination
FRAs	Forest Resources Assessments
GeoJSON	a format for encoding various geographic data structures
GFC	Global Forest Change
GGMC	Guyana Geology and Mines Commission
Hg	Mercury
HNO_3	Nitric acid
ICP-OES	Inductively coupled plasma optical emission spectrometry
INPE	Instituto Nacional de Pesquisas Espaciais
IUCN	International Union for Conservation of Nature
K	Potassium
$KMnO_4$	Potassium permanganate

LiDAR	Light Detection and Ranging
Mg	Magnesium
Mn	Manganese
MODIS	Moderate Resolution Imaging Spectroradiometer
MRVS	Monitoring, Verification and Reporting System
N	Nitrogen
Na	Sodium
NASA	National Aeronautics and Space Administration
P	Phosphorus
PPCDAm	Plano de Prevenção e Controle do Desmatamento na Amazônia
PRODES	Monitoramento do Desmatamento na Amazônia Legal por Satélite
RAISG	Rede Amazónica de Información Socioambiental Georreferenciada
REDD+	Reducing Emissions from Deforestation and Forest Degradation
RIL	Reduced Impact Logging
SST	Sea surface temperature
SUDAM	Superinterdency for development of Amazonia
TIPNIS	Territorio Indígena y Parque Nacional Isiboro Secure
TN	Total Nitrogen
TP	Total Phosphorus
UNFCCC	United Nations Framework Convention on Climate Change
USGS	United States Geological Survey
ΔAGB	Annual change in biomass

1
Introduction

1.1 Threats to tropical forests

Tropical forests are hotspots of carbon and biodiversity, storing 70% of all living biomass worldwide (Pan et al. 2011) and harbouring over half of the Earth's terrestrial biodiversity (ter Steege et al. 2015). These diverse ecosystems provide a wide range of critical ecosystem services from regulating water cycles to recycling nutrients to the storage of carbon. Nowhere is this more evident than in the Amazon Basin, a composite of nine countries possessing the largest remaining expanse of tropical forest worldwide (Hansen et al. 2013), and storing approximately 100 billion tonnes of carbon in their vegetation and soils (Feldpausch et al. 2012, Phillips et al. 2017). Ecological processes (e.g. species composition, dispersal mechanisms and demography) within the Amazonian forests are remarkably complex, but are highly sensitive to environmental changes (ter Steege et al. 2013, Lewis et al. 2015). Of particular concern is the continued forest loss across the Amazon due to (1) climate change resulting from global warming and deforestation, and (2) anthropogenic disturbances (Figure 1.1).

As these forests play a crucial role in Earth's carbon cycle, even small changes in their dynamics may have significant regional or global consequences (Lenton 2011, Figure 1.1). For instance, Amazonian forests offset ~25% of anthropogenic emissions stemming from fossil fuels, the main driver of climate change (Pan et al. 2011, Grace et al. 2014). Recent large-scale deforestation events, however, have resulted in the release of approximately 1.8 million tons of atmospheric carbon dioxide annually between 2000 and 2010 (Song et al. 2015) and a reduced carbon storage potential (Foley et al. 2007). Further, recent research revealed that carbon gains in intact forests offset losses due to deforestation (Galbraith et al. In Review). However, the natural Amazonian carbon sink is also in decline (Brienen et al. 2015). Therefore, despite recent reductions in

deforestation across some Amazonian countries such as Brazil (Tyukavina et al. 2017), the overall net effect is neutral (Galbraith et al. In Review).

Regionally, deforestation may also affect climate by reducing the rate of evapotranspiration (Bonan 2008, Gloor et al. 2013, Spracklen and Garcia-Carreras 2015), which in turn may affect ecosystem functioning and carbon dioxide fluxes during the transpiration process (Maeda et al. 2017). In western Amazonia, deforestation was shown to reduce rainfall by 20% downwind of the deforested area (Zemp et al. 2017), while meteorological stations in Rondônia, Brazil, indicated that seasonality of rainfall shifted due to forest loss. Here, the wet season was delayed by ~11 days in deforested regions while no change was observed in forested areas over the last 30 years (Butt et al. 2011). Unlike intact tropical forests, tree species from land uses such as pasture and agriculture have far less leaf area and shallower roots (Jipp et al. 1998) and declines in evapotranspiration may further decrease rainfall, thereby reducing precipitation downstream of the deforested region (Spracklen et al. 2012, Figure 1.1). However, the importance of this effect varies according to the size and pattern of deforestation patches (Lawrence and Vandecar 2014). For instance, in smaller patches, precipitation increased downwind, resulting in net increase in rainfall over the entire deforested patch. As size of the deforested patch increased, the magnitude of precipitation and rainfall declined (Lawrence and Vandecar 2014).

As the carbon dynamics of Amazonian forests are tightly coupled to variations in climate (Gloor et al. 2013), recent trends point to a variable seasonality when averaged over the entire Basin (Gloor et al. 2013, Marengo and Espinoza 2016). In the future, some areas across the basin are predicted to become hotter and drier with extreme climatic events such as El Niño–Southern Oscillation (ENSO) likely to be stronger in southern, eastern and north-central Amazon (Lejeune et al. 2015, Marengo and Espinoza 2016). ENSO events can cause extreme water deficits which decrease productivity, leading to widespread tree mortality, and can potentially weaken the carbon sink (Cavaleri et al. 2017).

Concurrently, the catchment of the Amazon Basin is experiencing a substantial wetting trend which coincides with increasing tropical Atlantic sea surface temperatures (SST) (Gloor et al. 2013).

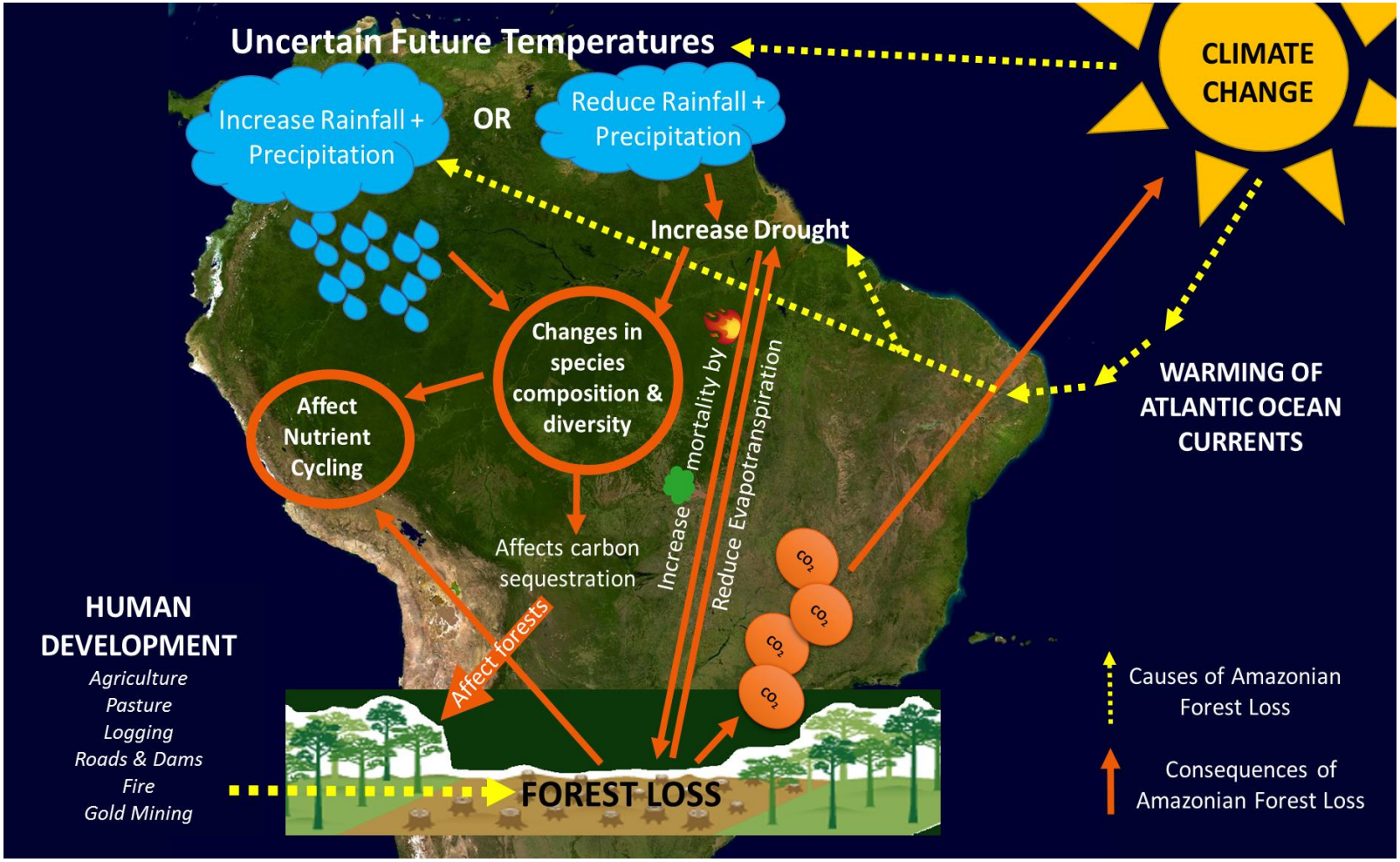

Figure 1.1 Causes and consequences of Amazonian forest loss.

This upward trend in SST may lead to increasing atmospheric water vapour transported across the northwestern Amazon while the southwestern Amazon may become drier due to shifting water circulation in the atmosphere from deforestation (Gloor et al. 2013).

Non-ENSO related droughts have also hit the Amazon in recent years (2005 and 2010). These were caused by warming of the tropical Atlantic, causing the rain-bearing inter-tropical convergence zone to shift northward, affecting both the seasonal parts of the basin as well as central and western Amazon (Lewis et al. 2011). These large drought events may temporarily reverse the longterm forest carbon sink in the Amazon (Phillips et al. 2009, Feldpausch et al. 2016), leading to the release of approximately 1.1 Pg C yr^{-1} (Feldpausch et al. 2016). In addition to changes in the carbon cycle, nutrient pools are also detrimentally affected by forest loss, particularly nitrogen and phosphorus cycles (Davidson et al. 2007, Kaspari and Powers 2016). Whether these anomalies will persist in the future is uncertain and climate model predictions in Amazonia vary from strong drying to modest wetting (Boisier et al. 2015; Figure 1.1). Irrespective of the direction of climatic changes, species diversity and composition may shift in response, potentially impacting on the rate of carbon sequestration and the regenerative capacity of tree species (Allen et al. 2010, Toledo et al. 2011, Mok et al. 2012, Exbrayat et al. 2017).

Additionally, an increase in global population and a concurrent increase in the exploitation of Amazonian forests for commercial and economic purposes have also resulted in significant impacts on both biodiversity and ecosystem services (Foley et al. 2007, Verboom et al. 2015). The net effect of these developments in the Amazon has resulted in the loss of millions of hectares of forest (FAO 2011), with many landscapes which were once dominated by old-growth forests quickly becoming replaced by alternative land uses (Lambin and Meyfroidt 2011). As wealth increases globally, along with other social, political and market forces that monetize Amazonian forests, further pressure is placed on these forests through resource extraction and land conversion that aid in the development and progress of human societies (Lambin and Meyfroidt 2011, Arima et al. 2014).

In determining the overall patterns of forest loss, it is important to recognize that land use change is complex as the underlying (indirect) and proximate (direct)

drivers are continually evolving across different temporal and spatial scales (Raunter et al. 2013, Nobre et al. 2016). Even within the Amazon Basin, the prevalence and drivers of forest loss shift across countries and even between Brazil and non-Brazilian countries (Killeen et al. 2007, IDEAM 2011, Asner et al. 2013, Nepstad et al. 2014). The shifting rates of forest loss throughout Amazonia raises several questions as to what is driving these changes, particularly across countries; the extent of forest cover change, and the extent to which forests can recover from land use perturbations.

As unprecedented changes occur across Amazonian forests, international concerns have increased regarding the global significance of forest loss. The 2015 Paris Agreement under the United Nations Framework Convention on Climate Change (UNFCCC) acknowledged the importance of forests for limiting future temperature increase (UNFCCC 2015). This included setting global targets like the 20 Aichi Biodiversity Targets, aimed at halving the rate of forest loss by 2020 (Target 5, CBD 2013), with incentives being negotiated to further reduce emissions from deforestation and forest degradation through forest restoration. Other international initiatives such as targets 14 and 15 of the Aichi Biodiversity Targets and the Bonn Challenge also recognise the carbon sequestration and biodiversity potential of recovering secondary tropical forests following anthropogenic land use disturbances (CBD 2013).

In fact, recovering secondary forests in many countries now exceeds the cover of primary forests (Wright 2005, Poorter et al. 2016), and can potentially sequester 3.05 $Mg\,C\,ha^{-1}\,yr^{-1}$, 11 times the uptake rates of old-growth Amazonia forests in 2010 (Houghton et al. 2015, Poorter et al. 2016). If allowed to persist, the second-growth potential across Latin America is substantial, with 240 million hectares available for offsetting carbon emissions from fossil fuel and industrial processes associated with these countries (Chazdon et al. 2016). Secondary forests may also help slow biodiversity loss by providing a habitat for forest-dwelling species and conserving distinct evolutionary lineages and high levels of evolutionary history (Chazdon et al. 2009, Edwards et al. 2017, Rocha et al. 2018). For secondary forests retaining less than 100 Mg ha^{-1} of carbon, carbon and biodiversity were recently shown to be strongly and positively linked (Ferreira et al. 2018). This makes secondary forest an important component for biodiversity conservation and carbon storage. Recent syntheses of

chronosequences from tropical secondary forests have concluded that secondary forest biomass recovery rates are 1) mainly controlled by rainfall (Poorter et al. 2016); 2) are faster in forests previously under pasture use than agricultural production (Martin et al. 2013); and 3) nutrient and biogeochemical processes, particularly nitrogen, recovers within 10-15 years of forest regrowth (Batterman et al. 2013). However, few studies have assessed the roles played by more intensive land uses such as mining for gold or other resources. Thus, we do not know how forest recovery and resilience (defined here a system's capacity to remain in the same state in the face of perturbations, Holling 1973) following these land uses compares with recovery from more traditional land uses such as pasture and agriculture.

This study thus seeks to answer the following questions: How has the forest landscape changed across Amazonia within the last decade and what influence does intensive land uses such as gold mining have on the current extent and recovery of forest in the region? Are protected areas effective in curbing forest loss from gold mining activities? By examining current forest loss across Amazonia, we can assess how different drivers may interact in diverse ways to influence this landscape as well as determine how fragmented systems will influence forest functioning. Further, by exploring the secondary succession process of other types of land uses directly associated with human development may help us predict how tropical forests respond to future environmental changes and disturbance events, which is crucial for improving climate change projections, and for land management and conservation.

1.2 Thesis Layout

The aim of this thesis is to better understand the current dynamics of forest loss across Amazonia, and how other types of developmental land uses such as gold mining impacts forest recovery. As such, this thesis was divided into two components encompassing different spatial scales: a) assessing land use change across the entire Amazon (Figure 1.2 – blue and purple boxes) using remote sensing products; and b) focusing on how gold mining influences forest loss, nutrient cycling and recovery patterns in specific mining intensive regions of

Guyana (Figure 1.2 – orange boxes) through remote sensing and field observations.

Chapter 1 explores the different drivers that influence forest loss across the Amazon Basin, followed by a description of features that are used to understand forest loss. A literature overview of remote sensing approaches used to quantify deforestation and forest recovery post-disturbance patterns is also presented (Figure 1.2 – blue box).

Chapter 2 investigates the temporal and spatial changes of forest loss across Amazonia according to size distribution of clearings, hotspots and geographical density events using a global forest cover dataset (Figure 1.2 – purple box).

Chapter 3 evaluates the extent of forest loss from the recent expansion of gold mining across Amazonia and assesses the accuracy of current high resolution satellite datasets in capturing gold mining-related forest loss (Figure 1.2 – orange box).

Chapter 4 assesses the impacts of small-scale gold mining on soil and plant mercury and nutrients (nitrogen, phosphorus, cations) concentrations.

Chapter 5 focuses on the regenerative abilities of forest biomass after gold mining-induced deforestation events and how these compare with other land uses such as agriculture and pasture.

Chapter 6 summarises and integrates the main findings from the data chapters and discusses the implications for conservation and suggest future directions for investigation (Figure 1.2 – orange box).

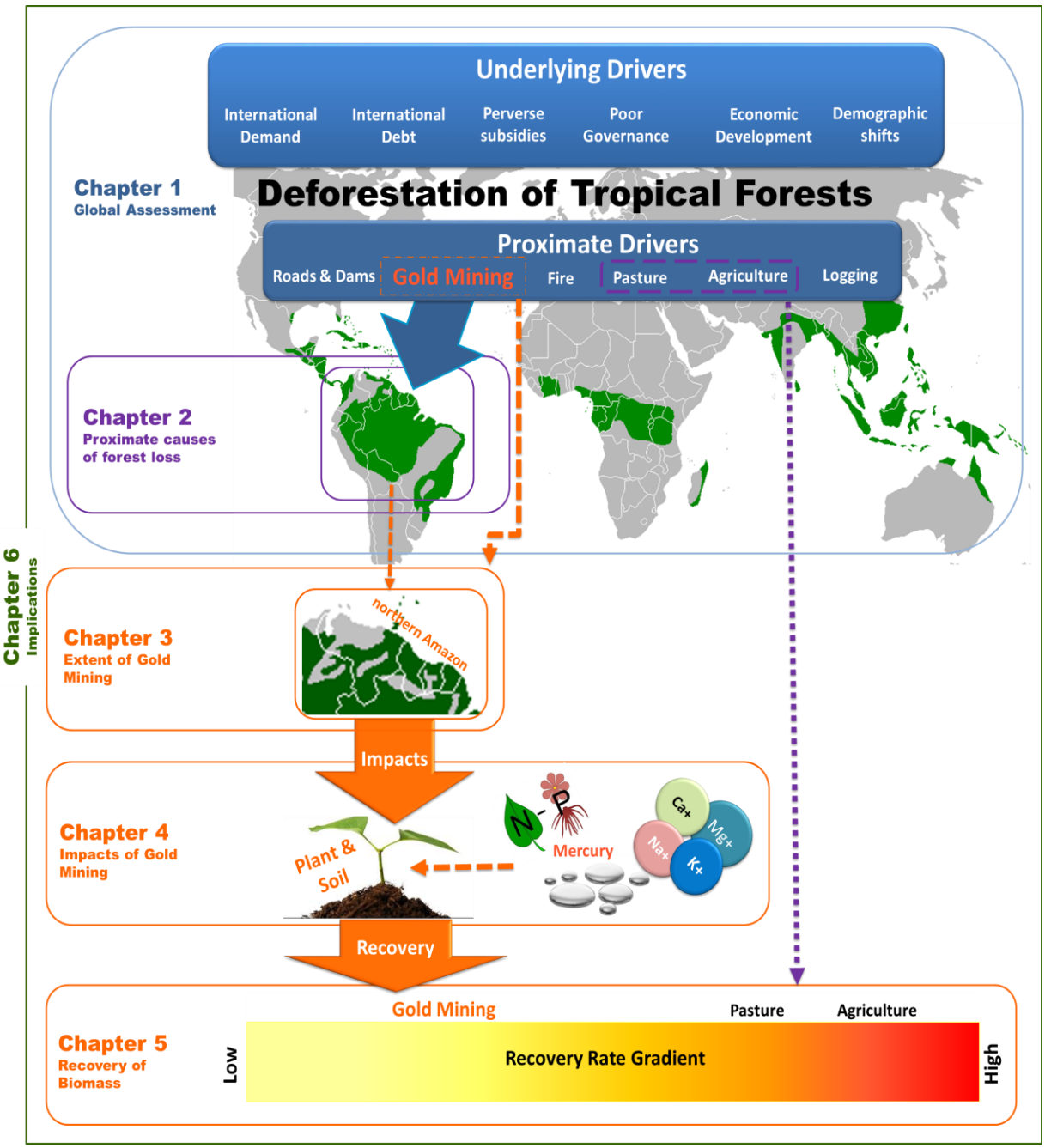

Figure 1.2 Conceptual diagram that summarizes the aims of this thesis. Different colour boxes represent the different objectives of this thesis: blue represents the global assessment of threats to tropical forests and different drivers (Chapter 1), the purple box focuses on the dynamics of the proximate causes of deforestation across Amazonia (Chapter 2), the orange boxes focus specifically on the extent (Chapter 3), impacts (Chapter 4) and recovery of biomass (Chapter 5) from gold mining while the green box represents the overall implication for conservation and management (Chapter 6).

1.3 Drivers of deforestation in Amazonia

Lambin et al. (2001) first conceptualised a simple way of categorizing different drivers of forest loss as either proximate (direct) or underlying (indirect). Underlying drivers are processes which have an indirect effect on forest loss, consisting of an interplay amongst demographic, economic, technological, institutional and socio-cultural factors (Figure 1.2). Proximate drivers are human activities which directly influence forest cover such as agriculture, pasture, logging, fires, infrastructure development such as roads and dams, and gold mining (Figure 1.2). In this section, I briefly describe how these drivers influence deforestation across Amazonia (Figures 1.2, 1.3).

1.3.1 Underlying drivers

Temporal and spatial patterns of deforestation have historically varied greatly from country to country (Figure 1.3) (Geist and Lambin 2001). Recent analysis suggest that economic globalization, rising incomes and increasing demands for commodities have accelerated forest conversion in high potential areas within the last decade (Lambin and Meyfroidt 2011). This has led to an increasing reliance on meat-based diets which has transformed old-growth forests into productive agriculture and pasture lands (Figure 1.3). For example, deforestation in the Brazilian Amazon is increasingly linked to globalized markets for timber, beef, soybean and biofuels (Rudorff et al. 2011). Moreover, the pace of forest loss in the region appears to be influenced by international demand for agricultural products once investments in infrastructure related to the national markets have integrated into the region (May et al. 2011). In the 1980s and 1990s, forest loss resulted primarily from smallholders clearing the forest for subsistence farming, but this shifted in the last decade to large-scale agriculture (Rudel 2007, Rudel et al. 2009). However, between 2002 and 2009, Rosa et al. (2012) showed that subsistence use once again dominated across the Brazilian Amazon, leading to 43% of all deforestation, whereas large-scale industries accounted for only 10% forest loss.

This shift in the pattern and size of forest loss clearings may result from changes in demand for different commodities and by different population pressures which manifests through forest loss across the region (Laurance 2015). As the demand increases, profits from deforestation vary extensively from a dollar to thousands of dollars, depending on the location, technologies and type of land use (Chomitz et al. 2007). In order to satisfy this demand, easier access to remote forests for land development and associated mechanization that increases production yield is required (Rademaekers et al. 2010). For example, in southern Brazil, forest loss surged in the 1970s due to agricultural mechanization (Chomitz et al. 2006), increasing at a rate of 3.66% annually between 1975 to 2010 (Contini and Martha 2010).

Ultimately, this demand for commodities, while growing the local cash economy (Lambin et al. 2003), also increases disparities in the distributions of goods between rich and poor nations, with many Amazonian countries overborrowing relative to their ability to repay. For example, the debt crisis of the 1980s highlighted the inability of many Amazonian countries to generate enough revenue to make payments to their mounting foreign debts (Pop-Eleches 2008). Thus, large sums of money were borrowed from the World Bank to finance massive agriculture, forestry, cattle ranching, mining and infrastructure projects. (Barbosa 2001). In turn, the World Bank rescheduled loan payments and provided new loans, called structural adjustments, which allowed Amazonian countries to institute economic policy reforms that encouraged them to spend less by devaluing currency, reducing government spending, liberalizing trade and privatizing government assets. While this ‘earn more’ and ‘spend less’ model facilitated some debt repayment, it increased forest loss across the region (Chakravarty et al. 2011). An analysis of the impact of loans at a local scale in the Peruvian Amazon indicated that forest loss rates were higher when loans were available for agriculture, with the highest rates found within 8 km of the Peruvian-Brazilian Interoceanic highway (Alvarez and Naughton-Treves 2003).

Other underlying drivers such as perverse subsidies also likely increase forest loss throughout the tropics. For instance, in Brazil, subsidies for cattle ranches approved by the Superintendency for Development of Amazonia (SUDAM) were a driving force for forest loss in the 1970s and 1980s (Fearnside 2005). Alongside this, poor governance may see the continuation and approval of

contracts that lead to forest loss via two routes: (1) large firms with political power may influence government policies or choices regarding concessions during the early stages of the decision-making process, or (2) smaller firms may bribe state officials to overlook stipulations of a contract during any part of the extractive phase (Pfaff et al. 2010). Several studies indicate that forest loss across the Amazon is determined by different combinations of these underlying drivers in varying geographical and historical contexts (Geist and Lambin 2001, Lambin et al. 2001, 2013); the direct consequences of these factors will be discussed below (Figure 1.3).

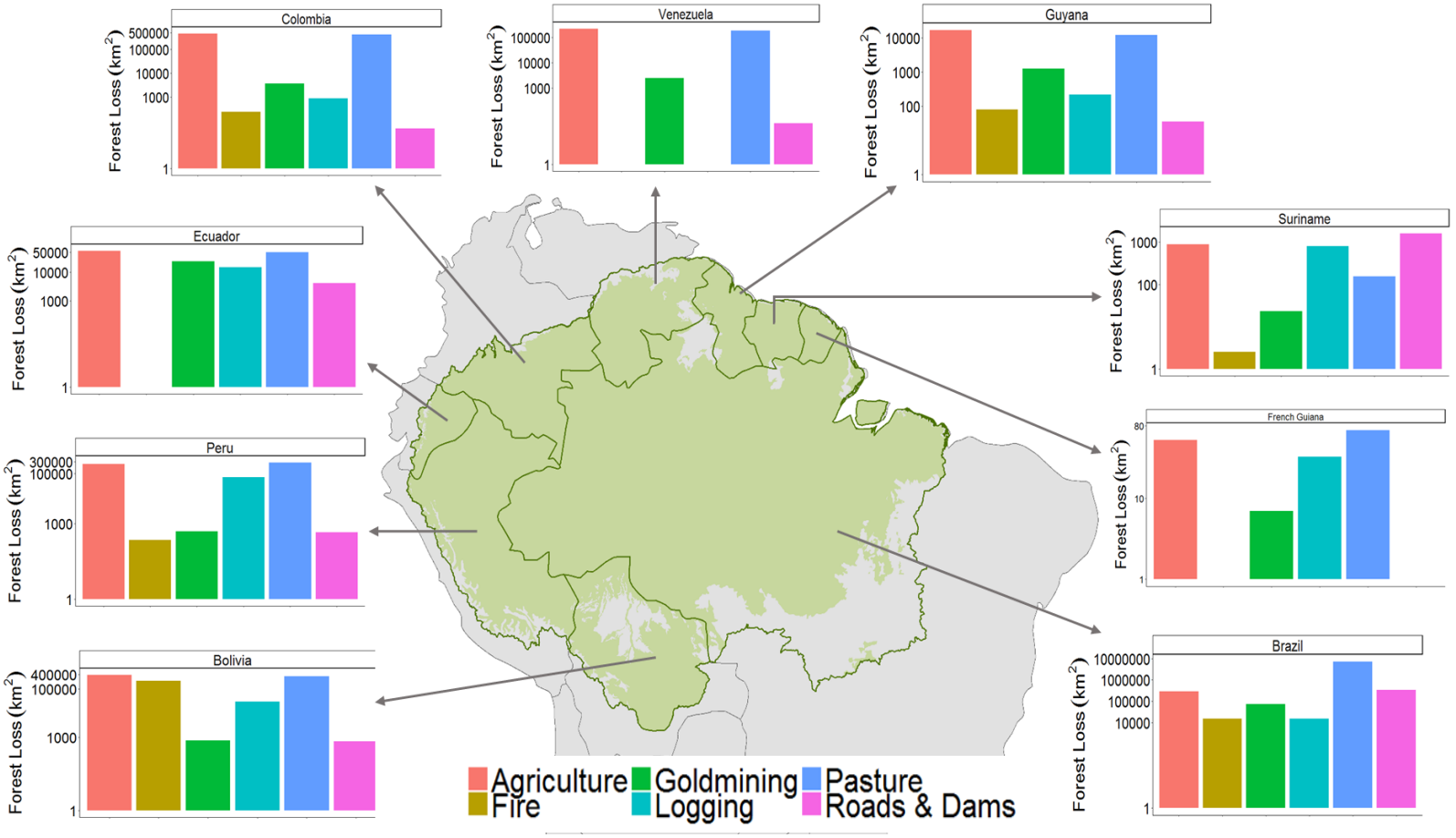

Figure 1.3 Proximate drivers of forest loss (km^2) across Amazonia. Missing data on individual graphs indicate no data found during the literature review[1].

[1] *Data for Figure 1.3 taken from Galbraith et al. (In review), FAO (2015), Asner et al. (2005, 2013), Rahm et al. (2015), Guitet et al. (2012), FAO (2001), FAO (2015b), Ledec and Quintero (2003), Finer and Novoa (2015), Salo et al. (2011), Pacheco (2006, 2012), Müller et al. (2014), Tyukavina et al. (2017), Massé and McDermott (2017), WorldStat, 2007 (http://en.worldstat.info/South_America/French_Guiana/Land), Vandegrift et al. (2017), Guyana Forestry Commission (2015), FAO (1993). It is important to note here that this figure was created using data from different sources across different timelines as a demonstration that no previous comprehensive analysis exists for comparison across all Amazonian countries.*

1.3.2 Proximate Drivers

1.3.2.1 Agriculture & Pasture

Since the 1970s, global demand for agricultural products has led to the expansion of agricultural areas and pastures across much of Amazonia. In order to meet this increasing demand for agricultural products, large swaths of rainforest are destroyed, with a focus on expanding arable land. Lower production costs and fewer environmental regulations have helped Amazonian countries such as Brazil, Peru, Bolivia and Guyana to respond quickly to increased demand for crops such as sugarcane, soybean and oil palm (Pacheco 2012, Figure 1.3) and pasture-based products such as beef (Lobato et al. 2014). For instance, large-scale soybean plantations now cover more than 21 million hectares in Brazil (Gibbs et al. 2010). As China's growing affluent classes consumes larger amounts of ration-fed poultry, pork and beef, soya continues to be the best source of vegetable protein in animal rations (Nepstad et al. 2008). With the world population expected to grow to 9 billion by 2050, and much of this growth forecast to occur in developing countries, the market demand for agricultural and pasture-based products will continue to increase.

Figure 1.4 indicates the increase of agricultural land fraction over time with Amazonian deforestation occurring across different parts of the region, from (i) the Andean Cordillera to Amazonian lowlands, a north-south axis over the western side of the region through Peru, Colombia, and Ecuador; (ii) from the south and east of Brazil to central Amazonia, (iii) from the North to South in Venezuela; and (iv) from the Atlantic coast along the Amazon River (Imbach et al. 2015). Here, Brazil followed by Peru show the largest variations in agricultural land use across the basin.

The rate of deforestation has declined across the Brazilian Amazon by 79% since 2005 (Assunção et al. 2012, Diniz et al. 2015), while agricultural and pasture outputs in the region have almost tripled during the same period (Assunção et al. 2012). Simultaneously, large-scale cattle ranching has also significantly expanded in Brazil since the 1990s with the number of cattle more than tripling (Fearnside 2008, Figure 1.5). Between 2001 and 2010, production increases corresponded to an area increase of 3 million hectares for cropland (soy) and 10 million hectares for pasture while deforestation across Brazil started to decreased by 2005 (Macedo et al. 2012). It is therefore clear that economic growth, particularly in Brazil, has become decoupled from deforestation (Macedo et al. 2012). Here, the efficiency of the land may have intensified where areas previously cleared have been re-utilized, thereby increasing the productivity of the land (Macedo et al. 2012, Lapola et al. 2014), despite cattle-dominated pastures decreasing over time in Brazil (Imbach et al. 2015, Figure 1.5). The Brazilian government contends that the fall in deforestation in 2004-2005 was a direct result of policy initiatives (such as the Soy and Beef Moratoria in 2006 and 2009 respectively) which ensured increased land productivity (Killeen et al. 2007) as opposed to a reduction in the demand for commodities. Whether this decoupling effect exists in other Amazonian countries is yet to be documented. This is mainly based on the lack of historical forest loss trend data on individual non-Brazilian countries. Figure 1.3 is an example of the lack of comprehensive and consistent data. For instance, deforestation trends in Guyana, despite being low, indicate an increase from the 1990 figures; which was originally projected as zero (FAO 2006). As a result of this seemingly limited forest loss, and large expanse of intact forests, the Governments of Guyana and Norway signed a Memorandum of Understanding (MoU) in 2009 to support Guyana's Reducing Emissions from Deforestation and Forest Degradation (REDD+) scheme in order to stem future forest loss (Gruining and Shuford 2012, Laing 2018). Other partnerships based on the concept of "Payment for Ecosystem Services" (PES) where an economic value is assigned to standing forests as a means to combat climate change also ensued in ~101 countries including Brazil, Ecuador, Colombia and Suriname (Kronenberg et al. 2015).

Nevertheless, other Amazonian countries are experiencing similar economic scenarios linked to placing a higher premium on agricultural commodities such as

soybeans and timber than on standing forests (Nobre et al. 2016, Figure 1.4). In Bolivia, deforestation was initially driven by demand for sugar and cotton in the 1970s, whereas the exponential growth from 1980s onwards coincided with infrastructural and agro-industrial expansion, particularly for soy and cocoa (UNODC 2006, Killeen et al. 2007). As agricultural expansion continued across Bolivia, a tripling of deforestation was also seen in protected areas (Killeen et al. 2007), while cattle ranching accounted for 27% of forest loss between 1994 and 2004 (Müller et al. 2012).

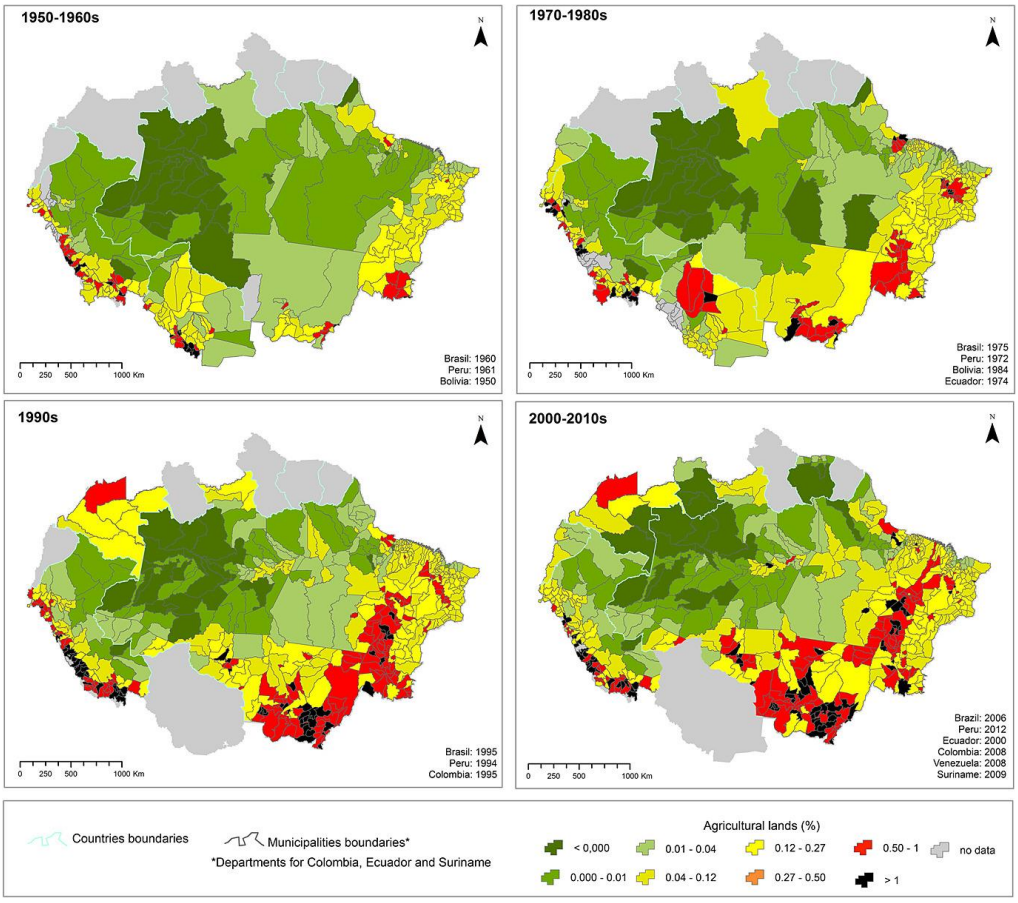

Figure 1.4 Fraction of agricultural lands over two consecutive decades across Amazonia. Map from Imbach et al. (2015).

This was further compounded by externalities such as Brazilian currencies, which played a noteworthy role in cattle-ranching investments, and therefore deforestation along the Bolivia-Brazil border (Killeen et al. 2008).

Peru also saw a mosaic of forest loss from agriculture and pastures between 2000 and 2012 (Lawson et al. 2014, Figures 1.4, 1.5), with oil palm monoculture

being the main driver, accompanied by economic incentives such as tax exemptions for oil palm cultivation (Dourojeanni et al. 2009, Gutiérrez-Vélez et al. 2011, Carrasco et al. 2014). From 2000 to 2010, an estimated 72% of industrial-scale high-yield oil palm expansion occurred in the Peruvian Amazon; particularly in old-growth forests (Gutiérrez-Vélez et al. 2011). Concurrently, pastures in Peru increased from 1950 until 2012 (Imbach et al. 2015), with a sudden decrease most likely correlated with other extractive industries such as gold mining (Asner et al. 2013).

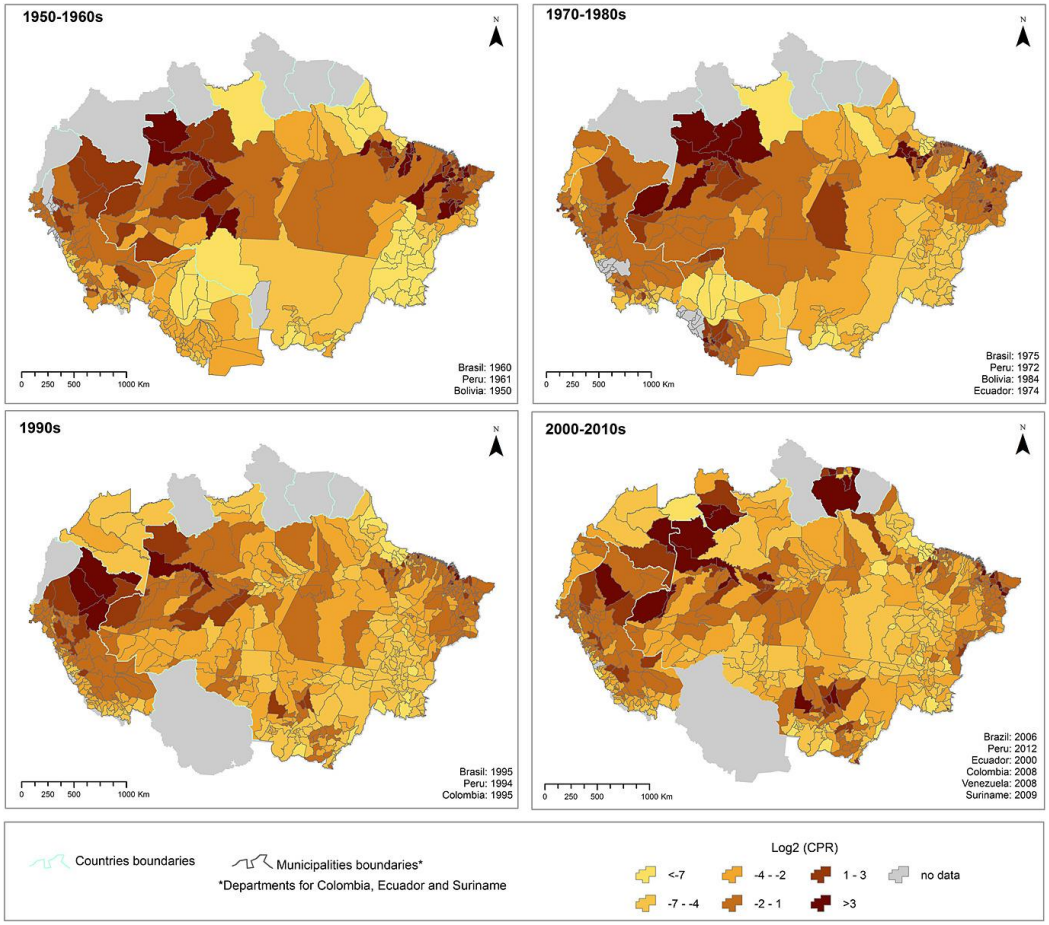

Figure 1.5 Planted/natural pastures over two consecutive decades across Amazonia. Map from Imbach et al. (2015).

Similar deforestation drivers suggest analogous effects in Ecuadorian and Colombian Amazon biome (Figures 1.4, 1.5). Governmental initiatives to expand agricultural colonization in the Ecuadorian Amazon was the initial cause of forest loss; commencing in 1964 with land reform laws that led to 18.6% deforestation

between 1965 and 2000 in the eastern lowlands (Wasserstrom and Southgate 2013). In Colombia, 75% of deforestation in its Amazon was a result of agriculture, a third of which was cleared for cattle ranching between 2000 and 2005 (Castiblanco et al. 2013).

Comparatively, deforestation trends in Northern Amazonia (Venezuela, Guyana, Suriname and French Guiana) remain remarkably low (4.1%) relative to Western Amazon and Brazil between 1990 and 2011 (Killeen 2012, Figures 1.4, 1.5). Multiple challenges such as the lack of accessibility, inactive development policies of the State and unavailable essential infrastructure and resources may explain why this region retains a relatively low deforestation rate (Rademaekers et al. 2010). However, this trend is changing as countries respond to international demands for commodities as a pathway for economic development. For instance, in Venezuela approximately 287,500 ha of forest was lost annually between 1990 and 2000, while the rate of forest change increased by 6% between 2000 and 2005 mainly due to cattle ranching (FAO 2011, Pacheco et al. 2014).

1.3.2.2 Logging

Over the past three decades, Amazonian forests have been threatened by increasing rates of forest loss from industrial logging. For instance, between 1996 and 1997, approximately 9000 to 15 000 km^2 has been logged (Asner et al. 2005). With over 800 million people depending on forests for timber and non-timber products (Chomitz et al. 2007), a central challenge for sustainable use of tropical forests was how to preserve the biodiversity and ecosystem services associated with forests while enhancing timber production. As such, selective logging was adopted as a viable forestry practice which involved the extraction of high-cost commercial tree species with a minimum trunk diameter (~40-60cm) (Salvini et al. 2014). This left non-commercial species unlogged, with only a small percentage of trees harvested, usually 1-10 trees per hectare (Edwards et al. 2014). Despite only harvesting a small number of trees, carbon sequestration rates may be affected by 47% (Asner et al. 2010). While conventional selective logging left the forest intact, little planned effort was made to reduce residual stand damage (Feldpausch et al. 2005b). As such, Reduce Impact Logging (RIL) was seen as a viable management option to further reduce damage and carbon accumulation as

coarse woody debris (CWD) production (see Feldpausch et al. 2005 for more details).

Despite selective logging and RIL being less detrimental than clear-cut logging, and with at least one-third of the Amazon now officially designated as timber concessions (Laurance et al. 2014), it can still have negative outcomes, resulting in localized extinctions and changes to community composition (Edwards et al. 2014, Bicknell et al. 2015). Logging intensity, species selection and canopy damage from logging have direct effects on stand structure, stand development, including major shifts in species dominance, densities and recruitment, and subsequent logging cycles (Feldpausch et al. 2005b). The direct impact of logging still remains from the networks of roads, tracks, and clearings created by bulldozers, skidders, and other heavy equipment during cutting operations (Bicknell et al. 2015). These networks cause collateral tree mortality, soil erosion and compaction, forest structure changes such as vine and grass invasions, and microclimatic changes associated with disruption of the forest canopy (Asner et al. 2004, Guitet et al. 2012). Moreover, localized corruption in regulatory documents may also enable further deforestation. For instance, in the Peruvian Amazon, legal logging concessions enabled widespread illegal logging activities in 69% of all concessions (Finer et al. 2014), thus threatening forested areas. Illegal logging may also be conducted by poor households accessing larger sections of the forests as demonstrated in the Ecuadorian Amazon (Vasco et al. 2017). In this regard, some authors have suggested that logged forests may take decades to fully recover (Osazuwa-Peters et al. 2015) with some insisting that it will negatively affect both carbon stocks (Berenguer et al. 2014, 2015) and ecosystem functioning (Foley et al. 2007, Edwards et al. 2014).

1.3.2.3 Roads and dams

Road and infrastructure development such as dams have shown to sharply increase deforestation rates in remote regions across Amazonia. Historically, the Amazon has been identified as a source of massive growth in hydropower capacity (Nobre et al. 2016) with more than 120 large dams planned across Amazonia (Figure 1.6). The rise in dam development is predominantly driven by greater electricity demands (Lees et al. 2016) with the debate on the detrimental

impacts of hydropower infrastructure in Amazonia largely focused on the displacement of human populations and habitat loss.

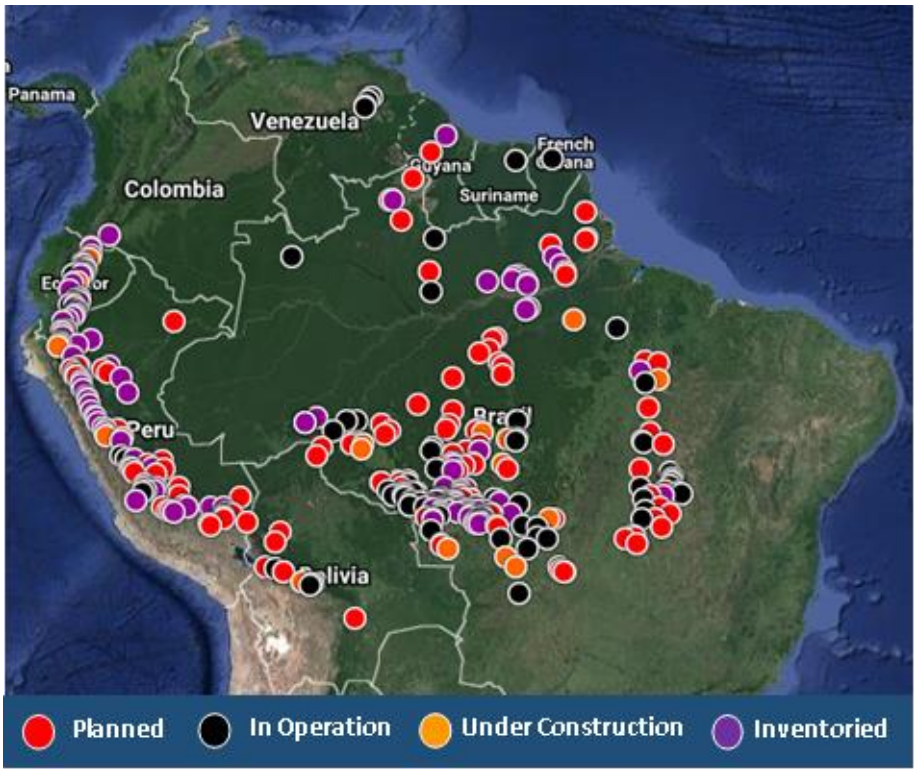

Figure 1.6 Total number of existing, planned and inventoried (registered sites) dams across Amazonia. Image from Dams for the Amazon Basin (http://dams-info.org/en), Fundacion Proteger, International Rivers, and ECOA

However the impacts of Amazonian dam projects have decisive ecological ramifications at local, regional and global scales with ~40 000 km^2 of forest being lost (Tundisi et al. 2014) as well as the significant increases of greenhouse gas emissions (Kemenes et al. 2007), habitat loss, hydrological alterations through water level change and reduction of fish catch potential (Nobre et al. 2016). Due to a combination of human displacement, environmental impacts and little subsidies for current mega-dam building, the Brazilian Government recently announced that the era of building big hydroelectric dams in the Brazilian Amazon is ending (Branford 2018). Unfortunately, similar actions were not observed in other Amazonian countries.

Further, expanding road networks across Amazonia can promote social and economic development, while bringing a multitude of environmental problems (Laurance et al. 2014, Figure 1.7). Assessments on the effects of roads in the

region showed that 95% of all forest loss occurred within a 5.5 km distance to roads (Barber et al. 2014a), with forest loss varying between 67% to 90% within 25-100 km of main roads (Laurance et al. 2001, Alves 2002, Asner et al. 2006). In Bolivia, for example, 58% of forest loss took place within 5 km of pre-existing roads in the recently downgraded legal protection of the Isiboro-Sécure National Park and Indigenous Territory (TIPNIS) between 2001 and 2017 (Fernández-Llamazares et al. 2018). As major roads open up large areas of forest to human settlement and much needed resources (Laurance et al. 2009), they also bring habitat and biodiversity loss, wildfires and overhunting, which may affect forest composition and structure due to changes in seed dispersals (Laurance et al. 2014).

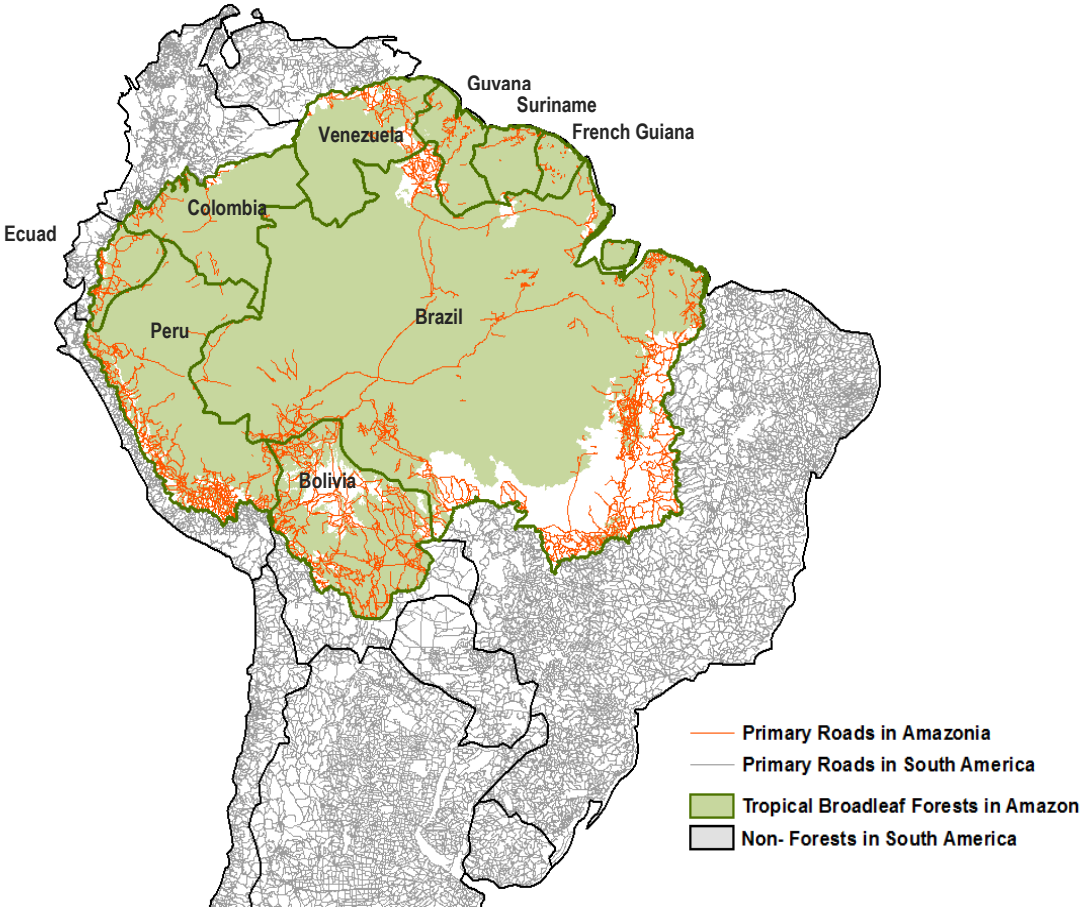

Figure 1.7 Major road network across Amazonia.
Map generated using data from the 2013 integrated gROADS database (http://sedac.ciesin.columbia.edu/data/set/groads-global-roads-open-access-v1); Columbia University; and University of Georgia.

For instance, Espinosa et al. (2018) showed that jaguar density was 6-18 times less at sites with increased accessibility via roads in Ecuador, while Ahmed et al. (2014) estimated that Para state in Brazil lost an average of 83 species of forest-associated birds between 2000 and 2008 due to road development and associated changes in vegetation structures.

As deforestation tends to spread contagiously, new roads will spawn networks of secondary or tertiary roads, with images of fishbone-like patterns emerging that may likely increase the spatial extent of forest loss (Figure 1.8). This expansion of roads may also occur regionally and across borders, reinforcing the previous forest loss trends while creating new ones. Within Ecuador, ~3 million hectares of forest was lost between 1990 and 2010 driven mainly through a shift from land settlements to more enterprise-driven activities with the discovery of oil (Rudel 2007).

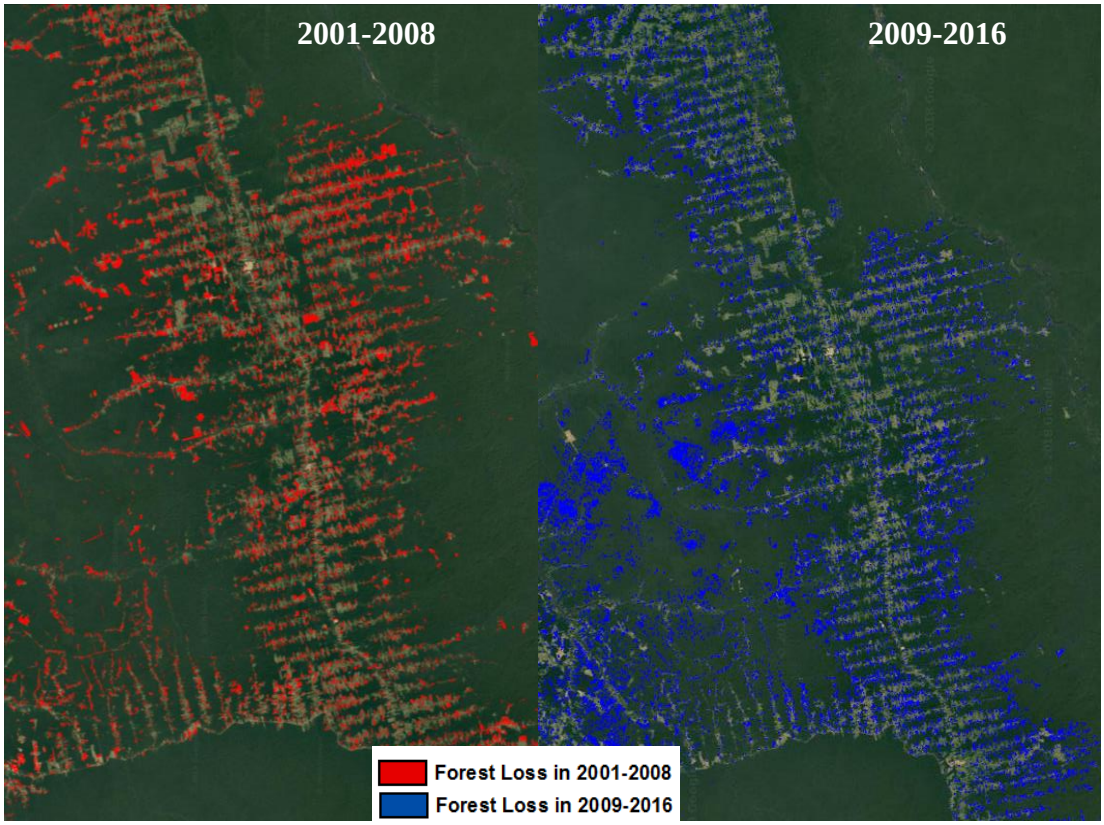

Figure 1.8 An example of the fishbone-like forest loss along primary and secondary roads between 2001-2008 and 2009-2016 in Brazil. Data for map used the Global Forest Cover (GFC) product in Google Earth Engine.

This opened and extended the northern Ecuadorian Amazon to rapid road construction and networks such as the Quito-Lago Agrio Highway (FAO 2011). Road developments along the Brazilian-Peruvian border also led to 64% deforestation rate between 1999 and 2005, with associated secondary road access, driving further forest loss through migration, human settlements, shifting cultivation and land trafficking (usurpation, illegal appropriation, and commerce of lands) within the Peruvian Amazon (Oliveira et al. 2007).

Despite roads playing a pivotal role in development, many are unmapped, with planning and management efforts extremely inadequate. Illegal roads may triple that of official roads (Laurance et al. 2014). In Brazil, for example, for every kilometre of legal road there are approximately three kilometre of illegal roads (Barber et al. 2014a), which further opens forested areas to illegal activities such as gold mining and logging, and may potentially create barriers for sensitive wildlife (Laurance et al. 2009). As road development and expansion continues, it increases the susceptibility of forests to further forest loss and fragmentation by exposing forest edges to increase disturbances.

1.3.2.4 Fire

Different land use activities also increase forest susceptibility to fire across the Amazon, providing ignition sources via forest fragmentation (Nepstad et al. 2008). Since the early 1970s, fire incidences soared across Amazonia as it was used as a primary tool for clearing forests in preparation for crops and pasture or to improve pasture forage. However, ignition sources frequently escaped beyond their intended boundaries into neighbouring forests (Cochrane et al. 2008, Figure 1.9), creating further forest loss and fragmentation. In this regard, fire is often associated with forest edges and fragmentations as they influence the occurrence and intensity of fire regimes, leading to increase tree mortality and forest loss (Vedovato et al. 2016, Armenteras et al. 2017). From 1993 to 2007, fires burned over 1 billion hectares of open and fragmented forests compared to 0.33 billion hectares of dense forest (Alencar et al. 2015).

In turn, fire-related disturbances induce changes in forest structure (size, shape and patterns of remaining fragments) and species composition, which may lead to many local and global consequences, especially under expected climate change conditions (Barlow et al. 2016). For instance, between 2001 and 2010,

approximately 126-221 Tg C were emitted to the atmosphere in the Brazilian Amazon due to edge effects (Numata et al. 2011).

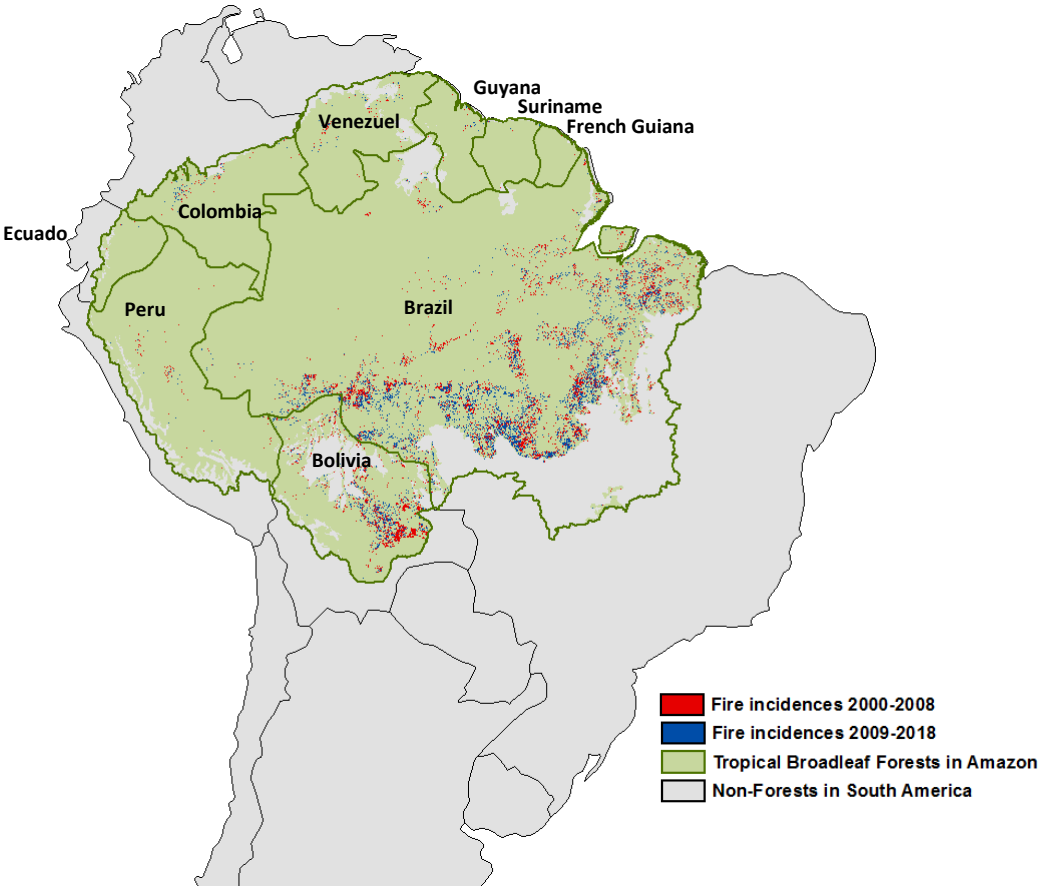

Figure 1.9 Fire incidences across Amazonia from 2000-2008 and 2009-2018. Map created using data from MOD14A1.006: Terra Thermal Anomalies & Fire Daily Global 1km in Google Earth Engine.

The return interval of a natural fire was historically estimated at ~500 -1000 years, but now fires occur every 5-10 years across the Amazon due to escaping agricultural fires (Pivello 2011). As most of the local species are not adapted to fire, their recovery may be hampered after repeated burns (Nobre et al. 2016, Massi et al. 2017), resulting in shifts in species composition. For instance, a woody non-fire-prone vegetation type may transition to a more herbaceous, flammable, and shade-intolerant vegetation type with frequent fire (Pinter et al. 2011). As episodic patterns of post-burn tree recruitment are strongly influenced by the number of times a forest is burned, a different suite of pioneer species may

dominate the vegetation composition after each fire event due to destruction of residual seed bank, mortality of entire cohorts or pioneer species and/or soil fertility (Barlow and Peres 2008). Further, these events increase in extent and intensity due to major drought events such as El Nino (Jiménez-Muñoz et al. 2016). Approximately 90% of all Amazonian forest burning occurs in El Nino events (Alencar and Vera 2006).

While historical fire regime, which result in the production of charcoal rich soils, *terra preta*, (Cordeiro et al. 2014), can be an important carbon pool for longterm storage, they occur on millennial scale biogeochemical cycling (Goulart et al. 2017, Koele et al. 2017). More modern fire incidences, which occurs on a much shorter timescale, tend to result in greater forest loss and reduction in above-ground biomass, primary productivity and disruption to biodiversity, energy and water cycles (Aragao et al. 2008, Cochrane et al. 2008). For instance, in the Brazilian Amazon, annual forest loss rates were closely linked to annual fire incidences from 1998 to 2005 (Aragao et al. 2008). However, in 2015 a drought-induced decoupling of forest loss and active fires was found across the Brazilian Amazon with fire events rising to 80% of the 2005 values despite a 76% decline in deforestation rates (Aragão et al. 2018). This decoupling effect was seen across Brazil, Peru and Bolivia, which may suggest that these countries may be entering a new land-use and land cover change phase (Aragão et al. 2018), driven by changes in large-scale atmospheric circulation patterns, resulting in below-average rainfall over Amazonia. As rainfall pattern decreases, water deficits increase, with drought-induced water stress on forests negatively impacting on photosynthetic capacity, leading to widespread tree mortality. Droughts can also increase the rate of fire incidences in Amazonia associated with increase pasture management and deforestation fires, opening areas adjacent to forest edges, fragments and human-modified forests, all of which are more susceptible to fire than large blocks of undisturbed primary forests. In this regard, degraded forests becomes even more susceptible to forest fires (Aragão et al. 2018).

1.3.2.5 Gold Mining

Gold mining often triggers significant forest loss as large tracts of forests are cleared in order to access the gold (Alvarez-Berrios and Mitchell Aide 2015, Sonter et al. 2017), with associated transportation and infrastructural support such

as roads leading to auxiliary forest loss (Asner and Tupayachi 2017). Much of this forest loss stems from artisanal and small-scale gold miners who take advantage of increases in international gold prices as a result of global financial recessions, opening up forested areas across Amazonia that were historically not profitable for extraction (Swenson et al. 2011, Alvarez-Berríos and Mitchell Aide 2015).

Artisanal and small-scale mining (ASM) continues to be an integral source of revenue for the local population and migrant miners, often forming part of a diversified livelihood strategy in combination with agriculture (Cremers et al. 2013). This is important as the ASM sector employs a greater number of people (Table 1.1) than large-scale mining, and has implications for deforestation trends. It is important to note that defining artisanal and small-scale mining (ASM) is problematic as the criteria used for classifying this type of mining is based on the production volume, size of claims and operational continuity (Hentschel et al. 2002). However, these characteristics are often site-specific with cultural and economic anomalies, and may not be based solely on size of the mine or amount of ore displaced daily (Veiga et al. 2006).

Despite this, it is generally accepted that ASM encompasses small, medium, informal, legal and illegal miners, with increased gold prices allowing for improved operations (Cremers et al. 2013). In fact, improved mechanization allows for a higher rate of return for the miner while simultaneously having a higher impact on the surrounding forests by uprooting trees, increasing sedimentation in rivers and higher deposits of mercury (Peterson and Heemskerk 2001, De Theije and Heemskerk 2009, Balzino et al. 2015). As such, forest loss from gold mining is likely to be further exacerbated across Amazonia due to further increases in the mechanization of the mining process (Cremers et al. 2013).

Given the unprecedented rise in gold mining in recent years, Alvarez-Berríos and Mitchell Aide (2015) estimated that between 2001 and 2013, ~1680 km^2 of forest was cleared within gold mining sites across the Amazon. Other studies have shown similar increases. For example, in Guyana, deforestation rates increased three-fold by 2012 as gold price increased to US$1200 per ounce; with 90% of forest loss attributed to increasing gold mining (Guyana Forestry Commission - Indufor 2013).

Table 1.1 Estimated total number of people employed in the Artisanal and Small-scale Mining (ASM) sector across Amazonia.

Country	Estimated total # of individuals	Data Sources
Brazil	200 000	Sousa et al. (2011), Cremers et al. (2013)
Peru	60 000	Cremers et al. (2013)
Ecuador	92 000	Hentschel et al. (2002)
Bolivia	80 000	Cremers et al. (2013)
Colombia	182 000	Cremers et al. (2013)
Venezuela	15 000	Veiga et al. (2006)
Guyana	130 000	Guyana Forestry Commission and Indufor (2012)
Suriname	20 000	Cremers et al. (2013)
French Guiana	10 550	Legg et al. (2015)

In Brazil, Sonter et al. (2017) showed that 37 830 km^2 of forests were cleared between 2005 and 2015. Likewise, Asner et al. (2013) observed a 400% increase in mining activities between 1999 and 2012 in the Madre de Dios region of Peru, resulting in a tripling of deforestation rate from ~5,350 acres per year to 15,180 acres annually, while in Colombia, the average area of deforestation between 2000 and 2010 increased by 3000 km^2 (Sánchez-Cuervo et al. 2012), partly due to FARC rebels turning to gold mining as an alternative source of revenue (Massé and Le Billon 2017).

Despite this increase in the extent of forest loss from gold mining, previous studies have been periodic, focusing mainly on mono-disciplinary subjects such as mercury impacts (Peterson and Heemskerk 2001, Hilson and Vieira 2007, Sousa et al. 2011), area-specific deforestation (Peterson and Heemskerk 2001, Swenson et al. 2011, Asner et al. 2012, Popescu et al. 2013) or socio-economics (Cremers et al. 2013), with no quantitative information on biomass recovery or nutrient cycling. Given the recent expansion of this sector across Amazonia, the geographic extent and ecological impacts of thousands of small mines have gone unexamined and remains to be properly quantified at a regional and temporal scale.

As forest trends in the Amazon Basin change profoundly, with marked decline of deforestation in Brazil, the reliability of different data sources becomes crucial. As demonstrated above, several studies have provided deforestation data from different land uses, with little consistency in time series. While the deforestation data in Brazil is considered relatively reliable due to consistent longterm monitoring via the Monitoramento do Desmatamento na Amazônia Legal por Satélite (PRODES) programme, for historical reasons, the PRODES data only considers deforestation above 6.25ha. Therefore, forest loss events smaller than 6.25ha are not captured. Furthermore, deforestation data for other Amazonian countries are not well quantified; with a strong indication that deforestation is increasing in Western and Northern Amazonia (Swenson et al. 2011, Asner et al. 2013, Pacheco et al. 2014). As these proximate and underlying drivers of forest loss change across different Amazonian countries, they create a more fragmented landscape (Laurance 2004). Understanding this fragmentation pattern may help us understand (1) how drivers interact in diverse ways and how they vary along spatial and temporal scales, and (2) how a fragmented system will effect forest functioning and therefore regional and local climate in a tropical system.

1.4 Metrics of forest loss

The analysis of spatial disturbance patterns within landscapes has been widely applied to the study of terrestrial ecosystems. When a disturbance is caused within a forest, it is generally parameterized by its frequency (per unit time and per unit area) and intensity (spatial scale), creating patterns and processes that are associated with the structural attributes of forest tree communities (Kellner and Asner 2009, Kellner et al. 2009, Asner 2013). These disturbances often create tree gaps with the resultant forest experiencing multi-layered patches or fragments, which may create spatial heterogeneity or homogeneity, i.e. the increasing similarity of biotas of large geographical areas over space and time (Gámez-Virués et al. 2015, Vallejos et al. 2016). In most human-dominated landscapes, small (less than 100 ha) patches of forest loss are usually the norm, though patches or clearings greater than 1000 ha can be present (Laurance 2004,

Rosa et al. 2012). As the biotic and abiotic conditions vary between forest gaps and within these forest loss patches, regenerating trees and species diversity also varies (Laurance 2004). Forest-climate interactions are also strongly influenced by forest loss patches through edge effects, especially if land use practices repeatedly disturb fragmented margins, for example through fire (Cochrane et al. 2008).

When clusters of patches increase along a spatial and temporal scale, they tend to form hotspots which can be used to identify regions of current and potential forest loss relative to their surroundings (Sanchez-Cuervo and Aide 2013, Isobe et al. 2015). Hotspots can also be areas that exhibit statistically significant clustering in the spatial pattern of forest loss, with observed patterns independent of random processes or subjective decisions (Getis and Ord 1992, Harris et al. 2017). Another metric that can be used to determine the extent of forest loss across a region temporally is geographic density, i.e. how widespread forest loss events are, even if the disturbance itself is not intense. By studying these spatial metrics of forest loss, we can better understand how forest recovery, and the mosaic and dynamics of forests will fare now and in the future, especially in light of climate change.

1.5 Forest Loss Detection

Several datasets have become available which provide information on forest loss since the 1990s, the majority of which rely on one of two imagery instruments – Landsat or MODIS (Moderate Resolution Imaging Spectroradiometer). Using MODIS, Coca-castro et al. (2013) employed the real-time (every 16 days) Terra-i monitoring system which incorporates rainfall and vegetation data to estimate land cover change in Amazonia from 2004-2016. MODIS-based systems such as Terra-i seek to address the time-lag issue for monitoring habitat change. This means that existing platforms are not yet capable of combining technical remote sensing data and analysis in a user-friendly interface. Alternatively, the Food and Agricultural Organization (FAO 2011) and Killeen (2012) initially utilized Landsat imagery to estimate forest change across Amazonia. By 2013, Hansen et al. (2013) employed data mining to the Landsat archive to quantify global tree cover change between 2000 and 2012, extended to

2017, mapping annual global cover extent, loss and gain at a high spatial resolution (30m). The Hansen et al. (2013) product is updated annually to provide wall-to-wall information on forest loss and gains globally, thus providing opportunities for quantifying trends in deforestation that were not historically available (Hansen et al. 2013). In this dataset, forests are defined by their physical attributes (i.e. tree or other vegetation exceeding a height of 5m, and >30% canopy cover prior to loss), rather than by their function or the land use. Therefore, this dataset not only include losses of primary forest, but also accounts, for example, for harvesting of commercial forestry and plantations. As such, I only considered forest loss and do not account for subsequent forest gain as a means to eliminate regrowth from other land uses such as plantations. Despite this limitation, GFC is still the best highest resolution map of global forest cover yet produced from 2000 to 2017.

Both Terra-i and the GFC products have enabled an alternative to the United Nations' Forest Resources Assessments (FRAs), which are hampered by inconsistencies in national reporting (Grainger 2008). The recent development of openly accessible and global satellite datasets has huge potential in facilitating countries that currently lack the capacity to develop independent forest monitoring and reporting systems (Goetz et al. 2015). They also provide an opportunity to estimate forest loss for non-Brazilian Amazonia, which to-date has been highly fragmented, with limited spatial and temporal coverage (see Figure 1.3) e.g. Perz et al. (2005). Using high resolution datasets such as Hansen et al. (2013) also allows for further exploration of forest loss metrics (as described in Section 1.4 above) such as shifts in deforestation size classes over time which can determine potential deforestation agents such as large agri-businesses or small farmers (Rosa et al. 2012).

1.6 Forest recovery from disturbance in the Neotropics and Amazonia

As discussed above, Amazonian forests undergo a panoply of disturbances occurring at multiple and often interacting, spatial and temporal scales. It is often accepted that if left long enough, between 20 to 200 years depending on the

measured variable (Chazdon et al. 2007, D'oliveira et al. 2011), tropical forests may recover to pre-disturbance levels from historical natural events such as blow downs and fires (Asner et al. 2004, Espírito-Santo et al. 2014, Pfeifer et al. 2016, Massi et al. 2017). For the most part, these ecosystems have shown resilience to natural disturbances in the past, ranging from instantaneous localised tree-fall to longer-term regional climatic change. This is often attributed to the (1) distance to primary forests which affected seed dispersal (Mesquita et al. 2001), and (2) the ability to sprout after damage for numerous Amazonian tree species, along with the availability of a rich seed bank (from 500 to 1000 seeds of successional woody species per square meter, Wilson 2007).

While these forests may likely recover from natural disturbances, the extent to which pre-Colombian human activities have shaped recovery patterns in modern Amazonian forests remains a matter of debate, simply because large swaths of the Amazon still remain unexplored (Roosevelt 2013, Levis et al. 2017, Palace et al. 2017). On one hand, some authors have suggested that Amazonian vegetation hid nutrient-poor soils incapable of supporting large populations (Meggers et al. 2003), with post-Colombian activities playing a much larger role in shaping Amazonian forests (McMichael et al. 2017). On the other hand, large pre-Colombian populations with spatially heterogenic settlement patterns across Amazonia may have influenced floristic composition (Bush et al. 2015, Stahl 2015, Levis et al. 2017, Palace et al. 2017), affecting the carbon cycle and global climate (Nevle et al. 2011). This pervasive historical human footprint across Amazonian forests may have dramatically altered woody plant regeneration due to repeated fire regimes (Bush et al. 2008). Intense or frequent fires often favours a distinctive suite of species from limited propagule sources, altering forest dynamics and composition (Balch et al. 2013).

However, recent anthropogenic disturbances, often in novel forms and with greater intensities, may jeopardize the potential for forest recovery and thus compromise forest resilience (Jakovac et al. 2015, Moreno-Mateos et al. 2017). Research conducted in the last few decades has attempted to understand how and whether forests from different types of land uses can recover (Peterson and Heemskerk 2001, Martin et al. 2013, Poorter et al. 2016, Bürgi et al. 2017). In human-induced disturbances, the disturbance regime – the frequency, size and type of disturbance - is often prolonged with curtailing of the successional process

numerous times prior to the sites being completely abandoned (Turner 2010). For instance, where large agriculture activities are prevalent, establishment of vegetation is often achieved through seed dispersal which may slow succession.

Successional pathways on anthropogencially altered lands often appear stochastic and extremely diverse, and may proceed differently from natural forest regeneration due to several factors. Firstly, forest recovery rates are related to biogeographical context. For example, recovery rates were found to be faster in Central American tropics than in Asia, while African forests recovered significantly faster compared to those in South America and Asia (Cole et al. 2014). In the Amazon, inter-regional differences in the average rates of basal area and height growth were best explained by differences in soil types, reflecting differences in soil fertility (Moran et al. 2000, Zarin et al. 2005). Secondly, forest attributes may recover at different rates depending on intensity, duration and frequency of disturbance. For instance, aboveground biomass may occur within decades while other processes, such as species composition may require centuries compared to natural regenerative processes (Chazdon et al. 2016, Poorter et al. 2016). Some disturbances such as from logging roads may recover quicker, with similar canopy cover, species diversity and leaf litter to nearby logged forests after 30 years (Kleinschroth et al. 2016). Moreover, under more traditional land uses such as agriculture and pasture, forests recovered on average 122 tons of aboveground biomass (dry matter) per hectare after 20 years, which corresponds to an uptake of 3.05 tons of carbon per hectare per year (Poorter et al. 2016). This rate of regrowth differed dramatically across Latin American sites, with larger rates associated with higher rainfall (Poorter et al. 2016). Biomass accumulation was found to be greater than 94% in Central Amazonia (Feldpausch et al. 2005a). Further, biomass recovery rates were faster in forests previously under pasture use than agricultural production (Martin et al. 2013). Thirdly, prior land use may influence different recovery and successional pathways. Pioneer species dominate the community during the first years of regeneration, leading to a forest composition very distinct from that of nearby old growth, particularly as some pioneer species can be very long lived (Chazdon 2003, Peña-Claros 2016). Studies across Latin America indicate that species from all functional groups such as shade-tolerant species establish themselves early in the successional process, and may continue to flourish even after canopy closure (van Breugel et al. 2007).

Two different floristic pathways were identified following land abandonment in Brazil, namely (1) *Cecropia*-dominated forests which arise on less severely impacted lands, and (2) *Vismia*-dominated forests which develop on more heavily used or more frequently burned areas (Steininger 2000, Mesquita et al. 2001). These pathways may become arrested or diverted by exotic species under extreme disturbances such as heavy grazing or high-impact logging due to residual vegetation and propagules sources being destroyed by fire or when soils are highly disturbed or compacted (Chinea 2002, Fine 2002, Chinea and Helmer 2003, Zarin et al. 2005). Lower leaf area accumulation relative to biomass was observed to influence different canopy development pathways following recovery from pasture (Feldpausch et al. 2005a). However, little or no such data exists for recovery potential of more intensive land use change such as mining for gold or other resources (see dos Santos et al. 2006 for nutrient recovery in degraded soils after oil exploration).

Despite potential recovery of forests, forest regrowth seems to stop short of 100% recovery, only achieving ~95%, due to either the onset of another disturbance event or the establishment of a lower forest proportion in the landscape as estimated through the percentage of fossil forest pollen (Cole et al. 2014). Moreover, this ability to regrow and recover often depends, to a large extent, on the availability of seeds and the essential soil nutrients, nitrogen and phosphorus. Despite both nutrients being crucial for tree growth, nitrogen limits regrowth in young forests, recovering within 10-15 years after disturbance (Davidson et al. 2004a, Silva et al. 2006, Batterman et al. 2013); while the abundance or scarcity of phosphorus sets the pace of growth in older stands (Turner et al. 2018). To add further complexity, recovery patterns may be influenced by distance to forested areas, regional species pool and competition, site factors such as soil fertility and texture, landscape configuration such as forest cover spatial organization and extent, and regional species composition (Chazdon et al. 2007). Knowledge on recovery rates and responses of Amazonian forests to past forms of disturbances and drivers may facilitate our understanding of the capacity of these systems to respond to current and future events.

1.7 Study Sites

Despite extensive research on forest loss in South America and its global impact (Malhi et al. 2008, Lawrence and Vandecar 2015, Spracklen and Garcia-Carreras 2015, Spracklen et al. 2015), the largely intact forests of northern Amazonia has been relatively overlooked (Hammond et al. 2007a, Bovolo et al. 2018). As such, in this study, measurement plots were installed in two important gold mining areas in Guyana, namely Mahdia and Puruni (Figure 1.10), from January to March, 2016, and subsequently re-censused in June to August, 2017 to provide the first quantitative measurements of forest biomass recovery from mining. Plot selection and date of abandonment was identified in collaboration with the Guyana Geology and Mines Commission (GGMC), the local authority that manages mineral resources within Guyana. Sites ranged in age from 0.6 to 3 years since abandonment of mining activity, with recensusing 18 months later. Time since abandonment was further confirmed through examination of RapidEye satellite imagery from 2010 to 2017 (https://www.planet.com/), by counting the nodes on *Cecropia obtusa* species present within my sites (Zalamea et al. 2012) and by interviewing local miners who worked in the area previously.

Both sites are utilized mainly by artisanal and small-scale miners. Mahdia has a long history of small scale and artisanal mining dating back to 1884 with the establishment of the area by Africans in search of gold following emancipation. Puruni was mainly the hub for the only large-scale operations of Peter's Mine, a hard rock mine, which was discovered in 1904 and worked until 1916, with no gold mining activities outside of this area. Small-scale and artisanal mining in Puruni began during the late 1990s – early 2000s.

Mean monthly temperature at Mahdia and Puruni vary little over the year and range between 24^{o}C and 29.6^{o}C. Mean annual rainfall is ~2900 mm and 2200 mm respectively (WorldClim), with two pronounced rainy seasons (April to July and November to January) and two dryer seasons (August to October and February to March).

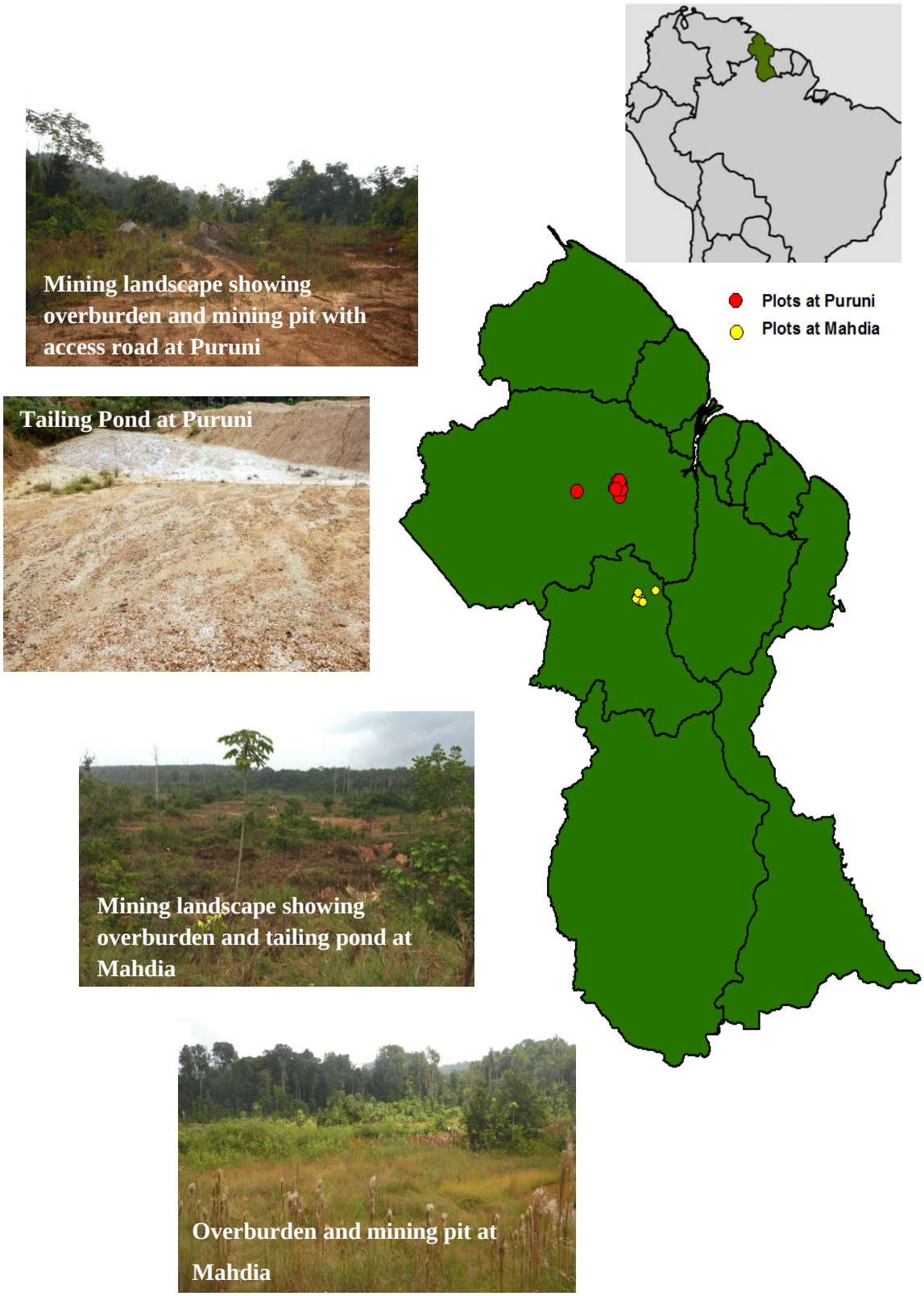

Figure 1.10 Field sites in Guyana, with image examples of plots at Puruni and Mahdia.

The alluvial soils are lateritic loam to sandy clay. Both sites are found at ~320 m elevation, along sedimentary rocks of the Guiana Shield (Hammond et al. 2007). For this reason, the sites contain large deposits of gold which may be more readily accessible to small and artisanal miners.

Each plot was positioned so as to include three important zones of an artisanal gold mining site, namely the mining pit, the mine tailings (deposits of material left over after the gold has been separated from the ore) and the overburden (areas overlying the ore which are displaced during the mining process) (Figure 1.11). More information on the plot installation and the additional data collected is provided in Chapters 4-5.

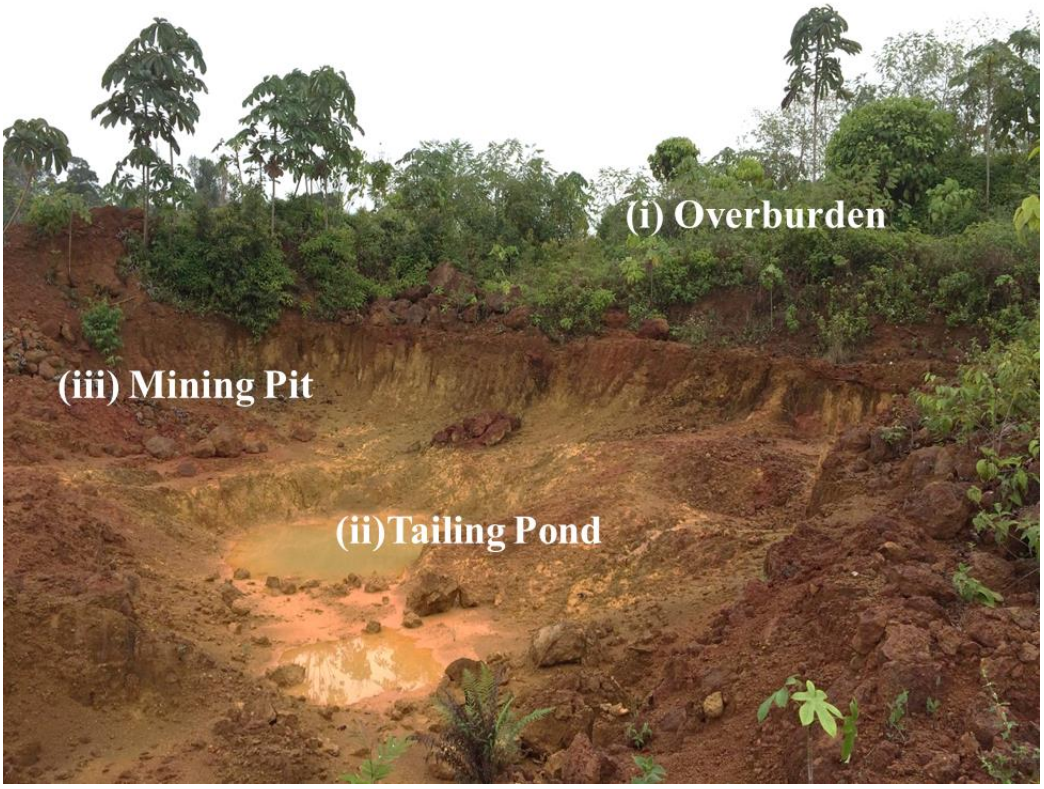

Figure 1.11 Zones of a small-scale mining process.

These are (i) Overburden: areas overlying the ore which are displaced during the mining process, (ii) Tailing Pond: deposits of material left over after the gold has been separated from the ore, and the (iii) Mining pit. Image © M. Kalamandeen (2016).

1.8 Important knowledge gaps

Despite their local and global significance, there are still many knowledge gaps concerning the dynamics and impacts of forest loss on Amazonian rainforests. Available resources are often lacking to collect real-time data on forest loss as it occurs. Until recently, a trade-off between spatial and temporal resolution existed, with higher-resolution sensors covering less area per day (Finer et al. 2018). As such, the availability of data on forest cover change is often dated when published, have limited time series, inconsistent definition of forest over time, questionable data reliability and may only have anecdotal knowledge for some Amazonian countries, with little information on non-Brazilian Amazonian countries. For instance, FAO reports such as its Global Forest Resource Assessments (FRAs) are dependent on government information, emphasizing the inconsistencies in methods and definitions of forests over time (Grainger 2008, Hansen et al. 2013). These reports also only capture net values for forest area changes, for example, forest loss in Guyana was estimated as zero from 1990-2000 (FAO 2006).

Despite the incredible wealth of information available within new global datasets such as the University of Maryland's Global Forest Change (GFC) (Hansen et al. 2013) and Terra-i (Coca-castro et al. 2013) products, a comprehensive pan-Amazonian analysis that considers multiple aspects of deforestation, not restricted simply to national trends, over time has not been achieved to-date. For example, deforestation characteristics such as deforested patches, an indication of the success of land and conservation policies (Rosa et al. 2012), have only been studied in the Brazilian Amazon for deforested patches >6.25 ha. Such information may also aid prioritizing the most important forest loss areas based on pattern (size and density), shape (linear) and location (overlap with areas of interest) (Finer et al. 2018) which can indicate (1) direct drivers such as agriculture or gold mining, (2) indirect drivers such as market forces that often determines appropriate policy action, and (3) future monitoring and conservation action based on a landscape assessment of hotspots. Little is also known about how effective protected areas are in stemming forest loss across Amazonia through a consistent time period. Understanding the current dynamics of forest

loss ultimately ensures that the goal of reducing deforestation can lead to actual policy or conservation action. Using the above datasets, I explore the temporal and spatial extent and distribution of forest loss features such as deforested patches, forest loss density and hotspots from 2001 to 2014 bringing clarity to important shifts in land use change across Amazonia and in protected areas (Chapter 2).

Further, the deforestation dynamics identified in Chapter 2 may be used to further assess how intensive land uses such as gold mining influence forest loss across the Amazon. Gold mining and its impact on Amazonian deforestation is a fairly recent and pervasive phenomenon but is often overlooked in deforestation analysis due to its relatively small extent (Alvarez-Berrios and Mitchell Aide 2015). Although gold mining is usually temporary, the impacts are profound and persistent (Sonter et al. 2017), with recent studies indicating the influence of mining activities on land use cover are through the territorial expansion of pasture and agribusinesses (Sonter et al. 2014). As northern Amazon (Venezuela, Guyana, Suriname and French Guiana) encompasses ~1 million km^2 of continuous, intact tropical forest (Hammond et al. 2007), it may increasingly represent a greater share of the remaining closed forest cover of Amazonia, with multi-scale impacts across South America if ~28% of the current area is deforested (Bovolo et al. 2018). The absence of forest loss information from gold mining is mainly due to (1) a lack of accurate mapping of mining areas due to the nature of the mining process which produces different types of land cover (e.g. barren soil, mining pits, water-bodies, degraded and recovering areas); and (2) a significant amount of small-scale mining occurs in relatively small areas (<10 000m^2) which are only detectably by high resolution images (≤30m) (Lobo et al. 2018). Numerous authors have tried to assess how gold mining influences deforestation in individual countries, for example, in Peru (Swenson et al. 2011, Asner et al. 2013), using relatively coarse remote sensing datasets such as MODIS (250m resolution) or inaccessible products such as CLASlite. However, evaluating the extent and pattern of gold mining influence on deforestation at a landscape level remains relatively unknown, particularly in areas with high cloud cover such as northern Amazonia. Further, little information exists on how gold mining impacts protected and conservation areas. In order to investigate gold mining-induced forest loss across the region, I explore the temporal and spatial extent and

distribution of forest loss in gold mining areas across northern Amazonia from 2001 to 2016 to bring clarity to important shifts in land use change across region (Chapter 3). I also examined whether high-resolution satellite images such as GFC (30m resolution) are able to adequately detect small-scale gold mining through comparison with 5m resolution RapidEye satellite imagery.

Additionally, little is known about the recovery process of forests from previously abandoned gold mining activities. In fact, only one previous study has attempted to evaluate the influence of gold mining on recovery of vegetation but used only visual assessment with no data from recensusing (Peterson and Heemskerk 2001). This is imperative as gold mining sites are often very dynamic with re-mining occurring several times on the same site, with little resting time in between mining activities. Compared to other land uses, gold mining is much more intensive due to the damage imposed. Therefore, it is unclear what may be influencing or limiting the ability of forests to recover within such sites. As such, with the collection of new data on plots established in previously mined regions, Chapters 4 and 5 will assess the impact of gold mining on soil and vegetation nutrients, and forest recovery dynamics at abandoned gold mining sites.

1.9 Research aims and objectives

1.9.1 Thesis aim

The aims of this thesis is to better understand how deforestation dynamics have evolved over the current Amazonian landscape and examine the extent, patterns and timing of ecological recovery from the recent increase in small-scale gold mining activities.

1.9.2 Thesis objectives

Objective 1: Evaluate the spatial and temporal changes in forest loss across Amazonia

1.1 Identify the hotspots (clusters of high rates of deforestation) of forest loss in the Amazon

1.2 Assess the different sizes of forest loss clearings

1.3 Identify forest loss events of different geographical density and determine how this has changed over time.

Objective 2: Evaluate the extent of forest loss from small-scale gold mining activities

2.1 Determine the extent of forest loss from gold mining activities across northern Amazonia

2.2 Quantify the accuracy of the 30m-resolution global forest cover product in detecting gold mining related forest loss events by assessing it with the 5m resolution RapidEye satellite imagery at two known gold mining sites

Objective 3: Evaluate the impact of small-scale gold mining activities on soil and plant nutrients

3.1 Assess the level of mercury concentrations in soil and vegetation at abandoned gold mining sites

3.2 Examine the available exchangeable cations for nutrient cycling

3.3 Quantify the levels of nitrogen and phosphorus in soils and vegetation across different mining zones

Objective 4: Investigate patterns of biomass recovery from gold mining

4.1 Determine the vegetation composition and biomass accumulation trajectories along abandoned gold mining sites

4.2 Investigate how observed biomass recovery patterns from gold mining sites compare with secondary forests recovering from other land uses (e.g. pasture, agriculture)

4.3 Assess which factors limit biomass recovery in previously mined gold mining sites

2

Pervasive Rise of Small-scale Deforestation in Amazonia

2.1 Abstract

Understanding forest loss patterns in Amazonia, the Earth's largest rainforest region, is critical for effective forest conservation and management. Following the most detailed analysis to date, spanning the entire Amazon and extending over a 14-year period (2001-2014), this chapter reveals significant shifts in deforestation dynamics of Amazonian forests. Firstly, hotspots of Amazonian forest loss are moving away from the southern Brazilian Amazon to Peru and Bolivia. Secondly, while the number of new large forest clearings (>50 ha) has declined significantly over time (46%), the number of new small clearings (<1 ha) increased by 34% between 2001-2007 and 2008-2014. Thirdly, small-scale low-density forest loss expanded markedly in geographical extent during 2008-2014. This shift presents an important and alarming new challenge for forest conservation, despite reductions in overall deforestation rates.

2.2 Introduction

Amazon rainforest deforestation has been a major issue on the environmental agenda, driven by concerns about deteriorating ecosystem services, biodiversity loss and increasing carbon emissions (Davidson et al. 2012, Aragão et al. 2014, Finer et al. 2015). For example, loss of forest cover has been shown to result in sharp reductions in species richness in southern Amazonia (Ochoa-Quintero et al. 2015). Furthermore, as the Amazon Basin accounts for ~ 5.4 million km^2 of contiguous tropical forests (Pokhrel et al. 2014) and 150 – 200 Pg of carbon (Feldpausch et al. 2012), changes in land use in Amazonia are expected to have significant regional and global climatic consequences (Coe et al. 2013, Lima et al. 2014), with potential impacts on climate and agriculture in other parts of South America and, via teleconnections, in other continents (Lawrence and Vandecar 2014).

Despite its significance, comprehensive assessments of the dynamics of forest loss across the entire Amazon region are rare. In fact, the majority of regional-level studies to date have focused only on the Brazilian Amazon (Nepstad et al. 2009, Rosa et al. 2012, 2013, Aragão et al. 2014, Nogueira et al. 2015). In part, this is due to the highly successful PRODES (Monitoramento do Desmatamento na Amazônia Legal por Satélite) programme, operated by the Brazilian Institute for Space Research (INPE), which provides annual estimates of deforestation for the entire Brazilian Amazon since 1988 based on 30m-resolution Landsat satellite images (INPE 2015). The PRODES data have been used to highlight the marked decline in deforestation in the Brazilian Amazon over the last decade, where deforestation was reported to have fallen from a record 27,772 km^2 in 2004 to 4,571 km^2 in 2012 (INPE 2015). In this regard, PRODES enabled government actions through the Plano de Prevenção e Controle do Desmatamento na Amazônia (PPCDAm) programme that led to a revolutionary impact on reducing deforestation in the Brazilian Amazon (Brasil - Ministério do Meio Ambiente (MMA) 2013). This steered renewed optimism about Brazil's capacity to contain Amazonian deforestation, with some authors predicting an end to deforestation of the Brazilian Amazon by 2020 (Nepstad et al. 2009).

PRODES-based studies, however, do not provide a complete picture of deforestation dynamics within the Basin for several reasons: 1) they do not consider deforestation events <6.25 ha; thus, smaller disturbances such as those associated with subsistence agriculture and artisanal or small-scale mining (typically < 5 ha) are not represented by PRODES unless accumulated over several years to >6.25ha (Lobo et al. 2016), 2) they only consider primary forests and do not account for secondary or regenerating forests and 3) they are restricted to Brazil (Hansen et al. 2008).

Furthermore, trends in Brazil may not reflect those occurring in other Amazonian countries or regions. In Bolivia, for example, forest loss has accelerated from ~400 km^2 y^{-1} in the 1960s to 2900 km^2 y^{-1} by 2004 (Killeen et al. 2007); while deforestation in the Colombian Amazon has also been reported to have increased over the last decade (Government of Colombia 2011, Armenteras et al. 2013). Other studies have highlighted sub-national, regional increases in deforestation. For example, significant increases in deforestation have been documented in the Madre de Dios region of Peru associated with a rapid surge in small-scale gold mining (Asner et al. 2013). Further, with increasing awareness of forest loss throughout the region, an exponential growth in protected areas was seen over the past decade as a means of protecting intact forest landscapes (Heino et al. 2015, Spracklen et al. 2015). Yet the effectiveness of protected area to curb forest loss using a uniform dataset that allowed for consistent forest extent comparisons over space and time has not been assessed.

Recent advances in data availability and processing power have enabled the emergence of high-resolution regional and global forest cover change datasets spanning over ten years of data, such as the University of Maryland's Global Forest Change (GFC) product (Hansen et al. 2013), based on hundreds of thousands of 30m-resolution Landsat satellite scenes, and the 250-m resolution Terra-i data (Coca-Castro et al. 2013) derived from USGS/NASA MODIS data, as described by Reymondin et al. (2012), allowing for in-depth assessment of forest loss extent and temporal dynamics. Thus, this chapter specifically addresses the following questions: 1) How has the spatial patterns of forest loss across Amazonia changed over a 14-year period (2001-2014)? 2) What are the temporal and spatial shifts of forest loss hotspots (clusters of high rates of deforestation) across Brazilian versus non-Brazilian Amazon? 3) Has the size of forest loss

patches and geographical density of forest loss events evolved across Amazonia within this timeline? 4) Are protected areas effective in reducing forest loss across Amazonia? For spatio-temporal analysis using the Terra-i product, see Appendix 2.15. These analyses provide critical insights into shifts in potential drivers of deforestation (Rosa et al. 2012) and establish a barometer for evaluating the effectiveness of conservation strategies such as protected areas.

2.3 Methods

2.3.1 Deforestation datasets and overarching temporal patterns

The Amazonian area of interest was defined following the boundaries proposed by Eva et al. (2005). This includes sections of nine countries: French Guiana, Suriname, Guyana, Venezuela, Colombia, Ecuador, Peru, Bolivia and Brazil. Deforestation data for the area of interest was obtained from the 30-m resolution Global Forest Change (GFC) data of Hansen et al. (2013), based on Landsat imagery. The Hansen et al. (2013) data was downloaded from http://earthenginepartners.appspot.com/science-2013-global-forest (Version 1.2). All results shown are for GFC Version 1.2, as this allowed analysis of the longest time series available. However, I also compared the results with GFC Version 1.0 data over the period for which there is data for both products (2001-2012). This was done to explore the potential effects of reprocessing changes in v. 1.2, where the reprocessing algorithm was changed for the 2011-2014 period. In v 1.0, consistent processing was used throughout the entire time series (2001-2012). I applied no further processing to the Hansen et al. (2013) dataset. The analysis indicated that overall patterns were very similar for both versions of the GFC data, over the period where both versions were available (Appendix 2.9 and 2.10). The study region spanned thirteen GFC (Landsat) tiles which were clipped to match the boundaries of my area of interest. I restricted my analysis to the Tropical and Subtropical Moist Broadleaf Forest (herein called the TMBF) biome using the definition and extent from Nature Conservancy (http://maps.tnc.org/gis_data.html). The TMBF is defined as large, discontinuous patches centred on the equatorial belt, between the Tropics of Cancer and Capricorn, and characterized by low variability in annual temperature and high

levels of rainfall (>200 centimetre annually). These forests are dominated by semi-evergreen and evergreen deciduous tree species.

Forest was defined as those pixels in GFC with >30% tree cover as per Kim et al. (2015). The total area deforested in the Amazonian region of each country was calculated annually for the GFC dataset (2001-2014). In the GFC dataset, deforestation was defined as a stand-replacement disturbance or the complete removal of tree cover canopy at the Landsat pixel scale (Hansen et al. 2013); with the exclusion of pixels after a deforestation event annually. Forest gain areas were therefore not considered in this analysis so as to eliminate secondary regrowth as non-forests such as plantations. As mentioned in Chapter 1.5, forests within the GFC dataset are defined by their physical attributes (i.e. tree or other vegetation exceeding a height of 5m, and >30% canopy cover prior to loss), rather than by their function or the land use. Therefore, this dataset included losses of primary and secondary forest, commercial forestry and plantations. Hansen et al. (2013) was able to assess tree cover through pre-processing 654 000 Landsat scenes for the growing season, correcting and normalising them, irrespective of calibration or atmospheric conditions, and developing an automated process to remove all cloud and cloud shadow. A set of variables was then applied to extracted all valid observations for each pixel, including features related to average greenness, and trends in that greenness through time. Using an extensive network of training data gleaned mostly from manual interpretation of hyperspatial (very high resolution, ≤5 m pixels) data, automated decision trees were set up to enable predictions of the percentage tree cover (in the year 2000), forest loss, and forest gain per pixel (see Hansen et al. 2013 for more details). The forest loss layer returned either 'no change', or a single year from 2001-2013 where loss occurred. Loss can occur only once using this algorithm, so such a pixel could never again be flagged as deforested.

The PRODES shapefile was derived from http://maps.csr.ufmg.br/, and indicates annual deforestation rates in the Brazilian Amazon since 1997. To compare PRODES data with the GFC product, yearly masks were created using the PRODES primary forest and associated yearly forest loss pixels to subset annual GFC data. This allowed the removal of all non-primary forests and non-forest regions from the analysis. Maps in figures 2.1, 2.3, 2.4, and Appendix 2.1,

2.5, 2.9 and 2.11 were generated using ArcGIS 10.4.1 software by Esri (Environmental Systems Resource Institute, www.esri.com).

For all analyses described below I divided the dataset into two periods of equivalent length: 1) 2001 – 2007 and 2) 2008 – 2014 to allow for statistical analysis of non-normally distributed and non-trend data. I statistically evaluated the differences in means of relevant metrics for both periods using the non-parametric Wilcoxon's signed rank test as the data was not normally distributed.

2.3.2 Analysis of size dynamics of deforested patches

Deforested patches were defined as contiguous areas of forest that were cleared within a year. Deforested patches were classified into eight categories, namely ≤1 ha, 1- 6.25 ha, 6.25 - 50 ha, 50 - 100 ha, 100 - 200 ha, 200 - 500 ha, 500 - 1000 ha and >1000 ha. This is the same size class breakdown used by Rosa et al. (2012), with the exceptions that I also consider deforestation patches ≤ 1 ha and 1-6.25 ha, which are below the annual deforestation threshold detected by the PRODES data analysed in this study.

2.3.3 Analysis of spatial patterns of deforestation

The GFC data were also used to investigate spatial patterns of deforestation density (number of deforested pixels per area), including their temporal dynamics using ArcGIS 10.4.1. To visualise deforestation density, I created a 10 x 10 km grid over the study area, within which total deforested area were classified within each gridcell into five categories following a log scale: 1) Negligible (<0.01 km^2 per 100 km^2 land area), 2) Light (0.0101– 0.1 km^2 per 100 km^2 land area), 3) Moderate (0.1001-1 km^2 per 100 km^2 land area), 4) Heavy (1.0001-10 km^2 per 100 km^2 land area) and 5) Very Heavy (> 10.0001km^2 per 100 km^2 land area). Annual data were grouped into two periods for analysis: 2001-2007 and 2008-2014. I conducted additional sensitivity analyses to explore the implications of the assumed lower boundaries for 'light' deforestation on the results. To do this, I performed additional calculations where the lower boundary was doubled (set to 0.02 km^2 per 100 km^2) or trebled (set to 0.03 km^2 per 100 km^2).

To evaluate whether similar patterns were observed inside and outside of protected areas, I applied a protected area mask using shapefiles provided by The

World Database on Protected Areas (WDPA), which include protected areas from all IUCN categories as well as indigenous protected areas, biological and biosphere reserves, cultural sites, sustainable reserves and hunting preserves (www.protectedplanet.net). I also utilized river and roads shapefiles from HydroSHEDS (http://www.hydrosheds.org/) and gROADS database (http://sedac.ciesin.columbia.edu/data/set/groads-global-roads-open-access-v1) respectively to assess accessibility across Amazonia. Separate Wilcoxon signed rank tests were conducted for areas inside and outside of protected areas to investigate changes in deforestation density between the two focal periods (2001-2007 and 2008-2014).

For each of the two study periods (2001-2007 and 2008-2014), I also statistically evaluated the spatial clustering patterns of deforestation, using the Getis-Ord Gi* statistic (Getis and Ord 1992) in ArcGIS 10.4.1. Getis-Ord Gi* is a local clustering statistic and was used to statistically determine the occurrence of deforestation hotspots (Getis and Ord 1992). Spatial statistics such as Getis-Ord Gi* can assist in quickly identifying spatiotemporal trends of forest loss without the explicitly need for pre-existing information on what underlying factors are driving these trend as well as measure the degree of correlation of weighted features within a specified distance threshold (Harris et al. 2017). Based on prediction accuracy index (PAI), Gi* gave the best results in predicting the spatial extension of hotspots and the best mapping technique for capturing local clusters with statistically significant hotpots (Chainey 2010). This metric has been utilized previously for hotspot analysis mainly in the health and urban sectors (Bereitschaft and Debbage 2014, López-Carr et al. 2014). The statistic is

$$G_i^*(d) = \frac{\sum_{j=1}^{n} w_{ij}(d) \times x_j}{\sum_{j=1}^{n} x_j}$$

where x_j is the number of spatially mapped deforested 30-m pixels within a 10 x 10 km gridcell j and $w_{ij}(d)$ is a weights matrix with values equal to 1 for gridcells located within a distance d from gridcell j and zero otherwise, and n is the total number of mapped deforestation rates (at locations j=1,...n). These analyses were conducted using the spatial statistics tools in ArcGIS 10.4, using a fixed distance d of 100 km, where features within this distance are its neighbours while features further away are not. The distance band

of 100km was selected after running multiple Moran's I statistics for a peak in z-scores. Hotspots (clustered deforestation patches) have comparably large positive Gi* values while absence of clustering is indicated by Gi* values close to zero. To detect hotspots Z-scores (standard deviations of all Gi* values) and corresponding p-values for Gi* were calculated for each gridcell to determine whether forest loss in a given gridcell is statistically clustered relative to neighbouring gridcells compared to all gridcells in the study region (Getis and Ord 1992). Significant positive Z-scores denote local clustering of high deforestation counts indicating a significant hotspot.

2.4 Results

2.4.1 Spatio-temporal evolution of forest loss hotspots

My analysis reveals important shifts in statistically significant forest loss hotspots (areas with concentrated forest loss activity) across Amazonia using a local clustering statistic, the Getis-Ord Gi* metric (see Methods). Over the first half of the study period (2001-2007), spatial hotspots of deforestation were concentrated along the widely known 'arc of deforestation' extending across the southern rim of the Brazilian Amazon from Pará to Rondônia, with an especially large hotspot in Mato Grosso (Figure 2.1). The only hotspot of note outside of Brazil during the 2001-2007 period was a relatively small region in western Santa Cruz state and bordering Beni state in Bolivia.

The distribution of deforestation hotspots during the 2008-2014 period differs from that of the 2001-2007 period due to three major notable features: 1) the weakening of the Brazilian 'arc of deforestation' as a deforestation hotspot, 2) the southward expansion of the Bolivian hotspot of deforestation and 3) the emergence of a new deforestation hotspot in Amazonian Peru. The apparent disappearance of the traditional 'arc of deforestation' is driven by a marked decline in the importance of Mato Grosso, and to a lesser extent Pará, as a forest loss hotspot. The Bolivian hotspot expanded rapidly from covering an area of ~300 km^2 in 2001-2007 to an area of ~9560 km^2 in 2008-2014, thus representing the largest deforestation hotspot (at 99% confidence levels) over the Amazon during that period (Figure 2.1, Appendix 2.1). The Peruvian forest loss hotspot is

much smaller in area (2066 km^2) than the Bolivian hotspot and only emerged during the second half of the study period. Accompanying the Peruvian hotspot is the emergence of a smaller, statistically weaker hotspot in western Colombia, also not evident during the first half of the study period.

2.4.2 Temporal patterns of forest loss patch size

I also found that mean forest loss patch size declined across Amazonia over the study period (2001-2014). Between 2001 and 2014, the mean forest loss patch size across the study region was 10.25 ha but varied considerably across countries, ranging from 0.5 ha in Ecuador to 15.6 ha in Brazil, (Appendix 2.2). Bolivia was the only country besides Brazil where mean forest loss patch size was >1 ha. I found a majority (96.4%) of deforested patches were below the 6.25 ha threshold considered by PRODES, with a large number of these (81.1%) below 1 ha. In area terms, patches below 6.25 ha accounted for ~39% and ~34% of total Amazonian and Brazilian Amazon forest loss across our study period respectively.

Mean patch size trajectories across time in Brazil and Bolivia were similar, increasing from 2001 up to 2004 and declining thereafter (Appendix 2.2). In both countries, mean patch size was significantly greater in 2001-2007 than in 2008-2014 (W=49, p=0.0005). Significant declines in mean size of forest loss patches between 2001-2007 and 2008-2014 were also found for Venezuela (W=41, p=0.038), French Guiana (W=45, p=0.006) and Guyana (W=43, p=0.017), but the total deforested area in these countries was much lower than in Brazil and Bolivia.

The declining mean patch size of forest loss across Amazonia reflects both a decline in the number of larger forest loss patches and an increase in the number of smaller patches (Figure 2.2). The number of very large (>500 ha) deforested patches declined significantly over time (W=49, p>0.001) by 67% between 2001-2007 and 2008-2014 (Table 2.1). This is driven by a 72% decline in very large forest loss patches in Brazil, the country with by far the greatest total number of forest loss patches, between the two time periods. Similarly, the number of very large forest loss patches in Bolivia also declined by 25% between both of my study periods.

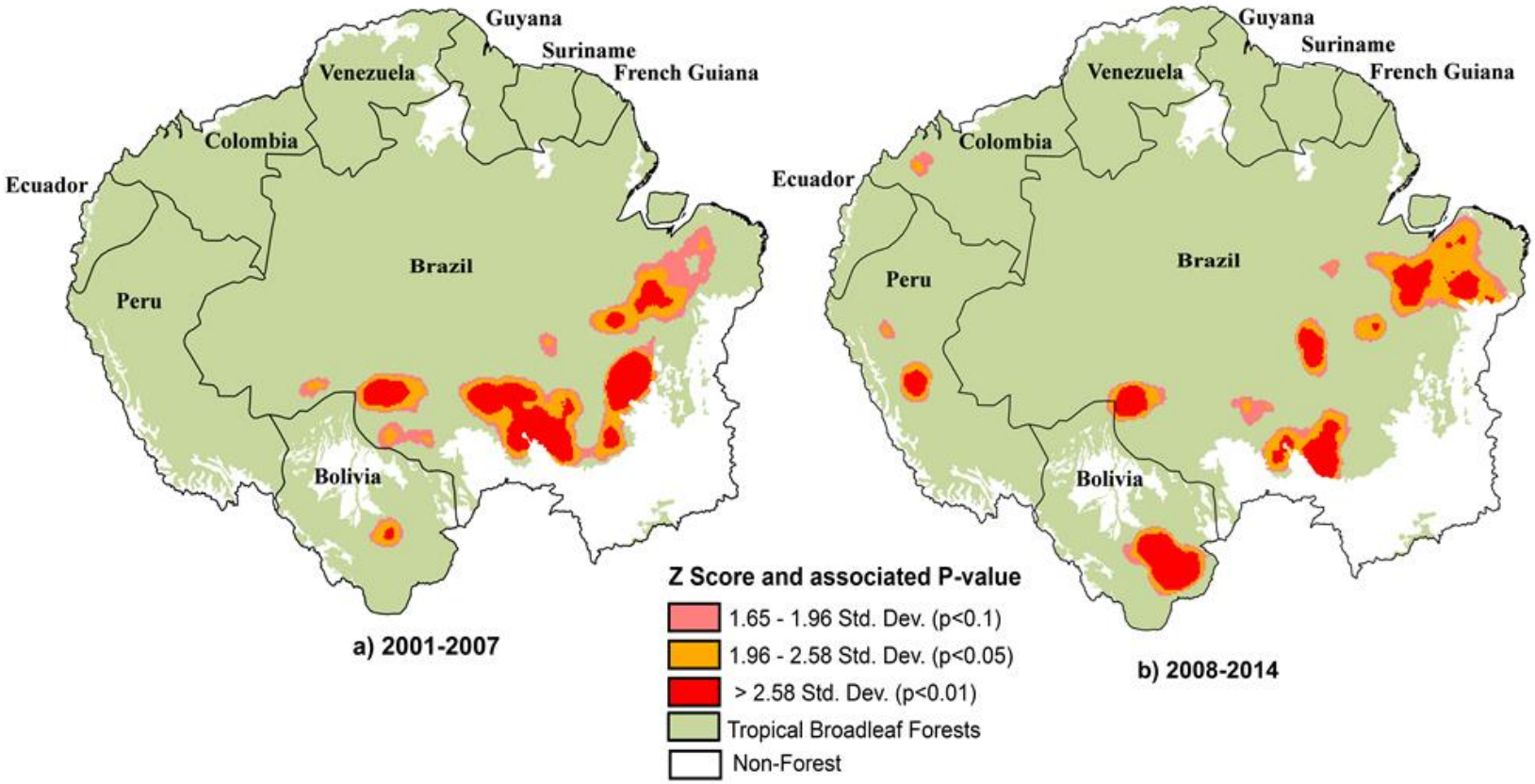

Figure 2.1 Hotspots of Amazonian forest loss.

Maps based on Getis Ord Gi* z-scores for GFC data for two time periods: 2001-2007 and 2008-2014 using ArcGIS 10.4.1 (www.esri.com). Higher values indicate increased clustering of deforestation patches.

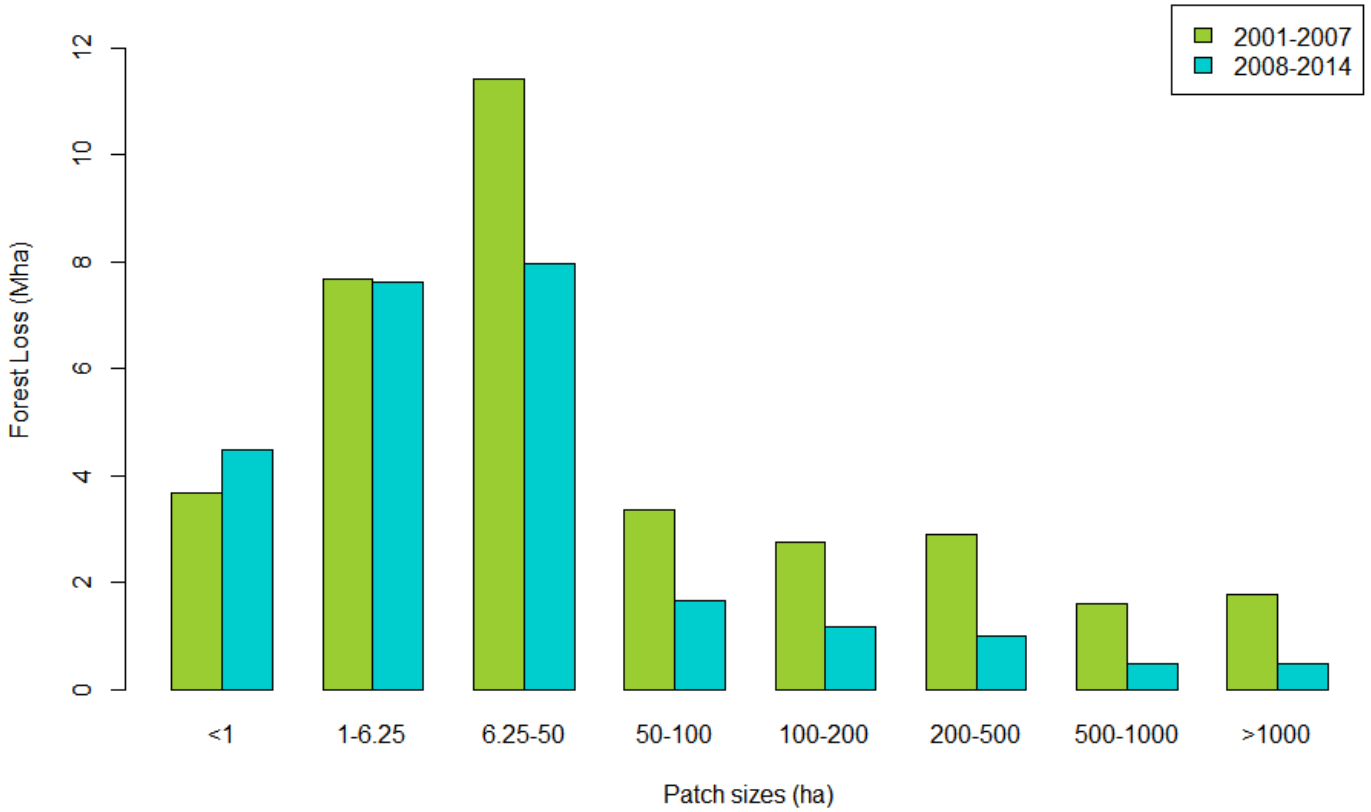

Figure 2.2 Change in deforested area (ha) of different size categories between 2001-2007 and 2008-2014 across Amazonia using the GFC dataset.

Table 2.1 Changes in the number of patches between 2001-2007 and 2008-2014 using the Hansen et al. GFC product. The significance of the difference between the two time periods (2001-2007 and 2008-2014) were estimated using the Wilcoxon signed rank test.

Patch Size	Mean number of forest loss patches		% Difference between time periods	Statistical Significance
	2001-2007	2008-2014		
<1ha	2069303	2709837	30.95	W = 13, p = 0.16
1 - 6.25 ha	445736	457348	2.61	W = 23, p = 0.9
6.25 – 50 ha	110007	82481	-25.02	W = 44, p = 0.01
50 – 100 ha	6965	3487	-49.93	W = 49 , p <0.001
100 – 200 ha	2870	1230	-57.12	W = 49, p <0.001
200 – 500 ha	1388	482	-65.31	W = 49, p <0.001
500 – 1000 ha	336	102	-69.71	W = 47, p = 0.002
>1000 ha	146	39	-73.24	W = 46, p = 0.004

There were also significant declines in forest loss patches of large and intermediate size (50-500 ha) by 27% (W=44, p=0.01), while the number of small forest loss patches (<6.25 ha) increased by ~34% (W=13, p=0.16) between the two study periods (Table 2.1). The overall pattern of increasing number of small forest loss patches was seen across all Amazonian countries (Appendix 2.3), although the multi-annual patterns of change varied according to country.

In Brazil and Bolivia, the number of small forest loss patches increased gradually throughout the study period (see Figure 2.5) while in northern Amazonian countries (French Guiana, Guyana, Suriname, Venezuela) and in western Amazonian countries (Colombia, Ecuador, Peru) there were pronounced increases in small forest loss events in 2012, with forest loss rates rebounding back to close to previous levels in 2013. For example, the number of forest loss patches <1 ha increased by 354% in French Guiana and 318% in Suriname between 2011 and 2012.

2.4.3 Geographical spread of deforestation events

Considerable changes were also observed in the geographical patterns of deforestation density between the two study periods (Figure 2.3, Appendix 2.4, 2.5). Whereas in 2001-2007, 45% of the 10 x 10 km gridcells in the study region were categorised as having negligible forest loss (<0.01 km^2 per 100 km^2), this declined to 35% in 2008-2014, despite overall Basin-scale declines in deforestation. On the other hand, the proportion of gridcells experiencing 'very heavy' deforestation (>10 km^2 per 100 km^2) declined by 66.7%, from 9% in 2001-2007 to 4.5% in 2008-2014. Conversely, an increase in the number of gridcells experiencing 'light' (0.01 – 0.1 km^2 per 100 km^2) and 'moderate' deforestation (0.1 – 1 km^2 per 100 km^2) was observed, increasing from 19% and 17.5% of gridcells in 2001-2007 to 23% and 18% in 2008-2014 respectively. The number of gridcells classified as having 'heavy' (1-10 km^2 per 100 km^2) deforestation increased from 17% to 20% of gridcells between the two time periods.

I tested whether patterns observed in protected areas differed from patterns observed outside of protected areas but found that temporal patterns were similar (Figure 2.4). Inside protected areas across the Amazon, the number of gridcells with negligible forest loss fell by 10% between 2001-2007 and 2008-2014 (W=13, p=0.2) while 'light' and 'moderate' deforestation increased by 18.4% (W=4,

p=0.3) and 30% (W=0, *p*=0.02) respectively. Conversely, 'very heavy' deforestation declined by 54% in protected areas between our two study periods (W=12, *p*=0.3), in line with patterns outside of protected areas.

Overall, these results suggest a progressive encroachment of low-density, small-scale deforestation into areas of Amazonia such as Amazonas, Roraima and Amapá (Figure 2.3, Appendix 2.5), which historically have had negligible deforestation, as well as the northern Amazonian countries of French Guiana, Guyana and Suriname.

2.4.4 Large-scale deforestation temporal patterns

Overall, Amazonian forest loss based on GFC declined between the two study periods (Appendix 2.6), from 238 km^2 yr^{-1} in 2001-2007 to 177 km^2 yr^{-1} in 2008-2014 (W=43, *p*=0.017). This is driven by statistically significant reductions in forest loss in Brazilian Amazonia which was 49.5% lower in 2008-2014 than 2001-2007 (W=48, *p*=0.001) but is offset somewhat by increasing forest loss in the non-Brazilian Amazon, which was 35% higher in 2008-2014 than 2001-2007 (W=1, *p*=0.001).

During the first half of the study period (2001-2007), I found that forest loss outside of Brazil accounted for 9.7% of total Amazonian forest loss, rising to 13.8% during the second half of the study period (2008-2014). The largest increases in forest loss occurred in Peru (106.73 km^2 yr^{-1}) and Bolivia (66.68 km^2 yr^{-1}), which together accounted for 72.3% of the increasing deforestation trend in the non-Brazilian Amazon (Appendix 2.7). Although I observed significant differences between the focal study periods, there is also evidence of a stabilisation of total forest loss rates during the second study period (2008-2014, Appendix 2.6), i.e. there is no clear trend between 2008-2014 in deforestation rates.

I also compared GFC-based deforestation estimates for Brazil with estimates from PRODES. For direct comparison with PRODES, I used the annual primary forest mask provided by PRODES to re-calculate forest loss with the GFC product. This removes any inconsistency between products due to potential deforestation of non-forest areas and secondary forests, while still preserving differences due to different size thresholds considered. Comparison of the GFC

forest loss temporal patterns for the Brazilian Amazon with deforestation data from PRODES revealed intriguing temporal differences between products. During the first three years of the study period (2001-2003), forest loss/deforestation estimates from GFC were on average ~34% lower than those of PRODES.

Over time, however, GFC forest loss estimates become progressively greater than PRODES deforestation estimates, so that over the last three years of the study period (2012-2014), GFC estimates of forest loss are ~72% greater than deforestation rates from PRODES (Appendix 2.8), with maximum divergence observed in 2012 (the year in which the new Brazilian Forestry Code was enacted), when GFC forest loss estimates were greater than PRODES deforestation rates by a factor of 2.52.

I found that this divergence can be at least partially explained by the increase in small-scale forest loss that are not incorporated within PRODES estimates. The fraction of total deforestation accounted for by patches <6.25 ha within the PRODES mask area increased from ~23% in 2004 to ~53% in 2013 (Appendix 2.9).

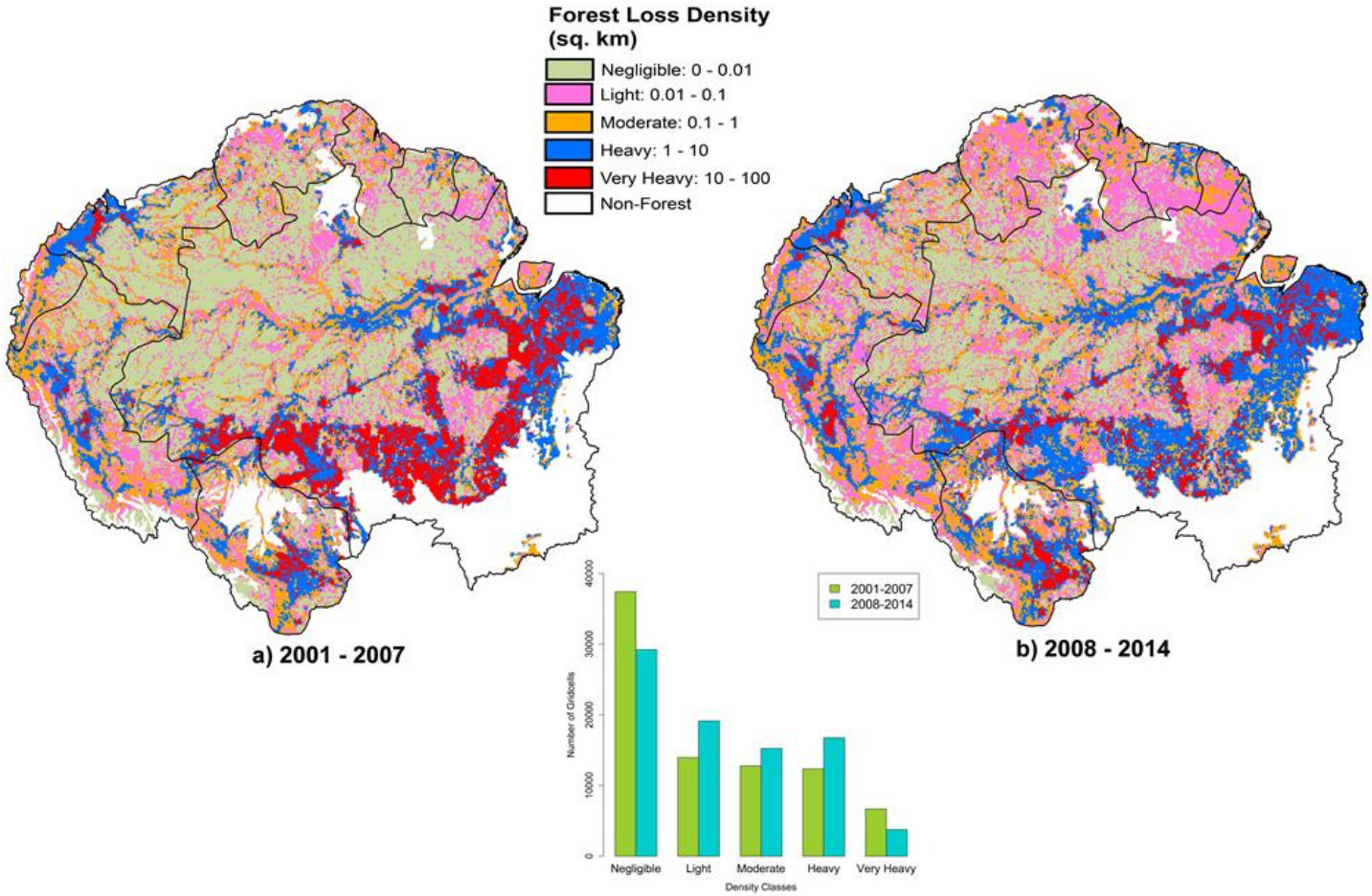

Figure 2.3 Forest loss density (km^2 forest loss per 100 km^2 land area) in Amazonia.

Map generated using the GFC product for two time periods: a) 2001-2007 and b) 2008-2014 in ArcGIS 10.4.1 (www.esri.com). Histogram indicates the number of gridcells for each density class.

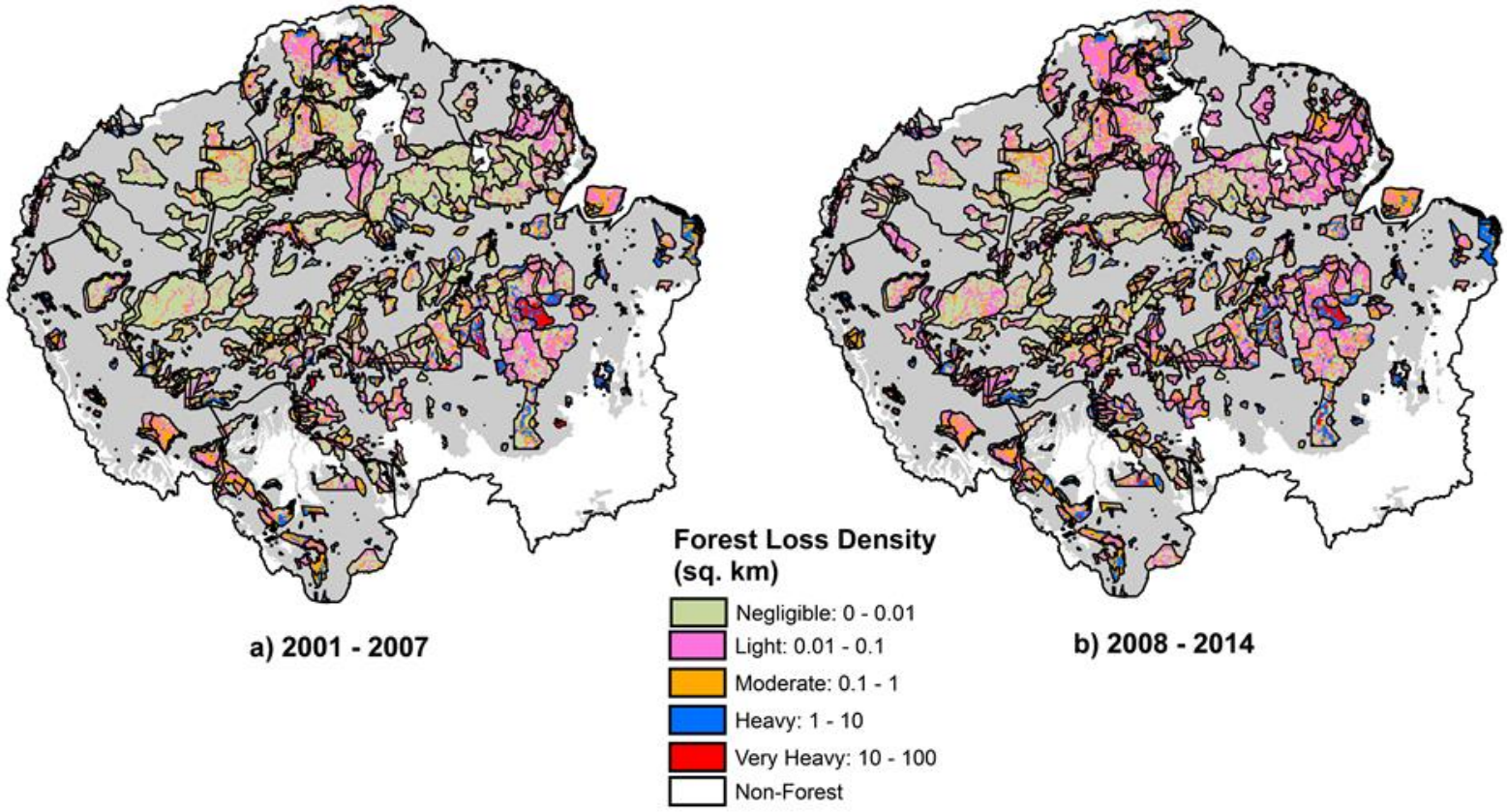

Figure 2.4 Forest loss density (km^2 forest loss per 100 km^2 land area) in Protected Areas across Amazonia. Map generated using the GFC product for two time periods: 2001-2007 and 2008-2014 using ArcGIS 10.4.1 (www.esri.com). For visualisation purposes, deforestation outside of protected areas is not shown. [Source of PA shapefiles: World Database on Protected Areas (WDPA) and International Union for Conservation of Nature (IUCN)]

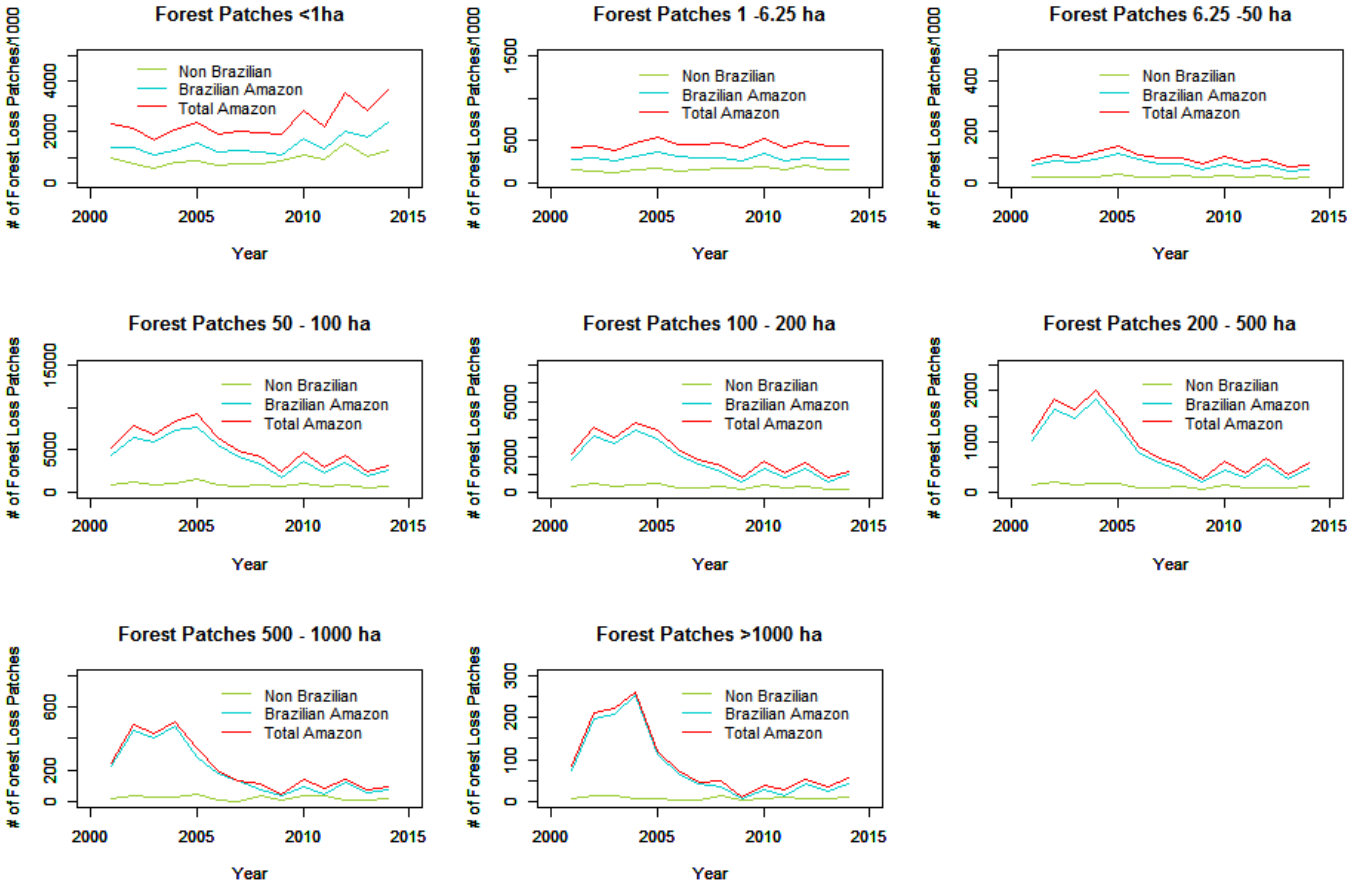

Figure 2.5 Forest loss across Brazil and Non-Brazilian Amazon based on GFC *Hansen et al* (2013) product according to patch sizes.

2.5 Discussion

2.5.1 Emerging hotspots in Bolivia and Peru

These findings paint a more complex picture of deforestation dynamics in Amazonia than has been reported thus far. While the widely-reported recent reduction in deforestation in the Brazilian Amazon is clearly observed in the analysis, I also highlight the growth of emerging deforestation hotspots in Bolivia and Peru. In 2001-2007, 99.5% of the area statistically defined as an Amazonian forest loss hotspot was found in Brazil, while in 2008-2014 this had fallen to 64%. This is associated with both the decline of deforestation in Brazil and the increasing importance of non-Brazilian deforestation hotspots. The declines in deforestation in the Brazilian Amazon are well-discussed in the literature and are likely associated with the implementation of the Plano de Prevenção e Controle do Desmatamento na Amazônia (PPCDAm) programme established in 2004 (Nepstad et al. 2014).

The new Peruvian hotspot, primarily in the Ucayali and San Martin regions of Peru, appears to be linked to the growth of palm oil agrobusiness (Chávez et al. 2014). In the Ucayali region, palm oil production commenced in 2000 and steadily increased until 2010, with San Martin expanding between 2006 and 2012. The completion of the Pacific or Interoceanic Highway from Brazil to Matarani Port in Peru in 2010, may have acted as a vector for the incursion of people and subsequent forest loss in this region.

Similarly, large agricultural expansion also contributes as a driver of the deforestation hotspot in Santa Cruz, Bolivia. This region has been the focal centre of Bolivian deforestation for over two decades (Pacheco and Mertens 2004), but the analysis shows a pattern of intensifying deforestation activity during the 2008-2014 period (Figure 2.1), so that the Santa Cruz region now represents the largest hotspot of deforestation in Amazonia. Much of this deforestation appears to be linked to the expansion of the soybean sector, and may be associated with a leakage of soybean plantations from Brazil as a result of the soybean moratorium established in Brazil in 2006 (Kaimowitz and Smith 2001, Rudorff et al. 2011, Gibbs et al. 2015).

2.5.2 Changing size distribution of deforested patches

My analysis also points to a considerable expansion of small-scale deforestation events between the two study periods (Figure 2.2) which somewhat offsets the previously reported declines in larger deforestation patches (Rosa et al. 2012) based on analysis of the PRODES data. This pattern is widespread, with increases in small-scale deforestation observed in almost all Amazonian countries (Appendix 2.2). Interestingly, the nature of these increases differs somewhat across countries. In Brazil and Bolivia, there is no obvious increasing trend up to 2008, after which there are progressive increases in small-scale deforestation. In the northern Amazonian countries (e.g. Guyana, French Guiana, Suriname), the temporal pattern is characterised by a sharp peak in 2012 (Figure 2.5). Overall, the results lend support to recent findings suggesting an increased contribution of small landholders to deforestation in Brazilian Amazonia (Godar et al. 2014) but I did not explicitly test this link between small patch size and small landholders. Examining the spatial patterns of rivers and roads across Amazonia may demonstrate how small landholders accessed forested areas and the type of driver associated with mode of access (Appendix 2.13). For instance, forest loss close to rivers may be indicative of gold mining, except where paving roads such as the Interoceanic Highway through Madre de Dios in Peru greatly increased access to forests in that region (Asner et al. 2010). Road networks have played a massive role in agriculture and palm oil expansion (Barber et al. 2014). However, the different national patterns may be indicative of different deforestation drivers across regions.

The increasingly small size of deforestation patches in Brazil may also partially reflect attempts by larger landowners to evade monitoring of deforestation activities, which has recently been strengthened through the introduction of the PPCDAm programme (Assunção et al. 2013). PRODES has a size cut-off of 6.25 ha, though deforestation events are collected at ~0.1 ha but not presented to maintain consistency with long-term data. Therefore, small-scale deforestation activities are only reported if they accumulate beyond that threshold. Additionally, PRODES may consider these small clearings as selective logging or ‘forests under use’ and not necessarily forest loss (Sato et al. 2011). Some of the forest loss events reported in Hansen et al. (2013) may also be due to the intense and increased degradation caused by forest fires and counted as deforestation

events. Due to methodological differences between PRODES and GFC, based on contextual and pixel-based classifications, respectively, degradation processes will not appear in PRODES estimates, but may inflate small deforestation estimates based on the GFC product. Therefore, causal attribution of small deforestation must be interpreted with caution. However, the same pattern was observed in Bolivia, where monitoring of deforestation and enforcement of penalties are not as effective as in Brazil (Brasil - Ministério do Meio Ambiente (MMA) 2013).

The 2012 peak in deforestation in northern Amazonia coincides with the peak of the Amazon gold boom, marking the point when gold prices reached their highest historical value ($1,660/oz) (WWF-Guianas 2012). Between 2012 and 2014, the price of gold fell by 28%; during this time, small forest loss activity in French Guiana, Guyana and Suriname declined back to baseline rates. Gold mining has recently been highlighted as an important driver of deforestation in both Peru (Asner et al. 2013) and northern Amazonia more generally (Alvarez-Berríos and Mitchell Aide 2015). My analysis supports these findings but also suggests that, in the Guianas at least, the increases in deforestation associated with gold mining were relatively short-lived.

2.5.3 Geographic spread of small-scale forest loss

Small-scale forest loss events have not only increased in number but have also increased greatly in geographical spread across Amazonia. Forest loss density (in km^2 per 100 km^2) increased by an order of magnitude or more across large areas of the Amazon typically associated with very low deforestation rates, between 2001-2007 and 2008-2014 (Figure 2.3). This phenomenon occurs across the Amazon Basin, highlighting the dispersed nature of small forest loss events. Thus, remote areas of the Amazon, largely thought to be isolated from deforestation pressures (Potapov et al. 2008), are now being impacted much more than before.

The small-scale nature of these events means that ultimately they would not be reported by monitoring systems such as PRODES which assume a much higher size threshold to be computed as deforestation. Additionally, in response to increasing awareness of rising small-scale forest loss events, the Brazilian government has plans to update its near real-time deforestation detection system

(DETER) (Diniz et al. 2015), which uses lower spatial resolution images than PRODES but with high temporal frequency, so that the threshold for deforestation has been reduced to 3 ha. Despite the DETER data being at a lower threshold, and in real-time, it is only available on a 3-monthly basis and is not included in the national deforestation statistics. This current trend of increasing small clearings would indicate that conservation efforts may now need to focus on fighting degradation and low density deforestation as large deforestation events are now relatively under control, despite an increase in these large scale events in 2015 and 2016 (Marcos Adami, personal communication). This study suggests that inclusion of small deforestation patches in national estimates is very important, given the growing divergence I found between PRODES and GFC estimates (Appendix 2.9).

In many areas, especially in the northern Amazonian countries (French Guiana, Guyana, Suriname, Venezuela), the geographical spread of small-scale deforestation events expanded greatly in 2012 (Appendix 2.3), mirroring the large increase in small deforestation events seen that year associated with the Amazonian gold boom. This suggests that the spatial footprint of deforestation tied to gold-mining activities in those countries is much greater than previously reported (Alvarez-Berríos and Mitchell Aide 2015), implying an important role of such activities in opening up remote areas of Amazonia to deforestation pressure, even if for short-lived periods.

Attribution of the specific causes of observed increases in small-scale forest loss is challenging. However, there are very strong reasons to believe that the increased small-scale forest loss events observed are linked to anthropogenic activity rather than natural disturbances. Most natural disturbance events in Amazonia occur at the sub-pixel scale. For example, Espírito-Santo et al. (2014) found that 98.6% of natural carbon losses in Amazonia are due to small-scale mortality events (<0.1 ha) with mean disturbance areas of 0.01 to 0.03 ha across different field-based and LiDAR datasets, equivalent to 1/9 to 1/3 of a Landsat pixel. This of course does not exclude the possibility that there has been an increase in larger natural disturbance events between both periods. I found no clear evidence, however, of anomalous patterns in small-scale forest loss in 2005 and 2010, the two large drought years encompassed by my study (Appendix 2.5). Further, a comparison of my forest loss density maps (Figure 2.3 and Appendix

2.5) with satellite-driven maximum climatological water deficit (MCWD), a measure of drought intensity that correlates with tree mortality (Lewis et al. 2011), indicates that the epicentres of the 2005 and 2010 drought events do not strongly correlate with the geographical location of small-scale forest loss increase seen in this study (see Appendix 2.14). This is further supported with recent findings from Yang et al. (2018) which showed drought-related tree mortality focused in southwest Brazil, with northern Amazonia remaining relatively unchanged even with one or more lag years.

Additional analysis also suggests that the observed increase in small deforestation events was not overly influenced by artefacts introduced by processing and classification problems. First, I found that my results were robust to the version of the GFC product used (Appendix 2.10 and 2.11), over the period for which I had data for both versions (2001-2012). Second, I found that the relative differences in increases in small-scale deforestation intensity between the two focal periods were robust to changes in the specific lower bounds used to delimit the 'light' deforestation category, with relative patterns between periods being maintained even after doubling and trebling of assumed deforestation cut-offs for that class (Appendix 2.12). Although Hansen et al. (2013) report a global accuracy of 99.5% for tropical regions, there are still some misclassification errors, as there are with all large-scale deforestation products. However, I can think of no major reasons beyond changes in processing, evaluated by comparing two versions of the GFC product, to expect classification accuracy to vary over time.

2.5.4 Implications for conservation efforts

These results also suggest that the protected area network in Amazonia has had limited success combating the pervasive spread of small-scale deforestation, as the relative increases in small-patch deforestation events were similar inside and outside protected areas over the two study periods. These small-scale losses in forest cover now present a new and alarming challenge for conservation efforts in Amazonia, as they are inherently more difficult to monitor and control. Protected areas are seen as a cornerstone for reducing deforestation and carbon emissions. My results suggest that the management strategies of Amazonian protected areas

may need revising to account for the increasing threat of low-density, small-scale forest losses.

In summary, this analysis of the high-resolution GFC data for Amazonia revealed three important insights. First, centres of high intensity deforestation have shifted away from the traditional arc of deforestation to Bolivia, Peru and the northeastern Brazilian Amazon. Second, there has been a marked increase in small-scale deforestation, partially offsetting the previously reported declines in deforestation of larger patch sizes. Thirdly, light deforestation events have spread pervasively across the entire Amazon in recent years, even in protected areas. Altogether these results raise awareness of new threats that national-level statistics do not capture and pose new challenges for conservation of Amazonian forests.

3

Forest Loss from Small-Scale Gold Mining underestimated in Amazonia

3.1 Abstract

Small-scale gold mining has significantly increased across northern Amazonian forests, making it the leading driver of deforestation in countries such as Suriname and Guyana. Though there are increasing efforts to stop deforestation in the region, there is a lack of datasets on where and how much forest is lost through small-scale gold mining. Using the satellite data-based 30m-resolution Global Forest Cover (GFC) product, this chapter quantifies the extent of forest loss from gold mining between 2001-2008 and 2009-2016 in northern Amazon by analysing the patterns of forest change at known gold mining sites. I also assessed the ability of the GFC dataset in detecting gold-mining forest loss through a comparison to 5m-resolution RapidEye imagery in the Guyanese Amazon. The total forest area lost due to gold mining in 2009-2016 was ~926 km^2 more than in 2001-2008. Gold mining also impacted protected areas within the region, with forest loss increasing by 32% (114 km^2) between the two study periods. Through analysis of remote sensing time series, the GFC product underestimated forest loss from gold mining by 74% in 2011-2016. This demonstrates that gold mining related forest loss across northern Amazonia has increased in extent and is higher than previously estimated, with GFC underestimating smaller forest loss events at a more regional scale. As such, post-processing and correcting this bias at a local-regional scale is required in order to support better land management and conservation policies.

3.2 Introduction

Small-scale deforestation in Amazonia has increased greatly in recent years (Kalamandeen et al. 2018, Chapter 2 of this thesis). However, ascertaining the contribution of different drivers to increasing small-scale deforestation is a substantial challenge. This chapter focuses specifically on the role of artisanal and small-scale gold mining activities, which have rapidly increased within the last decade across Amazonia (Alvarez-Berrios and Mitchell Aide 2015), in driving increases in small-scale deforestation in northern Amazonia. Despite widespread acknowledgement of its increased importance, the deforestation impacts of small-scale gold mining remains poorly quantified.

Historically, mapping forest loss from small-scale gold mining has been hindered by the availability of high resolution satellite images covering all nine Amazonian countries. Few countries in Amazonia except for Brazil have fully developed satellite monitoring systems for forest loss detection. With the recent availability of free, open and global datasets based on high resolution satellite images, the potential for assessing forest loss from small-scale activities has now become possible (Coca-castro et al. 2013, Hansen et al. 2013, Kalamandeen et al. 2018), and may be the basis for Amazonian countries to develop their own monitoring systems (Mitchard 2016). Yet, only a handful of studies have attempted to estimate deforestation driven by gold mining in Amazonia (see Table 3.1 for a summary). Of these, only one study focused on a spatial scale larger than national scale (Alvarez-Berrios and Mitchell Aide 2015), but this used relatively coarse (250m) resolution Moderate Resolution Imaging Spectroradiometer (MODIS) data to estimate forest loss, coupling this to a government database on mining in an effort to determine distribution of gold mining related deforestation. However, this resolution is too coarse to capture small-scale forest loss events, especially in areas such as northern Amazonia where the vast majority of deforestation events (96.4%) are below the resolution of a MODIS pixel (6.25ha) (Kalamandeen et al. 2018).

In this context, greater resolution of forest loss detection is of course desirable. The 30m-resolution University of Maryland's Global Forest Cover (GFC) (Hansen et al. 2013) dataset presents a higher-resolution alternative to

assess forest loss due to gold mining activity than has hitherto been possible through assessing patterns of forest loss at known gold mining sites. Small-scale mining is important across northern Amazonia, both in geographic extent and the number of mines (Hammond et al. 2007), and estimating forest loss where only artisanal and small-scale gold mining are known to operate may assist, to an extent, in distinguishing the type of gold mining that occurs in the region (i.e. small-scale versus large-scale activities). Overcoming the limits of detecting small-scale gold mining may also be achieved by using known small-scale gold mining areas as a proxy for practices (Reiche et al. 2013, Rahm et al. 2015).

Further, many gold mining sites occurred in or around protected areas (PAs) (Alvarez-Berríos and Mitchell Aide 2015), with several studies reporting the occurrence of mining operations within PAs (Swenson et al. 2011, Alvarez-Berríos and Mitchell Aide 2015, Asner and Tupayachi 2017). The creation and maintenance of PAs is considered one of the most effective ways to protect large areas of tropical forests. Collins and Mitchard (2017) showed that the majority of PAs experience little forest loss between 2000 and 2012. Though deforestation and degradation is still prevalent in the Amazon (Spracklen et al. 2015), the current extent and patterns of forest loss from gold mining within protected areas are poorly understood. Examining the current and future extent of gold mining pressures in PAs may be determined through assessing accessibility of PAs. Accessibility of PAs can be measured by evaluation of navigable rivers and roads that cross of form the boundaries of a given reserve (Peres and Lake 2003).

In this chapter, I specifically address the following questions: (1) what is the extent of forest loss associated with gold mining in northern Amazonia across two time periods: 2001-2008 and 2009-2016 using the GFC dataset? (2) Are protected areas effective in curbing forest loss from gold mining induced forest loss? (3) How accurate is the GFC dataset in identifying gold mining-related deforestation through comparison with 5m-resolution RapidEye satellite images for two main gold mining areas in Guyana? This is the first analysis conducted to evaluate the accuracy of the GFC product as it relates to gold mining in the northern Amazon.

Table 3.1 Defining mining-induced deforestation by various studies across Amazonia.

Studies	Summary	Defining gold mining sites
Asner et al. (2013)	Combined field surveys, airborne mapping, and high-resolution satellite imaging to assess road and river-based gold mining in the Madre de Dios, Peru from 1999 to 2012 using the Carnegie Landsat Analysis System-lite (CLASlite).	The fractional cover data, along with CLASlite's water-detection results, were classified to areas comprised of gold mining or clearings closely associated with gold mining (e.g., small clearings with miner huts and tents) using a Geographic Information System (ArcGIS 10.0; ESRI). The decision tree for gold mining was based on the presence of at least 25% bare substrate (for mining, includes bare soil and sand, tents, and other human-made objects) and standing water within each Landsat pixel. The resulting subpixel mapping classifications were evaluated using CAO high-resolution imagery and field data.
Swenson et al. (2011)	Analyzed satellite imagery from 2003 to 2009 to identify mined areas in Madre de Dios, Peru.	Distinct spectral signatures of mined areas were utilized by geographically isolating mining areas by hand-digitizing polygons around them that avoided rivers and naturally exposed soil and sand bars. An ISOData classification was applied and classes were separated into forest, edge or secondary forest, and mining by visual interpretation based on the image bands, tasseled-cap indices and the normalized difference vegetation index.
Alvarez-Berrios and Mitchell Aide (2015)	Combined geographical mining databases Google Earth images and maps derived from MODIS MOD 12Q1 imagery (250m resolution) from 2001 – 2013 for Tropical Moist Broadleaf Forest in South America.	Initially, a geographical database was created that included active or potential areas of gold extraction obtained from government and private mining GIS databases and by digitizing polygons around mining locations reported in peer-reviewed articles, news articles, and reports between 2000 and 2013. To map gold mining-related forest cover change, annual land cover maps derived from MODIS MOD13Q1 Vegetation indices from 2001 to 2013 was created and overlaid with the geographical databases and Google Earth images.
Reiche et	Used a combination	Defined mining-induced deforestation

al. (2013)	of ALOS PALSAR Fine Beam Duel and Landsat Imagery of 2007 and 2010 for detecting deforestation and forest degradation in central Guyana.	based on the idea that the location of deforestation, i.e. it is within a mining area, therefore assumption is that deforestation is directly related to mining. Deforestation is based on overall accuracy for mapping forest land cover (FLC) and Kappa coefficient. Also noted was the observed signatures of degraded forest which has a lower HV and increased HH-HV values compared to undisturbed forest.
Sonter et al. (2017)	Mining across Brazil from 2005 to 2015 using satellite data and propensity score matching	Assessed all types of mining activities, including gold, nickel, etc., using mining leases from 1960 to 2005 overlaid with Landsat TM imagery from 1985 and 2015.

3.3 Methods

3.3.1 Deforestation datasets and temporal patterns

The northern Amazonian area of interest was defined using the boundaries of the Amazon Basin as proposed by Eva et al. (2005). This includes sections of four countries: French Guiana, Suriname, Guyana and Venezuela (Figure 3.1a). The deforestation data for area of interest was taken from the 30-m resolution Global Forest Change (GFC) data of Hansen et al. (2013), based on Landsat imagery. For this Chapter, I utilized Version 1.4, which included the years 2015-2016, making it the longest time series to-date (https://earthenginepartners.appspot.com/science-2013-global-forest/download_v1.4.html). No further processing was applied to the GFC datasets. I restricted my analysis to the Tropical and Subtropical Moist Broadleaf Forest (herein called the TMBF) biome using the definition and extent from Nature Conservancy (http://maps.tnc.org/gis_data.html). The TMBF is defined as large, discontinuous patches centred on the equatorial belt, between the Tropics of Cancer and Capricorn, and characterized by low variability in annual temperature and high levels of rainfall (>200 cm annually). These forests are dominated by semi-evergreen and evergreen deciduous tree species.

Forests in the GFC data were defined as pixels with >30% tree cover (Kim et al. 2015), while forest loss was formally defined by Hansen et al. (2013) as a

stand-replacement disturbance or the complete removal of tree cover canopy at the Landsat pixel scale (30m); with the exclusion of pixels annually after a deforestation event. See Chapter 1.5 for limitations of the GFC dataset. Gold mining sites across northern Amazonia were geoferenced and digitized from two sources: (1) Alvarez-Berrios and Mitchell Aide (2015), which was created from government and private mining GIS databases, digitizing polygons around mining locations reported in peer-reviewed articles, news articles, and reports between 2000 and 2013 and systematically reviewing high and medium-resolution images available in Google Earth (very high resolution imagery (VHR) from Digital Globe and Landsat; from 2001 to 2013 (see Methods in Alvarez-Berrios and Mitchell Aide, 2015); and (2) Rede Amazônica de Informação Socioambiental Georreferenciada (RAISG, https://geo.socioambiental.org/webadaptor2/rest/services/raisg/), which sourced their data from SERGEOTECMIN, Bolivia (2005), National Department of Mineral Produces-DNPM, Brazil (2011), Colombian Mining Cadastre, Colombia (2010), Ministry of Non-Renewable Natural Resources, Ecuador (2010), Guyana Geology and Mines Commission, Guyana (2009), MINEM, Peru (2011), Natural Resource and Environmental Assessment-NARENA, Suriname and Ministry of Energy and Mines, Venezuela (2009). These mining polygons were then classified as active or potential (exploration/prospecting phases) gold mining activities (see Appendix 3.1 for location of gold mining sites).

The total area deforested in the northern Amazonian gold mining region of each country was calculated annually for the GFC dataset (2001-2016) by clipping the GFC dataset using the mining polygons. These datasets include both illegal and legal gold mining areas, though mining activities within protected areas may be considered as illegal. The illegality of mining within a protected area is highly contextual and may be based on the timeline of legal declaration of a site versus the commencement of mining activities, and/or the delineation or adjustment of a site's boundaries. Forest gain was not considered in this analysis as the GFC dataset captured all tree cover loss which may extend to plantations or recovering vegetation other than forests. Further, I assumed that forest loss within the stipulated gold mining sites resulted from gold mining and no other type of land use, though in reality this may not be the case.

3.3.2 Analysis of spatial patterns of deforestation

The GFC data was also used to investigate spatial patterns of deforestation density (number of deforested pixels per area), including their temporal dynamics using ArcGIS 10.4.1. To visualise deforestation density at a more regional scale, I created a 5x5 km grid over the study area, within which total deforested area was classified into three categories following a log scale, as per Chapter 2: 1) Negligible (<0.01 km^2 per 25 km^2 land area), 2) Light (0.01– 1 km^2 per 25 km^2 land area) and 3) Moderate (>1 km^2 per 25 km^2 land area). Annual data were grouped into two equal periods for analysis: 2001-2008 and 2009-2016. I did not attempt to map annual trends because it is known that GFC data often allocates deforestation events to incorrect years, due to the patchiness of cloud free data in this cloudy region of the world (Milodowski et al. 2016). Aggregating several years of data together negates this issue to a large degree.

To evaluate whether similar patterns were observed inside and outside of protected areas, we applied a protected area mask using shapefiles provided by The World Database on Protected Areas (WDPA) for northern Amazon, which includes protected areas from all IUCN categories as well as indigenous protected areas, biological and biosphere reserves, cultural sites, sustainable reserves and hunting preserves (www.protectedplanet.net). Legal mining areas have now been extended into several protected areas, particularly in Venezuela. Sequential buffer zones (5km, 10km and 20km) were created around gold mining sites to assess the extent of leakage of forest loss around these areas. I also utilized river and roads shapefiles from HydroSHEDS (http://www.hydrosheds.org/) and gROADS database (http://sedac.ciesin.columbia.edu/data/set/groads-global-roads-open-access-v1) respectively to assess accessibility to protected areas.

3.3.3 Statistical Analysis of spatial patterns of deforestation

For the GFC deforestation analyses described above the dataset was divided into two periods of equivalent length: 1) 2001 – 2008 and 2) 2009 – 2016. I statistically evaluated the differences in means for both periods using the non-parametric Wilcoxon's signed rank test as the data was not normally distributed. I also conducted separate Wilcoxon signed rank tests for areas inside and outside of protected areas to investigate changes in deforestation density from gold mining between the two focal periods.

3.3.4 Comparison of GFC dataset with RapidEye satellite images

In order to examine the accuracy of GFC for forest loss detection in gold mining sites, I used the 5m-resolution RapidEye images for two gold mining sites in Guyana, Mahdia and Puruni as a reference. Both sites are deforested primarily by artisanal and small-scale gold mining (Figure 3.1b). RapidEye satellite images were taken from www.planet.com for my area of interest. To estimate the size of both areas, a shapefile was created and area estimated in ArcGIS 10.4.1. An explanation is required here referring the circular shape of the RapidEye tiles of Figures 3.7, 3.8, 3.9 and 3.10. In order to access the RapidEye imagery, a radius of 10km^2 of Mahdia and Puruni were required via a GeoJSON format (a format for encoding a variety of geographic data structures), with a circular image output.

Only years where both products were available, with little cloud cover, were used for this comparison (2011-2016). Supervised maximum likelihood classification was performed on the RapidEye image in Excelis Software ENVI 5.1 using four classes (gold mining, forests, non-forest and clouds) for classification (see Table 3.2 for description of classes). I further used benchmark maps derived from the Guyana Forestry Commission Monitoring, Verification and Reporting System (MRVS) data (Guyana Forestry Commission - Indufor 2013) to exclude forest loss events in earlier years (i.e. 1990 -2010) in all RapidEye tiles to ensure a consistent timeframe across the two products. The MRV benchmark map was developed using 30m-resolution Landsat tiles and 5m-resolution RapidEye tiles to establish forest loss activities from 1990-2010. Hence, to determine forest loss in the composite years (2011-2016) all 1990-2010 forest loss events were masked using the MRVS benchmark map (Figures 3.8 and 3.9) in ArcGIS 10.4.1.

Spatio-temporal accuracy was based on three procedures. Firstly, spatial accuracy of the classification of classes in the RapidEye tile was assessed using a stratified random sampling in ENVI 5.1 leading to the generation of a confusion matrix, errors of commission (the fraction of values that were predicted to be in a class but do not belong to that class) and omission (the fraction of values that belong to a class but were predicted to be in a different class), and overall accuracy, producer accuracy and user accuracy for the confusion matrix. The overall kappa coefficient, *k*, for classified images, which assesses the agreement between classification and truth values was deduced. A kappa value of 1

represents perfect agreement while a value of 0 represents no agreement. The kappa coefficient is computed as follows:

$$\kappa = \frac{N \sum_{i=1}^{n} m_{i,i} - \sum_{i=1}^{n} (G_i C_i)}{N^2 - \sum_{i=1}^{n} (G_i C_i)}$$

Where i is the class number, N is the total number of classified values compared to truth values, $m_{i,i}$ is the number of values belonging to the truth class i that have also been classified as class i (i.e., values found along the diagonal of the confusion matrix), C_i is the total number of predicted values belonging to class i and G_i is the total number of truth values belonging to class i.

Table 3.2 Definition of forest and non-forest classes.

Class	Definition
Forest	Land dominated by semi-evergreen and evergreen deciduous tree species, with canopy height of ≥ 5m.
Gold Mining sites	Land surface without any vegetation and are clusters of tiny pits which can be recognized on the image by their high brightness and texture. Some pits can be filled with water, however the presence of the dry pits which signify high mining intensity, is the key identifying factor.
Clouds	Clouds, cloud shadows and haze were classed as clouds.
Non-Forest	Land surface without any vegetation.

Secondly, to assess the GFC forest loss data and how well it correlated with the mining sites identified in the reference RapidEye image, I overlay the GFC polygons in the classified RapidEye tile and assessed the intersect of the two products in R using the *rgeos* package. Finally, field survey of the study area has been done for further classification accuracy using nine (9) plots each at Mahdia and Puruni.

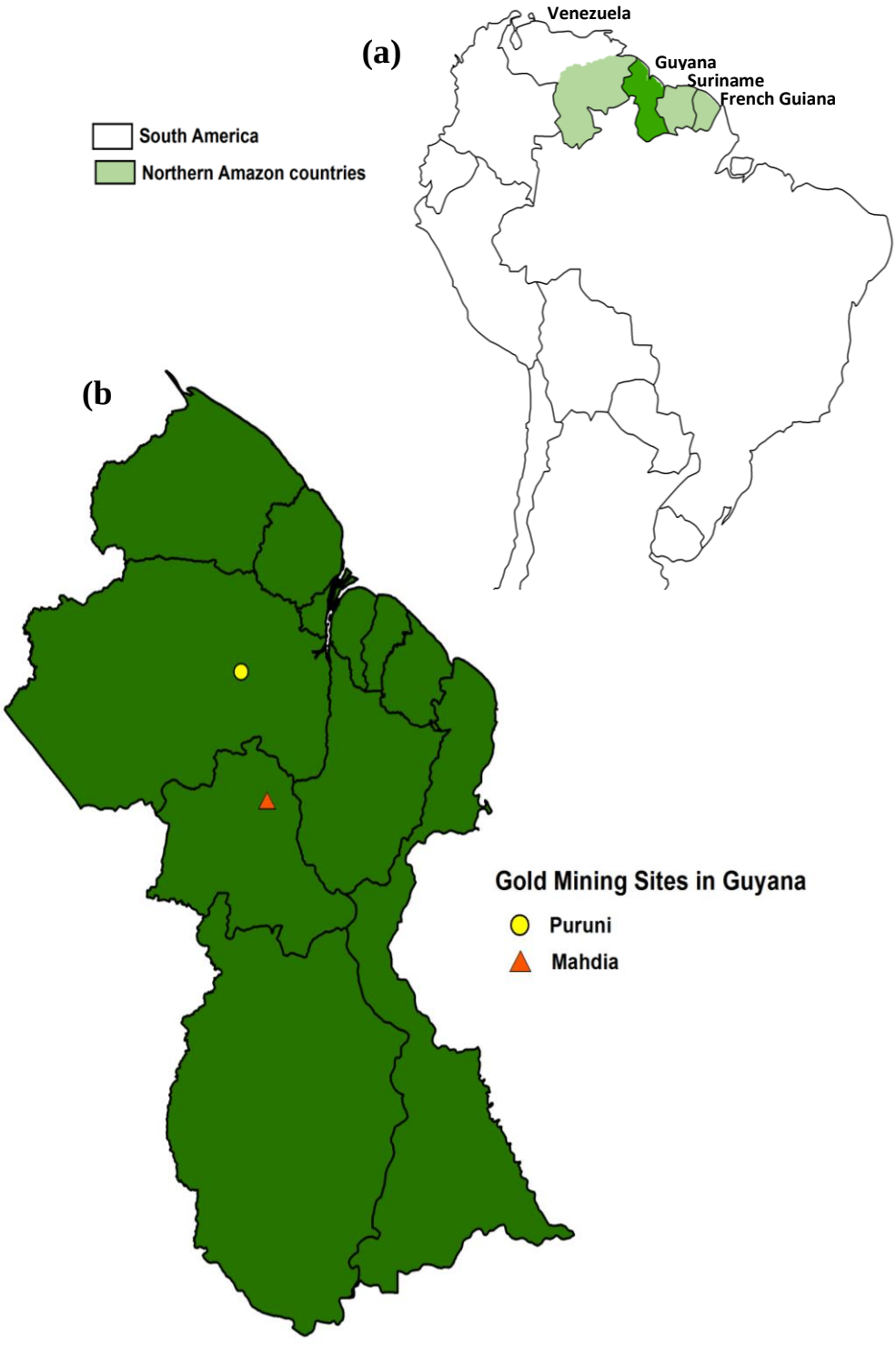

Figure 3.1 Map indicating (a) northern Amazonian countries and (b) the location of key gold mining areas, Mahdia and Puruni in Guyana.

3.4 Results

3.4.1 Extent of forest loss from gold mining

Across northern Amazonia, forest loss increased significantly at gold mining sites between 2001-2008 and 2009-2016 (W=1, p>0.001; Figure 3.2). In 2001-2008, total forest loss in the region was ~836.4 km^2 but grew by 111% to 1762.8 km^2 in 2009-2016. Within active mining areas, forest loss was estimated at 471 km^2 in 2001-2008 and 1178 km^2 in 2009-2016, while deforestation in sites slated for prospecting and exploratory phases were ~366 km^2 and 585 km^2 across the two periods respectively. In contrast, forest loss outside of immediate mining areas increased 90% between the two time periods (W=12, p=0.03), from 2454 km^2 in 2001-2008 to 4662 km^2 in 2009-2016 (Appendix 3.2). Forest loss also increased by 48.6% within a 20 km^2 buffer zone surrounding mining areas from 1124 km^2 in 2001-2008 to 1670.2 km^2 by the second half of the study period (Figure 3.3).

Considerable changes also occurred in the geographical pattern of deforestation density (number of deforested pixels per area), between the two study periods within gold mining areas (Figure 3.2). In 2001-2008, 62% of the 5x5 km gridcells in the study region were categorised as having negligible forest loss (<0.01 km^2 per 25 km^2) but this declined to 43.4% by 2009-2016. The proportion of gridcells experiencing 'light' (0.01-1 km^2 per 25 km^2) and 'moderate' (>1 km^2 per 25 km^2) deforestation grew by 14.4% and 4.3%, from 35.6% and 2.4% in 2001-2008 to 50% and 4.3% in 2009 – 2016 respectively.

I also tested whether deforestation patterns observed in gold mining areas differed from patterns observed outside of gold mining areas and within a 5 km^2, 10 km^2 and 20 km^2 buffer zone around mining sites. For areas outside of mining sites, gridcells experiencing 'light' and 'moderate' deforestation increased by 16% and 2.13% respectively between 2001-2008 and 2009-2016, while 'negligible' gridcells decreased by 18% between the two study periods (Appendix 3.2). Similar patterns of forest loss were seen within the sequential buffer zone around mining sites, with gridcells having 'negligible' forest loss declining by 23% between 2001-2008 and 2009-2016, while 'light' and 'moderate' gridcells

increased by 20.7% and 2% respectively between the two time periods (Figure 3.3).

Mining activities were also observed inside and outside (Appendix 3.3) protected areas and within a 5 km^2 and 10 km^2 buffer zone (Figure 3.4). Between 2001-2008 and 2009-2016, forest loss in protected areas grew by 32% from 242 km^2 to 358 km^2, and occurred mainly along rivers (Figure 3.5).

The majority of gold mining related forest loss in protected areas in 2001-2008 occurred in Venezuela (217 km^2), followed by French Guiana (14 km^2), Suriname (8 km^2) and Guyana (3.4 km^2). By 2009-2016, gold mining related forest loss in protected areas in Venezuela increased to 293 km^2, followed by Suriname (30 km^2), and equally in French Guiana and Guyana (17.2 km^2). Within the study period, gridcells with 'negligible' forest loss inside mining areas within protected areas decreased by 14.5% (W=16, p=0.02) while 'light' and 'moderate' gridcells grew by 12.5% (W=0, p=0.02) and 2% (W=10, p=0.5) respectively. Further, the buffer zones surrounding the mining areas in protected areas also saw similar temporal patterns. Gridcells with 'negligible' forest loss decreased from 56% in 2001-2008 to 30% in 2009-2016, while 'light' and 'moderate' gridcells increased by 24% and 2% respectively.

As the GFC data may lag across years, understanding annual trends may help us see the overall pattern of forest loss from gold mining. The largest forest loss values at gold mining sites in the first half of the study period were encountered in Venezuela (334 km^2), followed by Suriname (270.1 km^2), Guyana (200.8 km^2) and French Guiana (33.1 km^2). However, by 2009-2016, the highest forest loss events were seen in Suriname (819.5 km^2), followed by Venezuela (459.3 km^2), Guyana (455.8 km^2) and French Guiana (36.1 km^2). Overall, annual forest loss across northern Amazonia increased by 2 km^2 and 12 km^2 yearly in 2001-2008 and 2009-2016 respectively, with peak deforestation occurring in 2012 (244.7 km^2) and 2016 (269.5 km^2, Figure 3.6).

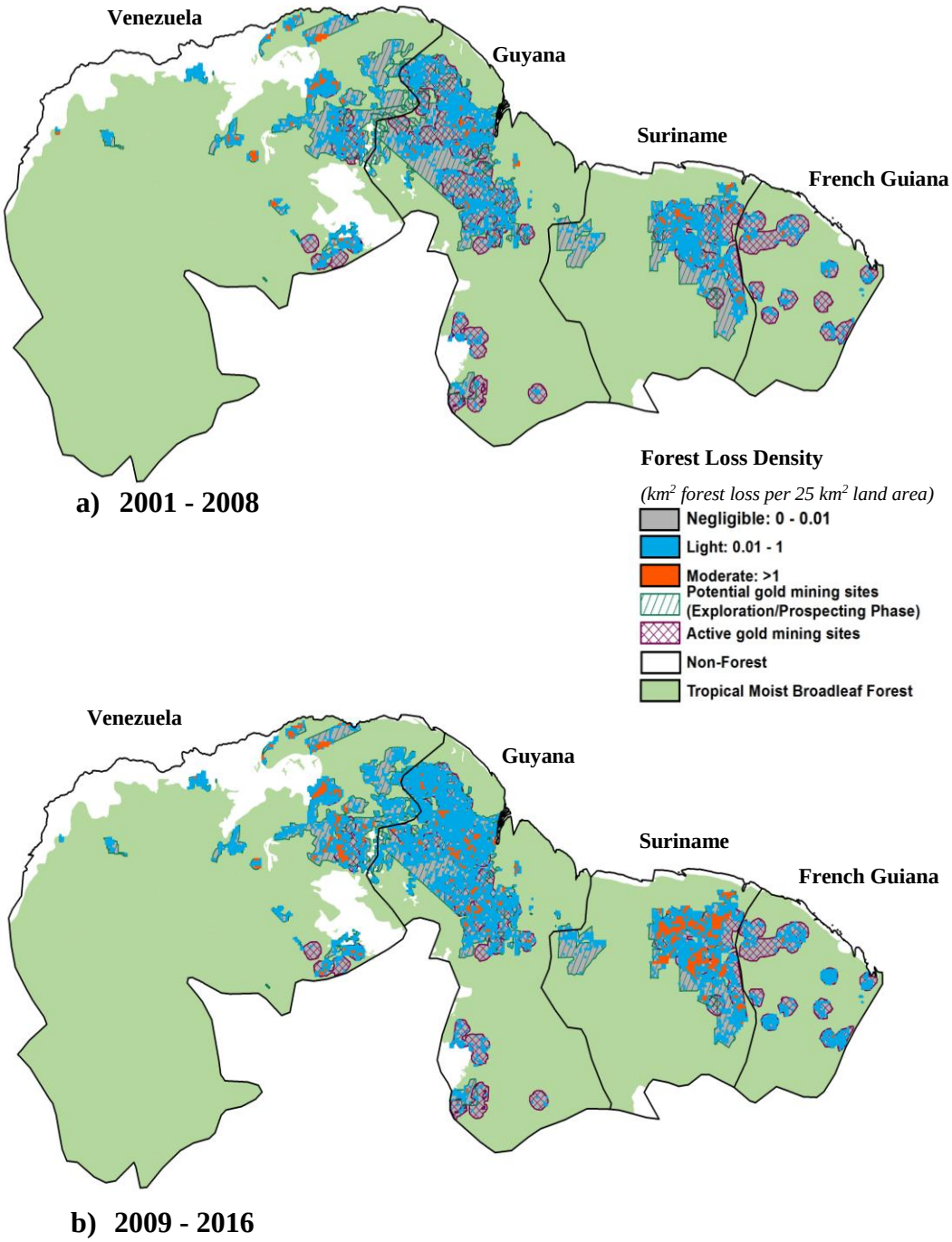

Figure 3.2 Forest Loss Density (km^2 forest loss per 25 km^2 land area) from gold mining activities across northern Amazonia.

Map generated using data from the GFC product for two time periods:(a) 2001-2008 and (b) 2009-2016.

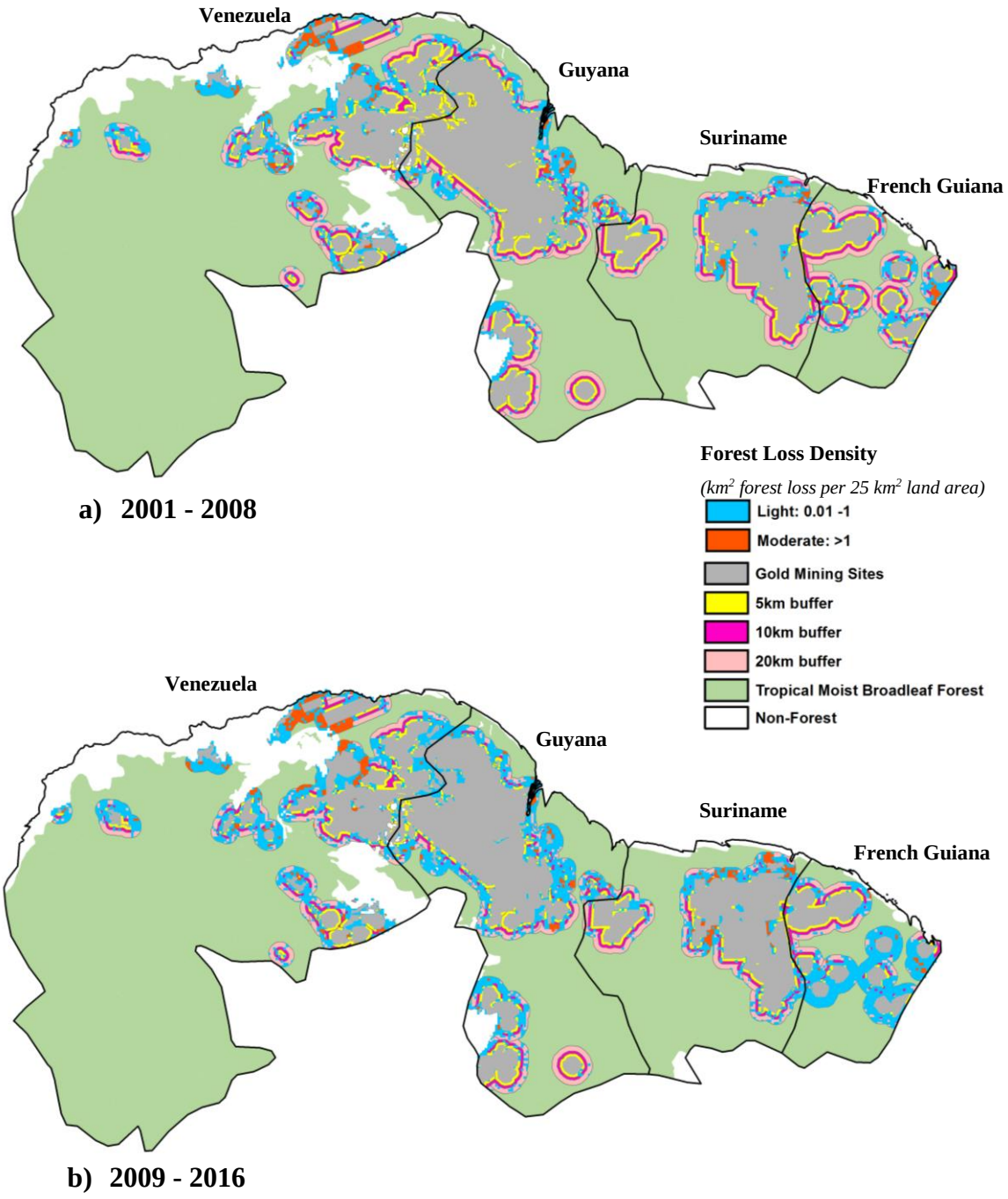

Figure 3.3 Forest Loss Density (km^2 forest loss per 25 km^2 land area) in sequential buffer zones around gold mining activities across northern Amazonia. Map generated using data from the GFC product for two time periods: (a) 2001-2008 and (b) 2009-2016. Forest loss in gold mining areas are not shown.

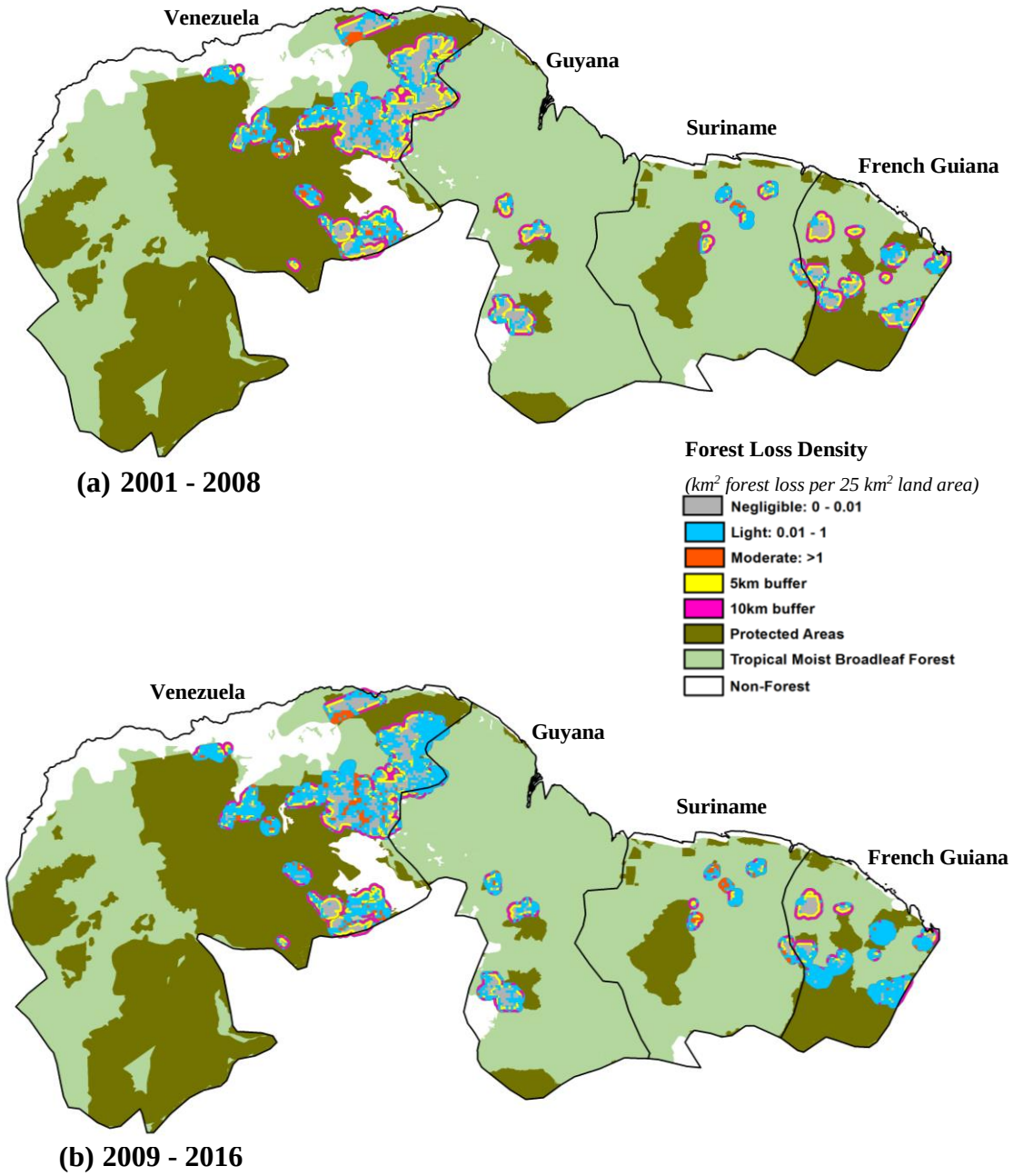

Figure 3.4 Forest Loss Density (km^2 forest loss per 25 km^2 land area) from gold mining activities in protected areas and within buffer zones across northern Amazonia. Map generated using data from the GFC product for two time periods: (a) 2001-2008 and (b) 2009-2016.

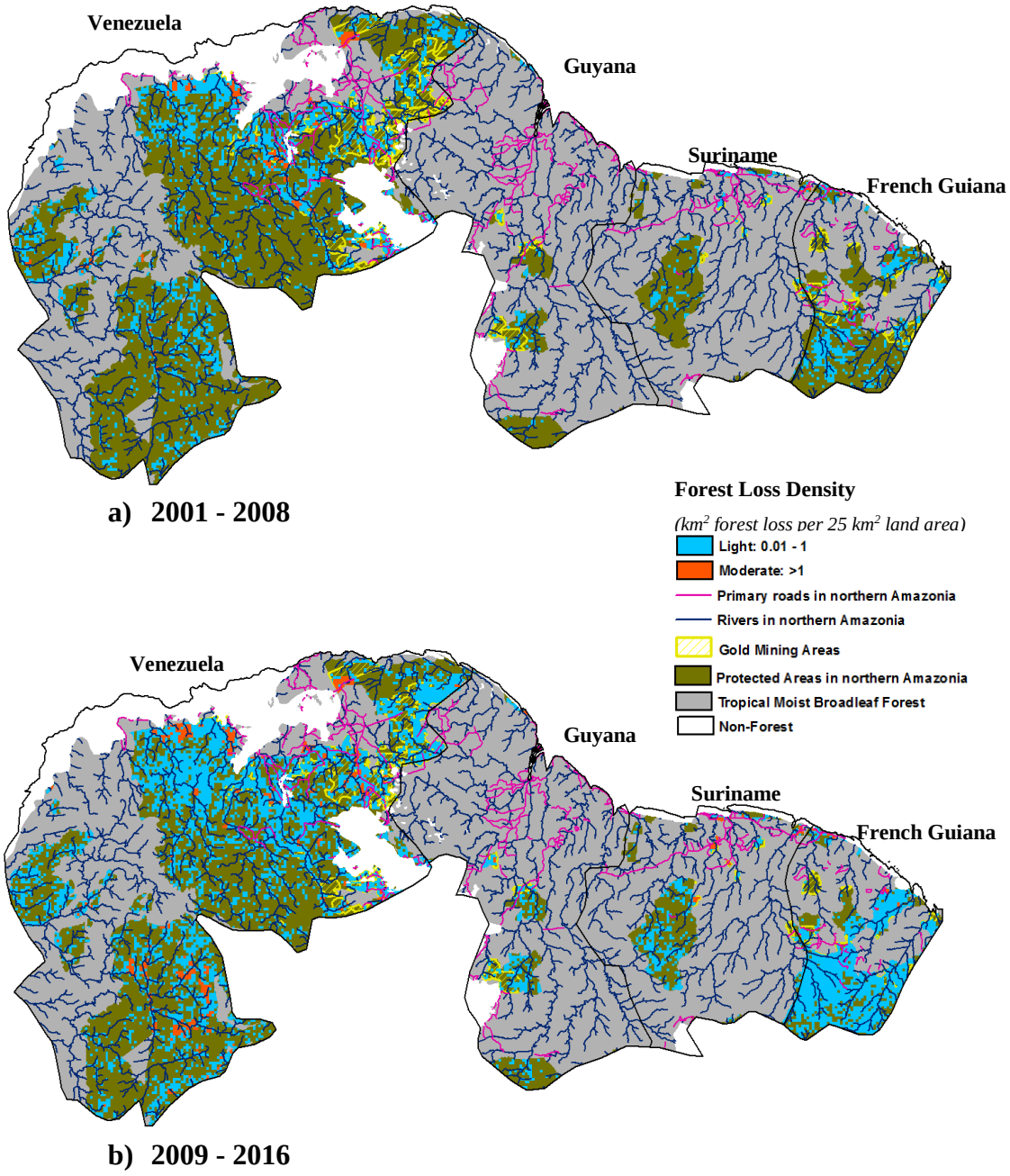

Figure 3.5 Forest loss from gold mining activities along rivers and roads in Protected Areas (PAs) across northern Amazon (NA) based on GFC product (2001-2016).

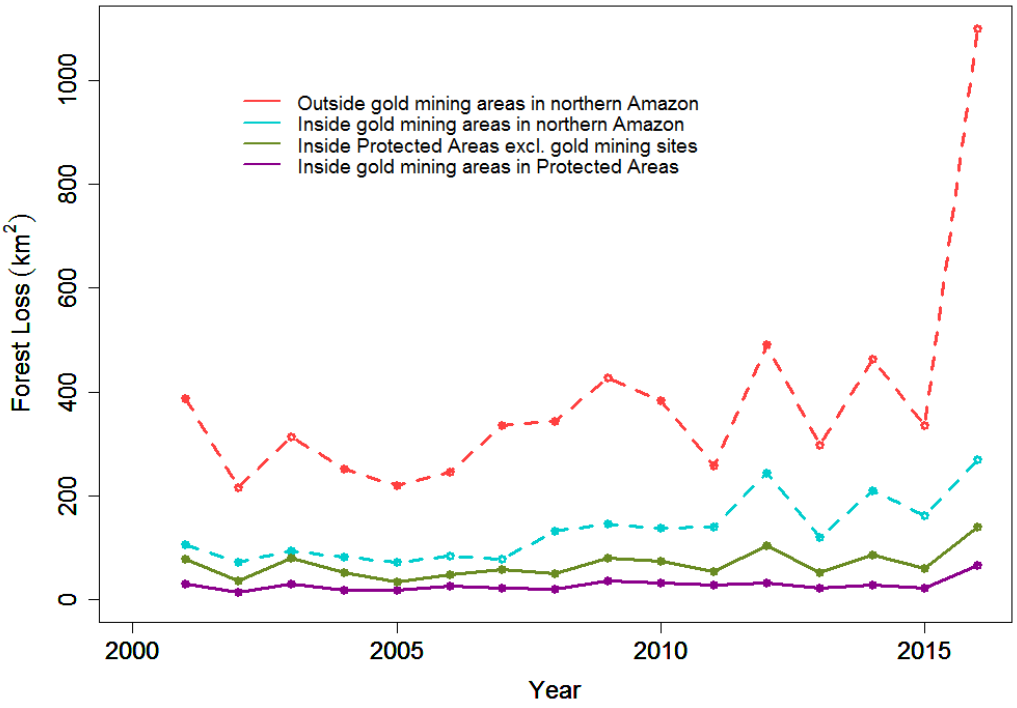

Figure 3.6 Forest loss from gold mining activities across northern Amazon (NA) based on GFC product (2001-2016).

3.4.2 Comparison of RapidEye versus GFC products

The classification of the RapidEye tiles utilized three classes, namely, gold mining sites, forests and cloud cover (Figure 3.7). Validation was made for classification of the RapidEye images using a stratified random sample for Mahdia and Puruni (Table 3.3a, b). Here, the classified RapidEye image of 2011-2016 in Mahdia had an overall accuracy of 99.9%, producer accuracy 99.7%, user accuracy 99.62% and overall kappa accuracy of 0.9 while in Puruni, overall accuracy of 99.4%, producer accuracy 99.6%, user accuracy 97.6% and overall kappa accuracy of 0.9. Error of commission and error of omission were relatively low for both sites when RapidEye images were classified and assessed using the stratified random sampling (Table 3.4) indicating that the classification of the classes were relatively good.

The classified RapidEye images allocated 330.5 km^2 and 390.4 km^2 as forests with 16.8 km^2 and 15.08 km^2 labelled as gold mining in Mahdia and

Puruni respectively. Overall forest loss based on GFC product was 5.35 km^2 in Mahdia and 9.06 km^2 in Puruni.

Table 3.3 Confusion Matrix (%) for Rapid Eye image (2011-2016) in (a) Mahdia and (b) Puruni using stratified random sampling.

(a)

Class (%)	Gold Mines	Clouds	Forests	Total
Gold Mines	99.74	0.26	0	100
Clouds	0.26	99.67	0.07	100
Forests	0	0.07	99.93	100
Total	100	100	100	100

(b)

Class (%)	Gold Mines	Clouds	Forests	Total
Gold Mines	99.3	0.59	0.11	100
Clouds	0.5	99.41	0.09	100
Forests	0.2	0	99.8	100
Total	100	100	100	100

Table 3.4 Error of Commission and error of omission of the RapidEye classified image in Mahdia and Puruni.

Sites	Mahdia		Puruni	
Classes	**Error of Commission (%)**	**Error of Omission (%)**	**Error of Commission (%)**	**Error of Omission (%)**
Gold Mines	0.38	0.6	1.4	0.4
Clouds	0.8	0.6	0.28	0.11
Forests	0	0.07	0.1	0.5

At the two gold mining sites in Guyana, forest loss captured by the GFC and RapidEye products were relatively similar (Figure 3.7). When the MRVS pre-2011 tiles were applied (Figure 3.8), between 2011 and 2016, there was 70.6% and 77.7% difference between the two products at Mahdia and Puruni respectively (Table 3.5). Intersection occurred when at least 25% of a GFC polygon overlapped with the classified RapidEye class (Figure 3.9). At Mahdia, GFC intersected the classified RapidEye tile at gold mining sites only 29.4% (an area covering 1.56 km^2) while at Puruni the GFC-RapidEye gold mining intersected 22.3% (an area covering 2 km^2) (Table 3.5), with greater correlation occurring at Mahdia. The rate of forest loss indicated by the GFC product is much lower than RapidEye detection, significantly underestimating forest loss at both Mahdia and Puruni (Table 3.5, Figures 3.8 and 3.9).

Validation using ground-truthing (field sites) showed that 44.4% of abandoned gold mining plots were classified within the RapidEye mining pixels while 11.2% of plots fell within the GFC forest loss pixels in Mahdia (Table 3.6). In Puruni, 55.6% and 44.4% of these plots intersected RapidEye mining sites and GFC forest loss polygons (Table 3.6). Intersection occurred between the field plots and the RapidEye-GFC mosaic if a pixel from the field plot correlated with any classes from the two products. An example of the intersection with field plots can be seen in Figure 3.10. Interestingly, 44.4% of abandoned gold mining plots were classified as forests in the RapidEye tile in Mahdia.

Table 3.5 Assessment (%) of GFC forest loss data correlating with the RapidEye classified image and MRVS pre-2011 image in Mahdia and Puruni.

GFC Forest Loss (%)	RapidEye Gold Mining Sites	RapidEye Forests	RapidEye Clouds	MRVS Pre2011	Total
Mahdia	29.4	26.7	19.9	24	100
Puruni	22.3	15.4	11	51.3	100

Table 3.6 Accuracy Assessment (%) of field sites within Rapid Eye, GFC and Forests pixels in Mahdia and Puruni.

Field Sites in Abandoned Gold mining areas (%)	RapidEye Gold Mining Sites	GFC Forest Loss	Forests	Total
Mahdia	44.4	11.2	44.4	100
Puruni	55.6	44.4	0	100

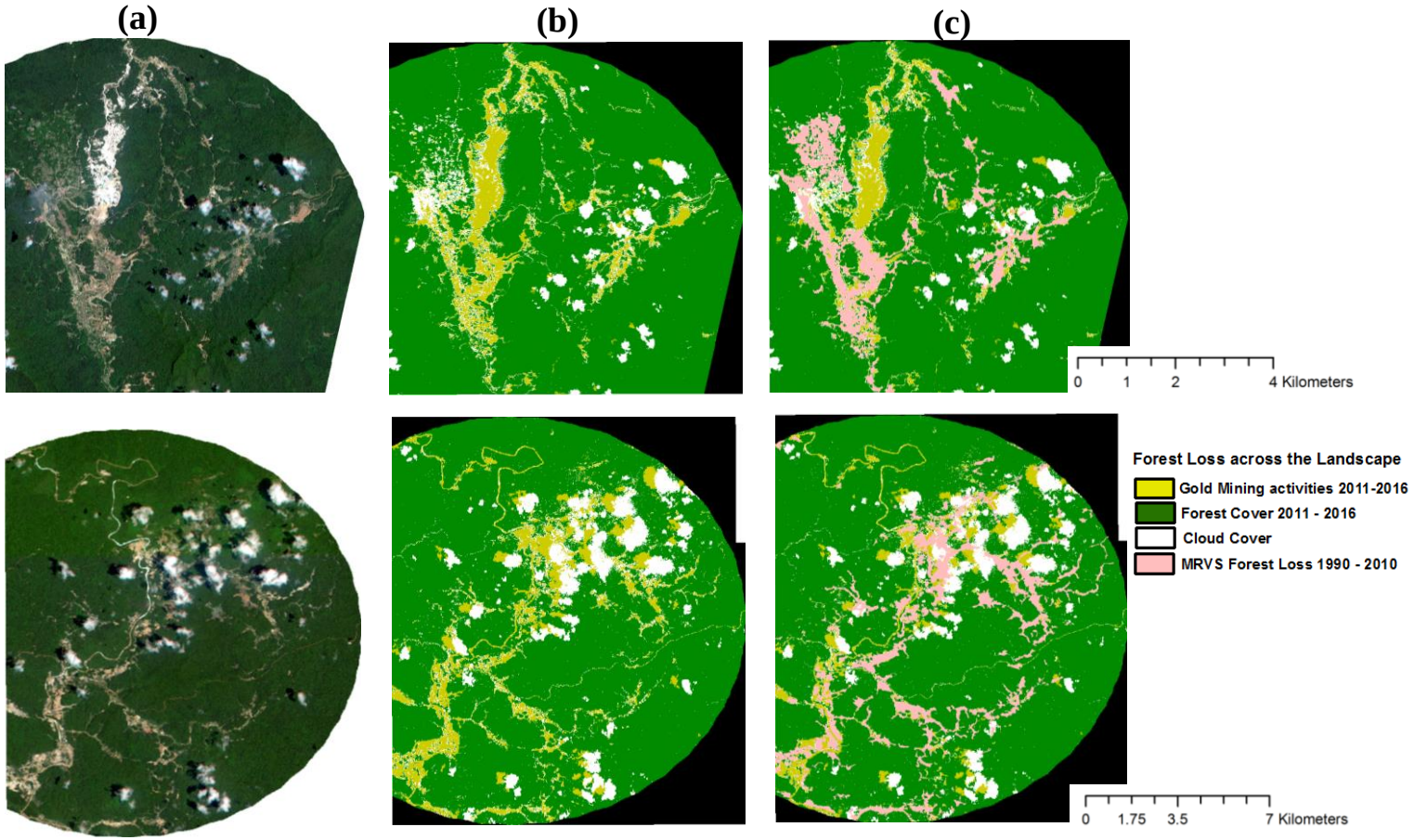

Figure 3.7 Forest loss detection using RapidEye Imagery (2011-2016) in Mahdia (top) and Puruni (bottom). Maps indicates (a) Original RapidEye image, (b) Supervised Maximum Likelihood Classification and (c) Supervised classification with pre-2011 MRV data.

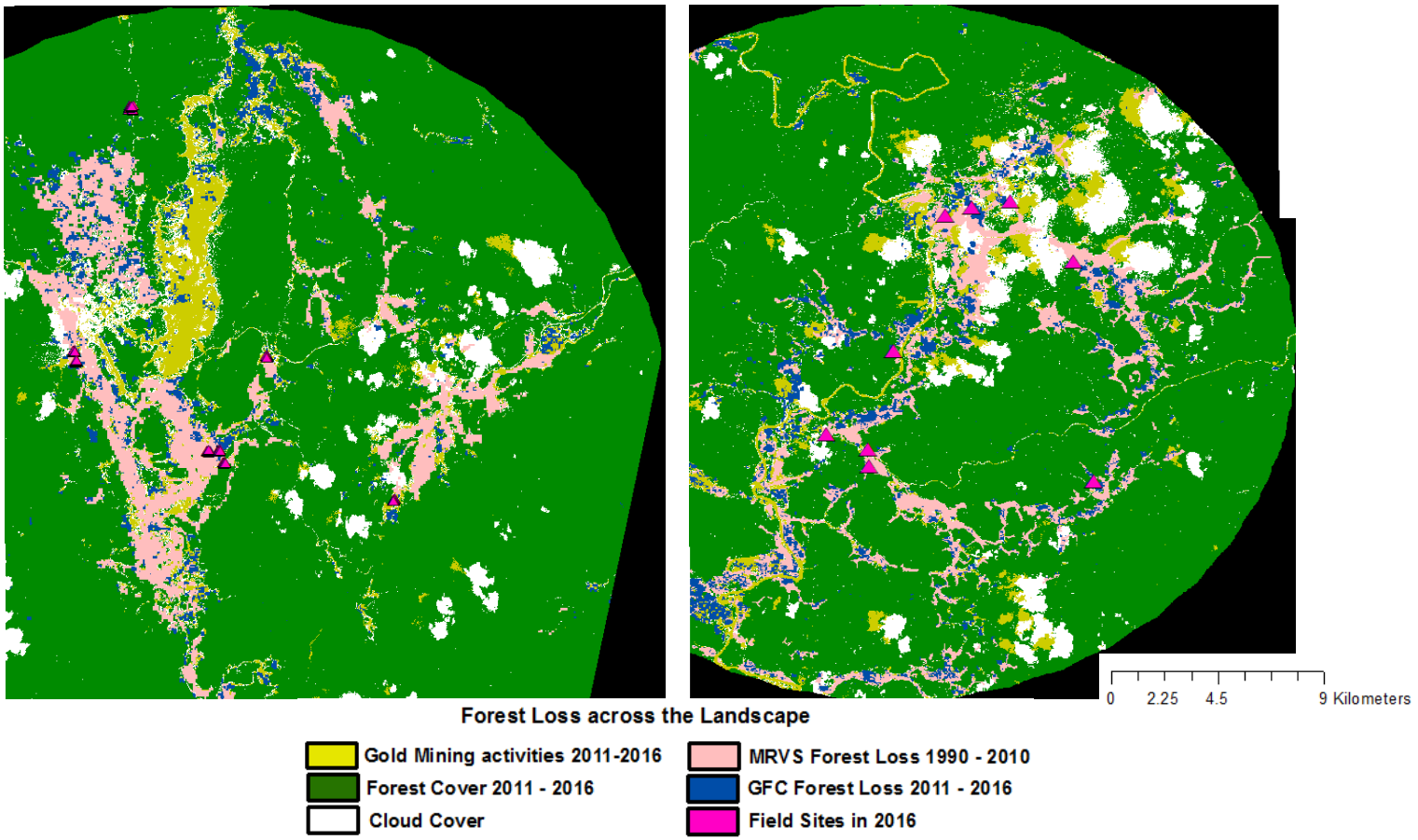

Figure 3.8 Comparison of forest loss detection with GFC, RapidEye and field sites (2011 - 2016) in Mahdia (left) and Puruni (right). Maps indicates supervised classification with 1990 - 2010 MRV (light pink), GFC data (dark blue) and field sites (deep pink). GFC was unable to detect gold mining activities based on RapidEye (yellow).

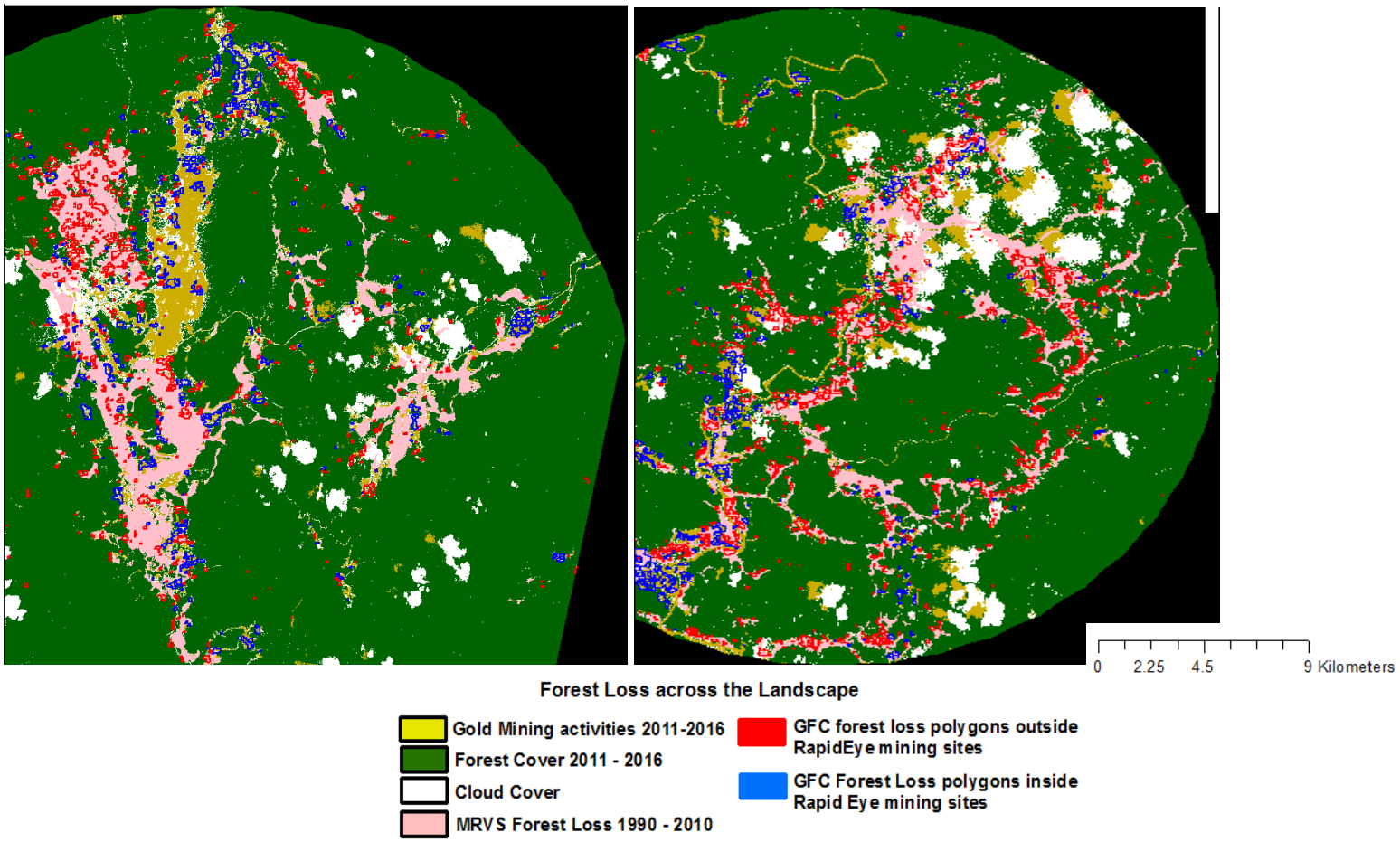

Figure 3.9 Intersection of GFC forest loss with RapidEye gold mining sites (2011 - 2016) in Mahdia (left) and Puruni (right).

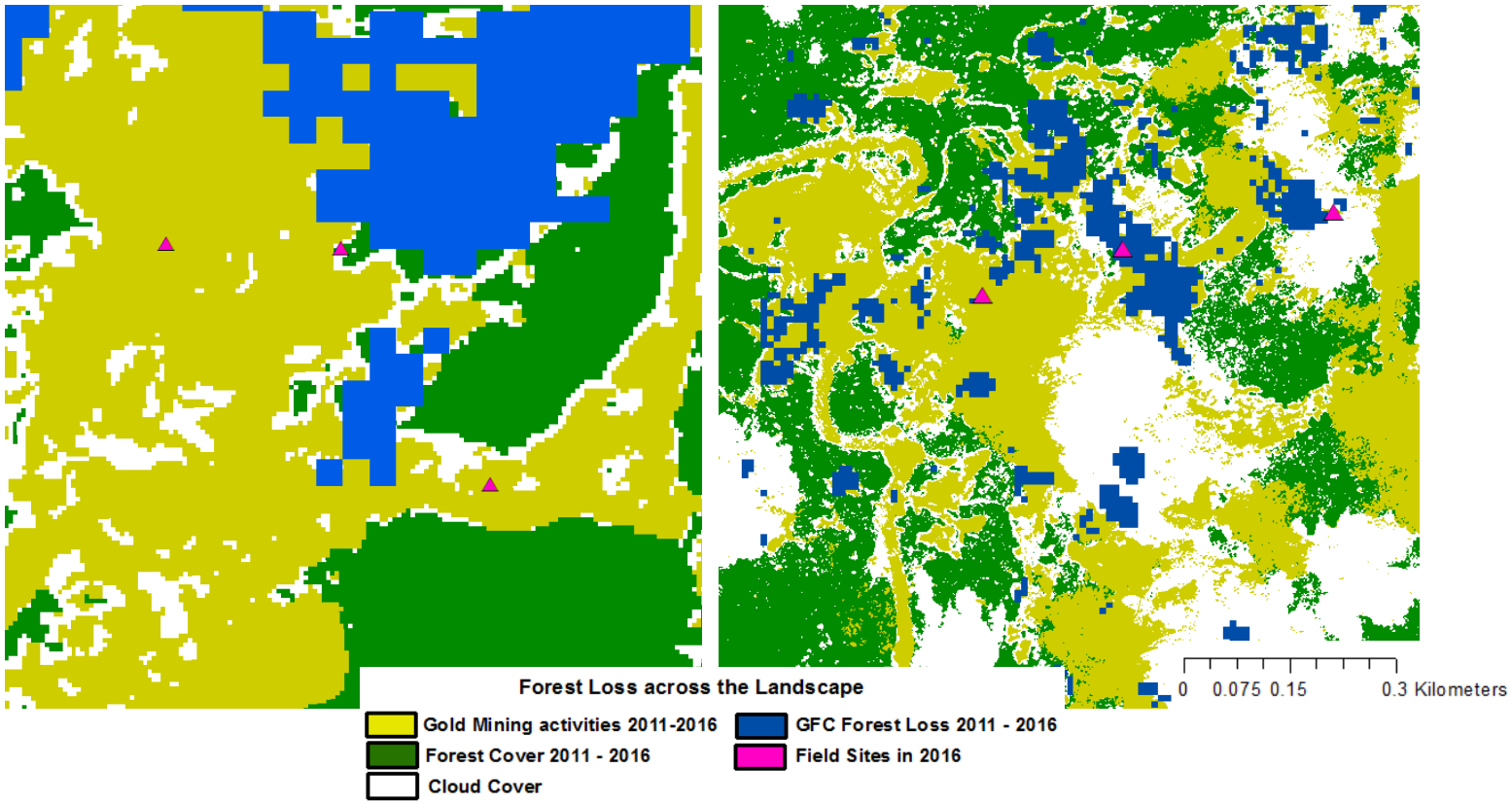

Figure 3.10 Example of accuracy of RapidEye and GFC detection with field sites (2011 - 2016) in Mahdia (left) and Puruni (right).

3.5 Discussion

3.5.1 Geographic spread of forest loss from small-scale gold mining and implications for conservation

In this study, forest area affected by gold mining activities increased by an additional 926.4 km^2 across northern Amazonia by the end of 2016. Much of this loss stems from deforestation within active and potential mining areas which increased by 60% and 37.5% respectively between 2001-2008 and 2009-2016. This analysis also showed that deforestation due to gold mining increased in extent after the 2008 financial crisis and again in 2012 when gold prices soared (Figure 3.5).

Between 2001-2008 and 2009-2016, gold mining related forest loss extent also increased by 32% within protected areas (Figure 3.4), indicating that protected area status does little to stem the onslaught from gold mining activities. A majority of total forest loss in protected areas (81% in 2009-2016) was seen in Venezuela's protected areas. In 2016 the Venezuelan government opened the legal Arco Minero del Orinoco, an area spanning 112 000 km^2 of forests and twelve protected areas (Rosales 2017) as a response to the current economic crisis. Guyana and Suriname had the biggest increase in mining activities in protected areas (403% and 298% respectively) between the two study periods. Mining activities observed within protected areas in other Amazonian countries may be regarded as illegal as these countries, despite some legal consignment of mining leases, may have restricted active mining in protected areas until further notice or upon decommissioning of protected areas. As mentioned previously (see Methods), the illegality of mining within a protected area is highly contextual and may be based on the timeline of legal declaration of a site versus the commencement of mining activities, and/or the delineation or adjustment of a site's boundaries.

Mining operations also occurred within a 10 km^2 buffer zone surrounding gold mining activities that are present within protected areas. Here, buffer zones do not limit the spread of gold mining activities and may likely indicate a leakage of potential impacts on soil and vegetation to surrounding conservation areas, which seems accessible via rivers (Figure 3.5). This may have far-reaching

consequences such as mercury contamination of water, soil and vegetation which may have deleterious effect on biodiversity. In fact, Asner and Tupayachi (2016) observed that once the soils underlying the forests have been stripped of gold, new areas of forests are opened, with no known examples of large-scale restoration successes on previously mined landscapes (Roman-Danobeytia et al. 2015). This makes accurate detection coupled with enforcement integral to preventing further damage to the environment.

Assigning specific causes of observed increases in small-scale forest loss witnessed in gold mining areas is challenging as current gold mining concessions do not delineate actual mines versus deforestation from other land uses such as selective logging prior to mining activities. It can be deduced that, at some point, on gold mining sites that mining activities will occur and as such forest loss is inevitable. Further, there is no evidence to indicate that the small-scale forest loss events in gold mining sites correlates with (1) the 2005 and 2010 droughts (see Appendix 2.14 for a comparison of maximum climatological water deficit and geographical location of small-scale forest loss increases) or (2) natural disturbance events in northern Amazonia at the sub-pixel scale (see Chapter 2.5.3, Espírito-Santo et al. 2014).

3.5.2 Accuracy of GFC product in detecting forest loss from small-scale gold mining

When the GFC product was tested for its accuracy in capturing gold mining activities at two known small-scale gold mining sites, Mahdia and Puruni, in Guyana, it was found that generally, temporal agreements between GFC and RapidEye is good where forest loss occurred within the period of interest, i.e. both GFC and RapidEye identified the general location of forest loss within a particular year (Figure 3.7, 3.8 and 3.9). However, the GFC product underestimated forest loss from gold mining by 70.6% and 77.7% at Mahdia and Puruni respectively from 2011-2016 relative to RapidEye.

This underestimation may be explained by lags or delays in forest loss detection. Delays may occur due to (1) cleared areas being missed during the year when forest was felled, especially if (2) subsequent Landsat scenes were obscured by cloud cover. Lags would be expected in the GFC product due to the resolution of scenes. Here, the higher resolution RapidEye imagery permits the detection of

smaller scale disturbances (Figures 3.8 and 3.9) which may only be detected by GFC later if expanded in size and intensity, as may be the case when forest loss was viewed as a total (i.e. 2011-2016). These findings also concur with other studies examining the GFC product with RapidEye imagery on traditional land uses such as agriculture (Milodowski et al. 2016).

While the spatial patterns of change indicated by GFC were relatively consistent with RapidEye, there were notable discrepancies in estimates of area deforested. Comparing across sites, the performance of the GFC product was notably better for Puruni than Mahdia, with the majority of GFC forest loss (51.3%) lagging within the MRVS pre2011 tile. As such, higher omissions were detected in Mahdia for mapped forest loss with a large number of pixels classified as either clouds (~27%) or pre2011 gold mining sites (~24%) (Figure 3.9, Table 3.5). Here, cloud cover, a lag and the impact of forest clearance size may be driving the detection processes seen across sites. Further, differences seen across products may be due to (1) pre-1990 forest loss activities which may be captured by the RapidEye tiles, especially in Mahdia which has a long history of gold mining dating back to the 1880s (see Chapter 1.7), (2) the MRVS benchmark map may include mining activities within government concessions but exclude illegal gold mining which RapidEye can detect, and (3) the cloud algorithm used by GFC may detect the surface reflectance of gold mining sites as clouds, such as what may have occurred in Mahdia (see Figures 3.7 and 3.8).

While GFC underestimated gold mining activities, it is important to note the advantages associated with this type of Landsat data including a long history of use, global acquisition, pre-processing and archiving of data, and free access to data. In contrast, RapidEye is costly and pre-processing and corrections are required. As such, Milodowski et al. (2017) suggested that areas of forest loss driven by a mosaic of small clearances may require a correction factor of +~25% in the GFC product to ensure comparable change estimates with those of RapidEye, while a correction of +~5-15% is required for large scale forest loss. This, however, was not tested in this study due to time limit.

3.5.3 Implication of gold mining underestimation and detection in Amazonia

The results presented in this chapter are significant in that they demonstrates that (1) forest loss resulting from gold mining activities is increasing across the northern Amazon and within protected areas, and (2) the performance of large scale deforestation products like GFC varies dependent on type and size of disturbances, suggesting that a negative bias is likely in regions dominated by small-scale forest loss such as those occurring initially due to small-scale gold mining. Mining activities within highly biodiverse protected areas will have far-reaching consequences on water, soil and vegetation which may reshape the dynamics of the forest landscape across Amazonia (from forests to bare lands). Further, if forest loss from gold mining activities are underestimated due to a lack of detection, it inherently becomes more difficult to monitor and control.

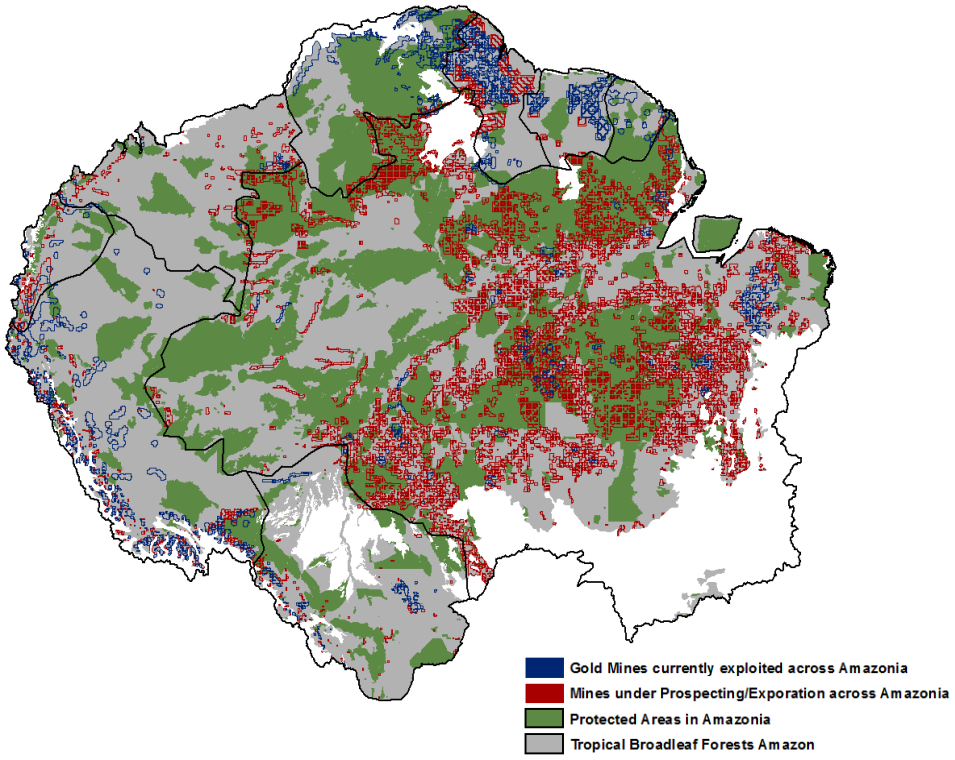

Figure 3.11: Gold Mining Sites across Amazonia digitized from Alvarez-Berríos and Mitchell Aide (2015) and RAISG (2012): blue polygons represent polygons that are currently exploited (370,396 km^2) while red polygons indicate mining sites under exploration and/or prospecting licenses (1,382,024 km^2).

Assuming that the underestimation of forest loss observed in our Guyanese plot applies more broadly to the Amazon, the implications are worrying, especially as 370,396 km^2 is under known active mining concessions with another 1,382,024 km^2 currently under prospecting for mining across Amazonia (Alvarez-Berríos and Mitchell Aide 2015, RAISG 2012, Figure 3.11).

Overall, the results presented here showed that expanding gold mining across the region will require at least sampling using global and open higher resolution (3m or 5m) forest cover imagery to accurately determine the level of underestimation of small-scale forest loss events, which can inform better enforcement and/or the development of conservation policies.

4

Small-Scale Gold Mining Inhibits Soil and Plant Nutrient Cycling

4.1 Abstract

The recent expansion of small-scale gold mining has contributed to the transformation of the Amazonian landscape, causing widespread environmental damage associated with mercury contamination, soil erosion and aquatic siltation, and loss of biodiversity. However, the impacts on soil and vegetation nutrient cycling remain poorly known. Here I quantify mercury and nutrient concentrations in soil and vegetation in the mining pits, tailing ponds and overburden zones of two sites recovering from small-scale gold mining disturbance in Guyana. I also assessed mercury tolerance of the most dominant species in the abandoned mining plots. Based on the results, gold mining leads to increased mercury levels and a severe depletion of soil nutrients (exchangeable cations, nitrogen and phosphorus) on tailing ponds and mining pits, compared to overburden zones. Plant nutrient concentrations across plots largely reflected the patterns of soil nutrient concentrations, with greatly reduced foliar N and P in tailing pond vegetation relative to control and overburden vegetation. Mercury levels were also ~240 times higher in active mines than at abandoned mining sites, indicating mercury may be leaching to neighbouring areas. *Andropogon bicornis, Cecropia obtusa, Miconia argyrophylla, Vismia angusta and Vismia guianensis* were shown to be tolerant of mercury. These results highlight species which may be utilized for rehabilitation of sites and that active restoration is required using the overburden to enhance soil and vegetation nutrient levels.

4.2 Introduction

As small-scale gold mining continues to flourish across Amazonia, with ~1680 km^2 of forest lost between 2001-2013 (Alvarez-Berrios and Mitchell Aide 2015), it exposes ecosystems to novel perturbations, threatening their integrity and functioning (Asner et al. 2013, Alvarez-Berríos and Mitchell Aide 2015). Extracting gold requires a combination of forest removal, hydraulic abstraction of soil with water jets from high pressure hoses and processing the ore in sluice boxes and gold pans (Hammond et al. 2007). Gold is then recovered from the heavy fraction of the sediment by amalgamation with mercury, as it is cost effective and allows for easy separation from the surrounding soil (Veiga et al. 2014). This gold-mercury complex is then burned in the open air. An estimated 30-150 tons of mercury vapour was released into the Brazilian Amazon atmosphere during the 1990s alone from burning this gold-mercury complex (Pfeiffer et al. 1993), while historically approximately 0.3 to 1kg of mercury for every 1kg of gold is lost to rivers and soils through handling in field conditions and due to its volatility (Pfeiffer and de Lacerda 1988, Veiga et al. 2006, Swenson et al. 2011, Esdaile and Chalker 2018). This amalgamation process may be repeated 3 or 4 times to maximize gold extraction (Esdaile and Chalker 2018), with mercury rich tailings left in most mining sites.

The majority of studies assessing the impacts of gold mining have focused primarily on mercury (Hg) pollution in aquatic systems in Amazonia (Mol et al. 2001, Mol and Ouboter 2004, Santos-Francés et al. 2011, Laperche et al. 2014), whereas the impact on soil and vegetation is often neglected. For the few existing studies, data on the distribution and contamination of soils from gold mining is often limited to only one of the three mining zones, specifically the tailing pond (Arets et al. 2006, Garcïa-Sánchez et al. 2006, Guedron et al. 2009, Howard et al. 2011, Santos-Francés et al. 2011, Grimaldi et al. 2015). The effects of gold mining on overburden and mining pit areas are rarely assessed. From Guedron et al. (2009), we know that mercury has a high affinity for organic matter, clay minerals and iron (Fe), aluminium (Al), and Manganese (Mn) oxides. Yet, the mining zones (overburden, mining pit and tailing pond) tend to vary in soil properties and structure, and hence, the retention capacity for mercury may also

vary. As natural vegetation may regrow on these areas, plants will uptake mercury and this may alter tree physiological functions by interfering with membrane functioning, water relations, protein metabolism, and seed germination (Espinosa-Reyes et al. 2014).

Further, important gaps remain in our knowledge on the role of small-scale gold mining on nutrient cycling (defined here as nutrient content), beyond the impacts of mercury. As many elemental cycles are coupled (Townsend et al. 2011), the ability of vegetation to regenerate from gold mining is likely influenced by the availability of certain nutrients. For instance, soil nutrients (exchangeable cations, nitrogen and phosphorus) are crucial for the successful establishment of plants (Litaor et al. 2017). The removal of topsoil during the mining process has the potential to greatly alter soil and plant nutrient status, but these impacts have been little quantified. Furthermore, the relative roles of nutrient depletion and soil mercury in inhibiting forest recovery post-mining remain largely unstudied.

Given that there is relatively limited information on how gold mining may impact on nutrient cycling, we can hypothesize potential changes based on more traditional land use disturbances caused by the complete clearance of forests such as agriculture, pasture and oil exploration (dos Santos et al. 2006, Powers and Marín-Spiotta 2017). While many intact lowland tropical systems are relatively poor in phosphorus and rich in nitrogen, land use disturbances such as agriculture and pasture, can cause nitrogen losses and can drive relatively phosphorus-poor systems towards nitrogen limitation in the early stages of secondary succession (Davidson et al. 2004a, Markewitz et al. 2004). As such, while there can be a brief surge of nitrogen mineralization following disturbance, nutrient losses and lower mineralization rates in degraded lands may limit available nitrogen and phosphorus, restricting vegetation regrowth (Nagy et al. 2017).

Several studies on forest recovery following deforestation have shown that nitrogen availability often controls how fast these systems can recover (Davidson et al. 2007, Batterman et al. 2013, Powers and Marín-Spiotta 2017). For these systems, nitrogen availability may recover over a time-scale of 10-15 years due in part to N_2-fixers (Batterman et al. 2013). However, phosphorus recovery may be more restricted. Conversion to pastures and agricultural lands creates a shift from phosphorus (P) limitation in mature forests to nitrogen (N) limitation in disturbed areas, with P constraints remaining despite vegetation recovery (Davidson et al.

2007). Low N availability may sometimes persist even after recovery from traditional disturbances (Pellegrini et al. 2014), but is strongly coupled to plant community composition and the presence of N_2-fixers (Batterman et al. 2013). When disturbances occur, legumes are often not abundant in recovering forests, and so mineralization of soil organic N is the most likely source of N needed to meet plant demand (Markewitz et al. 2004). Degraded sites such as pastures only possess ~2% of the N originally present in mature forest (149 kg N ha^{-1} yr^{-1} vs 46 kg N ha^{-1} yr^{-1}, Markewitz et al. 2004). Similarly, the level of phosphorus needed for growth may be species-specific, with no difference in community-wide response along a P gradient as some species may grow rapidly in infertile soils despite low P availability (Turner et al. 2018). Some studies across Amazonia have shown ~50% loss of P in soils shortly after fires (see Markewitz et al. 2004). Exchangeable cations, which are important for plant growth, greatly change base on the level of disturbance. For instance, soil nutrient analysis conducted by dos Santos et al. (2006) in soils formerly under oil exploration indicated that topsoil removal impoverished soil cations P, potassium (K), and Magnesium (Mg), with the exception of Calcium (Ca). dos Santos et al. (2006) also found that micronutrients concentrations (Fe, Mg and Mn) were also greater in soils formerly under oil exploration and may be linked to a significant reduction in soil pH levels. These metals are more soluble in acidic soils, and can dissolve to form toxic concentrations that may hinder plant growth. However, Markewitz et al. (2004) showed that degraded pastures possessed ~15% K, 11% Ca and 6% Mg compared to mature forests. Even lower Ca contents (3% compared to mature forests) were found in managed pastures where little woody material existed even after 10+ years since abandonment (Markewitz et al. 2004).

As gold mining removes the top 3-5m layer of nutrient rich soils, it leaves behind mining pits and tailing ponds with previously lower layers now forming their top layer. Therefore, mining pits and tailing ponds are likely to be depleted in nutrients, potentially leading to slow recovery and altered vegetation composition. Overall, this may restrict the ability of subsequent gold mining sites to fully recover. However, whether or not this mining-nutrient feedback emerges, and on what scale it operates (for example, across mining zones or soil type) is unknown.

To address these knowledge gaps, I conducted fieldwork in two known small-scale gold mining regions in Guyana to assess the impact of gold mining activity on soil and vegetation nutrient cycling across different mining zones (overburden, tailing pond and mining pit) following abandonment of gold mining. For each site, I specifically assess (1) What are the levels of mercury concentrations in soils and vegetation at my two field sites and across different mining zones? 2) What are the levels of available exchangeable cations (Mg, Ca, K, Na, Al, Fe, Mn) across sites and mining zones? 3) How does nitrogen and phosphorus concentrations in soils and vegetation vary across mining zones and sites? and 4) What dominant species present in the abandoned mining sites may be tolerant to higher mercury concentrations? This is, to my knowledge, the first study to provide detailed, field-based information on the impacts on soil and plant nutrients across different mining features at abandoned gold mining sites.

4.3 Methods

4.3.1 Study site and field collection

The study was conducted in two major gold mining sites in Guyana, namely Mahdia and Puruni, from January to March, 2016 (Figure 4.1). A description of both sites can be found in Chapter 1.7. At each of the two study sites, measurement plots were established on previously mined vegetation patches, ranging in age from 0.6 to 3 years since abandonment of mining activity. Sites were selected based on accessibility and abandonment. As gold mining sites tend to be re-mined, no site >3 years since abandonment was found. Each plot was positioned so as to include the three zones of artisanal gold mining sites, i.e. the mining pit, the mine tailings (deposits of material left over after the gold has been separated from the ore) and the overburden (areas overlying the ore which are displaced during the mining process). For reference, I also measured soil properties in (1) active tailing pond mines in both Mahdia and Puruni and (2) a reclamation site in Mahdia, which was planted with 5300 *Acacia mangium* trees since 2010. *Acacia mangium* is not native to Guyana and was planted in a previous mining pit. *Acacia* was selected for replanting as it fast growing, tolerant of low pH conditions and has a symbiotic relationship with nitrogen fixing

Rhizobium bacteria (GGMC 2011). The mercury concentrations on active sites provide further indication of the timescales for persistence of mercury in the soil.

Eight soil samples to 30 cm depth were collected with a 2.5 cm diameter corer in each plot, including old-growth control plots, in January to March, 2016. All soil samples were air-dried, mixed for homogeneity and brought back to the laboratory for determination of cation exchange capacity (CEC), total nitrogen concentration (TN), total phosphorus concentration (TP), mercury concentration and particle size distribution. Additionally, ten sunlit leaves from three individuals from the ten most dominant species (4 from overburden, 3 from the mining pit and 3 from the tailing pond) were collected in each plot, including old-growth control plots, in January to March, 2016. Dominant species within plots were *Andropogon bicornis, Cecropia obtusa, Miconia argyrophylla, Vismia angusta, Vismia guianensis, sedges, and Scleria secans* (Poaceae). All leaf samples were air-dried and brought back to the laboratory for determination of TN, TP and mercury concentration. Due to financial restrictions on lab analysis, I was only able to analyse material from one individual for each species per plot combination.

4.3.2 Analysis of Exchangeable Cations, Particle Size and Bulk Density in Soils

For determination of CEC, approximately 5g of soil was passed through a 500-μm sieve, to which 30 mL of silver-thiourea (Ag-TU) was added. Samples were shaken and centrifuged at 2000 rpm for 15 minutes and then analysed by inductively coupled plasma optical emission spectroscopy (ICP-OES) for exchangeable cations (Mg, Ca, K, Na, Al, Fe and Mn) as described by Dohrmann (2006). Due to financial restrictions on lab analysis, I was unable to analyse soils from the control sites. A range of methods described in BS: 1377:1967 (British Standards Institution 1967) was used to analyse the soil samples for texture and particle size. Confirmation was obtained for clay and silt fraction using laser diffraction (Brown et al. 1990), while soil bulk density analysis was done using the core method (Rowell, 1994).

4.3.3 Analysis of Total Nitrogen and Total Phosphorus in Soils and Plants

For determination of TN and TP, I utilized the method of Allen (1989) where approximately 0.25g soil and 0.25g of plant material were independently

passed through a 2-mm sieve with 4.4 mL of mixed digestion reagents (100 volume hydrogen peroxide, concentrated sulphuric acid, lithium sulphate and selenium powder) added to each sample. Using a hot block, samples were heated gently to 300°C and were then left to cool and deionised water was added to make up a volume of 50 mL. Samples were then analysed using a Skalar SAN++ continuous flow autoanalyser.

4.3.4 Analysis of Mercury in Soils and Plants

Mercury (Hg) concentrations were determined using a closed vessel acid digestion method (Ure and Shand 1974) by passing 1g of soil and 3-5g of plant material independently through a 2-mm sieve. The open acid digestion method was initially tested but mercury was lost during the process, especially in areas where high mercury concentrations were expected to be high such as active mines, reported as low levels. A 5mL aliquot of concentrated nitric acid (HNO_3) was added to each sample and the vessel was assembled with a Kevlar outer layer and run with a CEM MARS microwave digester programme for 30 minutes at 150^{o}C. Samples were quantitatively transferred into 50 mL centrifuge tube. A 6% m/v aqueous potassium permanganate ($KMnO_4$) solution was added drop wise with a permanent pink colour appeared in order to prevent loss of mercury and to remove oxides of nitrogen. The sample was then diluted to 50 mL and left overnight to allow the particulate residue to settle. The samples were then analysed by Thermo iCAP ICP-OES (soil) or ICP-OES-hydride generation (plant material). A total of 60 soil and 70 leaf samples were examined. An annotation should be made here that mercury may have been lost from samples during storage as I was only able to analyse samples one year after collection due to financial constraints.

4.3.5 Statistical Analysis

To examine the effects of mining sites (Mahdia vs. Puruni) and individual zones (overburden, mining pit, tailing pond) on soil and plant material, linear mixed effects models were used, with a random intercept for each plot. Nutrient and mercury contents were log-transformed prior to analysis to satisfy requirements of normality and homogeneity of variance. These analyses were conducted using *nlme* package in R (Pinheiro et al. 2018). Similar mixed effects models (with mining zones and sites as fixed effects and plot as a random effect),

were constructed to examine how soil nutrient content (exchangeable cations, TN, TP) and soil Hg differed between the two mining regions and across the mining features considered. Mixed effects models were also used to examine differences among sites and zones for nutrient and mercury concentrations in plant materials with plot and plant species as random effects.

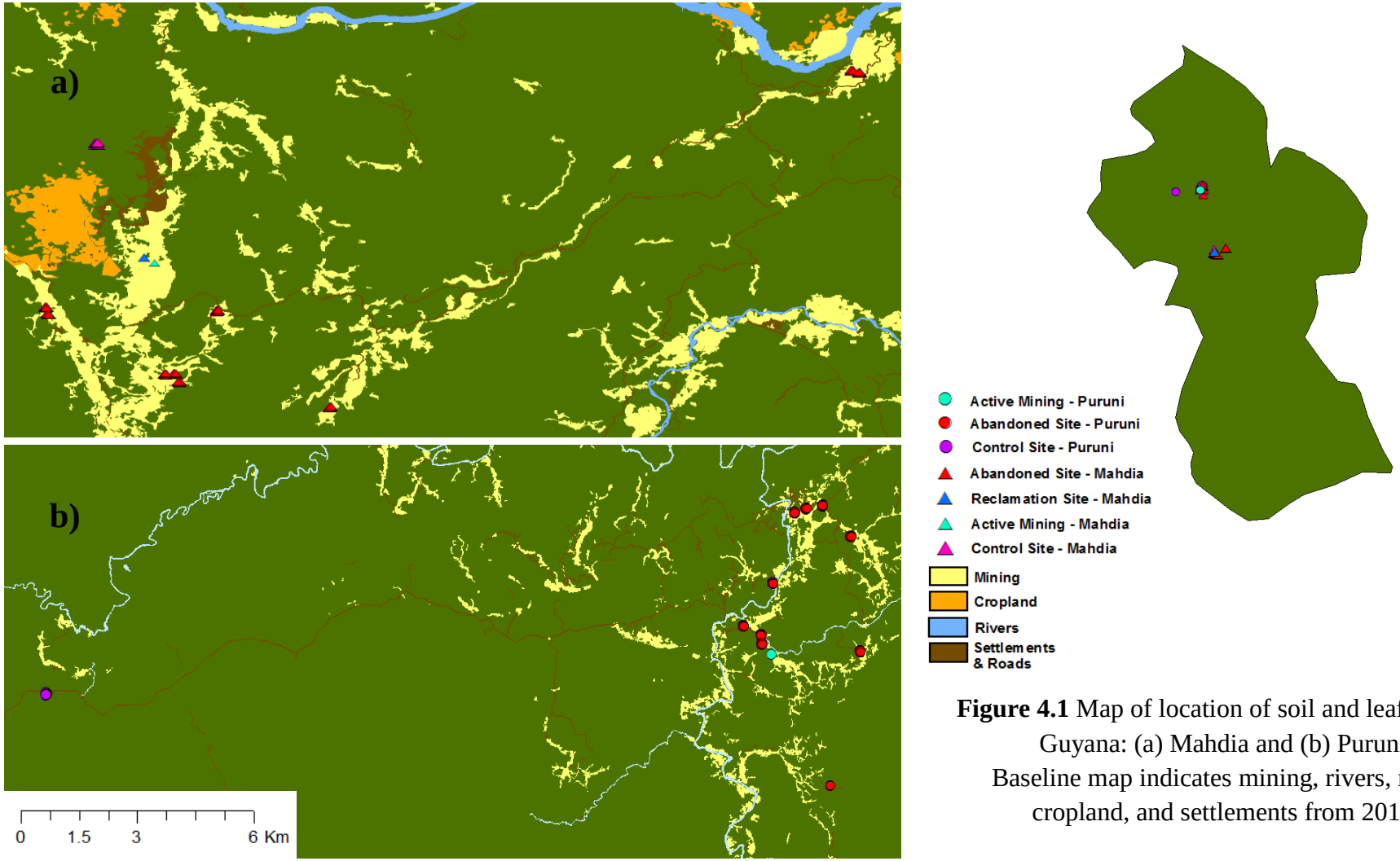

Figure 4.1 Map of location of soil and leaf samples Guyana: (a) Mahdia and (b) Puruni. Baseline map indicates mining, rivers, roads, cropland, and settlements from 2014.

4.4 Results

4.4.1 Soil nutrient and mercury levels

Significant differences were observed across mining zones (overburden, tailing pond and mining pit) for mercury concentration ($p<0.0001$), total nitrogen ($p=0.004$) and exchangeable cations ($p=0.04$) based on mixed effects models (Table 4.1), with study site showing no significance across all variables (Table 4.1). Total phosphorus showed no significant differences across site ($p=0.41$) or mining zones ($p>0.22$), but did show clear directional trends in both Mahdia and Puruni sites, with mean values being greatest in the control plots, followed by the overburden plots, with the lowest values in the tailing pond.

Table 4.1 Summary Results from Mixed-effects Models for Mercury concentrations, Total Nitrogen, Total Phosphorus and exchangeable cations (CEC) in soils

	log(Hg)		**log(TN)**		**log(TP)**		**log(CEC)**	
	F-value	*p-value*	*F-value*	*p-value*	*F-value*	*p-value*	*F-value*	*p-value*
Site	4.82	0.06	2.37	0.17	0.76	0.41	0.32	0.59
Zone	**16.11**	**0.0001**	**7.76**	**0.004**	1.69	0.22	**4.13**	**0.04**
Site*Zone	0.62	0.55	0.003	0.997	0.25	0.78	0.13	0.88

Comparison among mining zones and between sites for total nitrogen showed overburden at Mahdia contained 247% and 160% more TN than tailing pond and mining pit respectively, while TP levels were 88% and 60% higher than tailing pond and mining pit (Table 4.2, Figure 4.2). Similarly, overburden features at Puruni contained more TN (1560% and 730% respectively) and TP (633% and 5% respectively) than tailing pond and mining pit (Table 4.2, Figure 4.2). When compared to their respective control sites, the overburden zone at Mahdia and Puruni exhibited 145% and 254% less TN, while TP was 12.5% and 118% lower respectively. No vegetation was present in active mining sites.

Mercury concentrations in the overburden zone were 60% and 50% lower than tailing pond and mining pit at Mahdia respectively, while mercury concentration at Puruni was 80% and 63% lower than the two mining zones

respectively (Table 4.2, Figure 4.2). In contrast, mercury concentrations were considerably higher in the overburden at both Mahdia (85%) and Puruni (33%) compared to old growth forests (Figure 4.2).

A 48-to-120 fold increase in mercury concentration was observed at active mines in Mahdia compared to the abandoned mining zones, while in Puruni, active mines were 10-50 fold higher than abandoned mining zones (Figure 4.2). Substantially higher concentrations of mercury were also observed at active mines in Mahdia (800 fold increase) and Puruni (75 fold increase) compared to their respective old-growth forests (Figure 4.2). Although mining pits and tailing ponds had only been abandoned for 6 months to three years, their mercury concentrations were two orders of magnitude lower than active site concentrations. This suggests that leaching of mercury from soils of mining areas happens very quickly. This leached mercury likely enters water courses in the surrounding areas, but we did not quantify mercury concentrations in water bodies.

Differences between mining zones were also found for exchangeable cations (Table 4.2, Figure 4.3). On the overburden Mg+, Ca+, K+ and Na+ cations were high at Mahdia and Puruni compared to tailing pond and mining pits (Figure 4.3). In contrast, concentrations of Al+, Fe+ and Mn+ cations were higher in the tailing pond and mining pit relative to overburden zones at both sites (Figure 4.3). A positive correlation was observed between exchangeable cations and other soil nutrients such as nitrogen ($p<0.001$) and phosphorus ($p<0.05$), but negatively correlated with mercury concentrations ($p=0.6$) across sites and mining zones (Figure 4.4).

Exchangeable cations were also positively correlated with sandy and clay soils (Table 4.3, Figure 4.4), while mercury concentration was positively and significantly correlated with clay ($p<0.05$) soils. Soil bulk density was higher (>1.6 g/cm^3) in the tailing ponds, mining pits and at active mine sites at both Mahdia and Puruni compared to the control and overburden zones (Table 4.3). TN and TP were positively correlated, but not significant, with silt and clay soils only (Figure 4.4).

Table 4.2 Mean soil nutrient concentrations with standard errors (mg/g) in different mining features in Mahdia and Puruni.

Site	Feature	Hg	TN	TP	Mg	Ca	K	Na	Al	Fe	Mn
Mahdia	Control	0.00003 ± 0.00003	2.55 ± 1.27	0.36 ± 0.18	-	-	-	-	-	-	-
	Overburden	0.0002 ± 0.0001	1.04 ± 0.35	0.32 ± 0.07	0.01 ± 0.004	0.04 ± 0.01	0.004 ± 0.001	0.004 ± 0.001	0.005 ± 0.003	0.003 ± 0.002	0.0006 ± 0.0004
	Mining Pit	0.0004 ± 0.0001	0.4 ± 0.21	0.2 ± 0.05	0.0012 ± 0.0003	0.003 ± 0.0003	0.002 ± 0.0007	0.003 ± 0.0002	0.012 ± 0.007	0.003 ± 0.001	0.005 ± 0.004
	Tailing Pond	0.0005 ± 0.0001	0.3 ± 0.11	0.17 ± 0.1	0.003 ± 0.001	0.006 ± 0.003	0.002 ± 0.0004	0.003 ± 0.0002	0.013 ± 0.005	0.005 ± 0.003	0.008 ± 0.007
	Active Mine	0.024 ± 0.007	-	-	-	-	-	-	-	-	-
	Reclaimed Site	Undetectable	-	-	-	-	-	-	-	-	-
Puruni	Control	0.00004 ± 0.00002	2.94 ± 1.47	0.48 ± 0.24	-	-	-	-	-	-	-
	Overburden	0.00006 ± 0.00004	0.83 ± 0.55	0.22 ± 0.19	0.009 ± 0.005	0.03 ± 0.02	0.01 ± 0.004	0.005 ± 0.001	0.003 ± 0.001	0.0002 ± 0.0001	0.001 ± 0.001
	Mining Pit	0.00016 ± 0.00004	0.1 ± 0.06	0.21 ± 0.16	0.002 ± 0.001	0.004 ± 0.002	0.002 ± 0.0004	0.003 ± 0.0003	0.005 ± 0.001	0.001 ± 0.0002	0.005 ± 0.004
	Tailing Pond	0.0003 ± 0.0001	0.05 ± 0.01	0.03 ± 0.01	0.002 ± 0.002	0.005 ± 0.004	0.002 ± 0.001	0.003 ± 0.0003	0.014 ± 0.006	0.0018 ± 0.0007	0.007 ± 0.004
	Active Mine	0.003 ± 0.002	-	-	-	-	-	-	-	-	-

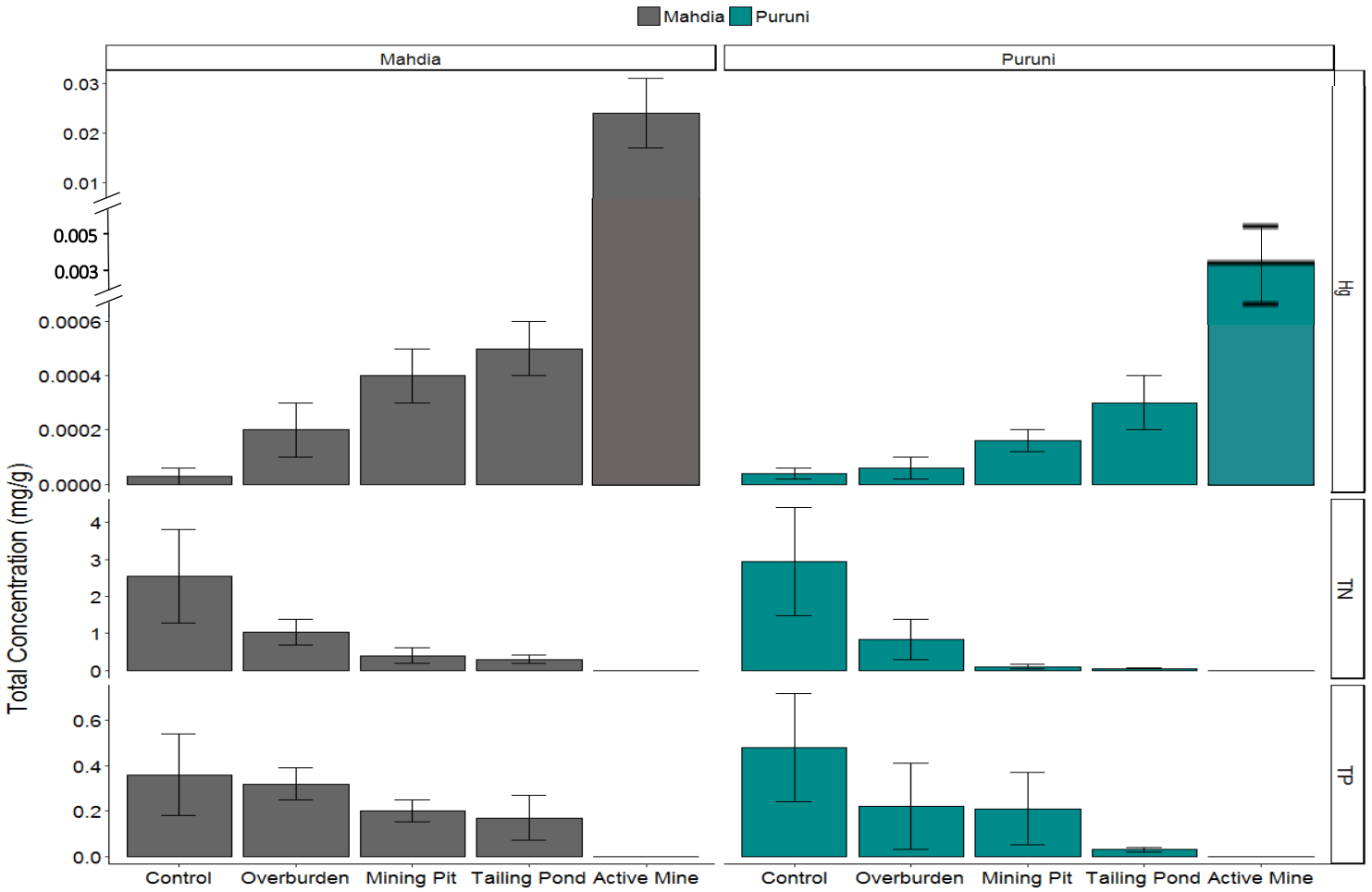

Figure 4.2 Mercury, Total Nitrogen and Total Phosphorus concentrations with standard error bars (mg/g) in soils from mining zones (overburden, tailing pond, mining pit) and active mines compared to old-growth sites at Mahdia and Puruni. Mercury levels were undetectable in the reclamation site.

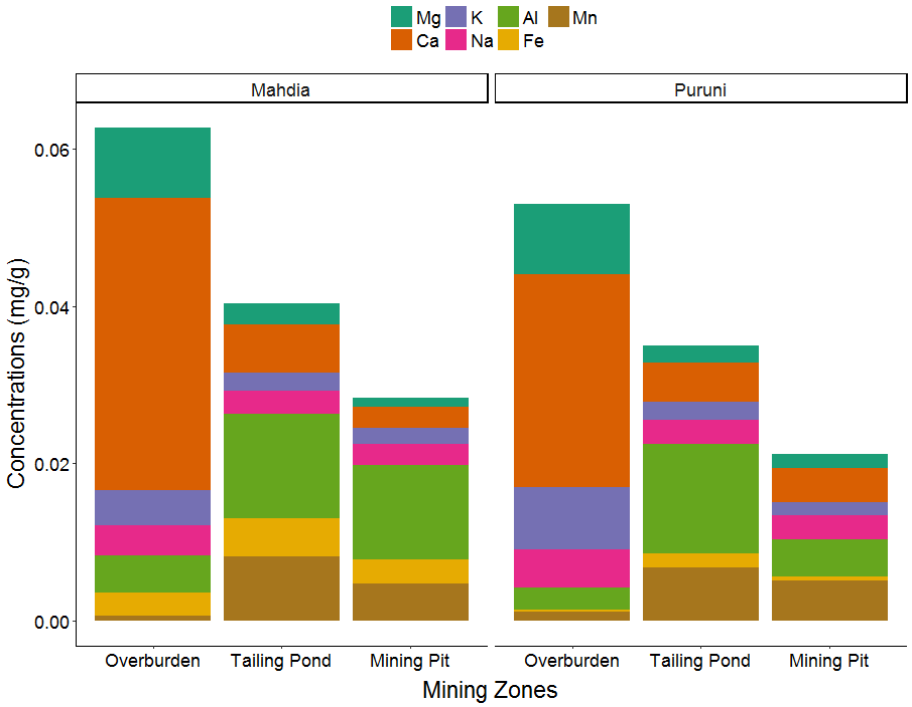

Figure 4.3 Exchangeable cations (mg/g) in soils from overburden, tailing pond and mining pit in Mahdia and Puruni.

Table 4.3 Soil texture and bulk density analysis across mining zones at abandoned gold mining sites in Mahdia and Puruni.

Site	Feature	Sand %	Silt %	Clay %	Bulk Density (g/cm^3)
Mahdia (n=7)	Control	86.82	11.06	2.34	1.2
	Overburden	3.93	54.64	38.24	0.7
	Mining Pit	21.21	32.48	44.80	1.8
	Tailing Pit	38.32	17.54	36.28	2.3
	Active Mine	84.47	14.56	0.97	1.9
	Reclamation Area	92.93	1.01	6.06	1.5
Puruni (n=6)	Control	72.73	12.24	12.23	1.2
	Overburden	86.76	5.78	7.45	1.3
	Mining Pit	31.68	43.20	10.87	1.7
	Tailing Pit	73.27	18.83	4.42	2.2
	Active Mine	88.89	11.23	2.22	1.6

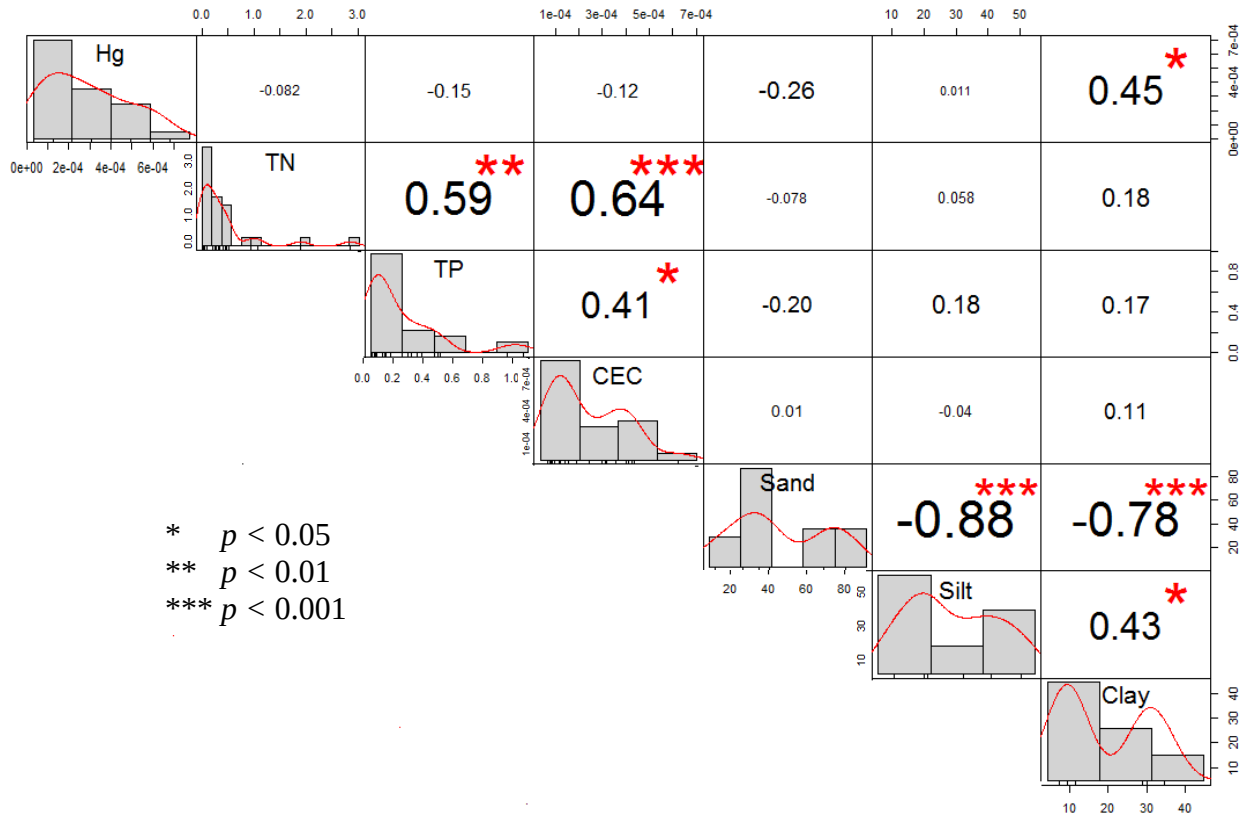

Figure 4.4 Correlation matrix of mercury concentration, soil nutrients (nitrogen and phosphorus), exchangeable cations (CEC) and soil textures with data distribution graphs (mg/g) and associated p-values. Red star (*) presents significant *p*-values.

4.4.2 Plant nutrient and mercury levels

Mercury concentration (p=0.01), total nitrogen (p<0.0001) and total phosphorus (p<0.01) were significantly different in plant nutrient composition across mining zones (overburden, tailing pond and mining pit) based on mixed effects models (Table 4.4). Site was not found to be a significant predictor of plant concentrations of Hg, TN and TP.

Table 4.4 Summary Results from Mixed-effects Models for Mercury concentrations, Total Nitrogen and Phosphorus concentrations in plants.

	log(Hg)		**log(TN)**		**log(TP)**	
	F-value	*p-value*	*F-value*	*p-value*	*F-value*	*p-value*
Site	1.20	0.3	0.61	0.46	0.61	0.46
Zone	**11.49**	**0.01**	**68.08**	**<0.0001**	**5.88**	**<0.01**
Site*Zone	1.49	0.36	**9.18**	**<0.001**	0.63	0.54

Difference across mining zones showed that the overburden at Mahdia contained an additional 190% and 104% TN than tailing pond and mining pit respectively, while TP levels were 151% and 77% higher compared to the two mining zones respectively (Table 4.5, Figure 4.5). Similarly, overburden zones at Puruni contained higher concentrations of TN (665% and 282% respectively) and TP (131% and 56% respectively) than tailing pond and mining pit (Table 4.5, Figure 4.5). Compared to their respective control sites, overburden zones contained 75% and 57% lower TN at Mahdia and Puruni respectively, while control sites contained 5.3% and 33% higher TP concentrations at the two study sties respectively (Figure 4.5).

In contrast, mercury concentrations on the overburden was 82% and 25% lower than tailing pond and mining pit at Mahdia, while at Puruni, overburden zones had 89% and 25% lower mercury levels than the other two zones respectively (Table 4.5, Figure 4.5). Mercury concentrations were 33% and 60% lower in control sites compared to overburden zones at Mahdia and Puruni respectively (Table 4.5). Reclamation area had 37% lower TN than old growth forests while containing an additional 22% TN relative to overburden zones at Mahdia. TP at the reclamation area was 138% and 126% lower than the control site and overburden zones respectively, while mercury concentration at the

reclamation area was 83% and 75% higher at the control site and overburden zones respectively (Table 4.5).

Table 4.5 Mean plant nutrients with standard error (mg/g) in different mining features in Mahdia and Puruni.

Site	Zones	Hg	TN	TP
Mahdia	Control	0.00002 ± 0.000003	27.84 ± 3.20	1.19 ± 0.22
	Overburden	0.00003 ± 0.00002	15.90 ± 1.39	1.13 ± 0.2
	Mining Pit	0.00004 ± 0.00001	7.78 ± 0.22	0.64 ± 0.09
	Tailing Pond	0.00017 ± 0.00005	5.48 ± 0.5	0.45 ± 0.11
	Reclamation Area	0.00012 ± 0.00005	20.28 ± 1.52	0.5 ± 0.03
Puruni	Control	0.000012 ± 0.0000005	32.02 ± 7.94	0.89 ± 0.11
	Overburden	0.00003 ± 0.00002	20.42 ± 3.76	0.67 ± 0.06
	Mining Pit	0.00004 ± 0.00001	5.34 ± 1.82	0.43 ± 0.14
	Tailing Pond	0.00027 ± 0.00011	2.67 ± 0.73	0.29 ± 0.1

Based on the analysis of dominant species present within the plots, different plant species exhibited varying concentrations of TN, TP and Hg (Table 4.6). In the overburden and tailing pond zones in Mahdia, *Miconia argyrophylla* contained the highest concentrations of mercury, while a seedling *Carapa guianensis*, though not dominant within the Mahdia plot where it was found, contained the highest mercury levels in the mining pit (Table 4.6). Analysis on the *Carapa guianensis* seedling was conducted as it is an important timber species in Guyana, with the seeds being utilized in cosmetic products. In contrast, *Vismia angusta*, which is common in secondary recovering forests, and sedges contained the lowest concentration of mercury across the three mining zones in Mahdia (Table 4.6). At Puruni, *Cecropia obtusa* had the highest mercury concentration on the overburden, while *Miconia argyrophylla*, *Andropogon bicornis* and sedges had the highest concentration of mercury in the tailing pond. The lowest concentrations of mercury was found in *Miconia argyrophylla* and sedges in the overburden and mining pit respectively at Puruni.

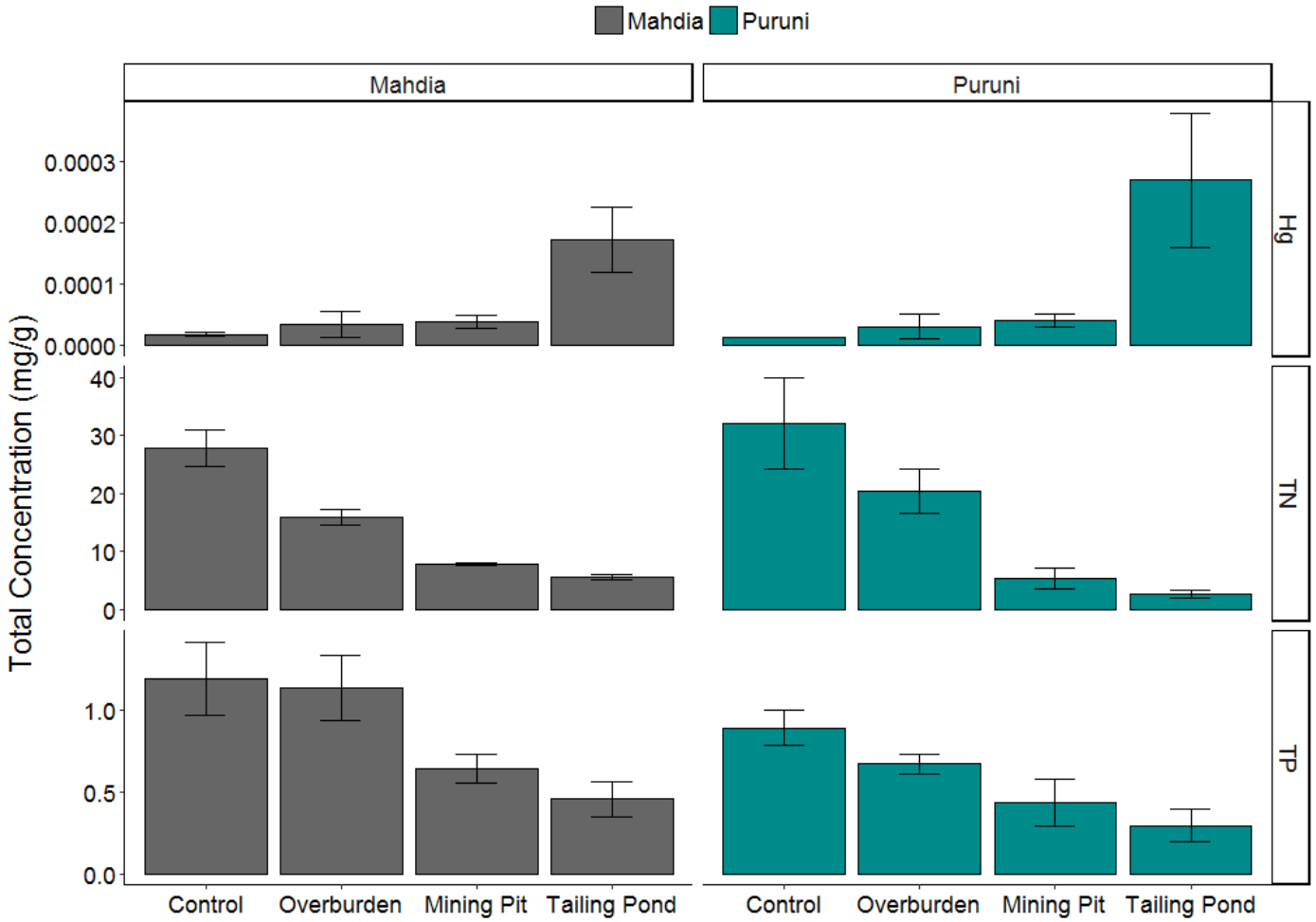

Figure 4.5 Mercury, Total Nitrogen and Total Phosphorus Concentrations with standard error bars (mg/g) in plant materials in Mahdia and Puruni.

Table 4.6 Total Nitrogen, Total Phosphorus and Mercury Concentrations (mg/g) of different species that were dominant across different mining zones in Mahdia and Puruni.

Site	Species	Zone	TN	TP	Hg
Mahdia	*Andropogon bicornis*	Mining Pit	5.81	0.33	0.00005
	Andropogon bicornis	Tailing Pond	4.57	0.45	0.0001
	Carapa guianensis	Mining Pit	8.34	0.49	0.0007
	Cecropia obtusa	Overburden	20.60	1.20	0.00007
	Miconia argyrophylla	Mining Pit	9.52	0.69	0.00006
	Miconia argyrophylla	Overburden	15.55	0.75	0.0007
	Miconia argyrophylla	Tailing Pond	8.57	0.55	0.0002
	Sedges	Mining Pit	7.55	0.96	0.00002
	Sedges	Tailing Pond	5.58	0.37	0.00005
	Vismia angusta	Overburden	14.86	2.21	0.000008
	Vismia guianensis	Mining Pit	5.92	1.11	0.00004
Puruni	*Andropogon bicornis*	Mining Pit	2.95	0.23	0.00002
	Andropogon bicornis	Tailing Pond	2.78	0.22	0.0002
	Cecropia obtusa	Overburden	23.66	1.04	0.00006
	Miconia argyrophylla	Mining Pit	5.13	0.81	0.00004
	Miconia argyrophylla	Overburden	27.06	0.65	0.000004
	Miconia argyrophylla	Tailing Pond	3.54	0.57	0.0003
	Sedges	Mining Pit	9.30	0.56	0.00001
	Sedges	Tailing Pond	4.26	0.45	0.0008
	Vismia guianensis	Overburden	17.68	0.53	0.00005

TN and TP concentrations were higher in *Cecropia obtusa, Vismia guianensis* and *Miconia argyrophylla* at overburden zones at both sites, while *Miconia argyrophylla* and sedges exhibited higher concentration in tailing ponds and mining pits.

4.5 Discussion

4.5.1 Nutrient and mercury dynamics in soils and plants following gold mining

These results demonstrate that gold mining is an important agent of disturbance and soil degradation in tropical forest ecosystems. After mining, the soil lost structure and fertility through deficiency in the nutrient content and cation exchange capacity and an increase in mercury concentrations. This caused decreased soil fertility to levels insufficient to support normal plant growth (Binkley and Fisher, 2013), particularly in the mining pits and tailing ponds. In fact, no woody species was recorded as dominant or present within the mining pits or tailing ponds at either Mahdia or Puruni. In contrast, overburden zones exhibited higher fertility capacity while displaying lower mercury concentrations. This combination of rich nutrient levels and lower mercury concentration allowed for the successful establishment of woody species such as *Cecropia obtusa*, *Vismia angusta* and *Vismia guianensis* which dominated the overburden zones.

As soil texture changed, the mining pits and tailing ponds showed higher retention of mercury due to its affinity to clay soils (Guedron et al. 2009), registering between ~0.0002 and ~0.0006 mg/g of mercury across these zones. The high level of soil degradation in mined pits and tailing ponds can be explained by the process of mineral extraction. As vast amounts of water is usually jetted onto soil surfaces at a very high pressure, disaggregation of the soil particles (Cremers et al. 2013) is prominent. The resulting gold-bearing slurry is then pumped into a sluice box, which collects gold particles, while mine tailings flow into either an abandoned mining pit or the adjacent forest (Peterson and Heemskerk 2001). As re-sedimentation takes place, the various size fractions settle in separate horizons of varying depths, giving rise to new textural classifications, different soil characteristics (Bradshaw 1997) and leaching of soil nutrients.

While plants were found to be tolerant of an external level of 0.0001 mg/g of mercury, physiological and biochemical processes were inhibited between 0.0005 – 0.1 mg/g mercury concentrations (Beauford et al. 1977). As mercury concentration increased, nutrient levels associated with fertility (i.e. TN, TP and exchangeable cations) decreased. Mined soils in the tailing ponds and mining pits at Mahdia and Puruni exhibited lower levels of nutrients (TN and TP) and cations (Mg^+, Ca^+, K^+ and Na+) strongly connected with soil and vegetation growth rates (Sheoran et al. 2010) while containing higher levels of cations (Al^+, Fe^+ and Mn^+) indicative of older, exhausted soils. The impact of nutrient availability can be seen

in the dominant species occurring in the overburden zone at Mahdia versus those on the mining pit at Puruni where similar mercury levels exist but nutrient levels vary. This suggests that nutrient requirements may influence vegetation growth more than mercury levels, though above 0.0005-0.1 mg/g, mercury concentrations start to inhibit the nitrogen fixing abilities of plants due to a breakdown of the nitrogen mineralisation process (Faassen 1973). Lower mercury levels associated with the overburden zone is likely due to the material being excavated prior to mercury application, while higher nutrient levels are likely associated with nutrient rich topsoil, which forms the majority of the overburden.

Cation availability, bulk density and correlation with soil type is site and zone specific (Table 4.3, Figure 4.5) and potentially an artefact of different mining practices used at Mahdia and Puruni, although this was not recorded here. It is expected that soils with sandy texture (2.0 – 0.05 mm) cannot hold as much nutrients as finer textured soils like loam (<0.002 mm) and silt (0.05-0.002 mm) (Sheoran et al. 2010). Therefore, soils with low clay content (i.e. sandy soils) should have a lower propensity for vegetation regrowth and therefore lower cation levels. This is suggested by the results here, although non-significant (Figure 4.5). Additionally, soil compaction, with a bulk density higher than 1.6 g/cm^3, directly limits plant growth and results in decreased capacity of soils to retain water and nutrients. Soils found at the mining pit and tailing pond zones at Mahdia and Puruni were found to have bulk density between 1.7 and 2.3 g/cm^3 indicating that most plant species would be unable to extend their roots effectively through these soils.

TP concentrations at both sites were similar between control and the overburden zone, indicating that P is a limited nutrient. Similarity in P concentrations between the overburden zones and their respective control sites may be due to the dumping of the original soils from the mining pit and tailing pond on the overburden zone. As P is a limiting nutrient, plants may expect to either function with less of it or cycle it more efficiently reflected in higher re-absorption efficiency of P. TP and TN levels at control plots at both Mahdia and Puruni were comparable to other Amazonian forests (Mercado et al. 2011).

Higher concentrations of mercury also differed between active mines and abandoned sites. Mercury levels in active mines were eight times higher in Mahdia than Puruni, potentially indicating (1) higher mercury use at this site, (2) a

longer history and/or reoccurring use of mercury which was reflected in the soil and vegetation of the tailing pond and mining pit, and (3) a higher retention of mercury in clay soils which was present in the Mahdia plots compared to the sandy soils in the Puruni plots. This difference between active and abandoned mines suggests that the majority of the mercury is not retained locally in the soils and may be transported out of the system to surrounding soils and waterways. Other studies have shown that mercury-rich tailings have been detected hundreds of kilometres away from mining sites (Diringer et al. 2015). If mercury is leached to neighbouring areas so quickly, this may lead to larger ecological impacts than previously estimated. Across Amazonia, the estimated level of mercury in soils was on average 0.0001 mg/g, with a reported range of 0.00005-0.00015mg/g (Santos-Francés et al. 2011). Mercury concentrations in active mines were ~3 to 240 times higher at Puruni and Mahdia respectively than reported levels in the literature (Howard et al. 2011, Santos-Francés et al. 2011, Figure 4.3). However, mercury concentration in the overburden in Puruni was the only mining zone that was within the range of reported mercury levels, while all other zones were higher.

As cation and nutrient (TN and TP) concentrations limit vegetation growth in most natural soils (Bell 2002, Mercado et al. 2011), the results presented here suggest that vegetation regrowth and soil fertility may decrease with increased mining activity in mining pit and tailing ponds, while overburden zones may recover to some extent. This indicates that refilling the mining pit and tailing ponds with the displaced overburden soils may improve rehabilitation at these zones. However, the effectiveness of rehabilitation has not been systematically tested.

4.5.2 Implications for soil and vegetation recovery and rehabilitation

These results indicate that the soils from the mining pit and tailing ponds are highly impoverished in terms of nutrients and high levels of mercury. Thus vegetation regrowth is likely to be very slow and few plants may be able to grow in such conditions. On the other hand, increased soil and plant nutrients on the overburden areas may permit plant recovery to former levels. As a result, the overburden may be effective as a restoration resource. To what extent refilling the

tailing ponds and mining pits with the overburden soils will aid recovery is not clear and should be further explored.

Gold mining activities also modified both the composition and structure of vegetation, with very specific species occupying this landscape, and may be dependent on nutrient and mercury levels. A *Miconia argyrophylla* successional pathway was dominant at overburden zone in Mahdia while a combination of *Miconia argyrophylla* and *Cecropia obtusa* was abundant in Puruni. This suggests that the overburden successional pathway behaves similarly to more traditional land uses such as pasture and agriculture (Chazdon et al. 2007). The dominant species growing on the overburden may reflect those that are capable of fixing nitrogen, especially at Puruni, as nutrients were high and mercury concentrations relatively low. On the other hand, species in the tailing pond and mining pit may be tolerant of high mercury levels or have lower nutrient requirements. *Andropogan bicornis, Miconia argyrophylla* and sedges dominated in the tailing pond and mining pits across both locations, which may suggest that these species are able to utilise a shallower root system due to the high compaction of soils and may be tolerant to high mercury concentrations (>0.005 mg/g) and low nutrient levels (Table 4.6).

From this study, possible species useful for phytoremediation and/or rehabilitation may be *Miconia argyrophylla*, *Vismia angusta*, *Vismia guianensis* and *Cecropia obtusa* on the overburden while *Andropogon bicornis*, *Miconia argyrophylla* and sedges may be important in mining pits and tailing ponds. *Miconia argyrophylla* emerges as a potential candidate species for phytoremediation across all three mining zones due to high concentrations of mercury in its leaf tissues. Tolerance to mercury can be mediated by bioaccumulation (i.e. survive despite concentrated contaminants) and bioexclusion (i.e. restrict contaminant uptake into their biomass) (Tangahu et al. 2011). Bioexclusion can play an important role in phytoremediation (Ritchie and Raina 2016) and therefore the rehabilitation of mined sites.

These findings offer an insight into how gold mining alters nutrient cycling and potentially offers a solution for recovery of these sites, indicating the prospective species for regeneration, while using the overburden for the potential rehabilitation of the tailing ponds and mining pits, theoretically increasing soil nutrient levels.

Through its current and continued expansion, gold mining will have serious impacts on soil and vegetation fertility levels across mined sites, consequently affecting forest regeneration in Guyana and Amazonia. It is important to note the lack of studies focused on soil nutrient levels and their influence in post-mining sites. Even at sites abandoned for 3 years, soil and vegetation nutrient levels were significantly lower in mining pits and tailing ponds with higher mercury concentrations, suggesting that it will take longer for plants to regrow within these zones and potentially lead to the establishment of a lower forest proportion compared to the overburden zone or primary forests (Cole et al. 2014). As local communities are modified through shifts in species diversity, ecosystem functioning may be affected leading to reduced evapotranspiration rate, decrease humidity and reduce regional rainfall (Morin et al. 2018). Ultimately, this will affect how resilient the recovered forests will be to future disturbances.

5

Limited Biomass Recovery from Gold Mining in Amazonian Forests

5.1 Abstract

Gold mining has rapidly become more prevalent across the Amazon Basin, especially in northern Amazonia within the last 16 years. Despite the regional significance of gold mining, the ability of forests to recover remains almost completely unquantified. In order to assess biomass accumulation in abandoned gold mining plots, I installed nine 0.25 ha forest inventory plots in recently abandoned mines in two major mining regions in Guyana (Mahdia and Puruni), re-censusing them 18 months later, to provide the first ground-based quantification of gold mining impacts on forest biomass recovery. I further examined how observed biomass recovery patterns from gold mining at my study sites compare with published tropical forest chronosequence data from other land uses (e.g. pasture, agriculture), and which factors most limit biomass recovery in previously mined sites. This study found that woody biomass recovery rates in abandoned mining pits and tailing ponds are the lowest previously recorded in tropical forests, with close to no woody biomass recovery after 3-4 years. On the overburden (areas not mined but where excavated soil is deposited), however, recovery rates (0.63 - 3.5 Mg ha^{-1} yr^{-1}) were comparable to those from other secondary forests (0.7 - 3.1 Mg ha^{-1} yr^{-1}) across the Neotropics following abandonment of pastures and agricultural lands. I estimate that the slow recovery rates in mining pits and ponds currently reduces carbon sequestration across Amazonian secondary forests by ~90,000 t C yr^{-1}. However, the significant recovery in overburden areas is heartening for potential remediation strategies and

suggests that back-filling of mining pits and ponds may help to promote biomass recovery.

5.2 Introduction

Within the last decade, gold mining activity has become more prevalent across the Amazon Basin, to the extent that it is now the major driver of deforestation in several northern Amazonian countries (Guyana Forestry Commission and Indufor 2012, Asner et al. 2013, Alvarez-Berríos and Mitchell Aide 2015). In Guyana, for example, gold mining has increased by 908% by area, since 1990 and now accounts for 94% of national deforestation (Guyana Forestry Commission and Indufor 2012, Guyana Forestry Commission 2015). Much of this forest loss stems from artisanal and small-scale miners, who respond rapidly to increases in international gold prices (Howard et al. 2011). These mining activities invariably lead to widespread environmental damage and deforestation, resulting in substantial soil erosion and contamination, increased fragmentation of forest patches and mercury pollution of rivers and streams (Veiga et al. 2006, Dedieu et al. 2014, Castilhos et al. 2015, Sonter et al. 2017).

The extent of soil physical damage and chemical contamination associated with gold-mining activities sets it apart from other traditional drivers of deforestation such as conversion to pasture or small-scale agriculture, which generally do not significantly alter soil structure or nutrient content (Santos-Francés et al. 2011, Wantzen and Mol 2013). Thus gold mining activity might be expected to arrest forest recovery rates compared to other land uses. Despite the importance of mining as a major driver of tropical forest deforestation, the impacts on forest biomass accumulation remain almost completely unquantified. In fact, only one previous field study has attempted to evaluate forest recovery following deforestation from gold mining in Amazonia (Peterson and Heemskerk 2001), but this study performed only visual assessments of vegetated area following 1-4 years of recovery with no quantitative measurements. With the availability of high-resolution satellite imagery, other authors such as Novoa et al. (2016) have also visually assessed forest regeneration following gold mining, finding vegetation regrowth in previously mined areas in Peru. Yet, such studies

have not incorporate a field-based ground-truthing and do not consider the complex nature of mining sites, which typically consist of three distinct mining zones: (1) overburden: areas overlying the gold ore, including the topsoil, which are displaced during the mining process, (2) tailing pond: deposits of material left over after the gold has been separated from the ore, and the (3) mining pit. The intensity of the disturbance caused by mining is much higher in the tailing pond and mining pit than the overburden and thus recovery rates are expected to be lower for the former two zones.

Several recent studies have shown that recovering, secondary forests, deliver a host of ecosystem services including maintenance of biodiversity, and significant accumulation of carbon in their biomass (Anderson-Teixeira et al. 2013, Lohbeck et al. 2015, Chazdon et al. 2016, Poorter et al. 2016). Indeed, across the Tropics, secondary forests are thought to constitute a significant carbon sink, which in some estimates is larger than that of intact primary forests per area (Pan et al. 2011). However, other studies have indicated the rapid early accumulation of aboveground biomass, with a levelling off in old-growth forest sites where biomass is at its highest (Silver et al. 2000, Feldpausch et al. 2005a, 2012b, Peña-Claros 2016). Recent syntheses of chronosequences from tropical secondary forests have concluded that secondary forest biomass recovery rates 1) are largely controlled by background rainfall conditions (Poorter et al. 2016), 2) only achieve 95% regrowth compared to old-growth forests (Cole et al. 2014), 3) differs between dry, moist and wet tropical forests (Saatchi et al. 2011), and 4) are faster in forests previously under pasture use than agricultural production (Martin et al. 2013), although Zarin et al. (2001) found no significant difference in biomass accumulation between former pastures and former slash-and-burn fallows. However, none of these syntheses contain chronosequences on previously mined areas. Thus, it is unclear how recovery of biomass and biodiversity following gold mining compares with recovery from more traditional land uses such as pasture and agriculture.

Further, species composition of secondary forests, in some cases, may not converge with that of old-growth forest (Marin-Spiotta et al. 2008). In some cases, exotic species may dominate parts of the successional process and eventually form a large portion of the forest canopy, especially in highly disturbed landscapes (Grau et al. 2003, Feldpausch et al. 2007, Franklin 2007). As a result

of this decoupling between structural and floristic components of forest change (Chazdon et al. 2007), different parameters may result in different answers as to how well would tropical forest recover from more intense land use disturbances such as gold mining.

To address these critical knowledge gaps, I established forest plots in focal gold mining regions in Guyana to investigate patterns of biomass recovery following abandonment of gold mining activity. Here, I specifically consider the following questions: 1) How has biomass changed over an 18-month period in nine recently abandoned gold mining plots (0.6 - 3 years since abandonment), 2) How observed biomass recovery patterns from gold mining at my study sites compare with published tropical forest chronosequence data from other land uses (e.g. pasture, agriculture), and 3) Which factors most limit biomass recovery in previously mined sites? This is the first study to provide detailed, recensused, field-based information on the regeneration of secondary forests following previous gold mining activity.

5.3 Methods

5.3.1 Study sites and sampling design

This chapter utilized measurement plots installed in two known gold mining sites in Guyana, namely Mahdia and Puruni (Figure 5.1), from January to March, 2016, and subsequently re-censused in June to August, 2017 (see Appendix 5.1 for images from field sites for both censuses). A description of both sites can be found in Chapter 1.7.

Nine 0.25 ha (50m x 50m) plots and a controlled old-growth forest plot (100m x 100m) were established at each site. Sites were selected based on the three mining zones being part of the same mining activity. However, approximately half of all plots (five in Mahdia and four in Puruni) were cut down and re-mined before the subsequent re-census in 2017. I only utilized plots which were present in 2016 and 2017. Each plot was positioned to include three important zones of artisanal gold mining sites, namely the mining pit, the mine tailings and the overburden (description and image of the zones are found in Chapter 1.7). Within each plot and within each mining zone (mining pit,

overburden, tailing pond), three nested subplots of 3m x 3m and 1m x 1m were established. All trees >2cm DBH (diameter at reference height of 1.3m) were measured in the larger 0.25 ha plot and identified to species level. All tree saplings 25-200 cm tall, and all tree seedlings 5-25 cm tall were identified and counted in the 3m x 3m and 1m x 1m subplots respectively. Nested subplots were also established in the 1-ha control plot, where all trees >10cm DBH were measured and recorded.

Heights of larger trees were measured using a laser rangefinder, whereas a tape measure was used to measure the height of saplings and seedlings. In the re-census in 2017, the diameter of all individuals still standing from the first census was re-measured, along with all new recruits > 2cm DBH in each 0.25 ha plot and >25cm and >5cm tall in our nested 3m x 3m and 1m x 1m subplots respectively. Trees not present in the second census but present in the first census were assumed to have died.

5.3.2 Biomass calculations

To calculate aboveground biomass (AGB) of individual trees (in kg), I used the allometric model of Chave et al. (2014):

$$AGB=0.0673 \times (\rho D^2 H)^{0.976}$$

where ρ = wood density (g cm^{-3}), D = DBH (cm) and H = height (m). This is a generic equation for tropical forests, based on a broad set of trees including primary and secondary forest species, and has previously been used for estimating biomass in young secondary forests (Poorter et al. 2016, Rozendaal et al. 2017). The Chave et al. (2014) allometric equation was used in this study as there is no specific published equation for smaller trees (i.e. <5cm DBH). Other authors such as Berenguer et al. (2015) have also demonstrated that the Chave et al equation can be used for assessing biomass in human-modified landscapes.

Wood density values for species were obtained from the global wood density database available from the Dryad data repository (http://datadryad.org/). Where species-specific wood densities were not available, genus mean or familial mean wood densities were used (e.g. Baker et al. 2004). As the relative proportions of overburden, pit and tailing areas varied across plots, I rescaled the total biomass estimates for each zone so that all values are expressed on a 1-ha basis. For each plot, I calculated the aboveground biomass (AGB), the total

change in biomass between our two measurement censuses (ΔAGB), the biomass change due to diameter growth (ΔAGB_{Growth}), the biomass change due to recruitment of new trees ($\Delta AGB_{Recruitment}$) and the biomass change due to mortality ($\Delta AGB_{Mortality}$).

5.3.3 Comparison with published secondary forest chronosequences

To place my study within the wider literature on tropical forest biomass recovery, I compared the AGB and ΔAGB values to published data for other tropical forests at 2-4 years since abandonment. Studies were retained in the comparison if they included: (i) at least one measurement of aboveground biomass for woody vegetation, (ii) the age or time since last disturbance occurred, (iii) the land use prior to abandonment, typically pasture or agriculture (Martin et al. 2013). Table 5.1 lists the published secondary forest AGB and ΔAGB data used for the comparative analysis. To allow for natural variation in aboveground biomass stocks, AGB was expressed as a proportion of the biomass stocks found in nearby old-growth forest plots, following approaches used in other published meta-analyses (Martin et al. 2013). If data from old-growth forests were not available in the reviewed studies, I utilized reference forest data from neighbouring plots (Johnson et al. 2016).

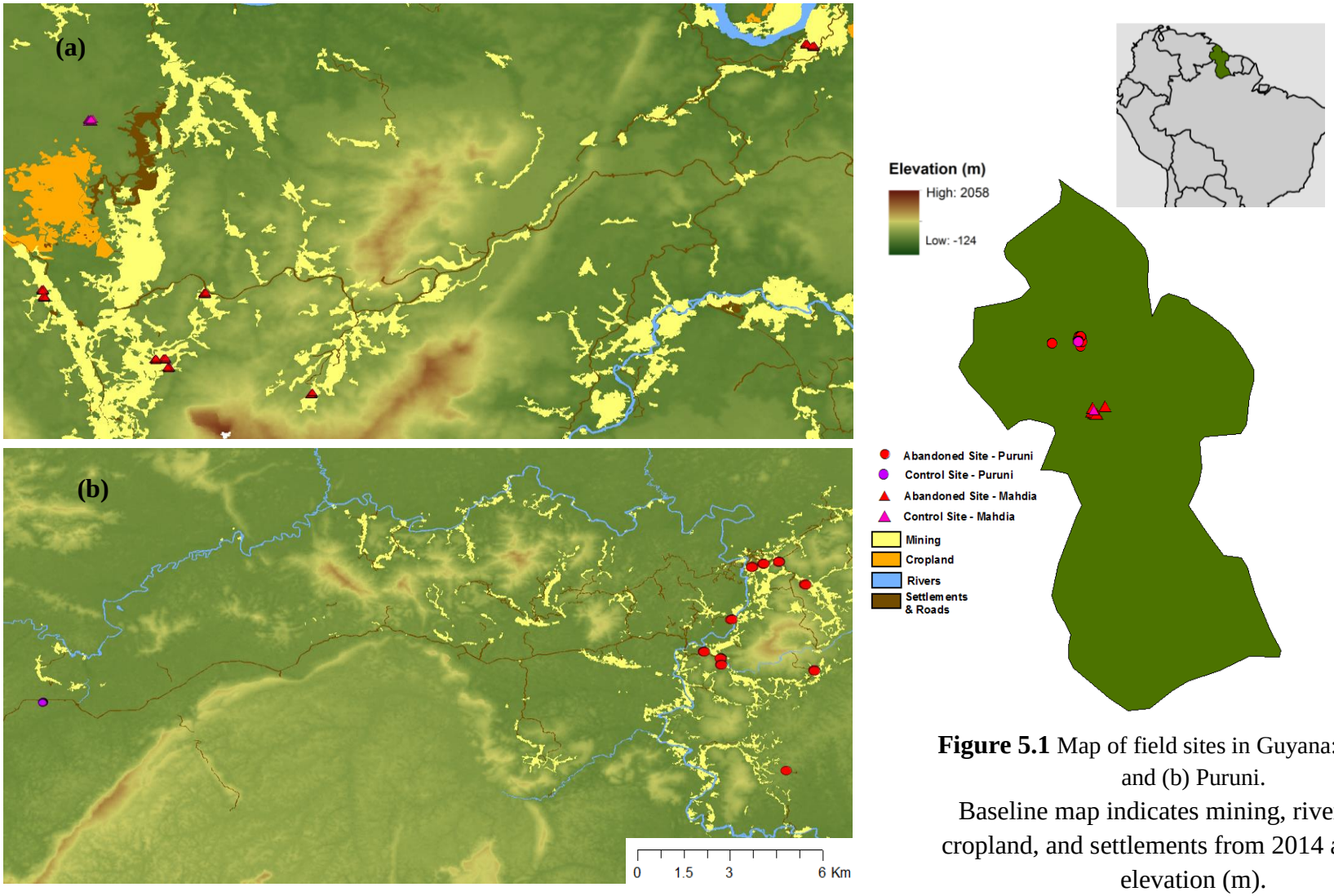

Figure 5.1 Map of field sites in Guyana: (a) Mahdia and (b) Puruni.
Baseline map indicates mining, rivers, roads, cropland, and settlements from 2014 and STRM elevation (m).

One of the assumptions of this study is that all sites have been subjected to the same environmental conditions, though in practice this condition is rarely met (Johnson and Miyanishi 2008).

Table 5.1 Sources of secondary forest chronosequences from different land uses.

Data Source	Land Use	Countries
Martin et al. (2013)	Pasture, Agriculture	Various
Vieira (2013)	Pasture	Brazil
Brondizio (unpublished)	Pasture	Brazil
Marin-Spiotta et al. (2008)	Pasture, Agriculture	Peru, Brazil, French Guiana, Colombia, Venezuela, Ecuador
Poorter et al (2016)	Pasture, Agriculture	Brazil, Bolivia, Colombia

5.3.4 Statistical Analysis

To examine the effects of mining sites (Mahdia vs. Puruni) and individual zones (overburden, mining pit and tailing pond) on AGB in census 1 and census 2, ΔAGB, $AGB_{Mortality}$, $AGB_{Recruitment}$ and AGB_{Growth}, linear mixed effects models were used, with a random intercept for each plot. AGB in Census I and II, ΔAGB, $AGB_{Mortality}$ and AGB_{Growth} data were log-transformed prior to analysis to satisfy requirements of normality and homogeneity of variance. For instance, ΔAGB was first translated (ΔAGB + 1) and then log-transformed due to the occurrence of negative values in the dataset such as those present for $AGB_{Mortality}$: ($\Delta AGB_{transformed} = \log(\Delta AGB + 1 - \min(\Delta AGB))$. These analyses were conducted using *nlme* package in R (Pinheiro et al. 2018). Mixed effects models were used as they are statistically rigorous even with a small dataset as in this case and can accommodate flexible data structures e.g. data that is non-normally distributed. I also tested whether structural equation models (SEMs) would work as variables were autocorrelated and this model assumes all variables impact on each other (Nachtigall et al. 2003). However, SEMs require normally distributed continuous

variables and a minimum number of parameters e.g. a sample size of 200 parameters which this study did not have (Nachtigall et al. 2003).

Using the soil data from Chapter 4, I conducted a second set of analyses to evaluate the importance of different continuous variables (CEC, N, P, Hg, Distance to Forest Edge) in predicting variation in AGB in Census I and II, ΔAGB, $AGB_{Mortality}$, $AGB_{Recruitment}$ and AGB_{Growth} across the study plots. For this analysis, I fitted generalized linear models in R, using the 'log' link option with the *glm* command. I compared models with all possible combinations of these variables but excluded interaction effects due to the larger number of variables in these analyses and relatively small sample size (n=27), so as to avoid model overfitting. Model selection was performed based on Akaike's information criterion (AIC). Following Rozendaal et al. (2017), I considered models differing by less than two AIC units as equally supported.

Finally, I compared the AGB values at census 2 (following 2-4 years of recovery) with published biomass estimates from secondary forest chronosequence studies for similar stages of succession (2-4 years) following abandonment from other, more traditional land uses (agriculture and pasture). As it was recently shown that dry forests accumulate biomass more slowly than wet forests (Poorter et al. 2016), I restricted comparison location to moist, evergreen forests. For this comparison, I grouped the data from Mahdia and Puruni into three groups, one for each zone (overburden, mining pit and tailing pond) and treated all studies reporting recovery from agriculture as a single group and all studies reporting recovery from pasture as another group. Most studies do not provide detailed land use histories for each site, thus finer-scale groupings were not possible. For this analysis, I performed non-parametric Kruskal-Wallis tests, followed by post-hoc Dunn tests.

5.4 Results

5.4.1 Aboveground biomass dynamics during secondary succession

Aboveground biomass in the control, old-growth plot in Mahdia (317.7 Mg ha^{-1}) was considerably higher than in the control, old-growth plot in Puruni (187.6 Mg ha^{-1}). However, mean aboveground woody biomass in the overburden plots was on average more than three times greater in Puruni in Census II than it

was in Mahdia (Figure 5.2, $p<0.001$), despite no significant difference between sites when plots were installed (Census I). In Puruni, overburden aboveground woody biomass following 4-5 years of forest recovery was 6.63 ± 1.63 Mg ha^{-1} (3.46 ± 0.74 Mg ha^{-1} yr^{-1}) , equivalent to 3.5% that of the control while in Mahdia, it was only 1.06 ± 0.38 Mg ha^{-1} (0.36 ± 0.36 Mg ha^{-1} yr^{-1}), amounting to <1% of the control plot. In both Mahdia and Puruni, aboveground woody biomass was very low in the mining pit areas (mean AGB of 0 ± 0.03 Mg ha^{-1} yr^{-1} in Mahdia and 0 ± 0.05 Mg ha^{-1} yr^{-1} in Puruni, $p>0.1$) and tailing ponds (mean AGB of 0.01 ± 0.01 Mg ha^{-1} yr^{-1} in Mahdia and 0.03 ± 0.06 Mg ha^{-1} yr^{-1} in Puruni, $p>0.1$) (Figure 5.2).

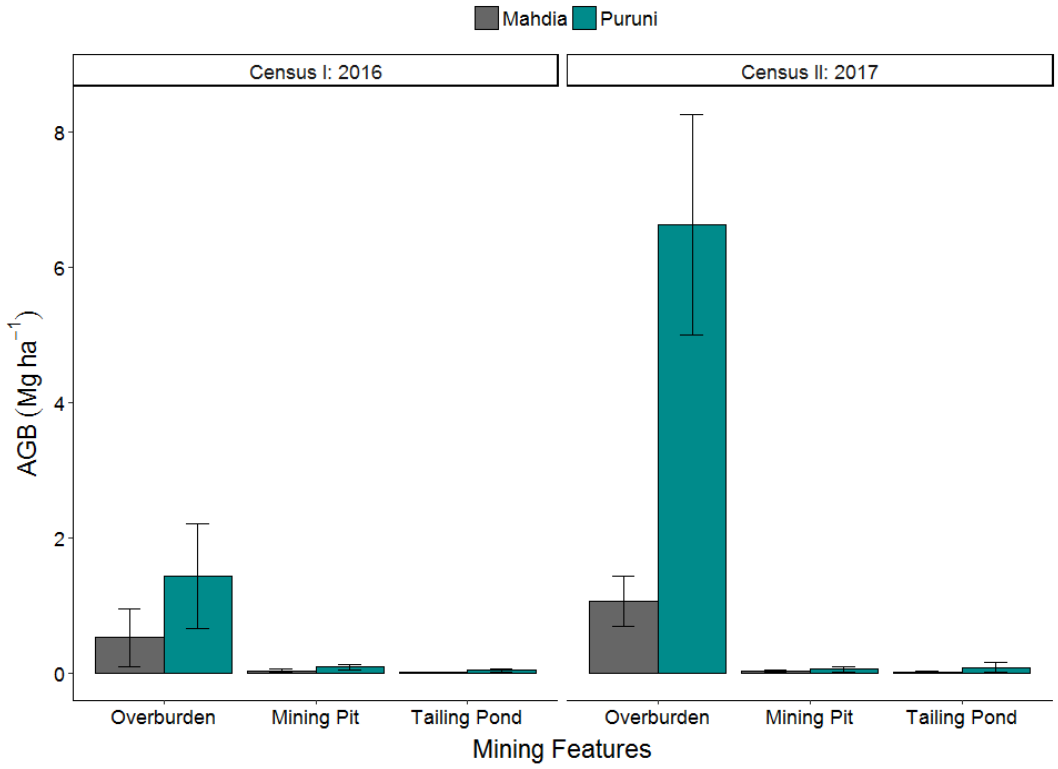

Figure 5.2 Mean above ground biomass (AGB) across mining zones (overburden, tailing pond & mining pit) in abandoned mining sites for Mahdia and Puruni. All abandoned sites were extrapolated to 1ha.

In fact, in approximately half of my plots, there was no recorded woody aboveground biomass in the pits and tailing ponds. No trees >10cm in height were found on the mining pit or tailing pond across plots at both sites in both censuses. In both sites, virtually all of the aboveground biomass in pits and ponds was accounted for by non-woody grasses and sedges, such as *Andropogon bicornis*.

Based on destructive harvesting undertaken in Census II, herbaceous (non-woody) aboveground biomass was estimated to be 0.03 ± 0.03 Mg ha^{-1} at Puruni and 0.17 ± 0.11 Mg ha^{-1} at Mahdia for the mining pit areas and 0.09 ± 0.07 Mg ha^{-1} (Puruni) and 0.2 ± 0.08 Mg ha^{-1} (Mahdia) for the tailing pit areas.

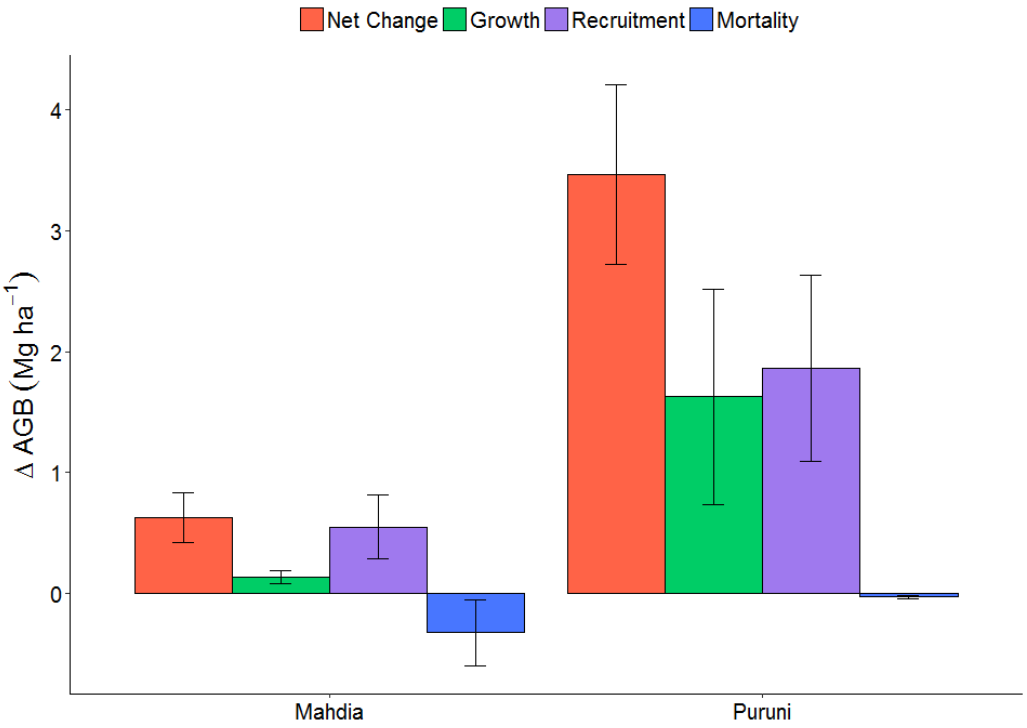

Figure 5.3 The contribution of tree growth, recruitment and mortality compared to annual biomass change between Census I and Census II for Mahdia & Puruni. Data was restricted to species on overburden and extrapolated to 1ha.

Annual rates of overburden aboveground biomass change (ΔAGB) differed strongly between sites and zones (Table 5.2, Figure 5.3, $p<0.0001$). ΔAGB was positive in all overburden plots except for one plot in Mahdia, indicating overall net AGB accumulation, with estimated annual ΔAGB approximately 5-fold lower in Mahdia (0.63 ± 0.41 Mg ha^{-1} yr^{-1}) than Puruni (3.46 ± 1.66 Mg ha^{-1} yr^{-1}). Woody biomass changes between censuses (ΔAGB) for mining pit and pond zones were not significant in either site, remaining close to zero in both censuses. Tree recruitment ($AGB_{Recruitment}$) was the main contributor to biomass increases for overburden areas in both sites, responsible for 80% and 54% of the biomass increases in Mahdia and Puruni respectively, although

$AGB_{Recruitment}$ was ~3.4 times greater (p=0.19, Table 5.2) in overburden plots in Puruni (1.86 ± 0.77 Mg ha^{-1} yr^{-1}) than in Mahdia (0.55 ± 0.26 Mg ha^{-1} yr^{-1}). Furthermore, ΔAGB_{Growth} was ~12 times greater (p=0.04, Table 5.2) in Puruni (1.63±0.9 Mg ha^{-1} yr^{-1}) than in Mahdia (0.13±0.5 Mg ha^{-1} yr^{-1}). Biomass mortality losses ($\Delta AGB_{Mortality}$), on the other hand, were on average 11 times higher (p=0.19, Table 5.2) in Mahdia (0.32±0.27 Mg ha^{-1} yr^{-1}) than in Puruni (0.03±0.01 Mg ha^{-1} yr^{-1}). $\Delta AGB_{Growth,}$ $AGB_{Recruitment}$ and $\Delta AGB_{Mortality}$ were close to zero in mining pit and tailing pond plots.

It is important to note that the results presented here on biomass may not reflect an effect of the 2015 El Nino event as all plots would have seen similar mortality rates. Analysis of mortality rate (see Condit et al. 1995 for mortality rate formula used) in neighbouring, long-term forest plots in Guyana (Iwok-22, Iwok-21 and Iwok-11) between 2006 and 2017 indicate a mean mortality rate of 0.003% while the mortality rate at Mahdia and Puruni between the two censuses were 0.1% and 0.03% respectively. Pioneer species such as those present at Mahdia and Puruni tend to have a higher mean mortality rate. The results here suggest that even if a lag was present with the 2015 El Nino event, it was not reflected in the mean mortality rate of long-term plots. However, the 2015 El Nino event may have impacts on observed climate anomalies, water deficits and heat stress which may still be documented.

5.4.2 Forest composition and structure

Taxonomic composition ranged widely across the plots and was not only very different between recovering secondary plots and nearby old-growth sites, but also between recovering forest plots in both sites (Figure 5.4). In the old-growth control plots, Fabaceae was the most dominant family in terms of AGB contribution, accounting for 63% of total AGB in both Mahdia and Puruni. This was followed by Lecythidaceae, which accounted for 21% of total AGB in Mahdia and 26% in Puruni. In Mahdia, overburden areas were initially dominated by Anacardiaceae and Ulmaceae, jointly responsible for 71% of total AGB across all previously disturbed plots in Census I, and then by Clusiaceae and Urticaceae, which were jointly responsible for 66% of total AGB in Census II. In Puruni, Fabaceae and Urticaceae were the dominant families in terms of AGB

contribution, being jointly responsible for 77% of total AGB in Census I and 74% in Census II across overburden plots.

Species composition varied considerably between sites and across plots within sites. Important woody species present in Census I (1-3 years post-abandonment) were *Tapirira marchandii* (Anacardiaceae, 1.3 Mg ha^{-1}), *Trema spp* (Ulmaceae, 0.23 Mg ha^{-1}) and *Caryocar microcarpum* (Caryocaraceae, 0.2 Mg ha^{-1}) in Mahdia and *Zygia collina* (Fabaceae, 3.03 Mg ha^{-1}), *Cecropia surinamensis* (Urticaceae, 2.29 Mg ha^{-1}) and *Byrsonima aerugo* (Malpighiaceae, 0.7 Mg ha^{-1}) in Puruni. In Census II, the species with the most biomass were *Zygia collina* (Fabaceae, 10.7 Mg ha^{-1}) and *Cecropia obtusa* (Urticaceae, 9.09 Mg ha^{-1}) in Puruni, while *Vismia guianensis* (Clusiaceae, 1.4 Mg ha^{-1}) and *Cecropia obtusa* (Urticaceae, 1.04 Mg ha^{-1}) dominated in Mahdia.

Tree heights also varied across mature and abandoned sites. Maximum height in mature forests were 32.04m and 42.37m in Mahdia and Puruni respectively. In Mahdia, maximum tree height recorded on overburden areas was 12m, but trees up to 23.5m were recorded in overburden areas of Puruni.

Table 5.2 Summary Results from Mixed-effects Models for Aboveground Biomass (AGB), Annual Biomass Change (ΔAGB), and Biomass Change resulting from Recruitment ($\Delta AGB_{Recruitment}$), Mortality ($\Delta AGB_{Mortality}$) and Tree Growth (ΔAGB_{Growth}).

	$log(AGB_{CensusI})$		**$log(AGB_{CensusII})$**		**$log(\Delta AGB)$**		**$log(\Delta AGB_{Recruitment})$**		**$log(\Delta AGB_{Mortality})$**		**$log(\Delta AGB_{Growth})$**	
	F-value	***p-value***	***F-value***	***p-value***	***F-value***	***p-value***	***F-value***	***p-value***	***F-value***	***p-value***	***F-value***	***p-value***
Site	0.89	0.38	14.69	**0.006**	6.62	**0.04**	2.13	0.19	0.96	0.36	5.49	**0.05**
Zone	5.63	**0.02**	71.98	**0.0001**	42.17	**0.0001**	18.45	**0.0001**	1.48	0.26	8.42	**0.004**
Site*Zone	0.58	0.57	14.54	**0.0004**	13.08	**0.001**	2.37	0.13	1.85	0.19	3.98	**0.04**

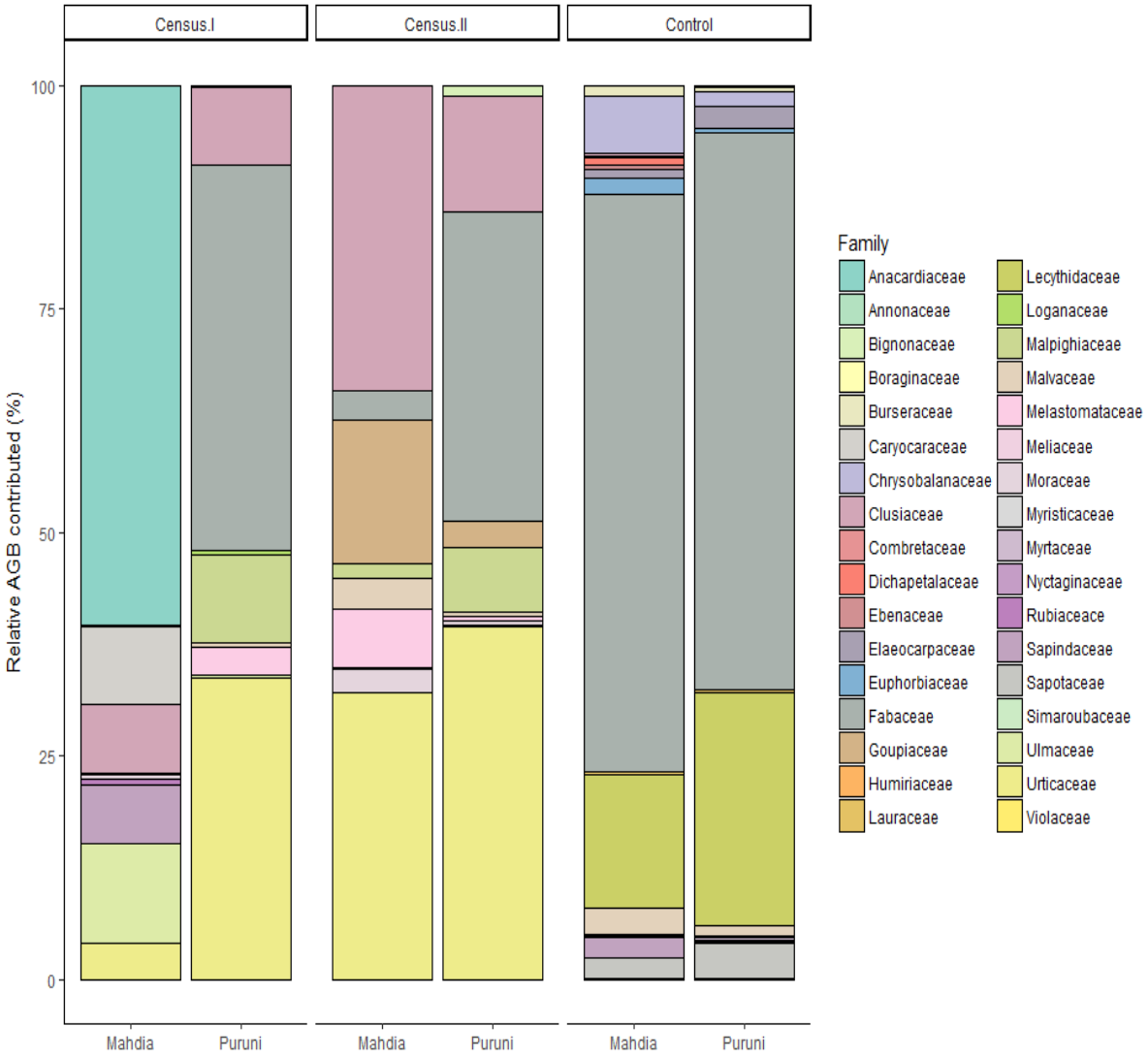

Figure 5.4 Relative biomass contributed by families in Census I and Census II on the overburden, compared to control sites. All sites extrapolated to 1ha.

5.4.3 Controls on Biomass Recovery

The best supported models for explaining variation in $AGB_{censusII}$ and annual biomass change (ΔAGB) involved combinations of total nitrogen and phosphorus, mercury and exchangeable cations (Table 5.3), with the models explaining 38-43% of the observed variation in AGB. Mercury concentrations, total nitrogen and distance to forest edge explained 70% of the observed variation in aboveground growth (AGB_{Growth}). Total nitrogen was particularly important, featuring in all best supported models for AGB, AGB_{Growth} and $AGB_{Mortality}$.

Overall predictive ability of the models was relatively weak for both $AGB_{Mortality}$ and $AGB_{Recruitment}$ where the best models explained only 20-25% of the variations. Mercury content and exchangeable cations were found to be the most important predictors of $AGB_{Recruitment.}$ Phosphorus content was found to be less important than other predictors in driving variation in biomass recovery across plots.

5.4.4 Biomass Recovery in Second-Growth Forests by land use

Figure 5.5 depicts how biomass estimates for Census II from this study compare with published data for other moist Neotropical secondary forests of equivalent age (2-4 years post-abandonment) recovering from agricultural and pasture use. Compared to agriculture and pasture, biomass recovery rates for the mining pits and tailing ponds are the lowest documented for any land use thus far. However, biomass stocks in overburden areas are not significantly different to those for other sites previously under pasture and agriculture. The annual rates of aboveground biomass change (ΔAGB) of the overburden of abandoned gold mining sites at both Mahdia and Puruni were comparable to the only other multi-census data published for second-growth forests across the Neotropics (see Table 5.1 for published data used, Figure 5.6). For instance, Puruni (3.5 Mg ha^{-1}) was similar in recovery to Nizanda, Mexico (3.1 Mg ha^{-1}) while Mahdia (0.63 Mg ha^{-1}) was similar to Chamela, Mexico (0.7 Mg ha^{-1}). Caution is necessary, however, as some of these estimates are from seasonally dry forests in Mexico, where recovery rates would be expected to be lower than for moister forests (Poorter et al. 2016). Further, forests established after agriculture appeared to recover biomass quicker than those following pasture and gold mining.

Table 5.3 Results of important continuous variables that may affect changes in aboveground biomass (AGB) in Census I and II, Annual Biomass Change (ΔAGB), and Biomass Change resulting from Recruitment ($\Delta AGB_{Recruitment}$), Mortality ($\Delta AGB_{Mortality}$) and Tree Growth (ΔAGB_{Growth}).

Model (fixed effects)	$log(AGB_{CensusI})$		$log(AGB_{CensusII})$		$log(\Delta AGB)$		$log(\Delta AGB_{Recruitment})$		$log(\Delta AGB_{Mortality})$		$log(\Delta AGB_{Growth})$	
	ΔAIC	**R^2**	**ΔAIC**	**R^2**	**ΔAIC**	**R^2**	**ΔAIC**	**R^2**	**ΔAIC**	**R^2**	**ΔAIC**	**R^2**
Hg + TP + TN + CEC + Distance	5.72	**0.38**	**1.24**	0.29	**1.23**	0.34	**0.66**	0.22	5.16	**0.23**	3.79	**0.70**
Hg + TP + TN + Distance	5.30	**0.38**	9.22	**0.38**	6.85	**0.43**	7.07	0.20	3.17	**0.23**	**1.85**	**0.70**
Hg + TP + TN + CEC	3.96	0.35	**0.00**	0.30	**0.00**	0.38	**1.01**	**0.25**	3.99	0.22	5.00	0.65
Hg + TN + TP	3.33	**0.37**	7.24	**0.38**	4.88	**0.43**	5.14	0.19	2.09	0.22	3.04	0.64
Hg + TP	8.57	0.20	8.51	0.27	8.21	0.30	3.28	0.20	5.64	0.08	35.13	0.34
Hg + TN	**1.41**	**0.37**	5.26	**0.39**	3.01	**0.42**	4.03	0.17	**0.50**	0.22	**1.86**	0.64
TN + CEC	**1.62**	0.34	14.91	0.25	14.61	0.24	10.71	0.03	2.44	0.19	15.14	0.56
TP + CEC	6.85	0.19	15.97	0.15	16.79	0.12	10.79	0.02	6.25	0.06	17.73	0.44
Hg + CEC	10.68	0.12	12.02	0.28	9.40	0.30	**0.00**	0.21	5.45	0.08	23.94	0.38
TN + TP	1.80	0.34	14.23	0.26	14.33	0.23	11.19	0.01	2.03	0.18	13.80	0.58
Hg + TP + Distance	10.53	0.20	10.33	0.25	10.20	0.30	5.21	0.21	6.29	0.12	37.05	0.33
Hg + TN + Distance	3.36	0.37	7.23	**0.38**	5.01	**0.42**	5.91	0.18	1.72	**0.24**	**0.23**	**0.69**
Hg + CEC + Distance	12.39	0.12	11.75	0.20	10.80	0.25	**0.77**	0.22	4.26	0.16	25.88	0.37
TP + CEC + Distance	8.84	0.19	17.28	0.20	17.65	0.17	11.72	0.06	4.16	0.17	18.97	0.46
TN + CEC + Distance	**1.96**	**0.39**	9.89	0.34	9.45	0.37	10.57	0.09	1.96	**0.23**	**1.76**	**0.69**
CEC + Distance	11.50	0.08	18.67	0.11	18.77	0.11	9.75	0.06	2.26	0.16	29.90	0.31
Hg + Distance	13.48	0.07	10.91	0.19	9.71	0.23	5.12	0.18	5.17	0.10	50.14	0.13
TN + Distance	**1.49**	**0.37**	10.37	0.36	9.58	0.35	10.65	0.03	**0.00**	**0.23**	**0.00**	**0.69**
TP + Distance	9.29	0.20	19.60	0.20	18.43	0.17	10.52	0.03	4.30	0.12	38.99	0.37
Hg	11.62	0.06	11.35	0.24	8.39	0.27	3.23	0.17	5.26	0.02	48.14	0.14
TP	7.46	0.18	19.16	0.13	18.39	0.09	9.25	0.01	4.88	0.04	38.61	0.31
TN	**0.00**	0.33	13.00	0.27	12.63	0.24	9.44	0.00	**0.73**	0.19	16.48	0.58
CEC	9.57	0.08	17.03	0.08	17.75	0.07	8.90	0.02	4.68	0.05	28.25	0.30
Distance	13.27	0.00	23.19	0.05	20.38	0.06	8.66	0.03	3.22	0.09	52.57	0.03
None (Intercept only)	11.37	0.00	22.62	0.00	19.99	0.00	7.45	0.00	3.90	0.00	51.51	0.00

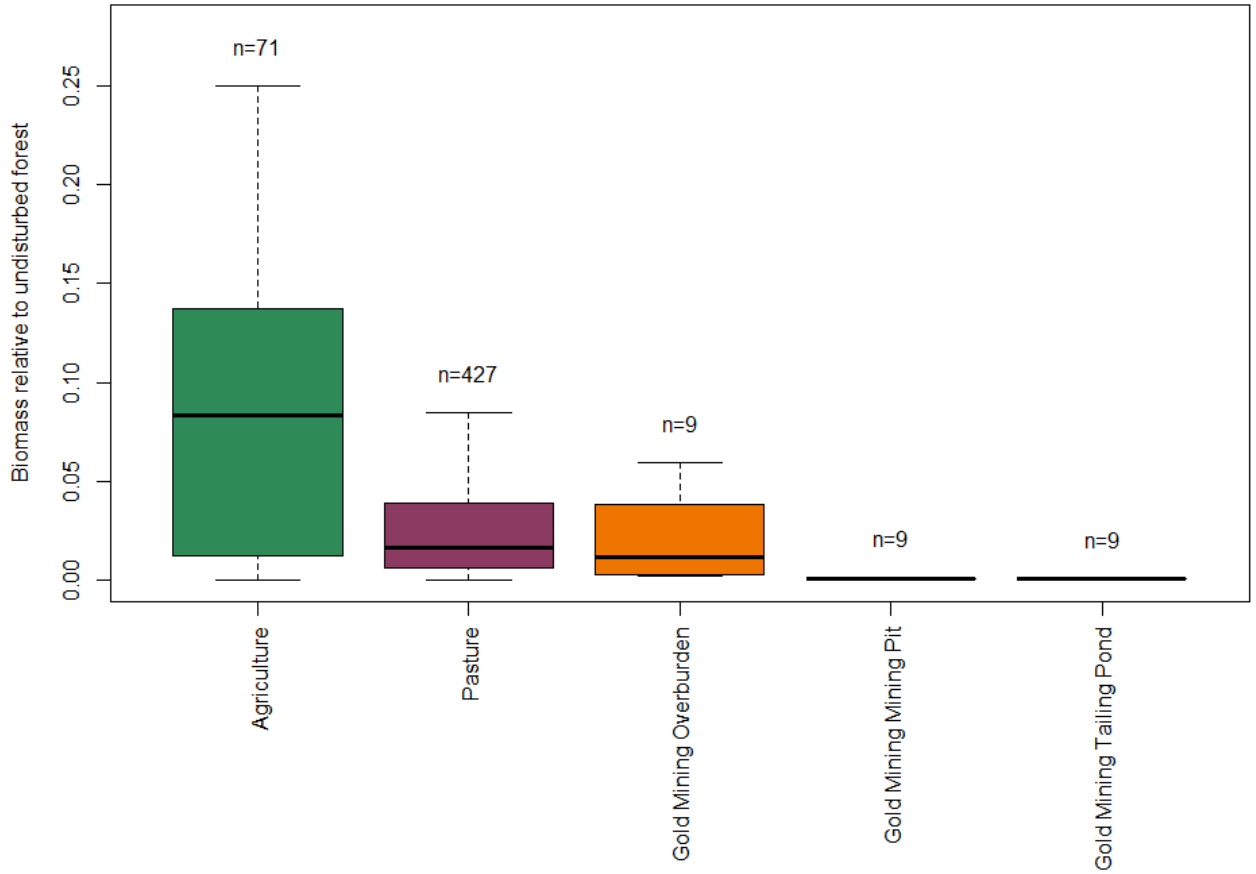

Figure 5.5 Recovery of biomass in different land use, relative to undisturbed reference forests.

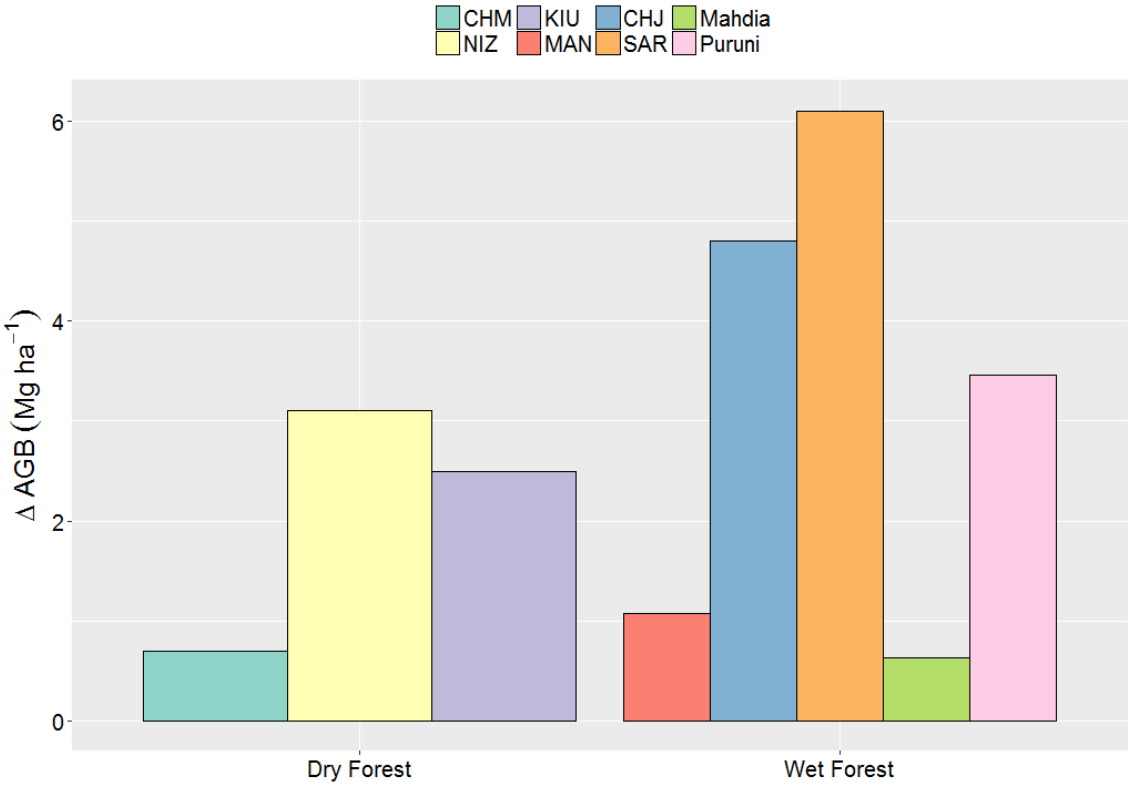

Figure 5.6 Comparison of annual biomass change of abandoned gold mining sites (overburden only) with six second-growth forests across the Neotropics (Dry Forests: CHM = Chamela, Mexico; NIZ = Nizanda, Mexico; Wet Forests: KIU = Kiuic, Mexico; MAN = Manaus, Brazil; CHJ = Chajul, Mexico; SAR = Sarapiqui, Costa Rica).

5.5 Discussion

5.5.1 Successional Recovery of Biomass and Species Composition Post-mining

This analysis finds clear evidence that gold mining heavily disrupts the secondary succession process and therefore forest recovery in former mining pit and tailing pond areas, but not on the overburden. While woody biomass recovery rates on mining pit and tailing ponds were amongst the lowest ever recorded, recovery rates on overburden areas were comparable to those from secondary forests recovering from agriculture and pasture.

The lack of woody biomass recovery, particularly on the mining pit and tailing pond, was found to be heavily influenced by available total nitrogen and mercury concentrations (Table 5.3). In Chapter 4, I showed that N content of soils across previously mined plots was much depleted relative to the control plots in both Mahdia and Puruni. This was especially true for the previously mined tailing ponds and mining pits. Nitrogen content in previously mined mining pits was only 10-38% of that in overburden plots while nitrogen content in previous tailing pond areas was only 4-6% of that in overburden areas (Chapter 4, Table 4.1). Recovery of Amazonian secondary forests is known to be heavily linked to nitrogen availability (e.g. Davidson et al. 2004, Feldpausch et al. 2004). The substantial stripping of nitrogen from mining pits and tailing ponds means that the concentrations found in this study would represent the lowest reported for Amazonian soils, considerably retarding their recovery. Given the infertility, some form of amendments for successful plant growth and development are required in these zones, and may involve the addition of organic material and/or inorganic fertilizer. Fertilization experiments have shown that phosphorus additions to soil, when combined with nitrogen additions, can also boost biomass recovery in secondary forests (Davidson et al. 2004b).

However, in this study, soil phosphorus content was not found to be an important predictor of biomass recovery following mining. Indeed, the differences in phosphorus content between overburden plots, which recovered well, and plots on previously mined tailing ponds and mining pits were not nearly as pronounced as for nitrogen. Previously mined tailing ponds and mining pits, which showed no

recovery in both sites, were found to contain 64-94% of the soil phosphorus content of the overburden plots.

Whereas available N likely drives the differential recovery observed across mining zones, these analyses suggest that other factors such as species may likely drive the differences in accumulation rates observed at the two study sites (Mahdia and Puruni). Indeed, overburden biomass accumulated approximately six times more slowly in Mahdia than Puruni, despite actual N and P concentrations in overburden soils being on average higher in Mahdia than Puruni (Chapter 4, Table 4.1). Soil mercury content and exchangeable cations emerged as important secondary predictors of biomass accumulation metrics (Table 5.3) and may have ultimately led to between-site differences in biomass accumulation. Mercury concentrations on overburden soils in Puruni was the only mining zone that was within range of reported mercury levels, while all other zones were higher. The statistical analyses suggests an important role for mercury in inhibiting recruitment.

Mercury concentrations have been found to strongly inhibit plant development and growth, but have differential impacts across taxa (Muddarisna and Krisnayanti 2015). My analyses suggest that mercury concentrations may have been particularly important for impairing woody plant recruitment (Table 5.3). Comparison of the plant composition data for overburden plots at both sites revealed that an important difference between the compositions of the overburden vegetation is the near absence of leguminous woody species with the capacity to fix nitrogen in Mahdia (Figure 5.7). While abundance of Fabaceae is similar in control plots in both sites, the abundance of Fabaceae increases sharply during succession in Puruni but not in Mahdia. Nitrogen fixers are known to drive biomass accumulation in recovering secondary forests (Batterman et al. 2013) and their suppression in Mahdia may be associated with higher mercury loads inhibiting the establishment of N fixing bacteria (Nuraini et al. 2015, Rafique et al. 2015). Experimental studies have previously found that application of mercury markedly decreases germination of selected leguminous tree species (Iqbal et al. 2014), including inhibiting the presence of nitrogen-fixing bacteria (Nuraini et al. 2015). I hypothesise that similar mechanisms may be limiting the establishment of N-fixing trees in Mahdia.

It is important to note the almost complete lack of specific studies focused on understanding the tolerance of rainforest tree species to mercury outside of this thesis (Chapter 4). Targeted experiments which directly test this hypothesis that the germination capacity of nitrogen fixers may be disproportionately reduced by different soil mercury loads need to be undertaken. Some studies on agricultural crops have shown that N fixing bacterium from the genera *Staphylococcus*, *Pseudomonas*, *Escherichia* and *Bacillus* may be resistant to some levels of mercury contamination by converting mercury into a less toxic form, such as hydrogen sulphide (Nuraini et al. 2015, Rafique et al. 2015). However, these are likely to involve threshold responses and these thresholds likely differ according to plant taxa. However, at present, there is simply no information in this regard.

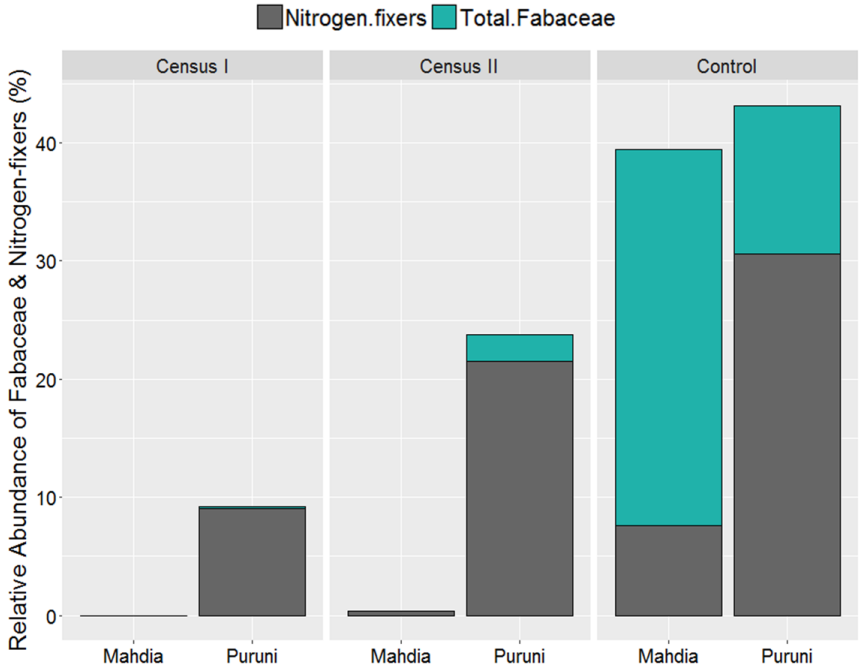

Figure 5.7 Relative Abundance of Fabaceae and Nitrogen-fixers for Mahdia and Puruni in Census I, Census II and Control.

Exchangeable cations were also shown to influence mainly annual biomass change (ΔAGB) and biomass change from tree recruitment ($\Delta AGB_{Recruitment}$, Table 5.3), and strongly correlated to soil fertility and the ability of new trees to enter the system, especially on the overburden zone. Distance to forest edge was significant for tree mortality ($\Delta AGB_{Mortality}$) and tree growth (ΔAGB_{Growth}). This was driven by two of the Mahdia plots being further away from the primary forest edge than any of the other plots (Appendix Figure 5.1).

In many tropical studies, biomass recovery has been found to decline with increasing distance from forest edge (>2 km) (Thomlinson et al. 1996, Valois-Cuesta et al. 2017) and this is linked to lower seed input from mature forest seed sources. However, all of my study plots were ≤1km from the nearest forest edge, which would allow for potentially high seed input for regeneration from nearby mature forests (Mesquita et al. 2015, Appendix 5.2). Recovery rates for plots located at roughly the same distance to edge were still much lower in Mahdia than Puruni, so this effect is likely of secondary importance in explaining the differences in recovery observed between the two sites.

5.5.2 Implications for forest recovery and rehabilitation

Relative to other previous land uses, biomass recovery in previously mined pits and tailing ponds are the slowest recorded in the literature (Figure 5.5). In Guyana alone, an area of 879 km^2 of forest was deforested due to gold mining and mining infrastructure in Guyana between 1990 and 2014 (Guyana Forestry Commission 2015). Across the entire Amazon, ~370,396 km^2 of forests are currently found within active mining concessions (Alvarez-Berríos and Mitchell Aide 2015, RAISG 2012, Figure 3.11). Within these areas, 1680 km^2 of tropical forest was lost to mining between 2001 and 2013 (Alvarez-Berríos and Mitchell Aide 2015), corresponding to an annual forest loss of ~130 km^2 yr^{-1} over this period. Assuming that the pit/pond/overburden proportions observed in our Guyanese landscape applies more broadly over the Amazon, I estimated that gold mining results in ~90,000 t C yr^{-1} less carbon being accumulated in relation to what would have accumulated under agriculture/pasture. Given that a further 1,382,024 km^2 of Amazonia is currently under prospecting license for mining (Alvarez-Berríos and Mitchell Aide 2015, RAISG 2012, Figure S5), the gold mining-induced carbon deficit in Amazonia is expected to increase greatly over coming years.

For most tropical forest ecosystems recovering from past clearing from pasture and agriculture, it takes 50-100 years to fully recover species diversity patterns (Martin et al. 2013). Given that recovery of woody biomass and diversity on tailing ponds and mining pits is practically non-existent even after 2-4 years following abandonment, one can expect that recovery within these systems to take significantly longer. The findings presented here indicate the limited and uneven

nature of forest regeneration in gold mining sites, and potentially reveals a very fragmented Amazonian landscape in the future. Clearly, gold mining is one of the most destructive land use disturbances, compared to pasture and agriculture, in terms of nutrient depletion, mercury contamination and disrupting the successional process, particularly in the mining pits and tailing ponds. As such, active recovery strategies may have to be applied.

These results clearly show that nutrient (especially nitrogen) depletion may strongly influence ability to recover biomass and that nitrogen concentrations on overburden soils can be up to 20 times higher than those in previously mined pits and tailing ponds. This is linked to the excavation of topsoil from the mining pits and tailing ponds, which is subsequently dumped on overburden areas.

A practical recommendation that emerges from this work is that the re-filling of mining pits and tailing ponds with soils dumped on the overburden may go a long way to boosting forest recovery on those zones. The overburden should therefore be viewed as a strategic resource and its removal, storage and replacement to retain the physical and chemical properties should be protected. However, I also found evidence that high mercury concentrations may also retard forest recovery. Thus, if background mercury concentrations are high (e.g. in Mahdia), simply re-filling of mining pits and tailing ponds with the overburden soil may not automatically result in high biomass accumulation rates. Here, phytoremediation with native species may also aid restoration efforts. The optimal selection of plants requires carefully planned field trials as the germination/establishment sensitivity of different taxa to high mercury concentrations remains unstudied. Given their central role in driving biomass recovery, phytoremediation strategies which promote the functional integrity of nitrogen fixation processes need to further studied. Finally, a context of restoration of mined sites that involves planned decommissioning associated with positive management practices (e.g. pit re-filling) rather than the common practice of simple abandonment is required.

6
Synthesis & Conclusion

6.1 Research synthesis

The Amazon Basin is experiencing rapid transition, driven in recent decades by agricultural expansion in the Brazilian Amazon (Davidson et al. 2012). This thesis highlights new spatial patterns in Amazonian forest loss which point to a more complex pattern where new smaller-scale drivers of forest loss are becoming progressively more important (Chapter 2). In northern Amazonia, I further showed that these changes are closely related to the expansion of gold mining (Chapter 3). In Chapters 4 and 5, I then documented the impacts of gold mining on soil and plant nutrient status and on forest recovery processes. This process will ultimately frame the dynamics of the Amazonian landscape in the future.

My work was divided into two sections to assess (a) the spatial extent of different drivers of forest loss including gold mining across Amazonia using metrics of forest loss (Chapter 1.4), and (b) whether forests are able to recover following gold mining activities through an understanding of the mechanism responsible for regrowth from perturbations (Scheffer et al. 2015).

The major findings of my thesis were as follows (Figure 6.1):

1) Over the past 14-16 years, the Amazonian landscape have changed dramatically in terms of the type of driver that now influences forest loss, with small-scale activities becoming prevalent (Chapter 2).
2) Small-scale gold mining has expanded extensively across northern Amazonia, increasing by 926.4 km^2. This growth was also observed within protected areas where gold mining activities increased by 114 km^2 between the two study periods (Chapter 3).

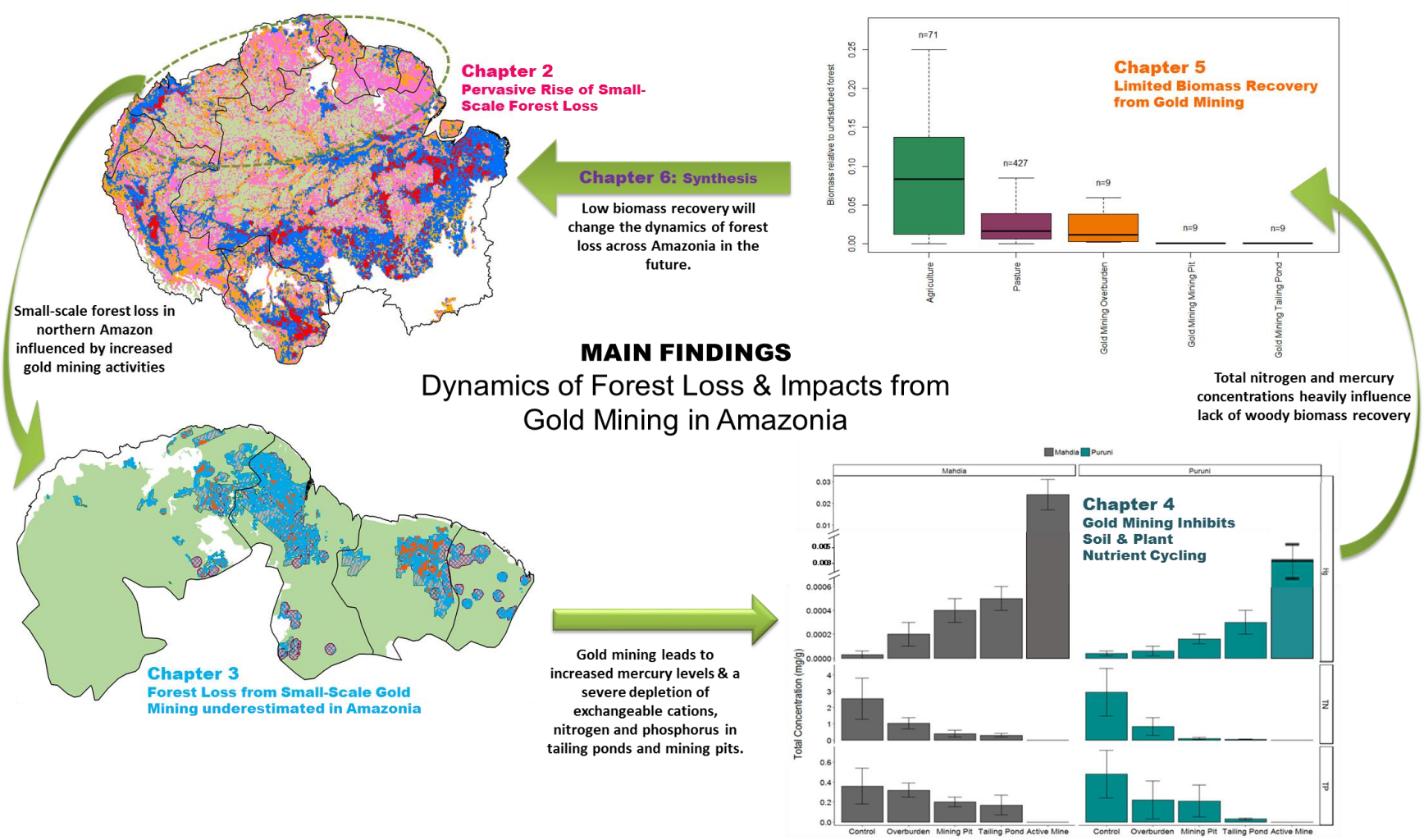

Figure 6.1 Summary of the main findings of the thesis.

3) Nutrient depletion was found to be the most important factor driving low biomass recovery in previously mined areas, with mercury contamination being a driver of secondary importance (Chapters 4 and 5).

4) Woody biomass recovery rates on previously mined tailing ponds and mining pits were the lowest recorded in any tropical forests after 2-4 years after abandonment, but were within normal range in overburden zones (Chapter 5).

In the following paragraphs, I summarize the main findings of each analytical chapter and how they contributed to achieving the aims of this thesis.

6.1.1 Small-scale forest loss persistent and increasing across Amazonia

To understand the dynamics of drivers of forest loss across the Amazon, remotely sensed data such as the Global Forest Cover (GFC) product based on 30-m resolution Landsat satellite images and 250-m resolution MODIS-based Terra-i product were used to assess the extent of forest loss events (Chapter 2, Appendix 2.13). The results of Chapter 2 indicate a shift of forest loss hotspots away from southern Brazil's 'arc of deforestation' to Peru and Brazil. Further, the number of small patches (<6.25ha) increased significantly between 2001-2007 and 2008-2014 across all Amazonian countries, extending in geographically remote areas which were previously considered isolated from deforestation pressures (Chapter 2). In northern Amazonia, this expansion of small-scale events was primarily driven by gold mining activities which increased by 926.4 km^2 between 2001-2008 and 2009-2016 (Chapter 3). This increase in gold mining also impacted protected areas which saw an increase of forest loss by 114 km^2 between the two time periods. Similar patterns of small-scale forest loss were also observed across all protected areas in the basin (Chapter 2). The results from protected area analysis in Chapters 2 and 3 suggests that protected areas have limited success in combating forest loss activities stemming from gold mining.

6.1.2 Underestimation of small-scale forest loss events from gold mining

I investigated whether remotely sensed products such as 30m-resolution Global Forest Cover (GFC) product are able to accurately detect forest loss from small-scale mining. As such, I compared GFC with 5m-resolution RapidEye satellite

images in Chapter 3. This chapter showed that GFC underestimated forest loss by area from gold mining activities by an average of 74% at known gold mining sites in Guyana. Higher omissions of forest loss were detected at the Mahdia site (70.6%) compared to Puruni (77.7%). This may indicate that initial size of forest clearance may be driving the detection process. As such, there is a probability that underestimation of forest loss may occur at sites driven by a mosaic of small-scale clearings.

6.1.3 Gold mining disrupts successional process in tailing pond and mining pit

One drawback of using satellite data of percentage tree cover as an indicator of environmental impacts of land uses is that it does not consider other impacts such as mercury poisoning or depletion of nutrients through the gold extraction process. As such, fieldwork was conducted where I measured changes in the soil and vegetation composition to test the recovery potential, and assessed the characteristics (e.g. nutrient composition and mercury concentration) behind such transitions. Nitrogen depletion was the main factor driving low biomass recovery in previously mined areas (Chapters 4 and 5). Chapter 4 analysis also suggested that mercury contamination at gold mining sites may further constrain the ability of selected plant species to establish themselves, including nitrogen-fixing species which are important for driving biomass accumulation in recovering secondary forests. Overall, gold mining can severely impair a forest's ability to recover, with preliminary evidence from Mahdia and Puruni, two gold mining study sites in Guyana, showing that abandoned mining pits and tailing ponds exhibit close to no woody biomass recovery even after 3-4 years of abandonment (Chapter 5). On the other hand, recovery rates of woody biomass on the overburden zone were comparable to other secondary forests across the Neotropics following abandonment of pastures and agriculture (Chapter 5). Thus, active rehabilitation measures are likely necessary to bolster recovery in previously mined tailing pond and mining pit zones but these have never been systematically evaluated. Assuming that the pit/pond/overburden proportions observed at my study sites applies more broadly over the Amazon, I estimated that gold mining results in ~90,000 t C yr^{-1} less carbon being accumulated in relation to what would have accumulated under agriculture/pasture.

6.2 Research implications

I showed that within the last 14-16 years small-scale forest loss has become pervasive throughout Amazonia (Chapter 2) with most of this clearing driven by gold mining activities in northern Amazon (Chapter 3). This result highlights the importance of small-scale deforestation events in determining total deforestation rates across each Amazonian country. While deforestation of large patches has steadily declined over time, deforestation of small patches (<1 ha) has increased over time. This is the most detailed assessment of forest loss across the entire Amazonian region (Chapter 2), which may help combat forest loss reporting inconsistencies for individual countries, helping them to achieve country level targets and accountability. Reporting and monitoring these forest loss changes is therefore critically important as Amazonian countries are required to document and record changes in forest extent, and therefore levels of deforestation-driven emissions, on a frequent basis under the Paris Agreement (UNFCCC 2015) and through schemes such as Reducing Emissions from Deforestation and Forest Degradation (REDD+). A key conclusion from this work is that national deforestation statistics need to include these small-scale events which are currently excluded from important official estimates such as PRODES.

Small-scale forest loss also opens up areas previously thought to be remote (Chapter 2) and may act as a catalyst for further development in the region. Understanding these drivers of forest loss has important implications for understanding forest dynamics and the global carbon cycle, especially the role of Amazonian forest as a global carbon pool. If forest loss is driven mainly by small-scale activities, detecting, monitoring and controlling them becomes inherently more difficult.

Significant forest loss from small-scale activities, including gold mining, were also tenacious within protected area networks including buffer zones in Amazonia (Chapters 2 and 3). Far-reaching consequences relating to mercury contamination and nutrient depletion will be present in these highly biodiverse regions, perhaps in the long-term (Chapter 4). Ultimately, current conservation strategies are ineffective in stopping small-scale deforestation events such as gold mining. Potential long-term solutions may likely require active law enforcement and

perhaps a de-emphasis on the use of gold as a financial commodity (Asner et al. 2013). The results presented in Chapters 2 and 3 also urge for a new way of mapping, detecting and tracking forest loss events across the Amazon.

It was evident from Chapters 4 and 5 that biomass recovery from gold mining activities was severely hampered because of nutrient depletion and mercury contamination, particularly on the tailing pond and mining pit. The potential area of impact covers over 1173 km^2 across northern Amazonia alone. As the successional processes are disrupted in these two mining zones, this indicates that active rehabilitation and restoration are required. In fact, restoration of former forested areas has been specifically outlined in the Paris Climate Agreement as a measure to limit global warming to below the 2^oC above pre-industrial levels (UNFCCC 2015), with the Bonn Challenge aiming to restore 350 million hectares of deforested areas by 2030 (IUCN 2014, Verdone and Seidl 2017). Besides protecting intact forests, restoration of former forests is the largest natural pathway to ensuring removal of existing carbon emissions from the atmosphere (Griscom et al. 2017). The results presented in this thesis (Chapters 4 and 5) may help restorative efforts in gold mining regions to channel limited resources towards depleted zones such as tailing ponds and mining pits. This means that countries will have clear conservation investment targets for restoration. However, the data in this thesis is based mainly on legal gold mining activities with no information on illegal activities. As such, knowing the actual extent of gold mining across Amazonia will assist in determining (1) where recovery is required, (2) the type of recovery necessary.

6.3 Future research directions

In this thesis I assessed information from remotely sensed data to examine the drivers of forest loss across the Amazon and determine the extent of more intense land use such as gold mining in northern Amazon. This methodological approach of using remote sensing has the strength to examine gold mining activities throughout the entire Amazon, with products such as 5m-resolution RapidEye being able to accurately detect small-scale activities compared to the 30m-resolution Landsat Global Forest Cover (GFC) and 250m-resolution MODIS

Terra-i products. As mentioned in Chapter 3, the accuracy of these products to detect different type of land uses is affected by cloud cover and scale of disturbance events: large-scale forest loss is easier to detect across all products. However, in Amazonian forests, forest loss and degradation are initially driven by more subtle processes that may be undetectable even at 30m-resolution, and may lead to underestimation of forest loss, as demonstrated in Chapters 2 and 3. Additionally, unlawful activities such as illegal gold mining often occurs in forests where full canopy clearance is not necessary. As such, combining products like the openly accessible GFC with complementary radar remote sensing may be more suitable to recording and detecting such disturbances. Hence, machine learning algorithms which are sensitive to small-scale forest loss events should be developed, potentially using radar, Landsat (GFC) and Sentinel time series. This machine learning algorithm can be developed further to map aboveground biomass across the Amazon based on FOTO and lacunarity analysis, a measure which determines multiple patterns across spatial and temporal scales that are inherent in high resolution imagery of forests (Butson and King 2006), that consider small-scale forest loss events.

As Amazonian forests did not co-evolve with such intense land uses, investigations on how effective forest rehabilitation can be at former gold mining sites should be also conducted. As shown in Chapters 4 and 5, nutrient depletion is an important factor driving low biomass recovery in previously mined areas. Thus, it might be expected that refilling of pits and ponds with displaced overburden soil which is richer in nutrients would improve the recovery of vegetation. However, the efficacy of refilling has not been systematically tested. Mercury contamination at gold mining sites can further impair the ability of selected plant species to establish, including nitrogen-fixing species which are important for driving biomass accumulation in recovering secondary forests. Thus, targeted planting of native forest species that are more resistant to mercury stress may also enhance recovery, but this too remains untested in the field. As such, I propose testing the efficacies of different restoration strategies which involves establishing replicates of the following treatments: a) control, i.e. no active management, b) re-filling using the overburden with natural regeneration, c) re-filling with planting of mercury tolerant forest species, and d) re-planting of mercury-tolerant forest species without re-filling. By examining these treatments,

we can assess the effectiveness of restoration and examine which species are more suited for enhanced regeneration of gold mining sites. I have recently won funding to test these ideas in practice.

Furthermore, the socioeconomic drivers and societal implications are complicated by a plethora of societal and political issues of gold mining all of which remain little studied and are likely complex. Poor people enter gold mining partly due to the perception of quicker returns of capital that can rapidly improve their economic status. Here, immediate prosperity is more highly valued than the long-lasting environmental impact. Due to this, it may be expected that in order for rehabilitation efforts to be achieved by these same people, their needs in terms of rapid financial or societal returns, should be prioritized through incentives. Further research into the causes and consequences of gold mining in tropical regions must therefore incorporate a social science perspective as well.

Almost all ecological research of human impacts on forests looks at changes after they occur using space-for-time substitution by comparing where a type of disturbance has happened to a nearby undisturbed site. The assumption of this approach is that the only thing that differs between sites is this disturbance. However, sites may have very different biodiversity, species composition and functions before any disturbance occurs. One potential research direction would be to use a before-after-control-impact (BACI) method where studies assess biodiversity and other ecological functions to sites prior to disturbance, during disturbance and after disturbance following gold mining activities. The sites impacted by the disturbance and the controls are measured before and after gold mining activities, which helps us to disentangle the effects of disturbance and any differences between sites. Additionally, we can compare the space-for-time methods to before-after-control-impact (BACI) methods. The BACI method was recently used to assess logging impacts on the Brazilian Amazon (França et al. 2016) but have not been extended to more intensive land uses such as gold mining.

6.4 Final Remarks

The analysis conducted in this thesis on forest loss dynamics and impacts from gold mining activities within the last 14 – 16 years across Amazonian forests revealed four important insights. Firstly, there has been a significant shift in the size of forest loss events across the region with small-scale clearings offsetting previously reported declines in deforestation by larger patch sizes. Secondly, these small-scale clearings are pervasive within protected areas and buffer zones which have had limited success in combating the spread of small-scale activities such as gold mining. Thirdly, the extent of forest loss from small-scale gold mining is underestimated due to current remote sensing products which are unable to detect smaller clearings. Finally, gold mining activities severely inhibit forest recovery due to nutrient depletion and mercury contamination, with some zones exhibiting close to no woody biomass recovery even after 2-5 years of abandonment. The results presented here highlights the vulnerability of Amazonian forests to newer, more intense types of land uses such as small-scale gold mining.

References

Ahmed, S. E., A. C. Lees, N. G. Moura, T. A. Gardner, J. Barlow, J. Ferreira, and R. M. Ewers. 2014. Road networks predict human influence on Amazonian bird communities. Proceedings of the Royal Society B: Biological Sciences 281:20141742–20141742.

Alencar, A. A., P. M. Brando, G. P. Asner, and F. E. Putz. 2015. Landscape fragmentation, severe drought, and the new Amazon forest fire regime. Ecological Applications.

Alencar, A., and C. Vera. 2006. Forest Understory Fire in the Brazilian Amazon in ENSO and Non-ENSO Years : Area Burned and. Earth Interactions 10.

Allen, C. D., A. K. Macalady, H. Chenchouni, D. Bachelet, N. McDowell, M. Vennetier, T. Kitzberger, A. Rigling, D. D. Breshears, E. H. (Ted. Hogg, P. Gonzalez, R. Fensham, Z. Zhang, J. Castro, N. Demidova, J. H. Lim, G. Allard, S. W. Running, A. Semerci, and N. Cobb. 2010. A global overview of drought and heat-induced tree mortality reveals emerging climate change risks for forests. Forest Ecology and Management 259:660–684.

Alvarez-Berríos, N. L., and T. Mitchell Aide. 2015. Global demand for gold is another threat for tropical forests. Environmental Research Letters 10:14006.

Alvarez, N. L., and L. Naughton-Treves. 2003. Linking National Agrarian Policy to Deforestation in the Peruvian Amazon: A Case Study of Tambopata, 1986–1997. AMBIO: A Journal of the Human Environment 32:269–274.

Alves, D. S. 2002. Space-time dynamics of deforestation in Brazilian Amaz??nia. International Journal of Remote Sensing.

Anderson-Teixeira, K. J., A. D. Miller, J. E. Mohan, T. W. Hudiburg, B. D. Duval, and E. H. DeLucia. 2013. Altered dynamics of forest recovery under a changing climate. Global Change Biology 19:2001–2021.

Aragao, L. E. O. ., Y. Malhi, N. Barbier, A. Lima, Y. Shimabukuro, L. Anderson, and S. Saatchi. 2008. Interactions between rainfall, deforestation and fires during recent years in the Brazilian Amazonia. Philosophical Transactions of the Royal Society B: Biological Sciences 363:1779–1785.

Aragão, L. E. O. C., L. O. Anderson, M. G. Fonseca, T. M. Rosan, L. B. Vedovato, F. H. Wagner, C. V. J. Silva, C. H. L. Silva Junior, E. Arai, A. P. Aguiar, J. Barlow, E. Berenguer, M. N. Deeter, L. G. Domingues, L. Gatti,

M. Gloor, Y. Malhi, J. A. Marengo, J. B. Miller, O. L. Phillips, and S. Saatchi. 2018. 21st Century drought-related fires counteract the decline of Amazon deforestation carbon emissions. Nature Communications 9:1–12.

Aragão, L. E. O. C., B. Poulter, J. B. Barlow, L. O. Anderson, Y. Malhi, S. Saatchi, O. L. Phillips, and E. Gloor. 2014. Environmental change and the carbon balance of Amazonian forests. Biological Reviews.

Arets, E. J. M. M., P. J. Van Der Meer, N. W. Van Den Brink, K. Tjon, V. P. Atmopawiro, and P. E. Ouboter. 2006. Assessment of the impacts of gold mining on soil and vegetation in Brownsberg Nature Park, Suriname.

Arima, E. Y., P. Barreto, E. Araújo, and B. Soares-Filho. 2014. Public policies can reduce tropical deforestation: Lessons and challenges from Brazil. Land Use Policy.

Armenteras, D., J. S. Barreto, K. Tabor, R. Molowny, and J. Retana. 2017. Changing patterns of fire occurrence in proximity to forest edges. Biogeosciences Discuss. Biogeosciences Discuss 5194:2016–532.

Armenteras, D., N. Rodríguez, and J. Retana. 2013. Landscape Dynamics in Northwestern Amazonia: An Assessment of Pastures, Fire and Illicit Crops as Drivers of Tropical Deforestation. PLoS ONE.

Asner, G. P. 2013. Geography of forest disturbance. Proceedings of the National Academy of Sciences 110:3711–3712.

Asner, G. P., E. N. Broadbent, P. J. C. Oliveira, M. Keller, D. E. Knapp, and J. N. M. Silva. 2006. Condition and fate of logged forests in the Brazilian Amazon. Proceedings of the National Academy of Sciences 103:12947–12950.

Asner, G. P., J. K. Clark, J. Mascaro, G. A. Galindo García, K. D. Chadwick, D. A. Navarrete Encinales, G. Paez-Acosta, E. Cabrera Montenegro, T. Kennedy-Bowdoin, Á. Duque, A. Balaji, P. Von Hildebrand, L. Maatoug, J. F. Phillips Bernal, A. P. Yepes Quintero, D. E. Knapp, M. C. García Dávila, J. Jacobson, and M. F. Ordóñez. 2012. High-resolution mapping of forest carbon stocks in the Colombian Amazon. Biogeosciences.

Asner, G. P., M. Keller, and J. N. M. Silva. 2004. Spatial and temporal dynamics of forest canopy gaps following selective logging in the eastern Amazon. Global Change Biology 10:765–783.

Asner, G. P., D. E. Knapp, E. N. Broadbent, P. J. C. Oliveira, M. Keller, and J. N.

Silva. 2005. Selective Logging in the Brazilian Amazon. Science 310:480–482.

Asner, G. P., W. Llactayo, R. Tupayachi, and E. R. Luna. 2013. Elevated rates of gold mining in the Amazon revealed through high-resolution monitoring. Proceedings of the National Academy of Sciences 110:18454–18459.

Asner, G. P., G. V. N. Powell, J. Mascaro, D. E. Knapp, J. K. Clark, J. Jacobson, T. Kennedy-Bowdoin, A. Balaji, G. Paez-Acosta, E. Victoria, L. Secada, M. Valqui, and R. F. Hughes. 2010. High-resolution forest carbon stocks and emissions in the Amazon. Proceedings of the National Academy of Sciences 107:16738–16742.

Asner, G. P., and R. Tupayachi. 2016. Accelerated losses of protected forests from gold mining in the Peruvian Amazon. Environmental Research Letters 12:94004.

Assunção, J., C. Gandour, and R. Rocha. 2012. Deforestation slowdown in the Brazilian Amazon: prices or policies? Environment and Development Economics.

Assunção, J., C. Gandour, R. Rocha, and R. Rocha. 2013. Does Credit A Deforestation? Evidence from a Rural Credit Policy in the Brazilian Amazon Climate Policy Initiative.

Baker, T. R., O. L. Phillips, Y. Malhi, S. Almeida, L. Arroyo, A. Di Fiore, T. Erwin, N. Higuchi, T. J. Killeen, S. G. Laurance, W. F. Laurance, S. L. Lewis, A. Monteagudo, D. A. Neill, P. Nunez Vargas, N. C. A. Pitman, J. N. M. Silva, and R. Vasquez Martinez. 2004. Increasing biomass in Amazonian forest plots. Philosophical Transactions of the Royal Society B: Biological Sciences.

Balch, J. K., T. J. Massad, P. M. Brando, D. C. Nepstad, L. M. Curran, P. T. R. S. B, J. K. Balch, T. J. Massad, P. M. Brando, D. C. Nepstad, and L. M. Curran. 2013. Effects of high-frequency understorey fires on woody plant regeneration in southeastern Amazonian forests. Philosophical Transactions of the Royal Society B: Biological Sciences 368.

Balzino, M., J. Seccatore, T. Marin, G. De Tomi, and M. M. Veiga. 2015. Gold losses and mercury recovery in artisanal gold mining on the Madeira River, Brazil. Journal of Cleaner Production.

Barber, C. P., M. A. Cochrane, C. M. Souza, and W. F. Laurance. 2014. Roads,

deforestation, and the mitigating effect of protected areas in the Amazon. Biological Conservation 177:203–209.

Barbosa, L. C. 2001. The Brazilian Amazon Rainforest: Global Ecopolitics, Development and Democracy. Lanham, MD: University Press of America, 2000:196.

Barlow, J., G. D. Lennox, J. Ferreira, E. Berenguer, A. C. Lees, R. Mac Nally, J. R. Thomson, S. F. D. B. Ferraz, J. Louzada, V. H. F. Oliveira, L. Parry, R. Ribeiro De Castro Solar, I. C. G. Vieira, L. E. O. C. Araga??, R. A. Begotti, R. F. Braga, T. M. Cardoso, R. C. D. O. Jr, C. M. Souza, N. G. Moura, S. S. Nunes, J. V. Siqueira, R. Pardini, J. M. Silveira, F. Z. Vaz-De-Mello, R. C. S. Veiga, A. Venturieri, and T. A. Gardner. 2016. Anthropogenic disturbance in tropical forests can double biodiversity loss from deforestation. Nature 535.

Barlow, J., and C. A. Peres. 2008. Fire-mediated dieback and compositional cascade in an Amazonian forest. Philosophical Transactions of the Royal Society B: Biological Sciences 363:1787–1794.

Batterman, S. A., L. O. Hedin, M. van Breugel, J. Ransijn, D. J. Craven, and J. S. Hall. 2013. Key role of symbiotic dinitrogen fixation in tropical forest secondary succession. Nature 502:224–227.

Bell, R. W. 2002. Restoration of Degraded Landscapes: Principles and Lessons from Case Studies with Salt-affected Land and Mine Revegetation. CMU Journal 1:1-.

Bereitschaft, B., and K. Debbage. 2014. Regional Variations in Urban Fragmentation Among U.S. Metropolitan and Megapolitan Areas. Applied Spatial Analysis and Policy.

Berenguer, E., J. Ferreira, T. A. Gardner, L. E. O. C. Aragão, P. B. De Camargo, C. E. Cerri, M. Durigan, R. C. De Oliveira, I. C. G. Vieira, and J. Barlow. 2014. A large-scale field assessment of carbon stocks in human-modified tropical forests. Global Change Biology.

Berenguer, E., T. A. Gardner, J. Ferreira, L. E. O. C. Aragão, P. B. Camargo, C. E. Cerri, M. Durigan, R. C. Oliveira, I. C. G. Vieira, and J. Barlow. 2015. Developing cost-effective field assessments of carbon stocks in human-modified tropical forests. PLoS ONE.

Bicknell, J. E., M. J. Struebig, and Z. G. Davies. 2015. Reconciling timber

extraction with biodiversity conservation in tropical forests using reduced-impact logging. Journal of Applied Ecology 52:379–388.

Boisier, J. P., P. Ciais, A. Ducharne, and M. Guimberteau. 2015. Projected strengthening of Amazonian dry season by constrained climate model simulations. Nature Climate Change 5:656–660.

Bonan, G. B. 2008. Forests and Climate Change: Forcings, Feedbacks, and the Climate Benefits of Forests. Science.

Bovolo, C. I., T. Wagner, G. Parkin, D. Hein-Griggs, R. Pereira, and R. Jones. 2018. The Guiana Shield rainforests—overlooked guardians of South American climate. Environmental Research Letters 13:74029.

Bradshaw, A. 1997. Restoration of mined lands—using natural processes. Ecological Engineering 8:255–269.

Branford, S. 2018. Brazil announces end to Amazon mega-dam building policy. Mongabay.

Brasil - Ministério do Meio Ambiente (MMA). 2013. Plano de Ação para Prevenção e Controle do Desmatamento na Amazônia Legal (PPCDAm). 3ª fase (2012-2015) pelo uso sustentável e conservação da Floresta Ministério do Meio Ambiente e Grupo Permanente de Trabalho Interministerial.

van Breugel, M., F. Bongers, and M. Mart. 2007. Species Dynamics During Early Secondary Forest Succession: Recruitment, Mortality and Species Turnover. Biotropica 35:610–619.

Brienen, R. J. W., O. L. Phillips, T. R. Feldpausch, E. Gloor, T. R. Baker, J. Lloyd, G. Lopez-Gonzalez, A. Monteagudo-Mendoza, Y. Malhi, S. L. Lewis, R. Vásquez Martinez, M. Alexiades, E. Álvarez Dávila, P. Alvarez-Loayza, A. Andrade, L. E. O. C. Aragão, A. Araujo-Murakami, E. J. M. M. Arets, L. Arroyo, G. A. Aymard C., O. S. Bánki, C. Baraloto, J. Barroso, D. Bonal, R. G. A. Boot, J. L. C. Camargo, C. V. Castilho, V. Chama, K. J. Chao, J. Chave, J. A. Comiskey, F. Cornejo Valverde, L. da Costa, E. A. de Oliveira, A. Di Fiore, T. L. Erwin, S. Fauset, M. Forsthofer, D. R. Galbraith, E. S. Grahame, N. Groot, B. Hérault, N. Higuchi, E. N. Honorio Coronado, H. Keeling, T. J. Killeen, W. F. Laurance, S. Laurance, J. Licona, W. E. Magnussen, B. S. Marimon, B. H. Marimon-Junior, C. Mendoza, D. A. Neill, E. M. Nogueira, P. Núñez, N. C. Pallqui Camacho, A. Parada, G. Pardo-Molina, J. Peacock, M. Peña-Claros, G. C. Pickavance, N. C. A. Pitman, L.

Poorter, A. Prieto, C. A. Quesada, F. Ramírez, H. Ramírez-Angulo, Z. Restrepo, A. Roopsind, A. Rudas, R. P. Salomão, M. Schwarz, N. Silva, J. E. Silva-Espejo, M. Silveira, J. Stropp, J. Talbot, H. ter Steege, J. Teran-Aguilar, J. Terborgh, R. Thomas-Caesar, M. Toledo, M. Torello-Raventos, R. K. Umetsu, G. M. F. van der Heijden, P. van der Hout, I. C. Guimarães Vieira, S. A. Vieira, E. Vilanova, V. A. Vos, and R. J. Zagt. 2015. Long-term decline of the Amazon carbon sink. Nature 519:344–348.

British Standards Institution. 1967. Methods of Testing Soils for Civil Engineering Purposes.

Brown, R. G. W., J. G. Burnett, J. Mansbridge, and C. I. Moir. 1990. Miniature laser light scattering instrumentation for particle size analysis. Applied Optics 29:4159.

Bürgi, M., L. Östlund, and D. J. Mladenoff. 2017. Legacy Effects of Human Land Use: Ecosystems as Time-Lagged Systems. Ecosystems 20:94–103.

Bush, M. B., C. H. Mcmichael, D. R. Piperno, M. R. Silman, J. Barlow, C. A. Peres, M. Power, and M. W. Palace. 2015. Anthropogenic influence on Amazonian forests in pre-history: An ecological perspective. Journal of Biogeography 42:2277–2288.

Bush, M. B., M. R. Silman, C. McMichael, and S. Saatchi. 2008. Fire, climate change and biodiversity in Amazonia: A Late-Holocene perspective. Philosophical Transactions of the Royal Society B: Biological Sciences 363:1795–1802.

Butson, C. R., and D. J. King. 2006. Lacunarity analysis to determine optimum extents for sample-based spatial information extraction from high-resolution forest imagery. International Journal of Remote Sensing 27:105–120.

Butt, N., P. A. De Oliveira, and M. H. Costa. 2011. Evidence that deforestation affects the onset of the rainy season in Rondonia, Brazil. Journal of Geophysical Research Atmospheres 116.

Carrasco, L. R., T. P. L. Nghiem, T. Sunderland, and L. P. Koh. 2014. Economic valuation of ecosystem services fails to capture biodiversity value of tropical forests. Biological Conservation 178:163–170.

Castiblanco, C., A. Etter, and T. M. Aide. 2013. Oil palm plantations in Colombia: A model of future expansion. Environmental Science and Policy 27:172–183.

Castilhos, Z., S. Rodrigues-Filho, R. Cesar, A. P. Rodrigues, R. Villas-Bôas, I. de Jesus, M. Lima, K. Faial, A. Miranda, E. Brabo, C. Beinhoff, and E. Santos. 2015. Human exposure and risk assessment associated with mercury contamination in artisanal gold mining areas in the Brazilian Amazon. Environmental Science and Pollution Research 22:11255–11264.

Cavaleri, M., M. G. Ryan, H. W. Loescher, M. A. Cavaleri, A. P. Coble, M. G. Ryan, W. L. Bauerle, and H. W. Loescher. 2017. Tropical rainforest carbon sink declines during El Niño as a result of reduced photosynthesis and increased respiration rates. New Phytologist 216:136–149.

CBD. 2013. Quick guides to the Aichi Biodiversity Targets:42.

Chainey, S. 2010. Spatial significance hotspot mapping using the Gi * statistic. POP Conference:1–43.

Chakravarty, S., S. K. Ghosh, and C. P. Suresh. 2011. Deforestation : Causes , Effects and Control Strategies:3–29.

Chave, J., M. Réjou-Méchain, A. Búrquez, E. Chidumayo, M. S. Colgan, W. B. C. Delitti, A. Duque, T. Eid, P. M. Fearnside, R. C. Goodman, M. Henry, A. Martínez-Yrízar, W. A. Mugasha, H. C. Muller-Landau, M. Mencuccini, B. W. Nelson, A. Ngomanda, E. M. Nogueira, E. Ortiz-Malavassi, R. Pélissier, P. Ploton, C. M. Ryan, J. G. Saldarriaga, and G. Vieilledent. 2014. Improved allometric models to estimate the aboveground biomass of tropical trees. Global Change Biology.

Chávez, A. B., E. N. Broadbent, and A. M. Almeyda Zambrano. 2014. Smallholder policy adoption and land cover change in the southeastern Peruvian Amazon: A twenty-year perspective. Applied Geography.

Chazdon, R. L. 2003. Tropical forest recovery : legacies of human impact and natural disturbances. Perspectives in Plant Ecol, Evol and Systematics 6:51–71.

Chazdon, R. L., E. N. Broadbent, D. M. A. Rozendaal, F. Bongers, A. M. A. Zambrano, T. M. Aide, P. Balvanera, J. M. Becknell, V. Boukili, P. H. S. Brancalion, D. Craven, J. S. Almeida-Cortez, G. A. L. Cabral, B. de Jong, J. S. Denslow, D. H. Dent, S. J. DeWalt, J. M. Dupuy, S. M. Duran, M. M. Espirito-Santo, M. C. Fandino, R. G. Cesar, J. S. Hall, J. L. Hernandez-Stefanoni, C. C. Jakovac, A. B. Junqueira, D. Kennard, S. G. Letcher, M. Lohbeck, M. Martinez-Ramos, P. Massoca, J. A. Meave, R. Mesquita, F.

Mora, R. Munoz, R. Muscarella, Y. R. F. Nunes, S. Ochoa-Gaona, E. Orihuela-Belmonte, M. Pena-Claros, E. A. Perez-Garcia, D. Piotto, J. S. Powers, J. Rodriguez-Velazquez, I. E. Romero-Perez, J. Ruiz, J. G. Saldarriaga, A. Sanchez-Azofeifa, N. B. Schwartz, M. K. Steininger, N. G. Swenson, M. Uriarte, M. van Breugel, H. van der Wal, M. D. M. Veloso, H. Vester, I. C. G. Vieira, T. V. Bentos, G. B. Williamson, and L. Poorter. 2016. Carbon sequestration potential of second-growth forest regeneration in the Latin American tropics. Science Advances 2:e1501639–e1501639.

Chazdon, R. L., S. G. Letcher, M. van Breugel, M. Martinez-Ramos, F. Bongers, and B. Finegan. 2007. Rates of change in tree communities of secondary Neotropical forests following major disturbances. Philosophical Transactions of the Royal Society B: Biological Sciences 362:273–289.

Chazdon, R. L., C. A. Peres, D. Dent, D. Sheil, A. E. Lugo, D. Lamb, N. E. Stork, and S. E. Miller. 2009. The potential for species conservation in tropical secondary forests. Conservation Biology.

Chinea, J. D. 2002. Tropical forest succession on abandoned farms in the Humacao Municipality of eastern Puerto Rico. Forest Ecology and Management 167:195–207.

Chinea, J. D., and E. H. Helmer. 2003. Diversity and composition of tropical secondary forests recovering from large- scale clearing : results from the 1990 inventory in Puerto Rico . For Ecol Manag recovering from large-scale clearing : results from the 1990 inventory in Puerto Rico. Forest Ecology and Management 180:227–240.

Chomitz, K. M., P. Buys, G. De Luca, T. S. Thomas, and S. Wertz-kanounnikoff. 2007. At Loggerheads? Agricultural Expansion, Poverty Reduction and Environment in the Tropical Forests. Page The International Bank for Reconstruction and Development, The World Bank.

Chomitz, K. M., G. A. B. da Fonseca, K. Alger, D. M. Stoms, M. Honzák, E. C. Landau, T. S. Thomas, W. W. Thomas, and F. Davis. 2006. Viable reserve networks arise from individual landholder responses to conservation incentives. Ecology and Society.

Coca-Castro, A., L. Reymondin, H. Bellfield, and G. Hymen. 2013. Land use Status and Trends in Amazonia: Terra-i. A report for the Amazonia Security Agenda Project.

Cochrane, M. A., W. F. Laurance, and L. Changes. 2008. Synergisms among Fire , Land Use , and Climate Change in the Amazon 37:522–527.

Coe, M. T., T. R. Marthews, M. H. Costa, D. R. Galbraith, N. L. Greenglass, H. M. A. Imbuzeiro, N. M. Levine, Y. Malhi, P. R. Moorcroft, M. N. Muza, T. L. Powell, S. R. Saleska, L. A. Solorzano, and J. Wang. 2013. Deforestation and climate feedbacks threaten the ecological integrity of south-southeastern Amazonia. Philosophical Transactions of the Royal Society B: Biological Sciences.

Cole, L. E. S., S. A. Bhagwat, and K. J. Willis. 2014. Recovery and resilience of tropical forests after disturbance. Nature Communications 5:1–7.

Collins, M. B., and E. T. A. Mitchard. 2017. A small subset of protected areas are a highly significant source of carbon emissions. Scientific Reports.

Condit, R., S. P. . Hubbell, and R. B. . Foster. 1995. Mortality Rates of 205 Neotropical Tree and Shrub Species and the Impact of a Severe Drought. Ecological Society of America 65:419–439.

Contini, E., and G. Martha. 2010. Brazilian agriculture , its productivity and change. Royal Swedish Academcy of Agricultur and Forestry:1–14.

Cordeiro, R. C., B. Turcq, L. S. Moreira, R. de A. R. Rodrigues, F. F. Lamego Simões Filho, G. S. Martins, A. B. Santos, M. Barbosa, M. C. Guilles da Conceição, R. de C. Rodrigues, H. Evangelista, P. Moreira-Turcq, Y. P. Penido, A. Sifeddine, and J. C. S. Seoane. 2014. Palaeofires in Amazon: Interplay between land use change and palaeoclimatic events. Palaeogeography, Palaeoclimatology, Palaeoecology 415:137–151.

Cremers, L., J. Kolen, and M. de Theije. 2013. Small-Scale Gold Mining in the Amazon: The cases of Bolivia, Brazil, Colombia, Peru and Suriname. Page Cente for Latin American Studies and Documentation, Amsterdam.

D’oliveira, M. V. N., E. C. Alvarado, J. C. Santos, and J. A. Carvalho. 2011. Forest natural regeneration and biomass production after slash and burn in a seasonally dry forest in the Southern Brazilian Amazon. Forest Ecology and Management 261:1490–1498.

Davidson, E. A., A. C. De Araüjo, P. Artaxo, J. K. Balch, I. F. Brown, M. M. Mercedes, M. T. Coe, R. S. Defries, M. Keller, M. Longo, J. W. Munger, W. Schroeder, B. S. Soares-Filho, C. M. Souza, and S. C. Wofsy. 2012. The Amazon basin in transition.

Davidson, E. A., C. J. R. De Carvalho, A. M. Figueira, F. Y. Ishida, J. P. H. B. Ometto, G. B. Nardoto, R. T. Sabá, S. N. Hayashi, E. C. Leal, I. C. G. Vieira, and L. A. Martinelli. 2007. Recuperation of nitrogen cycling in Amazonian forests following agricultural abandonment. Nature 447:995–998.

Davidson, E. A., C. J. R. De Carvalho, I. C. G. Vieira, R. De O, P. Moutinho, F. Y. Ishida, M. Tereza, J. Benito, K. Kalif, R. T. Sabá, and Y. Ishida. 2004a. Nitrogen and Phosphorus Limitation of Biomass Growth in a Tropical Secondary Forest 14:150–163.

Davidson, E. A., F. Y. Ishida, and D. C. Nepstad. 2004b. Effects of an experimental drought on soil emissions of carbon dioxide, methane, nitrous oxide, and nitric oxide in a moist tropical forest. Global Change Biology 10:718–730.

Dedieu, N., L. Allard, R. Vigouroux, S. Brosse, and R. Céréghino. 2014. Physical habitat and water chemistry changes induced by logging and gold mining in French Guiana streams. Knowledge and Management of Aquatic Ecosystems:2.

Diniz, C. G., A. A. D. A. Souza, D. C. Santos, M. C. Dias, N. C. Da Luz, D. R. V. De Moraes, J. S. A. Maia, A. R. Gomes, I. D. S. Narvaes, D. M. Valeriano, L. E. P. Maurano, and M. Adami. 2015. DETER-B: The New Amazon Near Real-Time Deforestation Detection System. IEEE Journal of Selected Topics in Applied Earth Observations and Remote Sensing 8:3619–3628.

Diringer, S. E., B. J. Feingold, E. J. Ortiz, J. A. Gallis, J. M. Araújo-Flores, A. Berky, W. K. Y. Pan, and H. Hsu-Kim. 2015. River transport of mercury from artisanal and small-scale gold mining and risks for dietary mercury exposure in Madre de Dios, Peru. Environmental Science: Processes & Impacts.

Dohrmann, R. 2006. Cation exchange capacity methodology II: A modified silver-thiourea method. Applied Clay Science 34:38–46.

Dourojeanni, M., A. Barandiarán, and D. Dourojeanni. 2009. Amazonía Peruana en 2021.

Edwards, D. P., M. R. Massam, T. Haugaasen, and J. J. Gilroy. 2017. Tropical secondary forest regeneration conserves high levels of avian phylogenetic diversity. Biological Conservation 209:432–439.

Edwards, D. P., J. A. Tobias, D. Sheil, E. Meijaard, and W. F. Laurance. 2014.

Maintaining ecosystem function and services in logged tropical forests. Trends in Ecology and Evolution 29:511–520.

Esdaile, L. J., and J. M. Chalker. 2018. The Mercury Problem in Artisanal and Small-Scale Gold Mining. Chemistry - A European Journal:1–13.

Espinosa-Reyes, G., D. J. González-Mille, C. A. Ilizaliturri-Hernández, J. Mejía-Saavedra, V. G. Cilia-López, R. Costilla-Salazar, and F. Díaz-Barriga. 2014. Effect of mining activities in biotic communities of Villa de la Paz, San Luis Potosi, Mexico. BioMed Research International 2014.

Espinosa, S., G. Celis, and L. C. Branch. 2018. When roads appear jaguars decline: Increased access to an Amazonian wilderness area reduces potential for jaguar conservation. PLoS ONE 13:1–18.

Espírito-Santo, F. D. B., M. Gloor, M. Keller, Y. Malhi, S. Saatchi, B. Nelson, R. C. O. Junior, C. Pereira, J. Lloyd, S. Frolking, M. Palace, Y. E. Shimabukuro, V. Duarte, A. M. Mendoza, G. López-González, T. R. Baker, T. R. Feldpausch, R. J. W. Brienen, G. P. Asner, D. S. Boyd, and O. L. Phillips. 2014. Size and frequency of natural forest disturbances and the Amazon forest carbon balance. Nature Communications.

Eva, H., O. Huber, F. Achard, H. Balslev, S. Beck, H. Behling, A. Belward, R. Beuchle, A. Cleef, M. Colchester, Duivenvoorden, M. Hoogmoed, W. Junk, P. Kabat, B. Kruijit, Y. Malhi, J. M. Müller, J. M. Pereira, C. Peres, G. T. Prance, J. Roberts, and J. Salo. 2005. A proposal for defining the geographical boundaries of Amazonia. Page A proposal for defining the geographical boundaries of Amazonia.

Exbrayat, J. F., Y. Y. Liu, and M. Williams. 2017. Impact of deforestation and climate on the Amazon Basin's above-ground biomass during. Scientific Reports 7:1–7.

Faassen, H. G. 1973. Effects of mercury compounds on soil microbes. Plant and Soil 38:485–487.

FAO. 1993. Management and conservation of closed forests in tropical America.

FAO. 2001. State of the World's Forest 2001. Food and Agriculture Organization of the United Nations.

FAO. 2006. Global Forest Resources Assessment 2005 Progress towards sustainable forest management. Food and Agricultural Organization of the United Nations.

FAO. 2011. The State of Forests in the Amazon Basin, Congo Basin and Southeast Asia.

FAO. 2015a. Global Forest Resources Assessment 2015: How are the world's forests changing? Food and Agriculture Organization of the United Nations, Rome, 2015.

FAO. 2015b. Global Forest Resources Assessment 2015 Country Report: Suriname. Food and Agriculture Organization of the United Nations, Roome 2015.

Fearnside, P. M. 2005. Deforestation in Brazilian Amazonia : History , Rates and Consequences. Conservation Biology 19:728–733.

Fearnside, P. M. 2008. The Roles and Movements of Actors in the Deforestation of Brazilian Amazonia. Ecology an 13 (1).

Feldpausch, T. R., C. da Conceicao Prates-Clark, E. C. M. Fernandes, and S. J. Riha. 2007. Secondary forest growth deviation from chronosequence predictions in central Amazonia. Global Change Biology 13:967–979.

Feldpausch, T. R., E. C. M. Fernandes, and S. J. Riha. 2005a. Development of Forest structure and leaf area in secondary forests regenerating from degraded pastures in central Amazônia. Earth Interactions 9.

Feldpausch, T. R., S. Jirka, C. A. M. Passos, F. Jasper, and S. J. Riha. 2005b. When big trees fall: Damage and carbon export by reduced impact logging in southern Amazonia. Forest Ecology and Management 219:199–215.

Feldpausch, T. R., J. Lloyd, S. L. Lewis, R. J. W. Brienen, M. Gloor, A. Monteagudo Mendoza, G. Lopez-Gonzalez, L. Banin, K. Abu Salim, K. Affum-Baffoe, M. Alexiades, S. Almeida, I. Amaral, A. Andrade, L. E. O. C. Aragão, A. Araujo Murakami, E. J. M. Arets, L. Arroyo, G. A. Aymard C., T. R. Baker, O. S. Bánki, N. J. Berry, N. Cardozo, J. Chave, J. A. Comiskey, E. Alvarez, A. De Oliveira, A. Di Fiore, G. Djagbletey, T. F. Domingues, T. L. Erwin, P. M. Fearnside, M. B. França, M. A. Freitas, N. Higuchi, E. Honorio C., Y. Iida, E. Jiménez, A. R. Kassim, T. J. Killeen, W. F. Laurance, J. C. Lovett, Y. Malhi, B. S. Marimon, B. H. Marimon-Junior, E. Lenza, A. R. Marshall, C. Mendoza, D. J. Metcalfe, E. T. A. Mitchard, D. A. Neill, B. W. Nelson, R. Nilus, E. M. Nogueira, A. Parada, K. S.-H. Peh, A. Pena Cruz, M. C. Peñuela, N. C. A. Pitman, A. Prieto, C. A. Quesada, F. Ramírez, H. Ramírez-Angulo, J. M. Reitsma, A. Rudas, G. Saiz, R. P. Salomão, M.

Schwarz, N. Silva, J. E. Silva-Espejo, M. Silveira, B. Sonké, J. Stropp, H. E. Taedoumg, S. Tan, H. Ter Steege, J. Terborgh, M. Torello-Raventos, G. M. F. Van Der Heijden, R. Vásquez, E. Vilanova, V. A. Vos, L. White, S. Willcock, H. Woell, and O. L. Phillips. 2012. Tree height integrated into pantropical forest biomass estimates. Biogeosciences 9:3381–3403.

Feldpausch, T. R., O. L. Phillips, R. J. W. Brienen, E. Gloor, J. Lloyd, Y. Malhi, A. Alarcón, E. Á. Dávila, A. Andrade, L. E. O. C. Aragao, L. Arroyo, G. A. C. Aymard, T. R. Baker, C. Baraloto, J. Barroso, D. Bonal, W. Castro, V. Chama, J. Chave, T. F. Domingues, S. Fauset, N. Groot, E. H. Coronado, S. Laurance, W. F. Laurance, S. L. Lewis, J. C. Licona, B. S. Marimon, C. M. Bautista, D. A. Neill, E. A. Oliveira, C. O. Santos, N. C. P. Camacho, A. Prieto, C. A. Quesada, F. Ramírez, A. Rudas, G. Saiz, R. P. Salomão, M. Silveira, H. Steege, J. Stropp, J. Terborgh, G. M. F. Heijden, R. V. Martinez, E. Vilanova, and V. A. Vos. 2016. Amazon forest response to repeated droughts. Global Biogeochemical Cycles 30:964–982.

Feldpausch, T. R., M. A. Rondon, E. C. M. Fernandes, and S. J. Riha. 2004. Carbon and Nutrient Accumulation in Secondary Forests Regenerating on Pastures in Central Amazonia Published by : Ecological Society of America Carbon and Nutrient Accumulation in Secondary Forests Regenerating on Pastures in Central Amazonia. Ecological Applications 14:164–176.

Fernández-Llamazares, Á., J. Helle, J. Eklund, A. Balmford, R. Mónica Moraes, V. Reyes-García, and M. Cabeza. 2018. New law puts Bolivian biodiversity hotspot on road to deforestation. Current Biology 28:R15–R16.

Ferreira, J., G. D. Lennox, T. A. Gardner, J. R. Thomson, E. Berenguer, A. C. Lees, R. Mac Nally, L. E. O. C. Aragão, S. F. B. Ferraz, J. Louzada, N. G. Moura, V. H. F. Oliveira, R. Pardini, R. R. C. Solar, I. C. G. Vieira, and J. Barlow. 2018. Carbon-focused conservation may fail to protect the most biodiverse tropical forests. Nature Climate Change.

Fine, P. V. A. 2002. The invasibility of tropical forests by exotic plants. Journal of Tropical Ecology 18:687–705.

Finer, M., B. Babbitt, S. Novoa, F. Ferrarese, S. E. Pappalardo, M. De Marchi, M. Saucedo, and A. Kumar. 2015. Future of oil and gas development in the western Amazon. Environmental Research Letters 10:24003.

Finer, M., C. N. Jenkins, M. A. B. Sky, and J. Pine. 2014. Logging concessions

enable illegal logging crisis in the peruvian amazon. Scientific Reports 4:1–6.

Finer, M., and S. Novoa. 2015. MAAP Synthesis # 1 : Patterns and Drivers of Deforestation in the Peruvian Amazon.

Finer, M., S. Novoa, J. Weisse, R. Petersen, T. Souto, and F. Stearns. 2018. Combating deforestation From satellite to intervention. Science 360:1303–1305.

Foley, J. A., G. P. Asner, M. Heil Costa, M. T. Coe, R. Defries, H. K. Gibbs, E. A. Howard, S. Olson, J. Patz, N. Ramankutty, and P. Snyder. 2007. Amazonia revealed: forest degradation and loss of ecosystem goods and services in the Amazon Basin. The Ecological Society of America 5:25–32.

França, F., J. Louzada, V. Korasaki, H. Griffiths, J. M. Silveira, and J. Barlow. 2016. Do space-for-time assessments underestimate the impacts of logging on tropical biodiversity? An Amazonian case study using dung beetles. Journal of Applied Ecology 53:1098–1105.

Franklin, J. 2007. Recovery from clearing, cyclone and fire in rain forests of Tonga, South Pacific: Vegetation dynamics 1995-2005. Austral Ecology 32:789–797.

Galbraith, D., M. Adami, Y. Wang, R. Brienen, P. M. Fearnside, E. Gloor, M. Kalamandeen, E. Mitchard, E. Nogueira, O. Phillips, L. Sadeck, A. Venturieri, G. Ziv, C. A. de Almeida, and A. Gomes. (in review.). High-resolution Assessment of the Net Biomass Balance of the Brazilian Amazon: 2004-2014. Global Change Biology.

Gámez-Virués, S., D. J. Perović, M. M. Gossner, C. Börschig, N. Blüthgen, H. De Jong, N. K. Simons, A. M. Klein, J. Krauss, G. Maier, C. Scherber, J. Steckel, C. Rothenwöhrer, I. Steffan-Dewenter, C. N. Weiner, W. Weisser, M. Werner, T. Tscharntke, and C. Westphal. 2015. Landscape simplification filters species traits and drives biotic homogenization. Nature Communications 6.

Garcïa-Sánchez, A., F. Contreras, M. Adams, and F. Santos. 2006. Atmospheric mercury emissions from polluted gold mining areas (Venezuela). Environmental Geochemistry and Health 28:529–540.

Geist, H. J., and E. Lambin. 2001. What drives tropical deforestation? Land-Use and Land-Cover Change (LUCC). International Human Dimeans Programme

on Global Environmental Change (IHDP) V. International Geosphere-Biosphere Programme (IGBP) Vi. LUCC Repor:373.

Getis, A., and J. K. Ord. 1992. The Analysis of Spatial Association by Use of Distance Statistics. Geographical Analysis 24:189–206.

GGMC. 2011. GGMC Annual Report 2011. Guyana Geology and Mines Commission (GGMC):45 pp.

Gibbs, H. K., L. Rausch, J. Munger, I. Schelly, D. C. Morton, P. Noojipady, B. Soares-Filho, P. Barreto, L. Micol, and N. F. Walker. 2015. Brazil's Soy Moratorium. Science 347:377–378.

Gibbs, H. K., A. S. Ruesch, F. Achard, M. K. Clayton, P. Holmgren, N. Ramankutty, and J. A. Foley. 2010. Tropical forests were the primary sources of new agricultural land in the 1980s and 1990s. Proceedings of the National Academy of Sciences 107:16732–16737.

Gloor, M., R. J. W. Brienen, D. Galbraith, T. R. Feldpausch, J. Schöngart, J. L. Guyot, J. C. Espinoza, J. Lloyd, and O. L. Phillips. 2013. Intensification of the Amazon hydrological cycle over the last two decades. Geophysical Research Letters.

Godar, J., T. A. Gardner, E. J. Tizado, and P. Pacheco. 2014. Actor-specific contributions to the deforestation slowdown in the Brazilian Amazon. Proceedings of the National Academy of Sciences.

Goetz, S. J., M. Hansen, R. A. Houghton, W. Walker, N. Laporte, and J. Busch. 2015. Measurement and monitoring needs, capabilities and potential for addressing reduced emissions from deforestation and forest degradation under REDD+. Environmental Research Letters 10:123001.

Goulart, A. C., K. D. Macario, R. Scheel-Ybert, E. Q. Alves, C. Bachelet, B. B. Pereira, C. Levis, B. H. Marimon Junior, B. S. Marimon, C. A. Quesada, and T. R. Feldpausch. 2017. Charcoal chronology of the Amazon forest: A record of biodiversity preserved by ancient fires. Quaternary Geochronology 41:180–186.

Government of Colombia. 2011. REDD Readiness Preparation Proposal. Working Draft Version 5 (revised): December 22, 2010.

Grainger, A. 2008. Difficulties in tracking the long-term global trend in tropical forest area. Proceedings of the National Academy of Sciences 105:818–823.

Grau, H. R., T. M. Aide, J. K. Zimmerman, J. R. Thomlison, E. H. Helmer, and X.

Zou. 2003. The Ecological Consequences of Socioeconomic and Land-Use Changes in Postagriculture Puerto Rico. BioScience 53:1159.

Grimaldi, Michel, Guédron, and Stéphane. 2015. Impact of gold mining on mercury contamination and soil degradation in Amazonian ecosystems of French Guiana.

Griscom, B. W., J. Adams, P. W. Ellis, R. A. Houghton, G. Lomax, D. A. Miteva, W. H. Schlesinger, D. Shoch, J. V. Siikamäki, P. Smith, P. Woodbury, C. Zganjar, A. Blackman, J. Campari, R. T. Conant, C. Delgado, P. Elias, T. Gopalakrishna, M. R. Hamsik, M. Herrero, J. Kiesecker, E. Landis, L. Laestadius, S. M. Leavitt, S. Minnemeyer, S. Polasky, P. Potapov, F. E. Putz, J. Sanderman, M. Silvius, E. Wollenberg, and J. Fargione. 2017. Natural climate solutions. Proceedings of the National Academy of Sciences 114:11645–11650.

Gruining, C., and L. S. Shuford. 2012. Case Study: Guyana REDD-Plus Investment Fund (GRIF). Frankfurt School-UNEP Centre for Climate and Sustainable Energy Finance.

Guedron, S., S. Grangeon, B. Lanson, and M. Grimaldi. 2009. Mercury speciation in a tropical soil association; Consequence of gold mining on Hg distribution in French Guiana. Page Geoderma.

Guitet, S., S. Pithon, O. Brunaux, G. Jubelin, and V. Gond. 2012. Impacts of logging on the canopy and the consequences for forest management in French Guiana. Forest Ecology and Management 277:124–131.

Gutiérrez-Vélez, V. H., R. DeFries, M. Pinedo-Vásquez, M. Uriarte, C. Padoch, W. Baethgen, K. Fernandes, and Y. Lim. 2011. High-yield oil palm expansion spares land at the expense of forests in the Peruvian Amazon. Environmental Research Letters 6:44029.

Guyana Forestry Commission. 2015. Guyana Forestry Commission Guyana REDD + Monitoring Reporting and Verification System.

Guyana Forestry Commission - Indufor. 2013. Guyana REDD+ Monitoring Reporting & Verification System (MRVS) Year 3 Interim Measures Report.

Guyana Forestry Commission, and Indufor. 2012. Guyana Forestry Commission Guyana REDD + Monitoring Reporting & Verification System (MRVS) Interim Measures Report 01 October 2010 – 31 December 2011.

Hammond, D. S., V. Gond, B. de Thoisy, P. M. Forget, and B. P. E DeDijn. 2007.

Causes and Consequences of a Tropical Forest Gold Rush in the Guiana Shield, South America. AMBIO: A Journal of the Human Environment 36:661–670.

Hansen, M. C., P. V. Potapov, R. Moore, M. Hancher, S. A. Turubanova, A. Tyukavina, D. Thau, S. V. Stehman, S. J. Goetz, T. R. Loveland, A. Kommareddy, A. Egorov, L. Chini, C. O. Justice, and J. R. G. Townshend. 2013. High-Resolution Global Maps of 21st-Century Forest Cover Change. Science 342:850–853.

Hansen, M. C., S. V Stehman, P. V Potapov, T. R. Loveland, J. R. G. Townshend, R. S. Defries, K. W. Pittman, B. Arunarwati, F. Stolle, M. K. Steininger, M. Carroll, and C. Dimiceli. 2008. Humid tropical forest clearing from 2000 to 2005 quantified by using multitemporal and multiresolution remotely sensed data. Proc. Natl. Acad. Sci. USA 105:9439–9444.

Harris, N. L., E. Goldman, C. Gabris, J. Nordling, S. Minnemeyer, S. Ansari, M. Lippmann, L. Bennett, M. Raad, M. Hansen, and P. Potapov. 2017. Using spatial statistics to identify emerging hot spots of forest loss. Environmental Research Letters.

Heino, M., M. Kummu, M. Makkonen, M. Mulligan, P. H. Verburg, M. Jalava, and T. A. Räsänen. 2015. Forest loss in protected areas and intact forest landscapes: A global analysis. PLoS ONE 10:1–21.

Hentschel, T., F. Hruschka, and M. Priester. 2002. Global Report on Artisanal & Small-Scale Mining.

Hilson, G., and R. Vieira. 2007. Challenges with minimising mercury pollution in the small-scale gold mining sector: Experiences from the Guianas. International Journal of Environmental Health Research.

Holling, C. S. 1973. Resilience and Stability of Ecological Systems. Annual Review of Ecology and Systematics 4:1–23.

Houghton, R. A., B. Byers, and A. A. Nassikas. 2015. A role for tropical forests in stabilizing atmospheric CO2. Nature Climate Change 5:1022–1023.

Howard, J., M. A. Trotz, K. Thomas, E. Omisca, H. T. Chiu, T. Halfhide, F. Akiwumi, R. Michael, and A. L. Stuart. 2011. Total mercury loadings in sediment from gold mining and conservation areas in Guyana. Environmental Monitoring and Assessment 179:555–573.

IDEAM. 2011. Estructura Ecológica Principal de Colombia. Proceso

metodológico y aplicación escala 1:500.000:44.

Imbach, P., M. Manrow, E. Barona, A. Barretto, G. Hyman, and P. Ciais. 2015. Spatial and temporal contrasts in the distribution of crops and pastures across Amazonia: A new agricultural land use data set from census data since 1950. Global Biogeochemical Cycles 29:1271–1288.

Iqbal, M. Z., M. Shafiq, and M. Athar. 2014. Phytotoxic effects of mercury on seed germination and seedling growth of Albizia lebbeck (L .) Benth . (Leguminosae) 3:207–216.

Isobe, A., K. Uchida, T. Tokai, and S. Iwasaki. 2015. East Asian seas: A hot spot of pelagic microplastics. Marine Pollution Bulletin 101:618–623.

IUCN. 2014. Forest landscape restoration potential and impacts. Arbovitae 45:16.

Jakovac, C. C., M. Peña-Claros, T. W. Kuyper, and F. Bongers. 2015. Loss of secondary-forest resilience by land-use intensification in the Amazon. Journal of Ecology.

Jiménez-Muñoz, J. C., C. Mattar, J. Barichivich, A. Santamaría-Artigas, K. Takahashi, Y. Malhi, J. A. Sobrino, and G. Van Der Schrier. 2016. Record-breaking warming and extreme drought in the Amazon rainforest during the course of El Niño 2015-2016. Scientific Reports 6:1–7.

Jipp, P. H., D. C. Nepstad, D. Cassel, and C. J. R. De Carvalho. 1998. Deep soil moisture storage and transpiration in forests and pastures of seasonally-dry amazonia. Climate Change 39:395–412.

Johnson, E. A., and K. Miyanishi. 2008. Testing the assumptions of chronosequences in succession.

Johnson, M. O., D. Galbraith, M. Gloor, H. De Deurwaerder, M. Guimberteau, A. Rammig, K. Thonicke, H. Verbeeck, C. von Randow, A. Monteagudo, O. L. Phillips, R. J. W. Brienen, T. R. Feldpausch, G. Lopez Gonzalez, S. Fauset, C. A. Quesada, B. Christoffersen, P. Ciais, G. Sampaio, B. Kruijt, P. Meir, P. Moorcroft, K. Zhang, E. Alvarez-Davila, A. Alves de Oliveira, I. Amaral, A. Andrade, L. E. O. C. Aragao, A. Araujo-Murakami, E. J. M. M. Arets, L. Arroyo, G. A. Aymard, C. Baraloto, J. Barroso, D. Bonal, R. Boot, J. Camargo, J. Chave, A. Cogollo, F. Cornejo Valverde, A. C. Lola da Costa, A. Di Fiore, L. Ferreira, N. Higuchi, E. N. Honorio, T. J. Killeen, S. G. Laurance, W. F. Laurance, J. Licona, T. Lovejoy, Y. Malhi, B. Marimon, B. H. Marimon, D. C. L. Matos, C. Mendoza, D. A. Neill, G. Pardo, M. Peña-

Claros, N. C. A. Pitman, L. Poorter, A. Prieto, H. Ramirez-Angulo, A. Roopsind, A. Rudas, R. P. Salomao, M. Silveira, J. Stropp, H. ter Steege, J. Terborgh, R. Thomas, M. Toledo, A. Torres-Lezama, G. M. F. van der Heijden, R. Vasquez, I. C. Guimarães Vieira, E. Vilanova, V. A. Vos, and T. R. Baker. 2016. Variation in stem mortality rates determines patterns of above-ground biomass in Amazonian forests: implications for dynamic global vegetation models. Global Change Biology 22:3996–4013.

Kaimowitz, D., and J. Smith. 2001. Soybean technology and the loss of natural vegetation in Brazil and Bolivia. Agricultural Technologies and Tropical Deforestation:195–212.

Kalamandeen, M., E. Gloor, E. Mitchard, D. Quincey, G. Ziv, D. Spracklen, B. Spracklen, M. Adami, L. E. O. C. Aragaõ, and D. Galbraith. 2018. Pervasive Rise of Small-scale Deforestation in Amazonia. Scientific Reports 8:1–10.

Kaspari, M., and J. S. Powers. 2016. Biogeochemistry and Geographical Ecology: Embracing All Twenty-Five Elements Required to Build Organisms. The American Naturalist 188:S62–S73.

Kellner, J. R., and G. P. Asner. 2009. Convergent structural responses of tropical forests to diverse disturbance regimes. Ecology Letters 12:887–897.

Kellner, J. R., D. B. Clark, and S. P. Hubbell. 2009. Pervasive canopy dynamics produce short-term stability in a tropical rain forest landscape. Ecology Letters 12:155–164.

Kemenes, A., B. R. Forsberg, and J. M. Melack. 2007. Methane release below a tropical hydroelectric dam. Geophysical Research Letters 34:1–5.

Killeen, T. J. 2012. Amazon Deforestation Rates by Country and Time Period. Compiled by WWF.

Killeen, T. J., V. Calderon, L. Soria, B. Quezada, M. K. Steininger, G. Harper, L. A. Solórzano, C. J. Tucker, and L. A. Soló Rzano. 2007. Thirty Years of Land-cover Change in Bolivia. Source: AMBIO: A Journal of the Human Environment 36:600–606.

Killeen, T. J., A. Guerra, M. Calzada, L. Correa, V. Calderon, L. Soria, B. Quezada, and T. Steininger, M. 2008. Total Historical Land- Use Change in Eastern Bolivia: Who, Where, When, and How Much? Ecology and Society 13:36.

Kim, D.-H., J. O. Sexton, and J. R. Townshend. 2015. Accelerated deforestation

in the humid tropics from the 1990s to the 2000s. Geophysical Research Letters 42:3495–3501.

Kleinschroth, F., J. R. Healey, P. Sist, F. Mortier, and S. Gourlet-Fleury. 2016. How persistent are the impacts of logging roads on Central African forest vegetation? Journal of Applied Ecology 53:1127–1137.

Koele, N., M. Bird, J. Haig, B. H. Marimon-Junior, B. S. Marimon, O. L. Phillips, E. A. de Oliveira, C. A. Quesada, and T. R. Feldpausch. 2017. Amazon Basin forest pyrogenic carbon stocks: First estimate of deep storage. Geoderma 306:237–243.

Kronenberg, J., E. Orligóra-Sankowska, and P. Czembrowski. 2015. REDD+ and Institutions. Sustainability (Switzerland) 7:10250–10263.

Laing, T. 2018. Guyana's REDD+ Agreement with Norway: Perceptions of and Impacts on Indigenous Communities. Working Paper 476, February 2018, Centre for Global Development.

Lambin, E. F., H. J. Geist, and E. Lepers. 2003. Dynamics of Land Use and Land Cover Change In Tropical Regions. Annual Review of Environment and Resources 28:205–241.

Lambin, E. F., H. K. Gibbs, L. Ferreira, R. Grau, P. Mayaux, P. Meyfroidt, D. C. Morton, T. K. Rudel, I. Gasparri, and J. Munger. 2013. Estimating the world's potentially available cropland using a bottom-up approach. Global Environmental Change.

Lambin, E. F., and P. Meyfroidt. 2011. Global land use change, economic globalization, and the looming land scarcity. Proceedings of the National Academy of Sciences 108:3465–3472.

Lambin, E. F., B. L. Turner, H. J. Geist, S. B. Agbola, A. Angelsen, C. Folke, J. W. Bruce, O. T. Coomes, R. Dirzo, P. S. George, K. Homewood, J. Imbernon, R. Leemans, X. Li, E. F. Moran, M. Mortimore, P. S. Ramakrishnan, J. F. Richards, W. Steffen, G. D. Stone, U. Svedin, T. A. Veldkamp, C. Vogel, and J. Xu. 2001. The causes of land-use and land-cover change : moving beyond the myths. Global Environmental Change 11:261–269.

Laperche, V., J. Hellal, R. Maury-Brachet, B. Joseph, P. Laporte, D. Breeze, and F. Blanchard. 2014. Regional distribution of mercury in sediments of the main rivers of French Guiana (Amazonian basin). SpringerPlus 3:1–11.

Lapola, D. M., L. A. Martinelli, C. A. Peres, J. P. H. B. Ometto, M. E. Ferreira, C. A. Nobre, A. P. D. Aguiar, M. M. C. Bustamante, M. F. Cardoso, M. H. Costa, C. A. Joly, C. C. Leite, P. Moutinho, G. Sampaio, B. B. N. Strassburg, and I. C. G. Vieira. 2014. Pervasive transition of the Brazilian land-use system.

Laurance, W. F. 2004. Forest-climate interactions in fragmented tropical landscapes. Philosophical Transactions of the Royal Society B: Biological Sciences 359:345–352.

Laurance, W. F. 2015. Emerging Threats to Tropical Forests [1, 2]. Annals of the Missouri Botanical Garden 100:159–169.

Laurance, W. F., G. R. Clements, S. Sloan, C. S. O'Connell, N. D. Mueller, M. Goosem, O. Venter, D. P. Edwards, B. Phalan, A. Balmford, R. Van Der Ree, and I. B. Arrea. 2014. A global strategy for road building. Nature 513:229–232.

Laurance, W. F., M. A. Cochrane, S. Bergen, P. M. Fearnside, P. Delamônica, C. Barber, S. D'Angelo, and T. Fernandes. 2001. The future of the Brazilian Amazon. Science 291:438–439.

Laurance, W. F., M. Goosem, and S. G. W. Laurance. 2009. Impacts of roads and linear clearings on tropical forests. Trends in Ecology and Evolution 24:659–669.

Lawrence, D., and K. Vandecar. 2014. Effects of tropical deforestation on climate and agriculture. Nature Climate Change 5:27–36.

Lawrence, D., and K. Vandecar. 2015. Effects of tropical deforestation on climate and agriculture. Nature Climate Change 5:27–36.

Lawson, S., A. Blundell, B. Cabarle, N. Basik, M. Jenkins, and K. Canby. 2014. Consumer Goods and Deforestation: An Analysis of the Extent and Nature of Illegality in Forest Conversion for Agriculture and Timber Plantations. Forest Trends Report:2012.

Ledec, G., and J. D. Quintero. 2003. Good dams and bad dams: environmental criteria for site selection of hydroelectric projects. Latin America and the Caribbean Region:Sustainable Development Working Paper No. 16 16:21.

Lees, A. C., C. A. Peres, P. M. Fearnside, M. Schneider, and J. A. S. Zuanon. 2016. Hydropower and the future of Amazonian biodiversity. Biodiversity and Conservation 25:451–466.

Legg, E. D., P. E. Ouboter, and M. a. Wright. 2015. Small-Scale Gold Mining Related Mercury Contamination in the Guianas : A Review:1–58.

Lejeune, Q., E. L. Davin, B. P. Guillod, and S. I. Seneviratne. 2015. Influence of Amazonian deforestation on the future evolution of regional surface fluxes, circulation, surface temperature and precipitation. Climate Dynamics 44:2769–2786.

Lenton, T. M. 2011. Early warning of climate tipping points. Nature Climate Change 1:201–209.

Levis, C., F. R. C. Costa, F. Bongers, M. Peña-Claros, C. R. Clement, A. B. Junqueira, E. G. Neves, E. K. Tamanaha, F. O. G. Figueiredo, R. P. Salomão, C. V. Castilho, W. E. Magnusson, O. L. Phillips, J. E. Guevara, D. Sabatier, J.-F. Molino, D. C. López, A. M. Mendoza, N. C. A. Pitman, A. Duque, P. N. Vargas, C. E. Zartman, R. Vasquez, A. Andrade, J. L. Camargo, T. R. Feldpausch, S. G. W. Laurance, W. F. Laurance, T. J. Killeen, H. E. M. Nascimento, J. C. Montero, B. Mostacedo, I. L. Amaral, I. C. Guimarães Vieira, R. Brienen, H. Castellanos, J. Terborgh, M. de J. V. Carim, J. R. da S. Guimarães, L. de S. Coelho, F. D. de A. Matos, F. Wittmann, H. F. Mogollón, G. Damasco, N. Dávila, R. García-Villacorta, E. N. H. Coronado, T. Emilio, D. de A. L. Filho, J. Schietti, P. Souza, N. Targhetta, J. A. Comiskey, B. S. Marimon, B.-H. Marimon, D. Neill, A. Alonso, L. Arroyo, F. A. Carvalho, F. C. de Souza, F. Dallmeier, M. P. Pansonato, J. F. Duivenvoorden, P. V. A. Fine, P. R. Stevenson, A. Araujo-Murakami, G. A. Aymard C., C. Baraloto, D. D. do Amaral, J. Engel, T. W. Henkel, P. Maas, P. Petronelli, J. D. C. Revilla, J. Stropp, D. Daly, R. Gribel, M. R. Paredes, M. Silveira, R. Thomas-Caesar, T. R. Baker, N. F. da Silva, L. V. Ferreira, C. A. Peres, M. R. Silman, C. Cerón, F. C. Valverde, A. Di Fiore, E. M. Jimenez, M. C. P. Mora, M. Toledo, E. M. Barbosa, L. C. de M. Bonates, N. C. Arboleda, E. de S. Farias, A. Fuentes, J.-L. Guillaumet, P. M. Jørgensen, Y. Malhi, I. P. de Andrade Miranda, J. F. Phillips, A. Prieto, A. Rudas, A. R. Ruschel, N. Silva, P. von Hildebrand, V. A. Vos, E. L. Zent, S. Zent, B. B. L. Cintra, M. T. Nascimento, A. A. Oliveira, H. Ramirez-Angulo, J. F. Ramos, G. Rivas, J. Schöngart, R. Sierra, M. Tirado, G. van der Heijden, E. V. Torre, O. Wang, K. R. Young, C. Baider, A. Cano, W. Farfan-Rios, C. Ferreira, B. Hoffman, C. Mendoza, I. Mesones, A. Torres-Lezama, M. N. U. Medina, T.

R. van Andel, D. Villarroel, R. Zagt, M. N. Alexiades, H. Balslev, K. Garcia-Cabrera, T. Gonzales, L. Hernandez, I. Huamantupa-Chuquimaco, A. G. Manzatto, W. Milliken, W. P. Cuenca, S. Pansini, D. Pauletto, F. R. Arevalo, N. F. C. Reis, A. F. Sampaio, L. E. U. Giraldo, E. H. V. Sandoval, L. V. Gamarra, C. I. A. Vela, and H. ter Steege. 2017. Persistent effects of pre-Columbian plant domestication on Amazonian forest composition. Science 355:925–931.

Lewis, S. L., P. M. Brando, O. L. Phillips, G. M. F. Van Der Heijden, and D. Nepstad. 2011. The 2010 Amazon drought. Science 331:554.

Lewis, S. L., D. P. Edwards, and D. Galbraith. 2015. Increasing human dominance of tropical forests. Science.

Lima, L. S., M. T. Coe, B. S. Soares Filho, S. V. Cuadra, L. C. P. Dias, M. H. Costa, L. S. Lima, and H. O. Rodrigues. 2014. Feedbacks between deforestation, climate, and hydrology in the Southwestern Amazon: Implications for the provision of ecosystem services. Landscape Ecology 29:261–274.

Litaor, M. I., L. Katz, and M. Shenker. 2017. The influence of compost and zeolite co-addition on the nutrients status and plant growth in intensively cultivated Mediterranean soils. Soil Use and Management 33:72–80.

Lobato, J. F. P., A. K. Freitas, T. Devincenzi, L. L. Cardoso, J. U. Tarouco, R. M. Vieira, D. R. Dillenburg, and I. Castro. 2014. Brazilian beef produced on pastures: Sustainable and healthy. Meat Science 98:336–345.

Lobo, F., M. Costa, E. Novo, and K. Telmer. 2016. Distribution of Artisanal and Small-Scale Gold Mining in the Tapajós River Basin (Brazilian Amazon) over the Past 40 Years and Relationship with Water Siltation. Remote Sensing 8:579.

Lobo, F. de L., P. W. M. Souza-Filho, E. M. L. de M. Novo, F. M. Carlos, and C. C. F. Barbosa. 2018. Mapping Mining Areas in the Brazilian Amazon Using MSI/Sentinel-2 Imagery (2017). Remote Sensing 10:1178.

Lohbeck, M., L. Poorter, M. Martínez-ramos, and F. Bongers. 2015. Biomass is the main driver of changes in ecosystem process rates during tropical forest succession Biomass is the main driver of changes in ecosystem process rates during tropical forest succession 96:1242–1252.

López-Carr, D., N. G. Pricope, J. E. Aukema, M. M. Jankowska, C. Funk, G.

Husak, and J. Michaelsen. 2014. A spatial analysis of population dynamics and climate change in Africa: Potential vulnerability hot spots emerge where precipitation declines and demographic pressures coincide. Population and Environment 35:323–339.

Macedo, M. N., R. S. DeFries, D. C. Morton, C. M. Stickler, G. L. Galford, and Y. E. Shimabukuro. 2012. Decoupling of deforestation and soy production in the southern Amazon during the late 2000s. Proceedings of the National Academy of Sciences 109:1341–1346.

Maeda, E., E. E. Maeda, X. Ma, F. H. Wagner, H. Kim, and T. Oki. 2017. Evapotranspiration seasonality across the Amazon Basin. Earth System Dynamics:439–454.

Malhi, Y., J. T. Roberts, R. A. Betts, T. J. Killeen, W. Li, and C. A. Nobre. 2008. Climate Change, Deforestation, and the Fate of the Amazon 169.

Marengo, J. A., and J. C. Espinoza. 2016. Extreme seasonal droughts and floods in Amazonia: Causes, trends and impacts. International Journal of Climatology 36:1033–1050.

Marin-Spiotta, E., D. Cusack, R. Ostertag, and W. Silver. 2008. Trends in above and belowground carbon with forest regrowth after agricultural abandonment in the Neotropics. Post-Agricultural Succession in the Neotropics.

Markewitz, D., E. Davidson, P. Moutinho, and D. Nepstad. 2004. Nutrient loss and redistribution after forest clearing on a highly weathered soil in Amazonia. Ecological Applications 14:177–199.

Martin, P. A., A. C. Newton, and J. M. Bullock. 2013. Carbon pools recover more quickly than plant biodiversity in tropical secondary forests. Proceedings of the Royal Society B: Biological Sciences 280:20132236–20132236.

Massé, F., and P. Le Billon. 2017. Gold mining in Colombia, post-war crime and the peace agreement with the FARC. Third World Thematics: A TWQ Journal 2014:1–19.

Massé, F., and J. McDermott. 2017. Responsible business conduct Due diligence in Colombia's gold supply chain gold mining in Chocó:24.

Massi, K. G., M. Bird, B. S. Marimon, B. H. Marimon, D. S. Nogueira, E. A. Oliveira, O. L. Phillips, C. A. Quesada, A. S. Andrade, R. J. W. Brienen, J. L. C. Camargo, J. Chave, E. N. Honorio Coronado, L. V. Ferreira, N. Higuchi, S. G. Laurance, W. F. Laurance, T. Lovejoy, Y. Malhi, R. V.

Martínez, A. Monteagudo, D. Neill, A. Prieto, H. Ramírez-Angulo, H. ter Steege, E. Vilanova, and T. R. Feldpausch. 2017. Does soil pyrogenic carbon determine plant functional traits in Amazon Basin forests? Plant Ecology 218:1047–1062.

May, P. H., B. Millikan, and M. F. Gebara. 2011. The context of REDD+ in Brazil.

McMichael, C. N. H., F. Matthews-Bird, W. Farfan-Rios, and K. J. Feeley. 2017. Ancient human disturbances may be skewing our understanding of Amazonian forests. Proceedings of the National Academy of Sciences.

Meggers, B. J., E. S. Brondizio, M. J. Heckenberger, and C. Fausto. 2003. Revisiting Amazonia Circa 1492. Science 302:2067–2070.

Mercado, L. M., S. Patino, T. F. Domingues, N. M. Fyllas, G. P. Weedon, S. Sitch, C. A. Quesada, O. L. Phillips, L. E. O. C. Aragao, Y. Malhi, A. J. Dolman, N. Restrepo-Coupe, S. R. Saleska, T. R. Baker, S. Almeida, N. Higuchi, and J. Lloyd. 2011. Variations in Amazon forest productivity correlated with foliar nutrients and modelled rates of photosynthetic carbon supply. Philosophical Transactions of the Royal Society B: Biological Sciences 366:3316–3329.

Mesquita, R. C. G., K. Ickes, G. Ganade, and G. B. Williamson. 2001. Alternative succesional pathways in the amazon basin. Journal of Ecology 89:528–537.

Mesquita, R. D. C. G., P. E. D. S. Massoca, C. C. Jakovac, T. V. Bentos, and G. B. Williamson. 2015. Amazon Rain Forest Succession: Stochasticity or Land-Use Legacy? BioScience 65:849–861.

Milodowski, D. T., E. T. A. Mitchard, and M. Williams. 2016. Forest loss maps from regional satellite monitoring systematically underestimate deforestation in two rapidly changing parts of the Amazon. Environmental Research Letters 12:94003.

Mitchard, E. 2016. A Review of Earth Observation Methods for Detecting and Measuring Forest Change in the Tropics. Ecometrica, Edingburgh, UK.

Mok, H.-F., S. K. Arndt, and C. R. Nitschke. 2012. Modelling the potential impact of climate variability and change on species regeneration potential in the temperate forests of South-Eastern Australia. Global Change Biology 18:1053–1072.

Mol, J. H., and P. E. Ouboter. 2004. Downstream Effects of Erosion from Small-

Scale Gold Mining on the Instream Habitat and Fish Community of a Small Neotropical Rainforest Stream. Conservation Biology 18:201–214.

Mol, J. H., J. S. Ramlal, C. Lietar, and M. Verloo. 2001. Mercury Contamination in Freshwater, Estuarine, and Marine Fishes in Relation to Small-Scale Gold Mining in Suriname, South America. Environmental Research.

Moran, E. F., E. S. Brondizio, J. M. Tucker, M. C. Da Silva-Forsberg, S. McCracken, and I. Falesi. 2000. Effects of soil fertility and land-use on forest succession in amazonia. Forest Ecology and Management 139:93–108.

Moreno-Mateos, D., E. B. Barbier, P. C. Jones, H. P. Jones, J. Aronson, J. A. López-López, M. L. McCrackin, P. Meli, D. Montoya, and J. M. Rey Benayas. 2017. Anthropogenic ecosystem disturbance and the recovery debt. Nature Communications 8:8–13.

Morin, X., L. Fahse, H. Jactel, M. Scherer-Lorenzen, R. García-Valdés, and H. Bugmann. 2018. Long-term response of forest productivity to climate change is mostly driven by change in tree species composition. Scientific Reports 8:1–12.

Muddarisna, N., and B. D. Krisnayanti. 2015. Selection of mercury accumulator plants for gold mine tailing contaminated soils. Journal of Degraded andMining Lands Management 2:341–346.

Müller, R., D. Müller, F. Schierhorn, G. Gerold, and P. Pacheco. 2012. Proximate causes of deforestation in the Bolivian lowlands: An analysis of spatial dynamics. Regional Environmental Change 12:445–459.

Müller, R., P. Pacheco, and J. C. Montero. 2014. The context of deforestation and forest degradation in Bolivia. Centre for International Forestry Research (CIFOR).

Nachtigall, C., U. Kroehne, F. Funke, and R. Steyer. 2003. (Why) should we use SEM? Pros and cons of structural equation modeling. Methods of Psychological Research 8:1–22.

Nagy, R. C., E. B. Rastetter, C. Neill, and S. Porder. 2017. Nutrient limitation in tropical secondary forests following different management practices. Ecological Applications.

Nepstad, D. C., C. M. Stickler, B. S. Filho, and F. Merry. 2008. Interactions among Amazon land use, forests and climate: prospects for a near-term forest tipping point. Philosophical Transactions of the Royal Society B: Biological

Sciences 363:1737–1746.

Nepstad, D., D. McGrath, C. Stickler, A. Alencar, A. Azevedo, B. Swette, T. Bezerra, M. DiGiano, J. Shimada, R. Seroa da Motta, E. Armijo, L. Castello, P. Brando, M. C. Hansen, M. McGrath-Horn, O. Carvalho, and L. Hess. 2014. Slowing Amazon deforestation through public policy and interventions in beef and soy supply chains. Science 344:1118–1123.

Nepstad, D., B. S. Soares-Filho, F. Merry, A. Lima, P. Moutinho, J. Carter, M. Bowman, A. Cattaneo, H. Rodrigues, S. Schwartzman, D. G. McGrath, C. M. Stickler, R. Lubowski, P. Piris-Cabezas, S. Rivero, A. Alencar, O. Almeida, and O. Stella. 2009. The End of Deforestation in the Brazilian Amazon. Science.

Nevle, R. J., D. K. Bird, W. F. Ruddiman, and R. A. Dull. 2011. Neotropical human-landscape interactions, fire, and atmospheric CO2during european conquest. Holocene 21:853–864.

Nobre, C. A., G. Sampaio, L. S. Borma, J. C. Castilla-Rubio, J. S. Silva, and M. Cardoso. 2016. Land-use and climate change risks in the Amazon and the need of a novel sustainable development paradigm. Proceedings of the National Academy of Sciences 113:10759–10768.

Nogueira, E. M., A. M. Yanai, F. O. R. Fonseca, and P. M. Fearnside. 2015. Carbon stock loss from deforestation through 2013 in Brazilian Amazonia. Global Change Biology.

Novoa, S., M. Finer, and F. Román. 2016. Regeneration of Vegetation in Zone Affected by Gold Mining in the Amarakaeri Communal Reserve. MAAP 44.

Numata, I., M. A. Cochrane, C. M. Souza Jr, and M. H. Sales. 2011. Carbon emissions from deforestation and forest fragmentation in the Brazilian Amazon. Environmental Research Letters 6:44003.

Nuraini, Y., N. Arfarita, and B. Siswanto. 2015. Isolation and characteristic of nitrogen-fixing bacteria and phosphate-solubilizing bacteria from soil high in mercury in tailings and compost areas of artisanal gold mine. Agrivita 37:1–7.

Ochoa-Quintero, J. M., T. A. Gardner, I. Rosa, S. F. de Barros Ferraz, and W. J. Sutherland. 2015. Thresholds of species loss in Amazonian deforestation frontier landscapes. Conservation Biology 29:440–451.

Oliveira, P., G. P. Asner, D. E. Knapp, A. Almeyda, R. Galvan-Gildemeister, S.

Keene, R. Raybin, and R. Smith. 2007. Land-Use Allocation Protects the Peruvian Amazon. Science 317:1233–1236.

Osazuwa-Peters, O., C. Chapman, and A. E. Zanne. 2015. Selective logging : does the imprint remain on tree structure and composition after 45 years? Conservation Physiology 3:1–12.

Pacheco, C. E., M. I. Aguado, and D. Mollicone. 2014. Identification and characterization of deforestation hot spots in Venezuela using MODIS satellite images. Acta Amazonica 44:185–196.

Pacheco, P. 2006. Agricultural expansion and deforestation in lowland Bolivia: the import substitution versus the structural adjustment model. Land Use Policy.

Pacheco, P. 2012. Soybean and oil palm expansion in South America. Center for International Forestry Research:1–28.

Pacheco, P., and B. Mertens. 2004. Land use change and agriculture development in Santa Cruz, Bolivia 280:29–40.

Palace, M. W., C. N. H. McMichael, B. H. Braswell, S. C. Hagen, M. B. Bush, E. Neves, E. Tamanaha, C. Herrick, and S. Frolking. 2017. Ancient Amazonian populations left lasting impacts on forest structure. Ecosphere 8.

Pan, Y., R. A. Birdsey, J. Fang, R. Houghton, P. E. Kauppi, W. A. Kurz, O. L. Phillips, A. Shvidenko, S. L. Lewis, J. G. Canadell, P. Ciais, R. B. Jackson, S. W. Pacala, A. D. McGuire, S. Piao, A. Rautiainen, S. Sitch, and D. Hayes. 2011. A Large and Persistent Carbon Sink in the World's Forests. Science.

Pellegrini, A., W. Hoffmann, and A. Franco. 2014. Carbon accumulation and nitrogen pool recovery during transitions from savanna to forest in central Brazil Carbon accumulation and nitrogen pool recovery during transitions from savanna to forest in central Brazil. Ecology 95:342–352.

Peña-Claros, M. 2016. Changes in Forest Structure and Species Composition during Secondary Forest Succession in the Bolivian Amazon Author (s): Marielos Peña-Claros Published by : Association for Tropical Biology and Conservation Stable URL : http://www.jstor.org/stable/3004. Biotropica 35:450–461.

Peres, C. a, and I. R. Lake. 2003. Extent of Nontimber Resource Extraction in Tropical Forests: Accessibility to Game Vertebrates by Hunters in the Amazon Basin\nAlcance de la Extracción de Recursos no Maderables en

Bosques Tropicales: Acceso a Vertebrados de Caza por Cazadores en la Cuenc. Conservation Biology 17:521–535.

Perz, S. G., C. Aramburú, and J. Bremner. 2005. Population, land use and deforestation in the Pan Amazon Basin: A comparison of Brazil, Bolivia, Colombia, Ecuador, Per?? and Venezuela. Environment, Development and Sustainability 7:23–49.

Peterson, G. D., and M. Heemskerk. 2001. Deforestation and forest regeneration following small-scale gold mining in the Amazon: the case of Suriname. Environmental Conservation 28:117–126.

Pfaff, A., E. O. Sills, G. S. Amacher, M. Coren, K. Lawlor, and C. Streck. 2010. Policy Impacts on Deforestation Lessons Learned from Past Experiences to Inform New Initiatives. Nicholas Institute for Environmental Policy Solutions, Duke University 121:54.

Pfeifer, M., L. Kor, R. Nilus, E. Turner, J. Cusack, I. Lysenko, M. Khoo, V. K. Chey, A. C. Chung, and R. M. Ewers. 2016. Mapping the structure of Borneo's tropical forests across a degradation gradient. Remote Sensing of Environment 176:84–97.

Pfeiffer, W. C. ., L. D. . Lacerda, W. . Salomons, and O. Malm. 1993. Environmental fate of mercury from gold mining in the Brazilian Amazon. Environmental Reviews 1:26–37.

Pfeiffer, W. C., and L. D. de Lacerda. 1988. Mercury inputs into the Amazon Region, Brazil. Environmental Technology Letters 9:325–330.

Phillips, O. L., L. E. O. C. Aragão, S. L. Lewis, J. B. Fisher, J. Lloyd, G. López-González, Y. Malhi, A. Monteagudo, J. Peacock, C. a Quesada, G. van der Heijden, S. Almeida, I. Amaral, L. Arroyo, G. Aymard, T. R. Baker, O. Bánki, L. Blanc, D. Bonal, P. Brando, J. Chave, A. C. A. de Oliveira, N. D. Cardozo, C. I. Czimczik, T. R. Feldpausch, M. A. Freitas, E. Gloor, N. Higuchi, E. Jiménez, G. Lloyd, P. Meir, C. Mendoza, A. Morel, D. a Neill, D. Nepstad, S. Patiño, M. C. Peñuela, A. Prieto, F. Ramírez, M. Schwarz, J. Silva, M. Silveira, A. S. Thomas, H. Ter Steege, J. Stropp, R. Vásquez, P. Zelazowski, E. Alvarez Dávila, S. Andelman, A. Andrade, K. Chao, T. Erwin, A. Di Fiore, E. Honorio C, H. Keeling, T. J. Killeen, W. F. Laurance, A. Peña Cruz, N. C. a Pitman, P. Núñez Vargas, H. Ramírez-Angulo, A. Rudas, R. Salamão, N. Silva, J. Terborgh, A. Torres-Lezama, G. Van Der

Heijden, Á. Cristina, A. De Oliveira, E. A. Dávila, A. Di Fiore, E. H. C, A. P. Cruz, and P. N. Vargas. 2009. Drought Sensitivity of the Amazon Rainforest. Science 323:1344–1347.

Phillips, O. L., R. J. W. Brienen, E. Gloor, T. R. Baker, J. Lloyd, G. Lopez-Gonzalez, A. Monteagudo-Mendoza, Y. Malhi, S. L. Lewis, R. Vásquez Martinez, M. Alexiades, E. Álvarez Dávila, P. Alvarez-Loayza, A. Andrade, L. E. O. C. Aragão, A. Araujo-Murakami, E. J. M. M. Arets, L. Arroyo, G. A. Aymard, O. S. Bánki, C. Baraloto, J. Barroso, D. Bonal, R. G. A. Boot, J. L. C. Camargo, C. V. Castilho, V. Chama, K. J. Chao, J. Chave, J. A. Comiskey, F. C. Valverde, L. da Costa, E. A. de Oliveira, A. Di Fiore, T. L. Erwin, S. Fauset, M. Forsthofer, D. R. Galbraith, E. S. Grahame, N. Groot, B. Hérault, N. Higuchi, E. N. Honorio Coronado, H. Keeling, T. J. Killeen, W. F. Laurance, S. Laurance, J. Licona, W. E. Magnusson, B. S. Marimon, B. H. Marimon-Junior, C. Mendoza, D. A. Neill, E. M. Nogueira, P. Núñez, N. C. Pallqui Camacho, A. Parada, G. Pardo-Molina, J. Peacock, M. Peña-Claros, G. C. Pickavance, N. C. A. Pitman, L. Poorter, A. Prieto, C. A. Quesada, F. Ramírez, H. Ramírez-Angulo, Z. Restrepo, A. Roopsind, A. Rudas, R. P. Salomão, M. Schwarz, N. Silva, J. E. Silva-Espejo, M. Silveira, J. Stropp, J. Talbot, H. ter Steege, J. Teran-Aguilar, J. Terborgh, R. Thomas-Caesar, M. Toledo, M. Torello-Raventos, K. Umetsu, G. M. F. van der Heijden, P. van der Hout, I. C. Guimarães Vieira, S. A. Vieira, E. Vilanova, V. A. Vos, R. J. Zagt, A. Alarcon, I. Amaral, P. P. B. Camargo, I. F. Brown, L. Blanc, B. Burban, N. Cardozo, J. Engel, M. A. de Freitas, A. de Oliveira, T. S. Fredericksen, L. Ferreira, N. T. Hinojosa, E. Jimenez, E. Lenza, C. Mendoza, I. Mendoza Polo, A. Peña Cruz, M. C. Peñuela, P. Petronelli, J. Singh, P. Maquirino, J. Serano, A. Sota, C. Oliveira dos Santos, J. Ybarnegaray, and J. Ricardo. 2017. Carbon uptake by mature Amazon forests has mitigated Amazon nations' carbon emissions. Carbon Balance and Management 12:1–9.

Pinheiro, J., D. Bates, S. DebRoy, and D. Sarka. 2018. Linear and NonLinear Mixed Effects Model: nlme R package.

Pinter, N., S. Fiedel, and J. E. Keeley. 2011. Fire and vegetation shifts in the Americas at the vanguard of Paleoindian migration. Quaternary Science Reviews 30:269–272.

Pivello, V. R. 2011. The use of fire in the cerrado and Amazonian rainforests of Brazil: Past and present. Fire Ecology 7:24–39.

Pokhrel, Y. N., Y. Fan, and G. Miguez-Macho. 2014. Potential hydrologic changes in the Amazon by the end of the 21st century and the groundwater buffer. Environmental Research Letters 9:84004.

Poorter, L., F. Bongers, T. M. Aide, A. M. Almeyda Zambrano, P. Balvanera, J. M. Becknell, V. Boukili, P. H. S. Brancalion, E. N. Broadbent, R. L. Chazdon, D. Craven, J. S. de Almeida-Cortez, G. A. L. Cabral, B. H. J. de Jong, J. S. Denslow, D. H. Dent, S. J. DeWalt, J. M. Dupuy, S. M. Durán, M. M. Espírito-Santo, M. C. Fandino, R. G. César, J. S. Hall, J. L. Hernandez-Stefanoni, C. C. Jakovac, A. B. Junqueira, D. Kennard, S. G. Letcher, J.-C. Licona, M. Lohbeck, E. Marín-Spiotta, M. Martínez-Ramos, P. Massoca, J. A. Meave, R. Mesquita, F. Mora, R. Muñoz, R. Muscarella, Y. R. F. Nunes, S. Ochoa-Gaona, A. A. de Oliveira, E. Orihuela-Belmonte, M. Peña-Claros, E. A. Pérez-García, D. Piotto, J. S. Powers, J. Rodríguez-Velázquez, I. E. Romero-Pérez, J. Ruíz, J. G. Saldarriaga, A. Sanchez-Azofeifa, N. B. Schwartz, M. K. Steininger, N. G. Swenson, M. Toledo, M. Uriarte, M. van Breugel, H. van der Wal, M. D. M. Veloso, H. F. M. Vester, A. Vicentini, I. C. G. Vieira, T. V. Bentos, G. B. Williamson, and D. M. A. Rozendaal. 2016. Biomass resilience of Neotropical secondary forests. Nature 530:211–214.

Pop-Eleches, G. 2008. Crisis in the eye of the beholder: Economic crisis and partisan politics in Latin American and East European International Monetary Fund programs. Comparative Political Studies 41:1179–1211.

Popescu, A., D. Faur, C. Vaduva, M. Datcu,] J Reiche, C. M. Souza, D. H. Hoekman, J. Verbesselt, H. Persaud, and M. Herold. 2013. Feature Level Fusion of Multi-Temporal ALOS PALSAR and Landsat Data for Mapping and Monitoring of Tropical Deforestation and Forest Degradation. IEEE Journal of Selected Topics in Applied Earth Observations and Remote Sensing IEEE Transactions on Information Theory Journal of Machine Learning Research 6:2159–2173.

Potapov, P., A. Yaroshenko, S. Turubanova, M. Dubinin, L. Laestadius, C. Thies, D. Aksenov, A. Egorov, Y. Yesipova, I. Glushkov, M. Karpachevskiy, A. Kostikova, A. Manisha, E. Tsybikova, and I. Zhuravleva. 2008. Mapping the World's Intact Forest Landscapes by Remote Sensing. Ecology and Society

13.

Powers, J. S., and E. Marín-Spiotta. 2017. Ecosystem Processes and Biogeochemical Cycles in Secondary Tropical Forest Succession. Annual Review of Ecology, Evolution, and Systematics 48:497–519.

Rademaekers, K., L. Eichler, J. Berg, M. Obersteiner, and P. Havlik. 2010. Study on the evolution of some deforestation drivers and their potential impacts on the costs of an avoiding deforestation scheme:114.

Rafique, A., A. Amin, and Z. Latif. 2015. Screening and characterization of mercury-resistant nitrogen fixing bacteria and their use as biofertilizers and for mercury bioremediation. Pakistan Journal of Zoology 47:1271–1277.

Rahm, M., B. Jullian, A. Lauger, R. de Carvalho, L. Vale, J. Totaram, K. A. Cort, M. Djojodikromo, M. Hardjoprajitno, S. Neri, R. Vieira, E. Watanabe, M. do Carmo Brito, P. Miranda, C. Paloeng, V. Moe Soe Let, S. Crabbe, and M. Calmel. 2015. Monitoring the impact of gold mining on the forest cover and freshwater in the Guiana Shield:1–60.

Raunter, M., M. Legget, and F. Davis. 2013. The Little Book of Big Deforestation Driver. The Global Canopy Programme, Oxford.

Reiche, J., C. M. Souzax, D. H. Hoekman, J. Verbesselt, H. Persaud, and M. Herold. 2013. Feature level fusion of multi-temporal ALOS PALSAR and Landsat data for mapping and monitoring of tropical deforestation and forest degradation. IEEE Journal of Selected Topics in Applied Earth Observations and Remote Sensing.

Reymondin, L., A. Jarvis, A. Perez-Uribe, J. Touval, K. Argote, A. Coca, J. Rebetez, E. Guevara, and M. Mulligan. 2012. Terra-i A methodology for near real-time monitoring of habitat change at continental scales using MODIS-NDVI and TRMM.

Ritchie, M. E., and R. Raina. 2016. Effects of herbivores on nitrogen fixation by grass endophytes, legume symbionts and free-living soil surface bacteria in the Serengeti. Pedobiologia 59:233–241.

Rocha, R., O. Ovaskainen, A. López-Baucells, F. Z. Farneda, E. M. Sampaio, P. E. D. Bobrowiec, M. Cabeza, J. M. Palmeirim, and C. F. J. Meyer. 2018. Secondary forest regeneration benefits old-growth specialist bats in a fragmented tropical landscape. Scientific Reports 8:1–9.

Roman-Danobeytia, F., M. Huayllani, A. Michi, F. Ibarra, R. Loayza-Muro, T.

Vazquez, L. Rodriguez, and M. Garcia. 2015. Reforestation with four native tree species after abandoned gold mining in the Peruvian Amazon. Ecological Engineering 85:39–46.

Roosevelt, A. C. 2013. The Amazon and the Anthropocene: 13,000 years of human influence in a tropical rainforest. Anthropocene 4:69–87.

Rosa, I. M. D., D. Purves, C. Souza, and R. M. Ewers. 2013. Predictive Modelling of Contagious Deforestation in the Brazilian Amazon. PLoS ONE.

Rosa, I. M. D., C. Souza, and R. M. Ewers. 2012. Changes in Size of Deforested Patches in the Brazilian Amazon. Conservation Biology 26:932–937.

Rosales, A. 2017. Venezuela's Deepening Logic of Extraction. NACLA Report on the Americas 49:132–135.

Rozendaal, D. M. A., R. L. Chazdon, F. Arreola-Villa, P. Balvanera, T. V. Bentos, J. M. Dupuy, J. L. Hernández-Stefanoni, C. C. Jakovac, E. E. Lebrija-Trejos, M. Lohbeck, M. Martínez-Ramos, P. E. S. Massoca, J. A. Meave, R. C. G. Mesquita, F. Mora, E. A. Pérez-García, I. E. Romero-Pérez, I. Saenz-Pedroza, M. van Breugel, G. B. Williamson, and F. Bongers. 2017. Demographic Drivers of Aboveground Biomass Dynamics During Secondary Succession in Neotropical Dry and Wet Forests. Ecosystems 20:340–353.

Rudel, T. K. 2007. Changing agents of deforestation: From state-initiated to enterprise driven processes, 1970-2000. Land Use Policy 24:35–41.

Rudel, T. K., R. Defries, G. P. Asner, and W. F. Laurance. 2009. Changing Drivers of Deforestation and New Opportunities for Conservation Conservation Bioh Changing Drivers of Deforestation and New Opportunities for Conservation. Conservation Biology 23:1396–1405.

Rudorff, B. F. T., M. Adami, D. A. Aguiar, M. A. Moreira, M. P. Mello, L. Fabiani, D. F. Amaral, and B. M. Pires. 2011. The soy moratorium in the Amazon biome monitored by remote sensing images. Remote Sensing 3:185–202.

Saatchi, S. S., N. L. Harrisc, S. Brownc, M. Lefskyd, E. T. A. Mitcharde, W. Salasf, B. R. Zuttaa, W. Buermannb, S. L. Lewisg, S. Hagenf, S. Petrovac, L. Whiteh, M. Silmani, and A. Morelj. 2011. Benchmark map of forest carbon stocks in tropical regions across three continents. Proceedings of the National Academy of Sciences 108:9899–9904.

Salo, M., S. Helle, and T. Toivonen. 2011. Allocating logging rights in Peruvian Amazonia-does it matter to be local? PLoS ONE 6.

Salvini, G., M. Herold, V. De Sy, G. Kissinger, M. Brockhaus, and M. Skutsch. 2014. How countries link REDD+ interventions to drivers in their readiness plans: Implications for monitoring systems. Environmental Research Letters 9.

Sanchez-Cuervo, A. M., and T. M. Aide. 2013. Identifying hotspots of deforestation and reforestation in Colombia (2001–2010): implications for protected areas. Ecosphere 4:art143.

Sánchez-Cuervo, A. M., T. M. Aide, M. L. Clark, and A. Etter. 2012. Land Cover Change in Colombia: Surprising Forest Recovery Trends between 2001 and 2010. PLoS ONE 7.

Santos-Francés, F., A. García-Sánchez, P. Alonso-Rojo, F. Contreras, and M. Adams. 2011. Distribution and mobility of mercury in soils of a gold mining region, Cuyuni river basin, Venezuela. Journal of Environmental Management 92:1268–1276.

dos Santos, U. M., J. F. de Carvalho Gonçalves, and T. R. Feldpausch. 2006. Growth, leaf nutrient concentration and photosynthetic nutrient use efficiency in tropical tree species planted in degraded areas in central Amazonia. Forest Ecology and Management 226:299–309.

Sato, L. Y., F. Da, S. Ramos, V. Martins, R. Zecchini Cantinho, T. S. Korting, L. Maria, G. Fonseca, C. Almeida, D. De, and M. Valeriano. 2011. Classificação de áreas exploradas por sistema de corte seletivo na Amazônia. Anais XV Simpósio Brasileiro de Sensoriamento Remoto - SBSR, Curitiba, PR, Brasil, 30 de abril a 05 de maio de 2011, INPE p.6688.

Scheffer, M., S. R. Carpenter, V. Dakos, and E. H. van Nes. 2015. Generic Indicators of Ecological Resilience: Inferring the Chance of a Critical Transition. Annual Review of Ecology, Evolution, and Systematics 46:145–167.

Sheoran, V., A. S. Sheoran, and P. Poonia. 2010. Soil Reclamation of Abandoned Mine Land by Revegetation : A Review. International Journal of Soil, Sediment and Water 3:1–21.

Silva, C. E. M., J. F. C. Gonçalves, T. R. Feldpausch, F. J. Luizão, R. R. Morais, and G. O. Ribeiro. 2006. Eficiência no uso dos nutrientes por espécies

pioneiras cresidas em pastagens degradadas na Amazônia central. Acta Amazonica 36:503–512.

Silver, W. L., W. L. Silver, R. Ostertag, R. Ostertag, a E. Lugo, and a E. Lugo. 2000. The potential for carbon sequestration through reforestation of abandoned agricultural and pasture lands. Restoration Ecology 8:394–407.

Song, X. P., C. Huang, S. S. Saatchi, M. C. Hansen, and J. R. Townshend. 2015. Annual carbon emissions from deforestation in the Amazon basin between 2000 and 2010. PLoS ONE 10:1–21.

Sonter, L. J., D. Herrera, D. J. Barrett, G. L. Galford, C. J. Moran, and B. S. Soares-Filho. 2017. Mining drives extensive deforestation in the Brazilian Amazon. Nature Communications.

Sonter, L. J., C. J. Moran, D. J. Barrett, and B. S. Soares-Filho. 2014. Processes of land use change in mining regions. Journal of Cleaner Production 84:494–501.

Sousa, R., M. Veiga, D. Van Zyl, K. Telmer, S. Spiegel, and J. Selder. 2011. Policies and regulations for Brazil's artisanal gold mining sector: Analysis and recommendations. Journal of Cleaner Production 19:742–750.

Spracklen, B. D., M. Kalamandeen, D. Galbraith, E. Gloor, and D. V. Spracklen. 2015. A global analysis of deforestation in moist tropical forest protected areas. PLoS ONE.

Spracklen, D. V., S. R. Arnold, and C. M. Taylor. 2012. Observations of increased tropical rainfall preceded by air passage over forests. Nature 489:282–285.

Spracklen, D. V., and L. Garcia-Carreras. 2015. The impact of Amazonian deforestation on Amazon basin rainfall. Geophysical Research Letters 42:9546–9552.

Stahl, P. W. 2015. Interpreting interfluvial landscape transformations in the pre-Columbian Amazon. Holocene 25:1598–1603.

ter Steege, H., N. C. A. Pitman, T. J. Killeen, W. F. Laurance, C. A. Peres, J. E. Guevara, R. P. Salomao, C. V. Castilho, I. L. Amaral, F. D. de Almeida Matos, L. de Souza Coelho, W. E. Magnusson, O. L. Phillips, D. de Andrade Lima Filho, M. de Jesus Veiga Carim, M. V. Irume, M. P. Martins, J.-F. Molino, D. Sabatier, F. Wittmann, D. C. Lopez, J. R. da Silva Guimaraes, A. M. Mendoza, P. N. Vargas, A. G. Manzatto, N. F. C. Reis, J. Terborgh, K. R. Casula, J. C. Montero, T. R. Feldpausch, E. N. Honorio Coronado, A. J. D.

Montoya, C. E. Zartman, B. Mostacedo, R. Vasquez, R. L. Assis, M. B. Medeiros, M. F. Simon, A. Andrade, J. L. Camargo, S. G. W. Laurance, H. E. M. Nascimento, B. S. Marimon, B.-H. Marimon, F. Costa, N. Targhetta, I. C. G. Vieira, R. Brienen, H. Castellanos, J. F. Duivenvoorden, H. F. Mogollon, M. T. F. Piedade, G. A. Aymard C., J. A. Comiskey, G. Damasco, N. Davila, R. Garcia-Villacorta, P. R. S. Diaz, A. Vincentini, T. Emilio, C. Levis, J. Schietti, P. Souza, A. Alonso, F. Dallmeier, L. V. Ferreira, D. Neill, A. Araujo-Murakami, L. Arroyo, F. A. Carvalho, F. C. Souza, D. D. d. Amaral, R. Gribel, B. G. Luize, M. P. Pansonato, E. Venticinque, P. Fine, M. Toledo, C. Baraloto, C. Ceron, J. Engel, T. W. Henkel, E. M. Jimenez, P. Maas, M. C. P. Mora, P. Petronelli, J. D. C. Revilla, M. Silveira, J. Stropp, R. Thomas-Caesar, T. R. Baker, D. Daly, M. R. Paredes, N. F. da Silva, A. Fuentes, P. M. Jorgensen, J. Scho ngart, M. R. Silman, N. C. Arboleda, B. B. L. Cintra, F. C. Valverde, A. Di Fiore, J. F. Phillips, T. R. van Andel, P. von Hildebrand, E. M. Barbosa, L. C. de Matos Bonates, D. de Castro, E. de Sousa Farias, T. Gonzales, J.-L. Guillaumet, B. Hoffman, Y. Malhi, I. P. de Andrade Miranda, A. Prieto, A. Rudas, A. R. Ruschell, N. Silva, C. I. A. Vela, V. A. Vos, E. L. Zent, S. Zent, A. Cano, M. T. Nascimento, A. A. Oliveira, H. Ramirez-Angulo, J. F. Ramos, R. Sierra, M. Tirado, M. N. U. Medina, G. van der Heijden, E. V. Torre, C. Vriesendorp, O. Wang, K. R. Young, C. Baider, H. Balslev, N. de Castro, W. Farfan-Rios, C. Ferreira, C. Mendoza, I. Mesones, A. Torres-Lezama, L. E. U. Giraldo, D. Villarroel, R. Zagt, M. N. Alexiades, K. Garcia-Cabrera, L. Hernandez, I. Huamantupa-Chuquimaco, W. Milliken, W. P. Cuenca, S. Pansini, D. Pauletto, F. R. Arevalo, A. F. Sampaio, E. H. Valderrama Sandoval, and L. V. Gamarra. 2015. Estimating the global conservation status of more than 15,000 Amazonian tree species. Science Advances.

ter Steege, H., N. C. A. Pitman, D. Sabatier, C. Baraloto, R. P. Salomão, J. E. Guevara, O. L. Phillips, C. V. Castilho, W. E. Magnusson, J. F. Molino, A. Monteagudo, P. N. Vargas, J. C. Montero, T. R. Feldpausch, E. N. H. Coronado, T. J. Killeen, B. Mostacedo, R. Vasquez, R. L. Assis, J. Terborgh, F. Wittmann, A. Andrade, W. F. Laurance, S. G. W. Laurance, B. S. Marimon, B. H. Marimon, I. C. G. Vieira, I. L. Amaral, R. Brienen, H. Castellanos, D. C. López, J. F. Duivenvoorden, H. F. Mogollón, F. D. D. A.

Matos, N. Dávila, R. García-Villacorta, P. R. S. Diaz, F. Costa, T. Emilio, C. Levis, J. Schietti, P. Souza, A. Alonso, F. Dallmeier, A. J. D. Montoya, M. T. F. Piedade, A. Araujo-Murakami, L. Arroyo, R. Gribel, P. V. A. Fine, C. A. Peres, M. Toledo, G. A. Aymard C., T. R. Baker, C. Cerón, J. Engel, T. W. Henkel, P. Maas, P. Petronelli, J. Stropp, C. E. Zartman, D. Daly, D. Neill, M. Silveira, M. R. Paredes, J. Chave, D. D. A. Lima Filho, P. M. Jørgensen, A. Fuentes, J. Schöngart, F. C. Valverde, A. Di Fiore, E. M. Jimenez, M. C. P. Mora, J. F. Phillips, G. Rivas, T. R. Van Andel, P. Von Hildebrand, B. Hoffman, E. L. Zent, Y. Malhi, A. Prieto, A. Rudas, A. R. Ruschell, N. Silva, V. Vos, S. Zent, A. A. Oliveira, A. C. Schutz, T. Gonzales, M. T. Nascimento, H. Ramirez-Angulo, R. Sierra, M. Tirado, M. N. U. Medina, G. Van Der Heijden, C. I. A. Vela, E. V. Torre, C. Vriesendorp, O. Wang, K. R. Young, C. Baider, H. Balslev, C. Ferreira, I. Mesones, A. Torres-Lezama, L. E. U. Giraldo, R. Zagt, M. N. Alexiades, L. Hernandez, I. Huamantupa-Chuquimaco, W. Milliken, W. P. Cuenca, D. Pauletto, E. V. Sandoval, L. V. Gamarra, K. G. Dexter, K. Feeley, G. Lopez-Gonzalez, and M. R. Silman. 2013. Hyperdominance in the Amazonian tree flora. Science 342.

Steininger, M. K. 2000. Secondary forest structure and biomass following short and extended land - use in central and southern Amazonia. Journal of Tropical 16:689–708.

Swenson, J. J., C. E. Carter, J. C. Domec, and C. I. Delgado. 2011. Gold mining in the peruvian amazon: Global prices, deforestation, and mercury imports. PLoS ONE 6.

Tangahu, B. V., S. R. Sheikh Abdullah, H. Basri, M. Idris, N. Anuar, and M. Mukhlisin. 2011. A review on heavy metals (As, Pb, and Hg) uptake by plants through phytoremediation. International Journal of Chemical Engineering 2011.

De Theije, M., and M. Heemskerk. 2009. Moving Frontiers in the Amazon: Brazilian Small-Scale Gold Miners in Suriname. European Review of Latin American and Caribbean Studies 87:5–25.

Thomlinson, J. R., M. I. Serrano, T. M. Lopez, T. M. Aide, and J. K. Zimmerman. 1996. Land-Use Dynamics in a Post-Agricultural Puerto Rican Landscape (1936-1988) Source : Biotropica , Vol . 28 , No . 4 , Part A . Special Issue : Long Term Responses of Caribbean Ecosystems to Disturbances (Dec .,

1996), pp . 525-536 Published by : Assoc 28:525–536.

Toledo, M., L. Poorter, M. Peña-Claros, A. Alarcón, J. Balcázar, C. Leaño, J. C. Licona, O. Llanque, V. Vroomans, P. Zuidema, and F. Bongers. 2011. Climate is a stronger driver of tree and forest growth rates than soil and disturbance. Journal of Ecology 99:254–264.

Townsend, A. R., C. C. Cleveland, B. Z. Houlton, C. B. Alden, and J. W. C. White. 2011. Multi-element regulation of the tropical forest carbon cycle. Frontiers in Ecology and the Environment 9:9–17.

Tundisi, J. G., J. Goldemberg, T. Matsumura-Tundisi, and A. C. F. Saraiva. 2014. How many more dams in the Amazon. Energy Policy 74:703–708.

Turner, B. L., T. Brenes-Arguedas, and R. Condit. 2018. Pervasive phosphorus limitation of tree species but not communities in tropical forests. Nature.

Turner, M. G. 2010. Disturbance and landscape dynamics in a changing world. Ecology 91:2833–2849.

Tyukavina, A., M. C. Hansen, P. V. Potapov, S. V. Stehman, K. Smith-Rodriguez, C. Okpa, and R. Aguilar. 2017. Types and rates of forest disturbance in Brazilian Legal Amazon, 2000–2013. Science Advances.

UNFCCC. 2015. Adoption of the Paris Agreement. United Nations Framework Convention on Climate Change (UNFCCC) 21930:1–32.

UNODC. 2006. Coca Cultivation in the Andean Region: A survey of Bolivia, Colombia and Peru. United Nations Office of Drugs and Crime, Illicit Crop Monitoring Programme.

Ure, A. M., and C. A. Shand. 1974. The determination of mercury in soils and related materials by cold-vapour atomic absorption spectrometry. Analytica Chimica Acta 72:63–77.

Vallejos, M. A. V., A. A. Padial, and J. R. S. Vitule. 2016. Human-induced landscape changes homogenize atlantic forest bird assemblages through nested species loss. PLoS ONE 11:1–17.

Valois-Cuesta, H., C. Martínez-Ruiz, and Y. Urrutia-Rivas. 2017. FormValois-Cuesta, H., Martínez-Ruiz, C., & Urrutia-Rivas, Y. (2017). Formación del banco de semillas durante la revegetación temprana de áreas afectadas por la minería en un bosque pluvial tropical del Chocó, Colombia. Revista de Biologia Tropical, 65(1). Revista de Biologia Tropical 65:393–404.

Vandegrift, R., D. C. Thomas, B. A. Roy, and M. Levy. 2017. The extent of

recent mining concessions in Ecuador 2017.

Vasco, C., B. Torres, P. Pacheco, and V. Griess. 2017. The socioeconomic determinants of legal and illegal smallholder logging: Evidence from the Ecuadorian Amazon. Forest Policy and Economics 78:133–140.

Vedovato, L. B., M. G. Fonseca, E. Arai, L. O. Anderson, and L. E. O. C. Aragï¿½o. 2016. The extent of 2014 forest fragmentation in the Brazilian Amazon. Regional Environmental Change 16:2485–2490.

Veiga, M. M., G. Angeloci-Santos, and J. A. Meech. 2014. Review of barriers to reduce mercury use in artisanal gold mining. Extractive Industries and Society 1:351–361.

Veiga, M. M., P. A. Maxson, and L. D. Hylander. 2006. Origin and consumption of mercury in small-scale gold mining. Journal of Cleaner Production 14:436–447.

Verboom, J., B. Kruijt, M. P. Soba, H. Baveco, M. Van Eupen, C. Von Randow, T. Parr, K. Thonicke, L. Jones, A. Boit, P. Balvanera, E. L. Abarca, C. Huntingford, E. Blyth, I. Cisowska, L. Martorano, M. Toledo, B. Purse, D. Masante, and M. P. Claros. 2015. Exploring causes risks, and consequences for ecosystem services of tipping points in Latin American forests - the role of biodiversity 117:7058.

Verdone, M., and A. Seidl. 2017. Time, space, place, and the Bonn Challenge global forest restoration target. Restoration Ecology 25:903–911.

Wantzen, K., and J. Mol. 2013. Soil Erosion from Agriculture and Mining: A Threat to Tropical Stream Ecosystems. Agriculture 3:660–683.

Wasserstrom, R., and D. Southgate. 2013. Deforestation, Agrarian Reform and Oil Development in Ecuador, 1964-1994. Natural Resources.

Wilson, E. . 2007. Biodiversity. National Academy Press, Washington D.C., 1988.

Wright, S. J. 2005. Tropical forests in a changing environment. Trends in Ecology and Evolution 20:553–560.

WWF-Guianas. 2012. REDD+ Developments in the Guianas. The evolution of the concept and activities undertaken in Guyana, Suriname and French Guiana.

Yang, Y., S. S. Saatchi, L. Xu, Y. Yu, S. Choi, N. Phillips, R. Kennedy, M. Keller, Y. Knyazikhin, and R. B. Myneni. 2018. Post-drought decline of the Amazon carbon sink. Nature Communications 2018 9:1 9:3172.

Zalamea, P. C., P. Heuret, C. Sarmiento, M. Rodríguez, A. Berthouly, S. Guitet,

E. Nicolini, C. Delnatte, D. Barthélémy, and P. R. Stevenson. 2012. The genus Cecropia: A biological clock to estimate the age of recently disturbed areas in the neotropics. PLoS ONE.

Zarin, D. J., E. a Davidson, E. Brondizio, I. C. G. Vieira, T. Sá, E. a G. Schuur, R. Mesquita, E. Moran, P. Delamonica, J. Mark, G. C. Hurtt, C. Salimon, and M. Denich. 2005. Legacy of fire slows carbon accumulation in. Ecology 3:365–369.

Zarin, D. J., M. J. Ducey, J. M. Tucker, and W. A. Salas. 2001. Potential biomass accumulation in Amazonian regrowth forests. Ecosystems 4:658–668.

Zemp, D. C., C. F. Schleussner, H. M. J. Barbosa, and A. Rammig. 2017. Deforestation effects on Amazon forest resilience. Geophysical Research Letters 44:6182–6190.

Appendix

Appendix 2.1 Bi-annual hotspots of forest loss (km^2) across Amazonia (2001-2014) using the Getis-Ord Gi* analysis in ArcGIS 10.4.1.

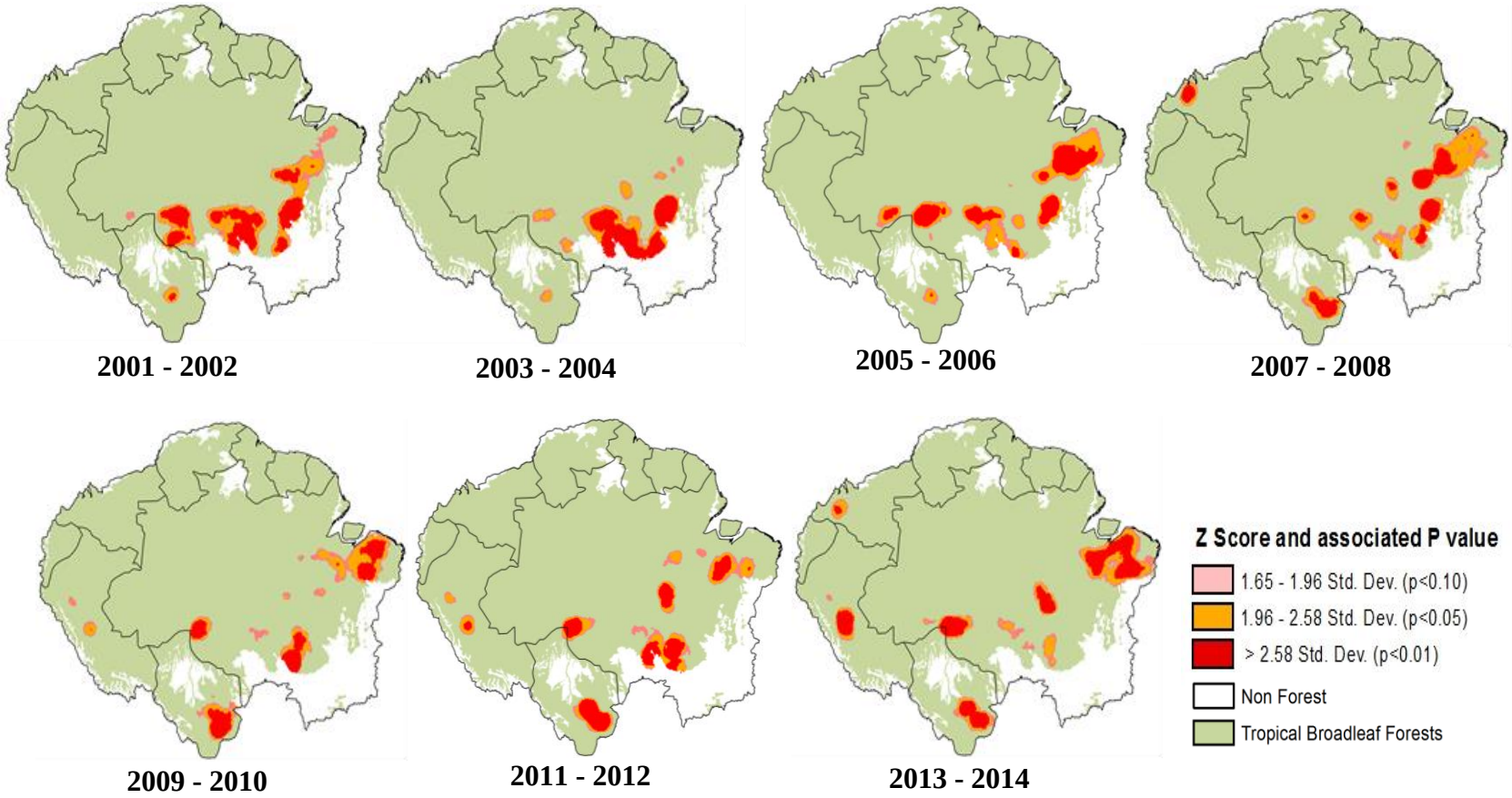

Appendix 2.2 Mean Deforested Patch Sizes (ha) across Amazonia, 2001-2014.

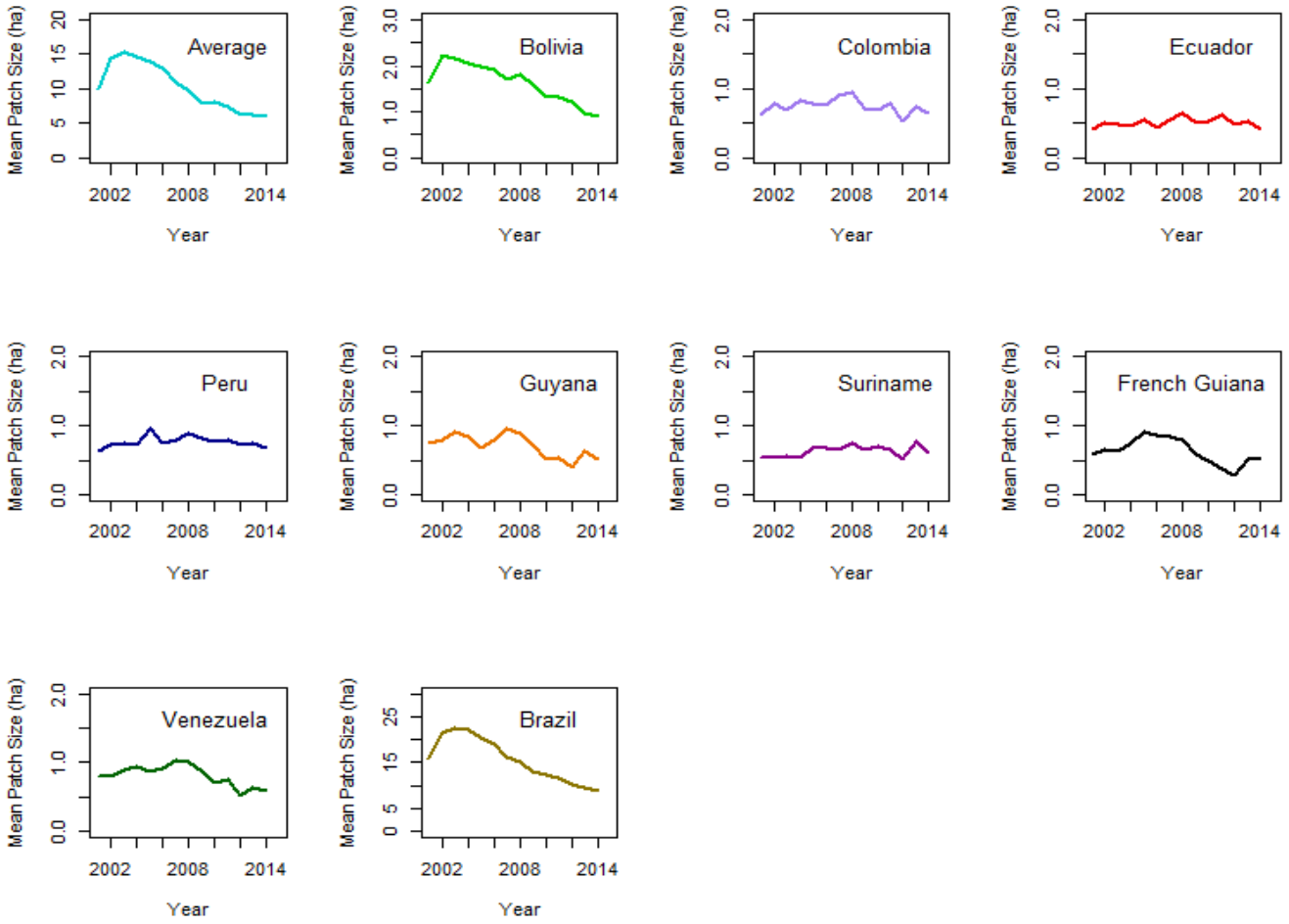

Appendix 2.3 Trajectory of area of small-scale forest loss (<1ha) across Amazonia, 2001-2014.

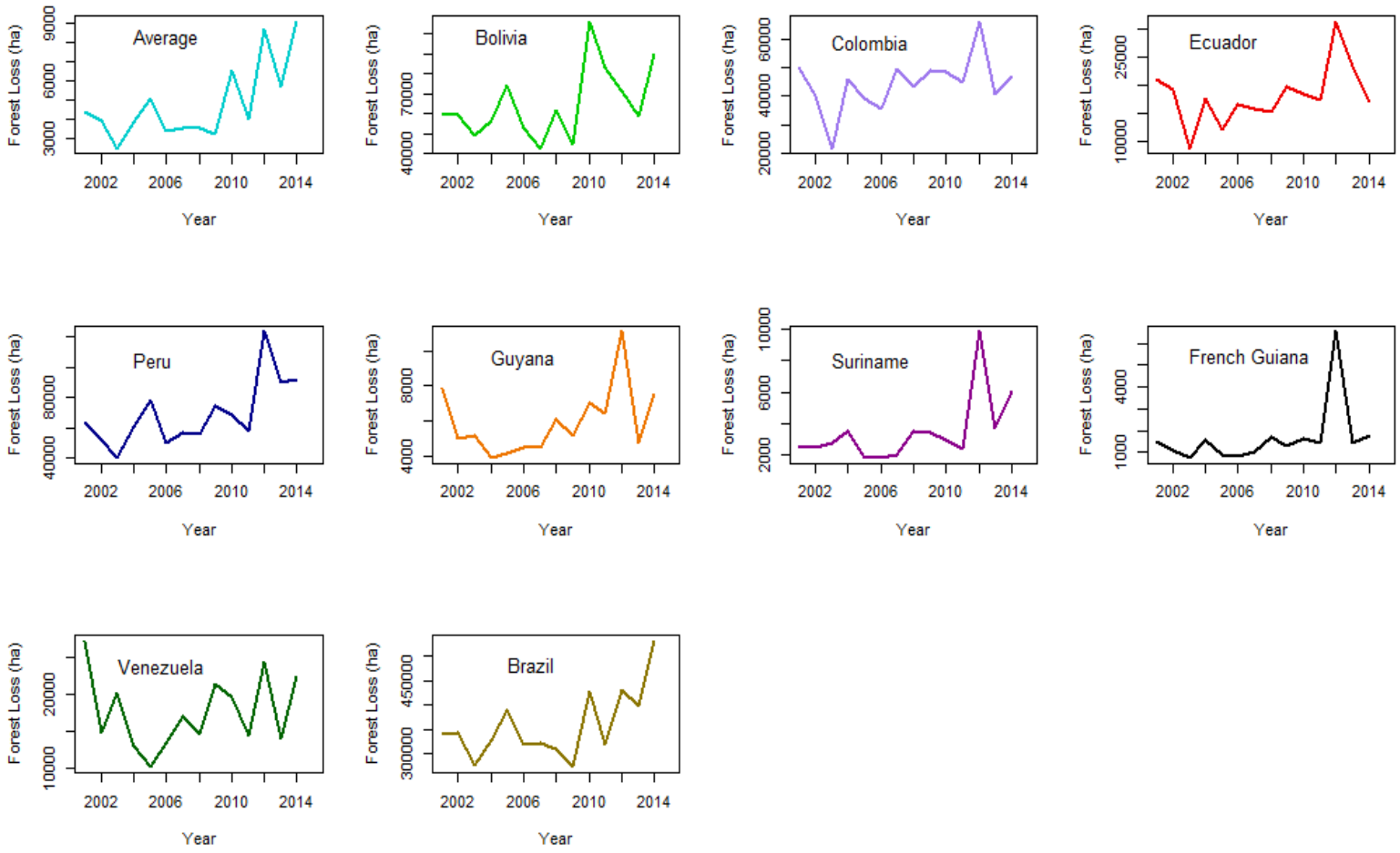

Appendix 2.4 Change (%) in number of 10x10 km gridcells between 2001-2007 and 2008-2014 for five different forest loss density categories. Negligible: < 0.01 km^2 / 100 km^2. Light: 0.01 – 0.1 km^2 /100 km^2. Moderate: 0.1 – 1 km^2/ 100 km^2. Heavy: 1-10 km^2/100 km^2. Very heavy: 10-100 km^2/100 km^2.

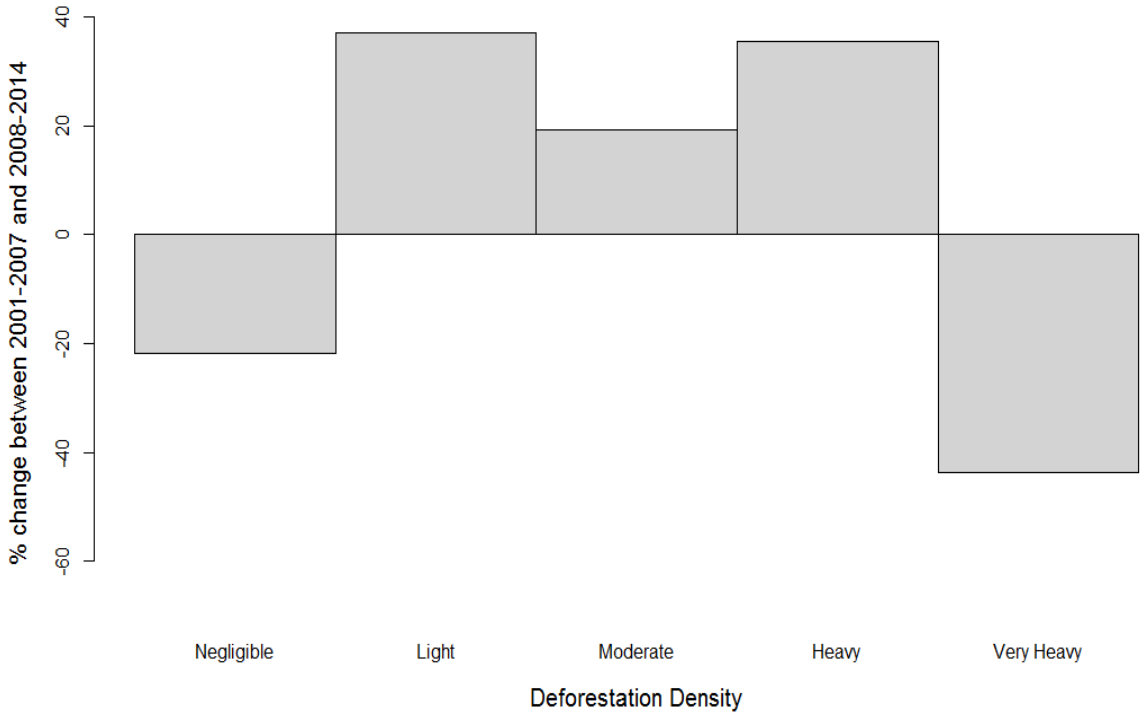

Appendix 2.5 Bi-annual forest loss density (km^2 deforested area over the target period per 100km^2 land area) across Amazonia (2001-2014) using ArcGIS 10.4.1 (www.esri.com).

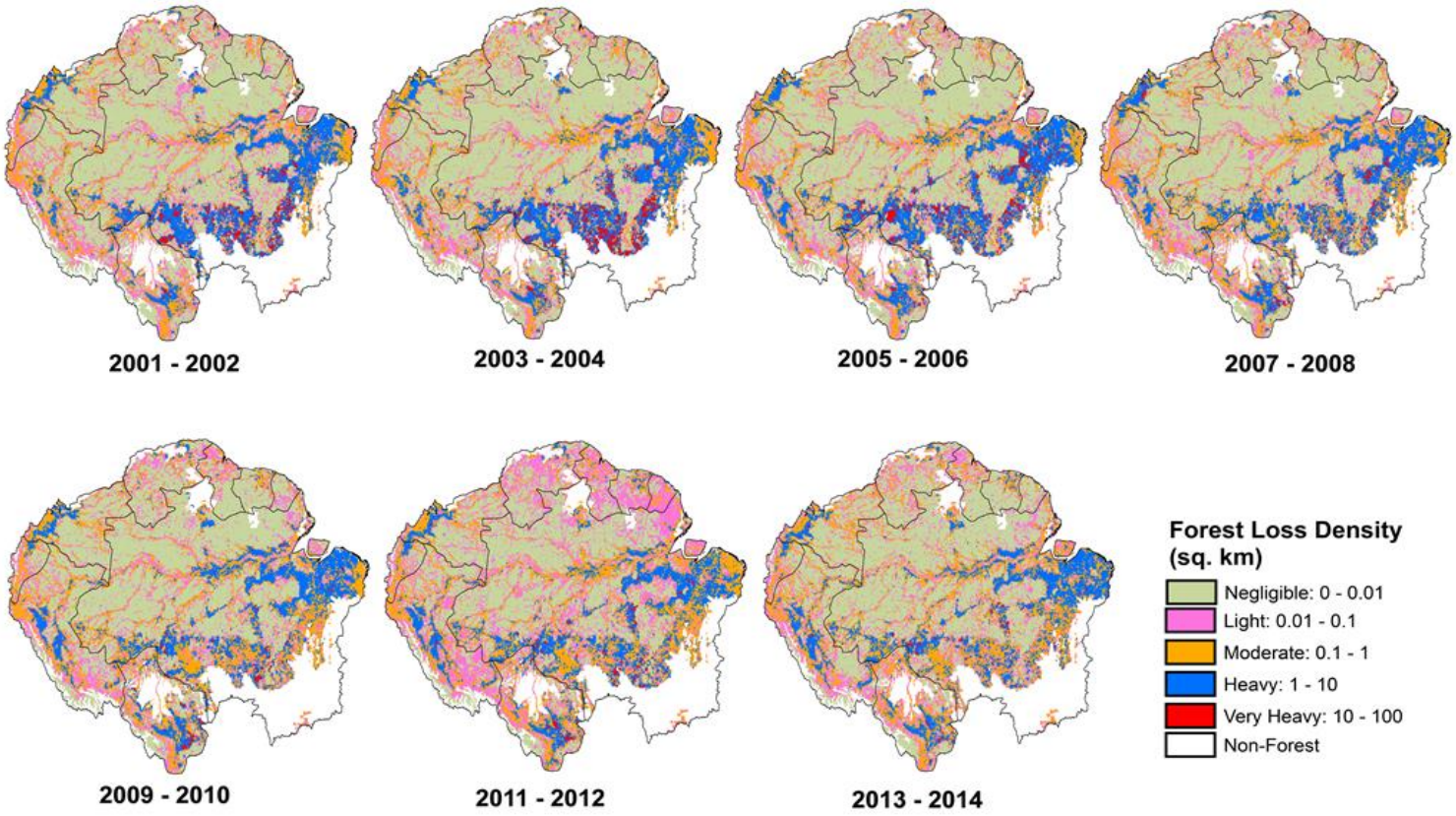

Appendix 2.6 Annual forest loss (km^2) across Amazonia for 2001-2014, based on the Global Forest Change (GFC) product.

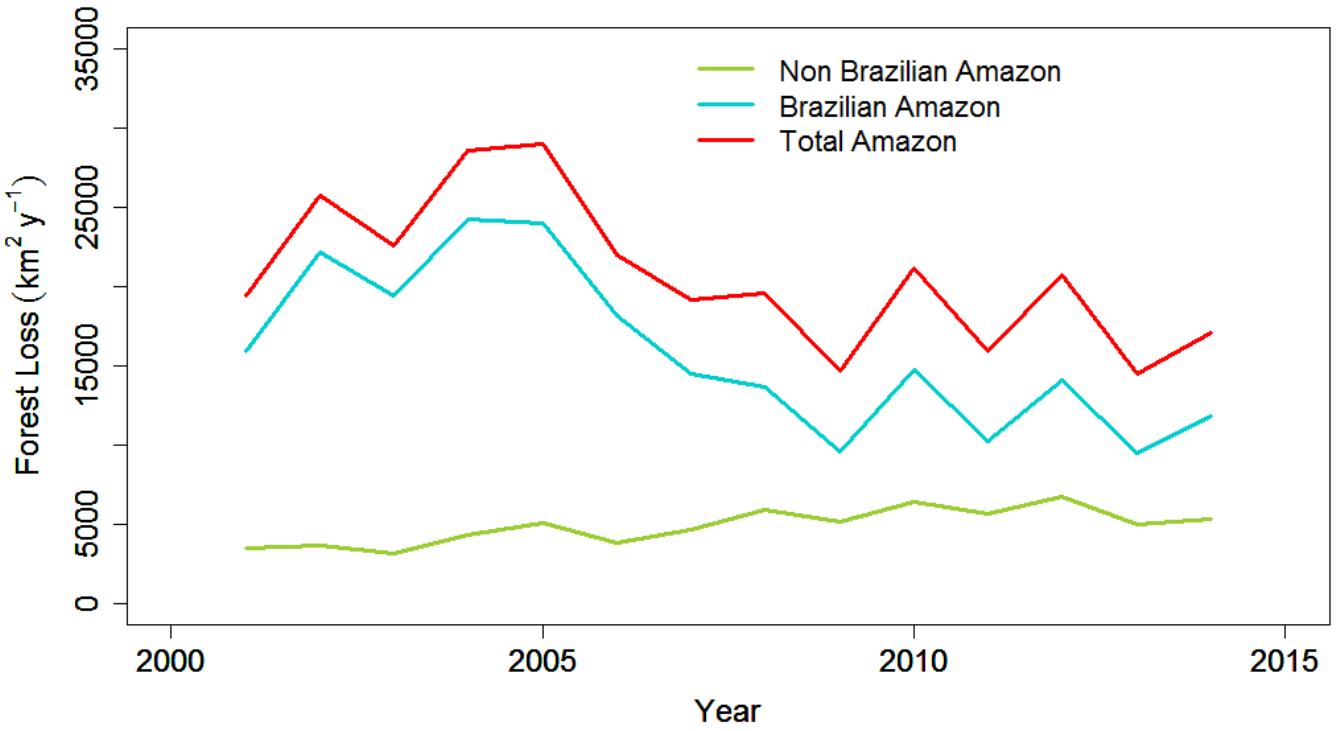

Appendix 2.7 Significant (*p*-value) of forest loss (km^2) across Amazonia for *Hansen et al* GFC product, 2001-2014. The significance was calculated on the means of the two time periods (2001-2007 & 2008-2014) using the Wilcoxon signed-ranked test.

Country	GFC		
	Annual mean loss rate		Significance of mean
	2001-2007	2008-2014	
Bolivia	79.39	175.62	0.04**
Colombia	65.29	-24.47	0.7
Ecuador	-1.22	0.71	0.01**
Peru	70.84	130.85	0.004**
French Guiana	0.11	0.26	0.62
Guyana	-4.87	-0.76	0.02**
Suriname	0.32	11.62	0.001***
Venezuela	-1.94	-8.09	0.1
Brazil	-273.66	-230.22	0.001***

***p* < 0.1**

** *p* < 0.05**

*** *p* < 0.001**

Appendix 2.8 Ratio of annual forest loss area for the Brazilian Amazon estimated from Hansen *et al*. GFC product relative to PRODES deforestation estimates.

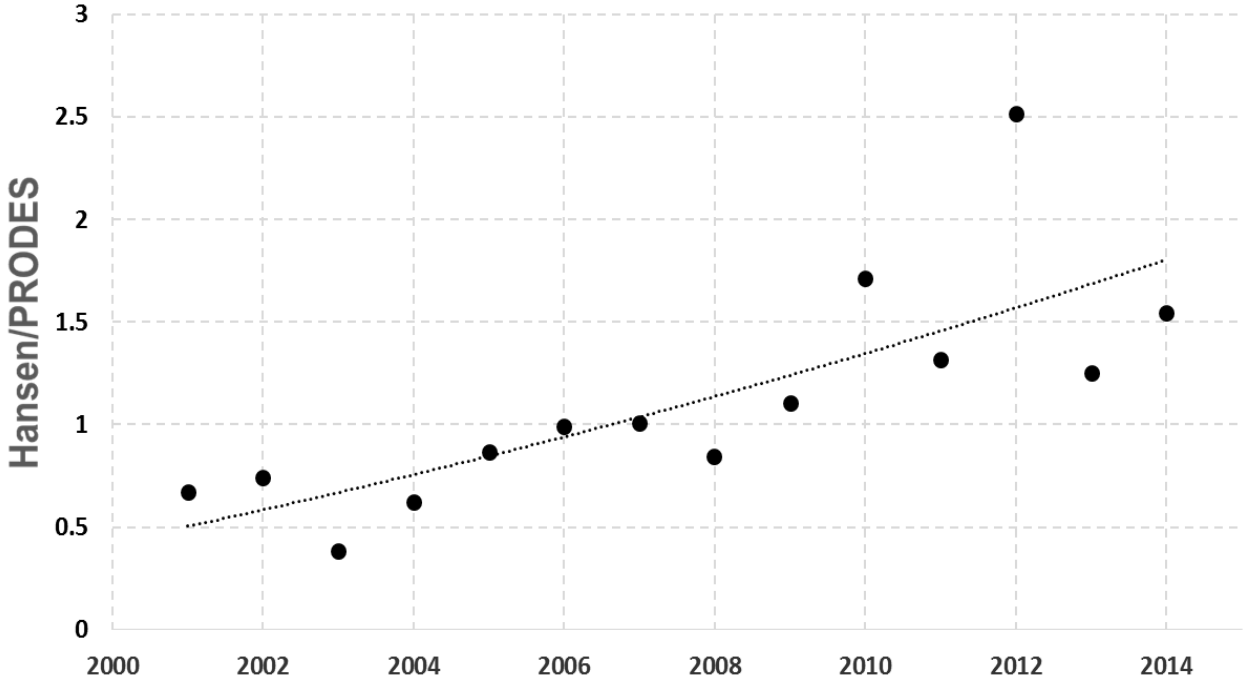

Appendix 2.9 The fraction of total Hansen et al. GFC deforestation attributed to small patches <6.25 ha (PRODES threshold).

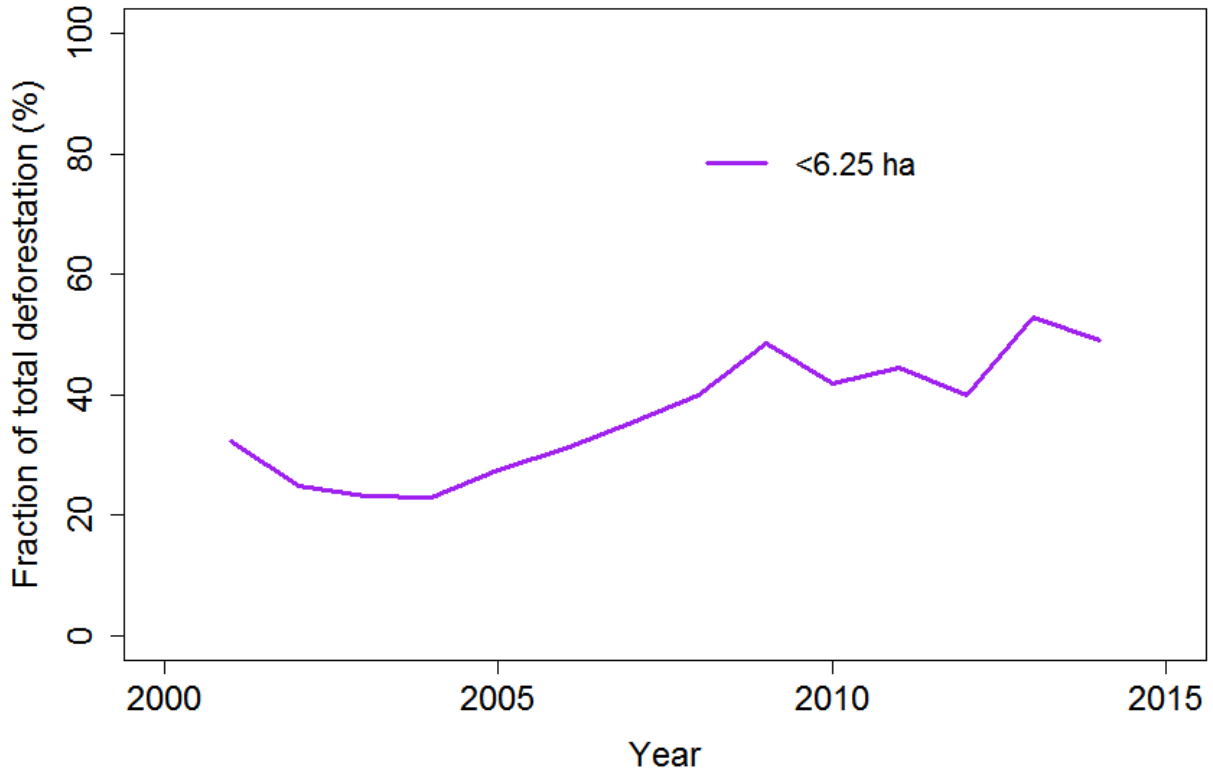

Appendix 2.10 Comparison of forest loss density (km^2 forest loss per 100km^2 land area) in Amazonia using the GFC (a) version 1.0 and (b) version 1.2 products for two time periods: 2001-2007 and 2008-2012 using ArcGIS 10.4.1 (www.esri.com).

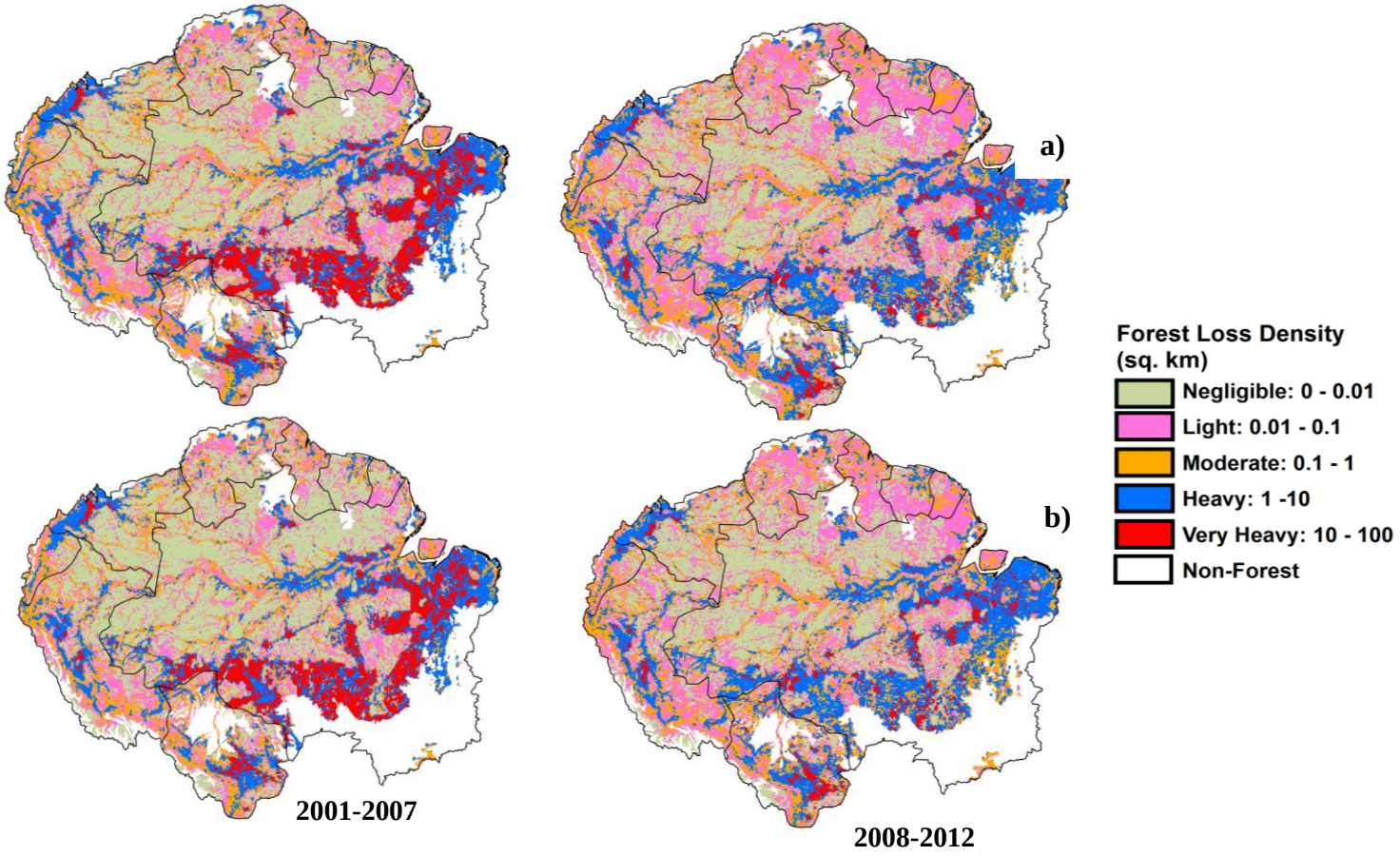

Appendix 2.11 Percent change forest loss density categories for GFC versions 1.0 and 1.2 for 2001-2007 and 2008-2012 across Amazonia.

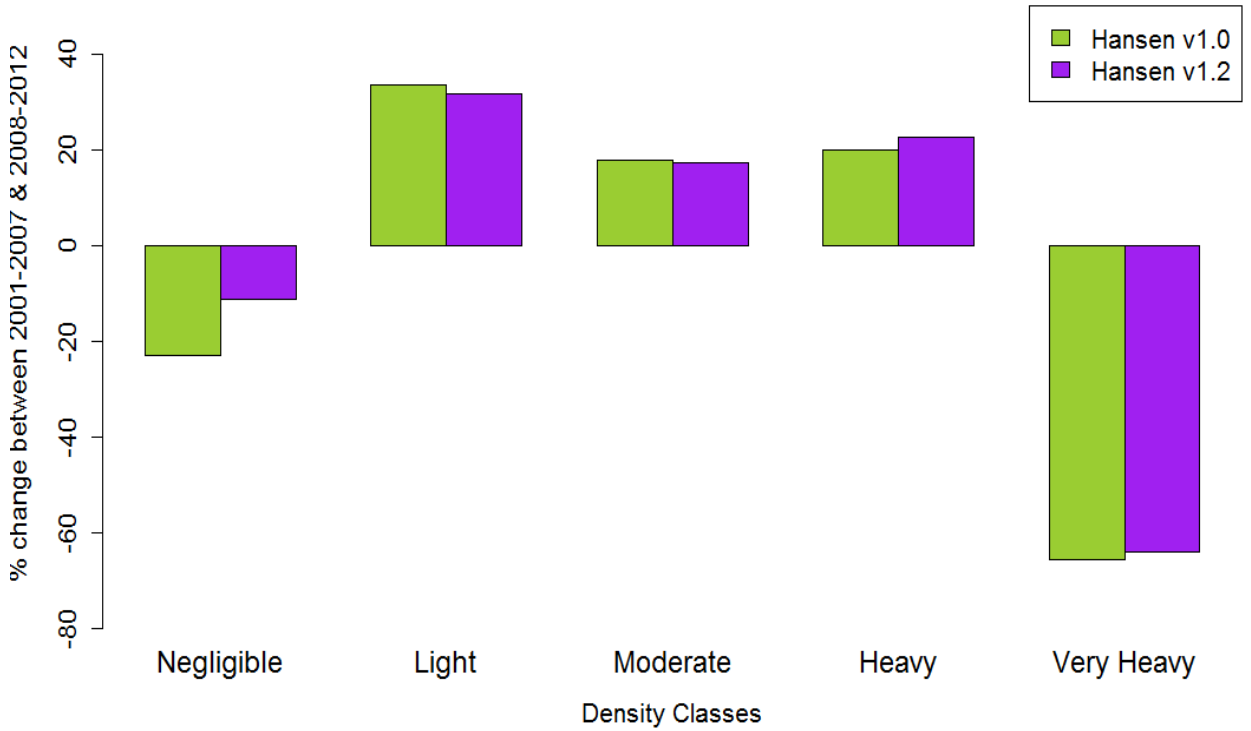

Appendix 2.12 Forest loss density (km^2 forest loss per 100km^2 land area) in Amazonia, as calculated using the GFC Version 1.2 product for two time periods: 2001-2007 and 2008-2014 using ArcGIS 10.4.1 (www.esri.com). Here, we (a) doubled and (b) trebled the lower classification to examine whether classification influenced our density results. Relative differences were sustained at 15.6% between 2001-2007 and 2008-2014 across all classifications.

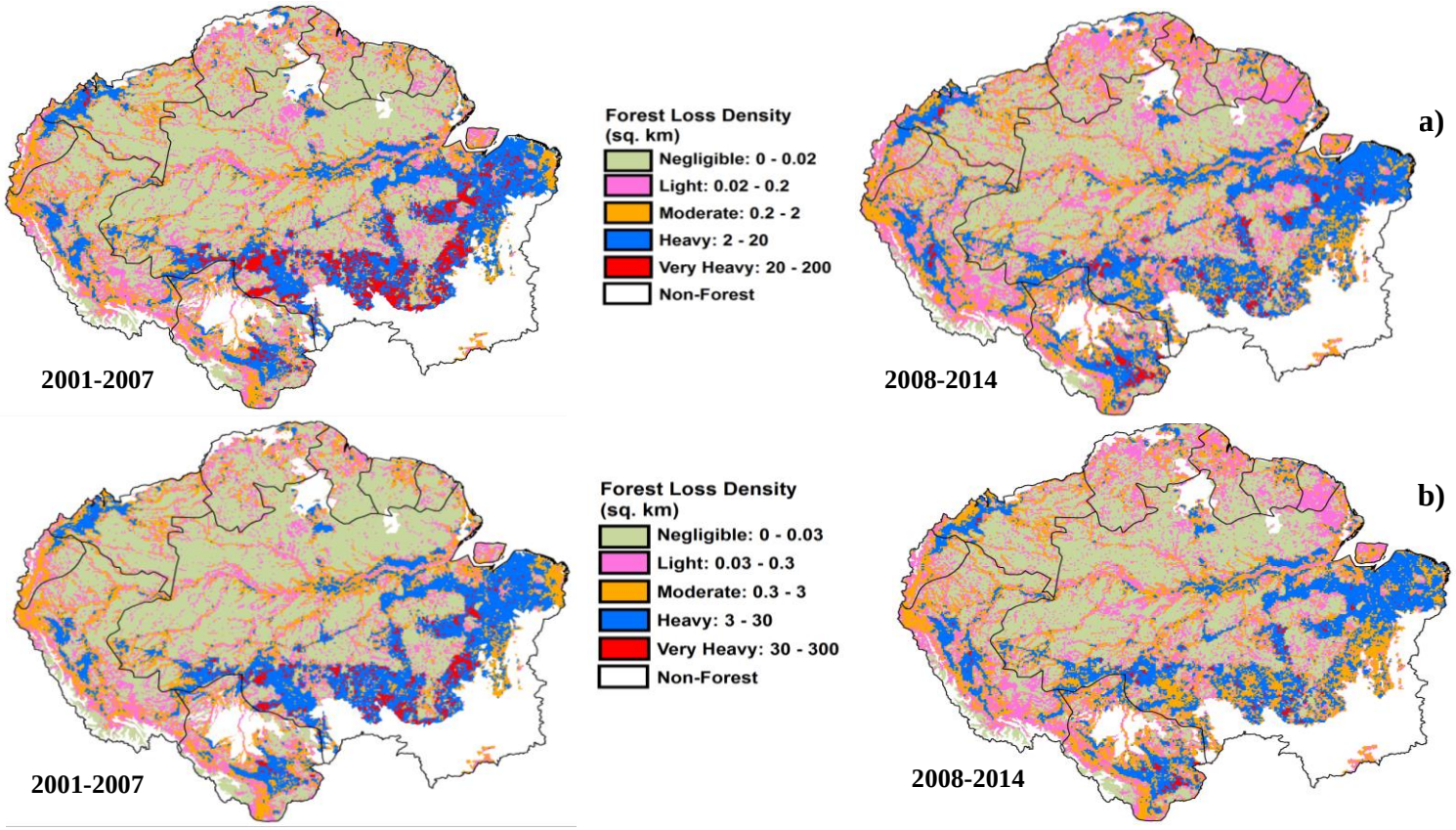

Appendix 2.13 Forest Loss Density (km^2) along primary roads and rivers between 2001-2007 and 2008-2014 in Amazonia.

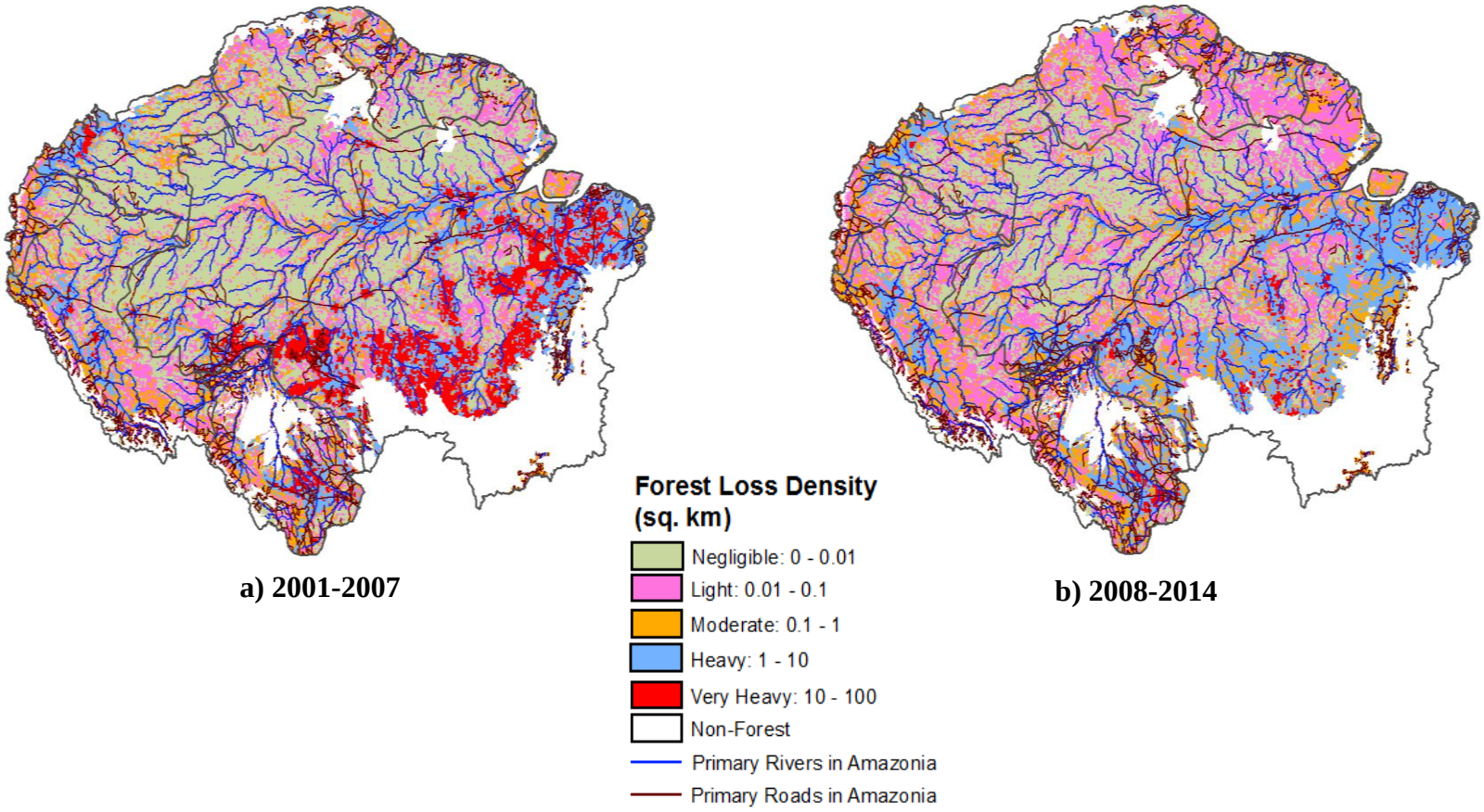

a) 2001-2007

b) 2008-2014

Appendix 2.14 Comparison of 2005 and 2010 drought-related tree mortality using maximum climatological water deficit (MCWD, Lewis et al. 2011) with small-scale forest loss events from this study.

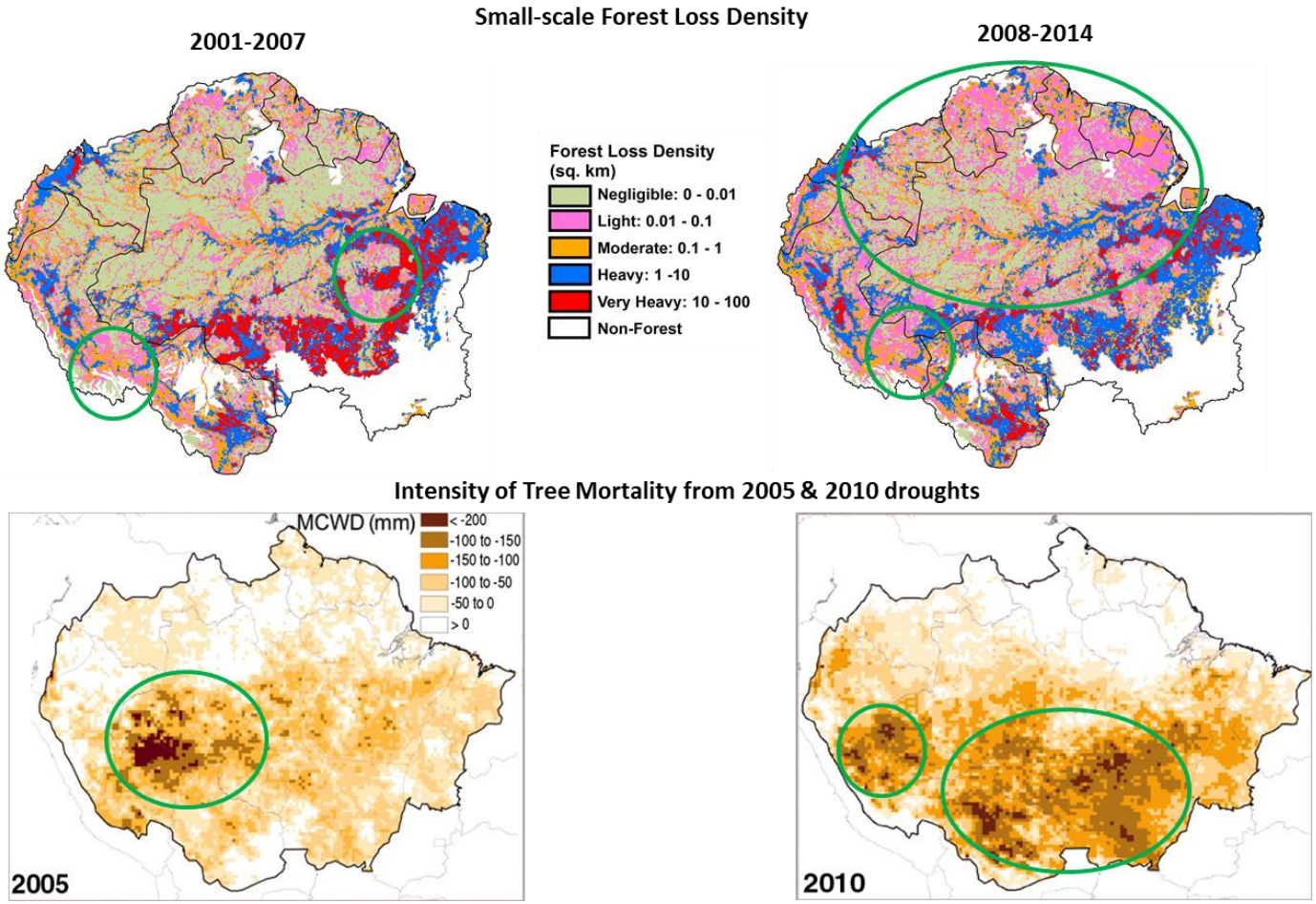

Appendix 2.15 Forest Loss Extent using Terra-i/MODIS product

This analysis of deforestation patterns in Chapter 2 was repeated with the 250-m resolution Terra-i data (Coca-Castro et al. 2013), derived from USGS/NASA MODIS data, as described by Reymondin et al. (2012) and processed by the International Centre for Tropical Agriculture (CIAT). As per my analysis of the Hansen et al. (2013) GFC forest loss product, I evaluated the spatial and temporal dynamics of deforestation across Amazonia from 2004-2014, specifically consider 1) forest loss hotspots, 2) size of forest loss patches and 3) the geographical density of forest loss events.

For MODIS/Terra-i, 132 tiles representing forest loss between 2004 and 2014 for Amazonia were downloaded from Terra-i (http://www.terra-i.org/terra-i.html). Due to the difference in resolution of the MODIS/Terra-i data (250m resolution) and Landsat/Hansen (30m resolution), resampling the coarser resolution datasets to the high resolution dataset using "nearest neighbour" was necessary for suitable comparison. MODIS/Terra-i data commenced in 2004, therefore comparison with GFC was limited to 2004-2014 period. The Terra-i dataset was resampled to 30m-resolution in ArcGIS 10.4.1, without changing the value of deforested pixels. Similar processing as described in Chapter 2.3 (Methods) above was used to define the extent of Amazonia and various features of forest loss using the Terra-i product.

2.15.1 Extent of forest loss hotspots

This analysis reveals significant difference in the spatial hotspots using the 250m-resolution Terra-i product when compared to the 30m-resolution GFC product (Figure A2.13.1). In 2004-2008, hotspots were concentrated along Brazil's arc of deforestation. The extent of forest loss hotspots in Brazil in the first period was 83% less than that captured by the GFC product. By 2009-2014, hotspots in Brazil's arc of deforestation decreased by 76% from 9784 km^2 to 2307 km^2, and was 88% lower than forest loss captured by the GFC product. Hotspots in Santa Cruz, Bolivia (382.47 km^2) and Ucayali, Peru (21.08 km^2) also emerged during the second half of the study period, while a statistically weaker hotspot was present near the Pilon Lajas Indigenous Territory Park in Bolivia. The Terra-i

product did not reveal hotspots in Colombia, which was detected by the GFC product.

2.15.2 Forest loss patches

Overall, the number of forest loss patches of intermediate (6.25 – 50 ha) and large (> ha) sizes grew between 2004-2008 and 2009-2014 (Figure 2.13.2). Intermediate patches grew by 46.5%, while clearings >100ha increased on average by 37.7%. Here, the number of small forest loss patches (1 – 6.25ha) declined by 13.5%, while very large patches (>1000ha) declined by 24% between 2004-2008 and 2009-2014. Forest loss patches <1ha were not detected across both time periods. This contrasted with the GFC dataset in that only small forest loss patches (<6.25ha) grew while intermediate and large patches declined between the two study periods.

2.15.3 Geographical Density of Forest Loss events

Considerable changes were also observed in the geographical patterns of deforestation density between the two timelines and between the two products (Figure A2.13.3). In 2004–2008, 56% of the 10×10 km gridcells in the study region were categorised as having negligible forest loss (<0.01 km^2 per 100 km^2), this declined to 37% in 2009–2014. On one hand, the proportion of gridcells experiencing 'moderate' (0.1–1 km^2 per 100 km^2) and 'heavy' (1–10 km^2 per 100 km^2) deforestation increased by 83% and 54% respectively, from 19% and ~9% in 2004–2008 to 34.7% and 13.8% in 2009-2014 respectively. On the other hand, gridcells experiencing 'light' (0.01–0.1 km^2 per 100 km^2) and 'very heavy' (>10 km^2 per 100 km^2) forest loss decreased between the two study periods by 7% and 21% respectively. Gridcells experiencing 'negligible', 'moderate', 'heavy' and 'very heavy' forest loss agreed on the nature of the deforestation trend when compared with the GFC product. In contrast, gridcells categorised as having 'light' deforestation decreased in the Terra-i product, while it increased using the GFC product.

2.15.4 Large-scale deforestation temporal patterns

Regionally, both GFC and Terra-i products agreed on the nature of deforestation trends in Amazonia (Figure A2.13.4). However, there was substantial variability in annual deforestation rates between the two datasets from 2004 to 2014. The Terra-i product reported a decline in forest loss by 391.08 km^2 yr^{-1} while Hansen et al. (2013) data detected a decrease of 1259.2 km^2 yr^{-1}. In the Brazilian Amazon, both datasets indicate a significant reduction in deforestation, by 1403.8 km^2 yr^{-1} for the Hansen et al. dataset and by 589.25 km^2 yr^{-1} for the Terra-i product.

Figure A2.15.1 Hotspots of Amazonian forest loss based on Getis Ord Gi* z-scores for Terra-i data for two time periods: 2004-2008 and 2009-2014 using ArcGIS 10.4.1 (www.esri.com). Higher values indicate increased clustering of deforestation patches.

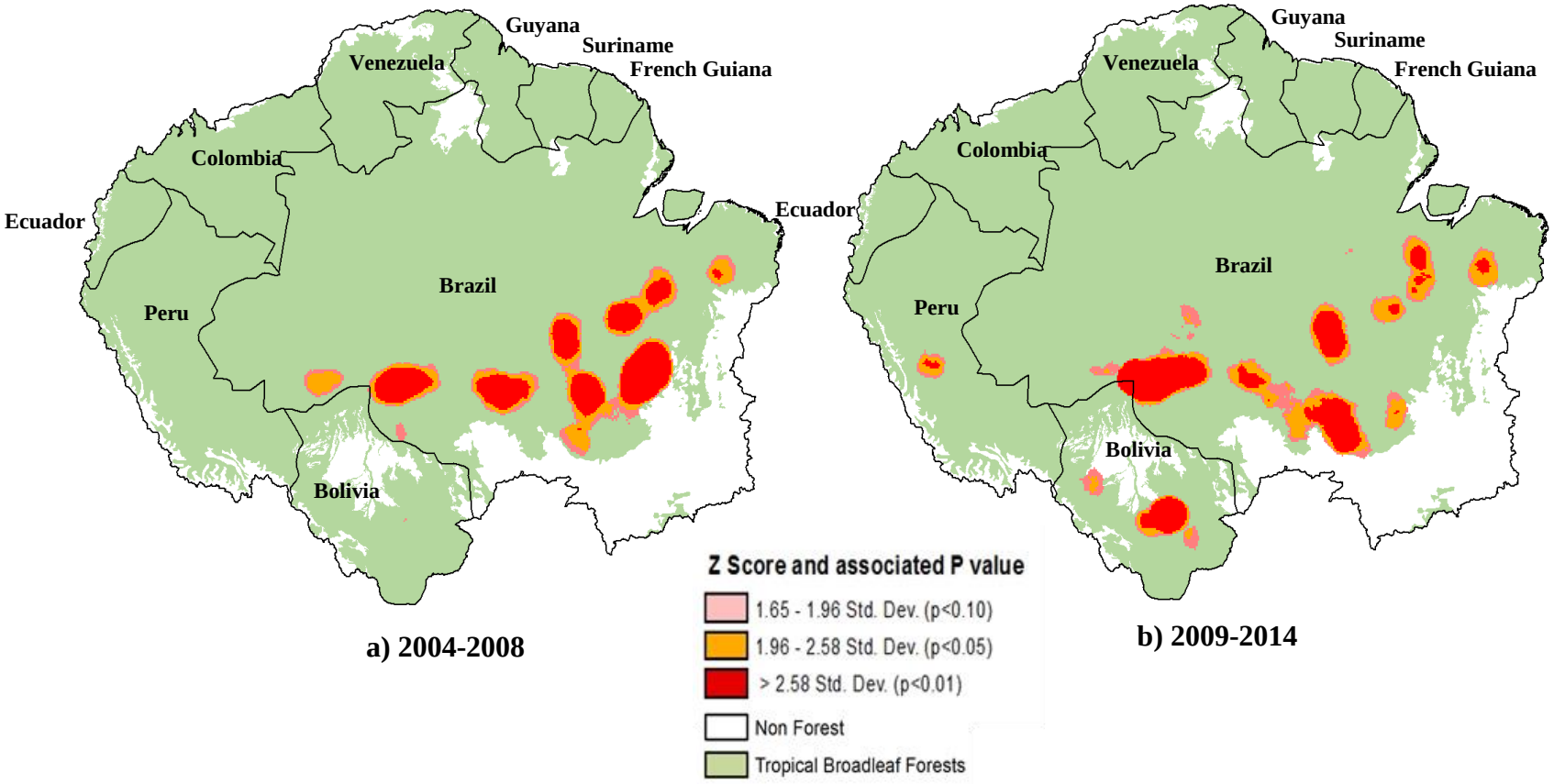

Figure A2.15.2 Change in deforested area (thousands of hectares) of different size categories between 2004-2008 and 2009-2014 across Amazonia using the resampled Terra-i dataset.

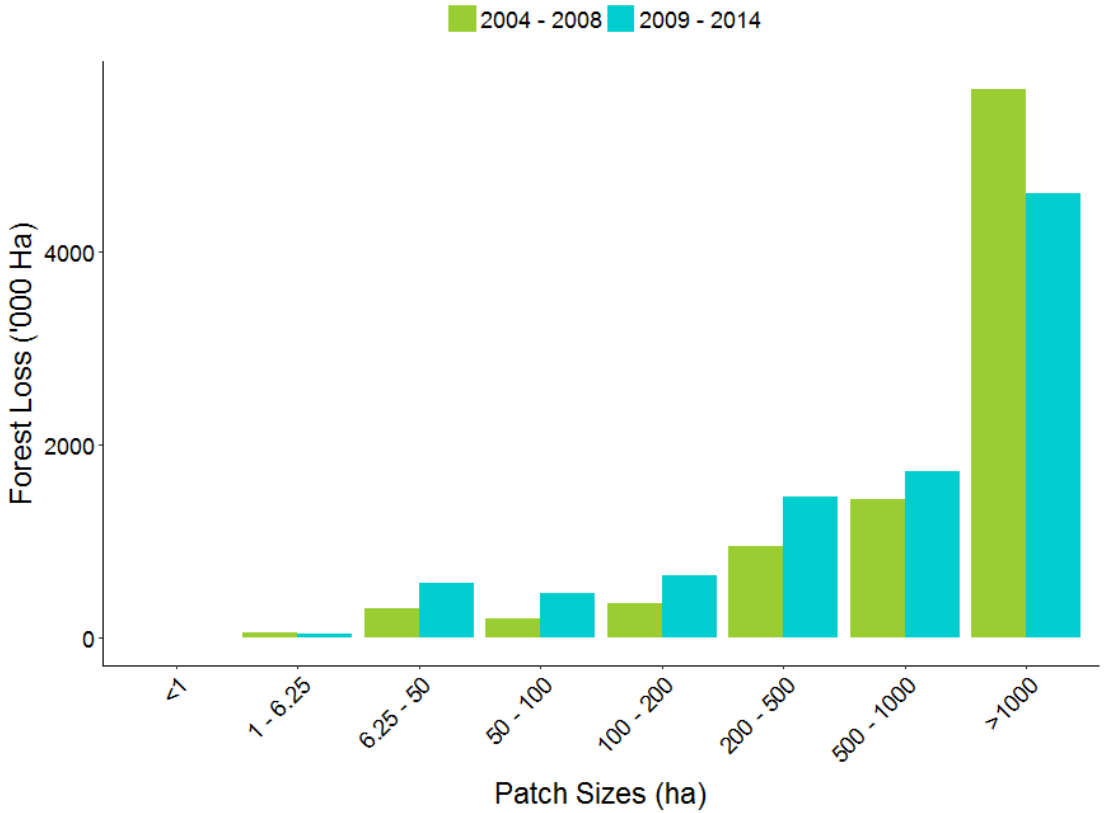

On the other hand, both datasets reported a sharp increase in deforestation rate in non-Brazilian countries. Here, Terra-i reported an annual increase of 198.19 km^2 yr^{-1} from 2004-2014 while GFC reported an increase of 144.59 km^2 yr^{-1}.

GFC-based deforestation estimates were higher compared with estimates from the MODIS-based Terra-i product and the PRODES data for Brazil (Figure A.2.13.5). Analysis of the MODIS-based Terra-i data revealed similar patterns to the GFC analysis (1403.81 km^2 yr^{-1}), although the magnitude of the decline in forest loss in the Brazilian Amazon was considerably lower when calculated using Terra-i data (589.3 km^2 yr^{-1}). The annual decline in deforestation in the Brazilian Amazon throughout the study period (2004-2014), as estimated by PRODES was 1925.6 km^2 yr^{-1}. Thus, the decline in deforestation according to PRODES is 37.1% greater than that calculated from the GFC data, and 2.27% greater than the Terra-i data (Figure A.2.13.5). Over time, both GFC and Terra-i forest loss estimates became progressively greater than PRODES deforestation estimates. Within the last three years (2012-2014), Terra-i estimates of forest loss are ~91% greater than deforestation rates from PRODES, with a maximum divergence observed in 2012 by a factor of 3, while the maximum divergence in GFC from PRODES was 2.52 (see Chapter 2.4.4).

Overall, despite resampling to 30m-resolution, Terra-i product fails to detect much of the smaller forest loss activities that occurred across the Amazon. This has important implications for conservation and management efforts such as those applied to protected areas. For instance, if small-scale activities are neglected with only large scale activities reported, there may be an inclination to develop management strategies that only produce large scale forest loss events such as agriculture and pasture, while ignoring growing small-scale activities such as gold mining.

Figure A2.15.3 Forest loss density (km^2 forest loss per 100km^2 land area in Amazonia**,** as calculated using the Terra-i product for two time periods: 2004-2008 and 2009-2014 using ArcGIS 10.4.1 (www.esri.com).

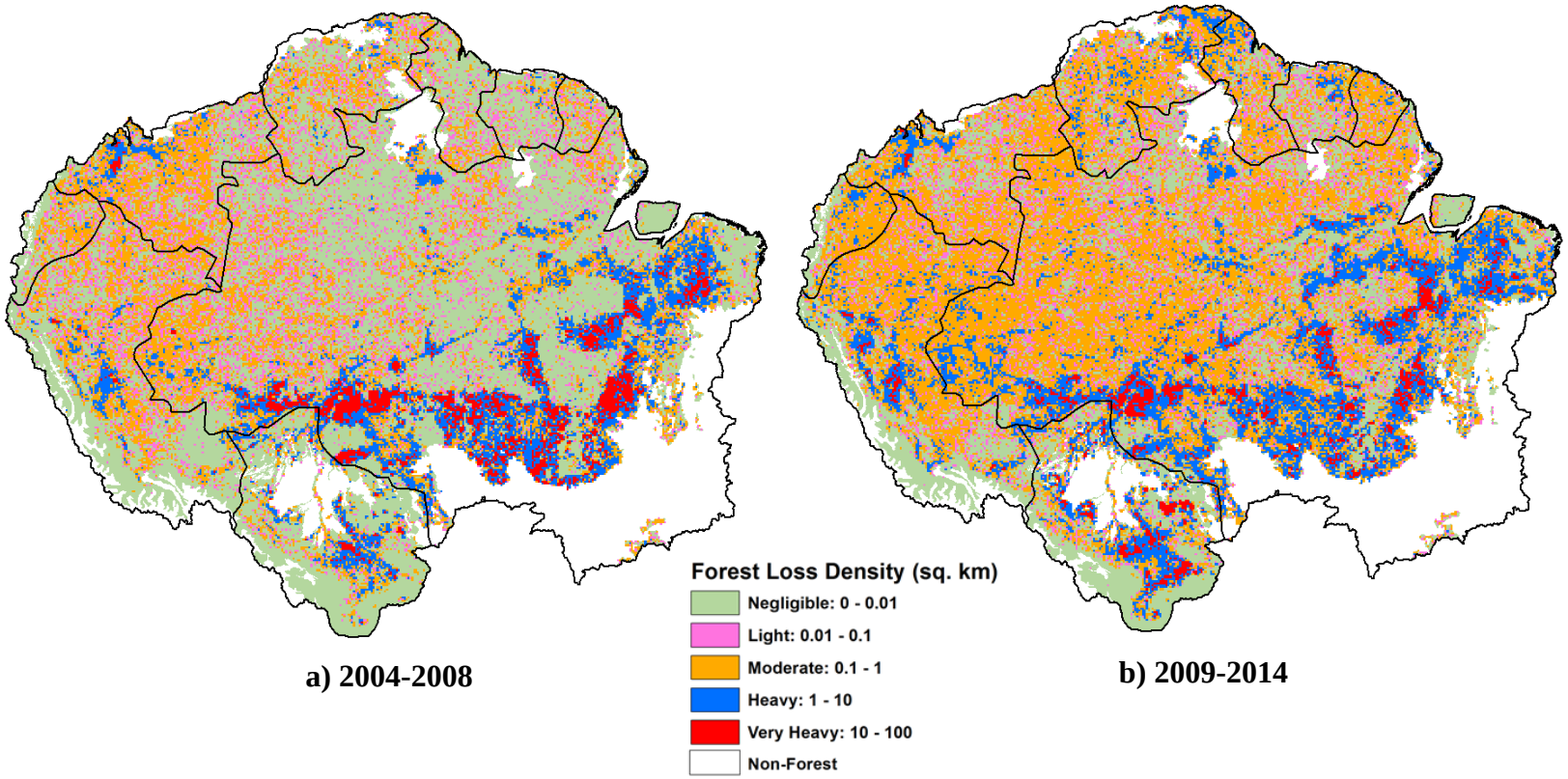

a) 2004-2008 **b) 2009-2014**

Figure A2.15.4 Annual forest loss (km^2) across Amazonia for 2004-2014 based on the Global Forest Change (GFC) and resampled Terra-i products.

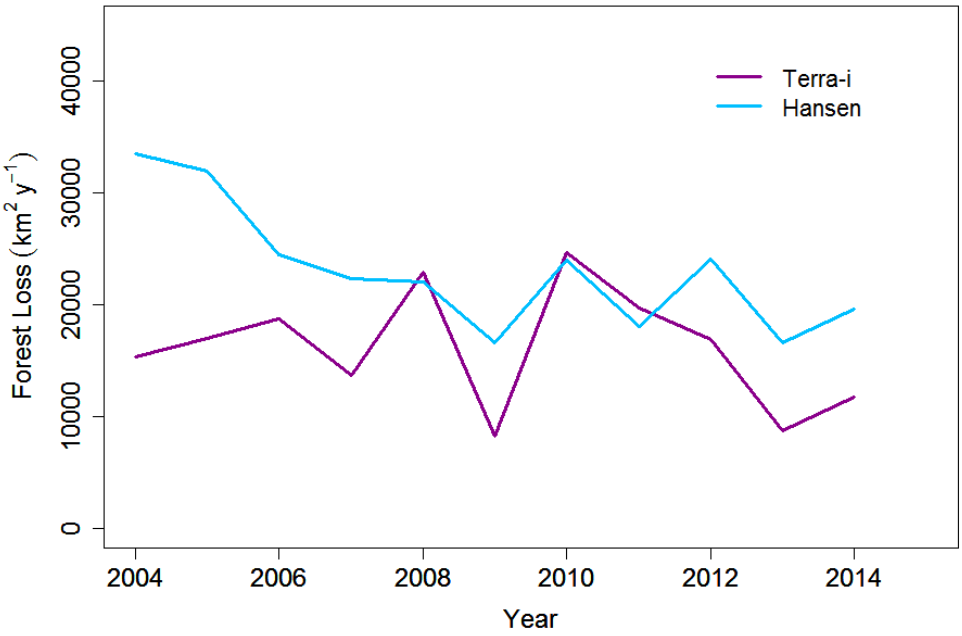

Figure A2.15.5 Ratio of annual forest loss area for the Brazilian Amazon estimated from Terra-i product relative to PRODES deforestation estimates.

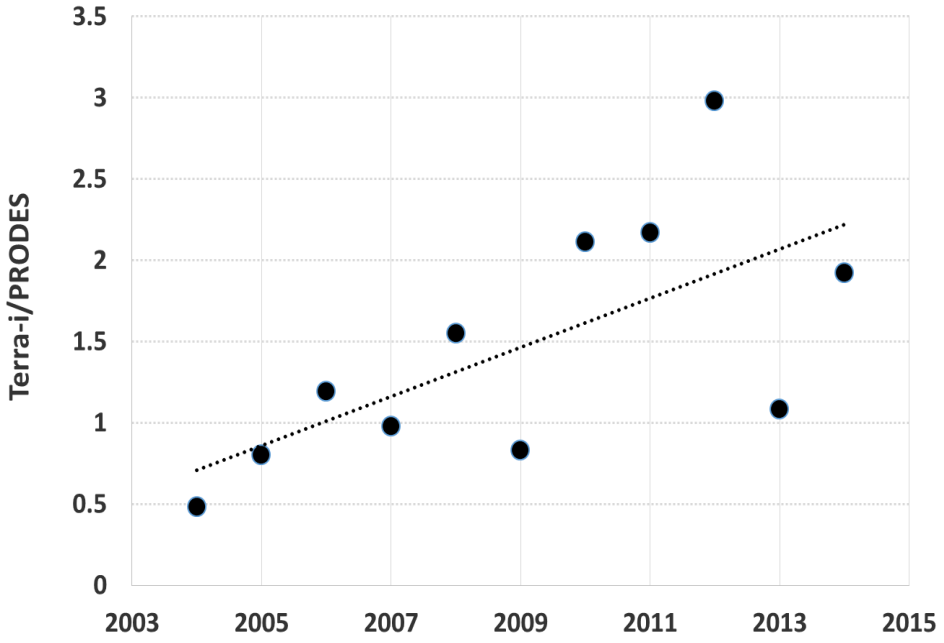

Appendix 3.1 Map of active and potential gold mining sites across Amazonia.

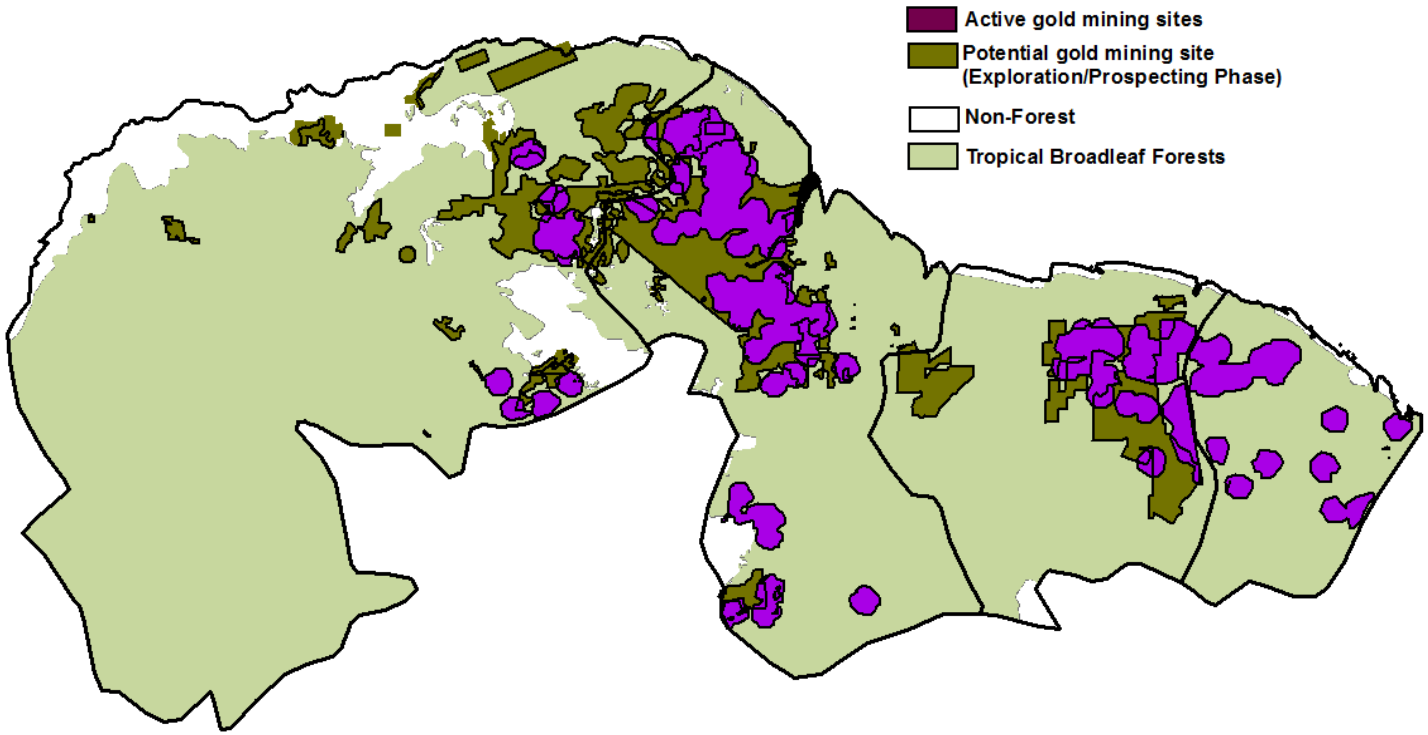

Appendix 3.2 Forest Loss Density (km^2 forest loss per 25km^2 land area) inside and outside of gold mining areas across northern Amazonia**,** as calculated using the GFC product for two time periods: (a) 2001-2008 and (b) 2009-2016.

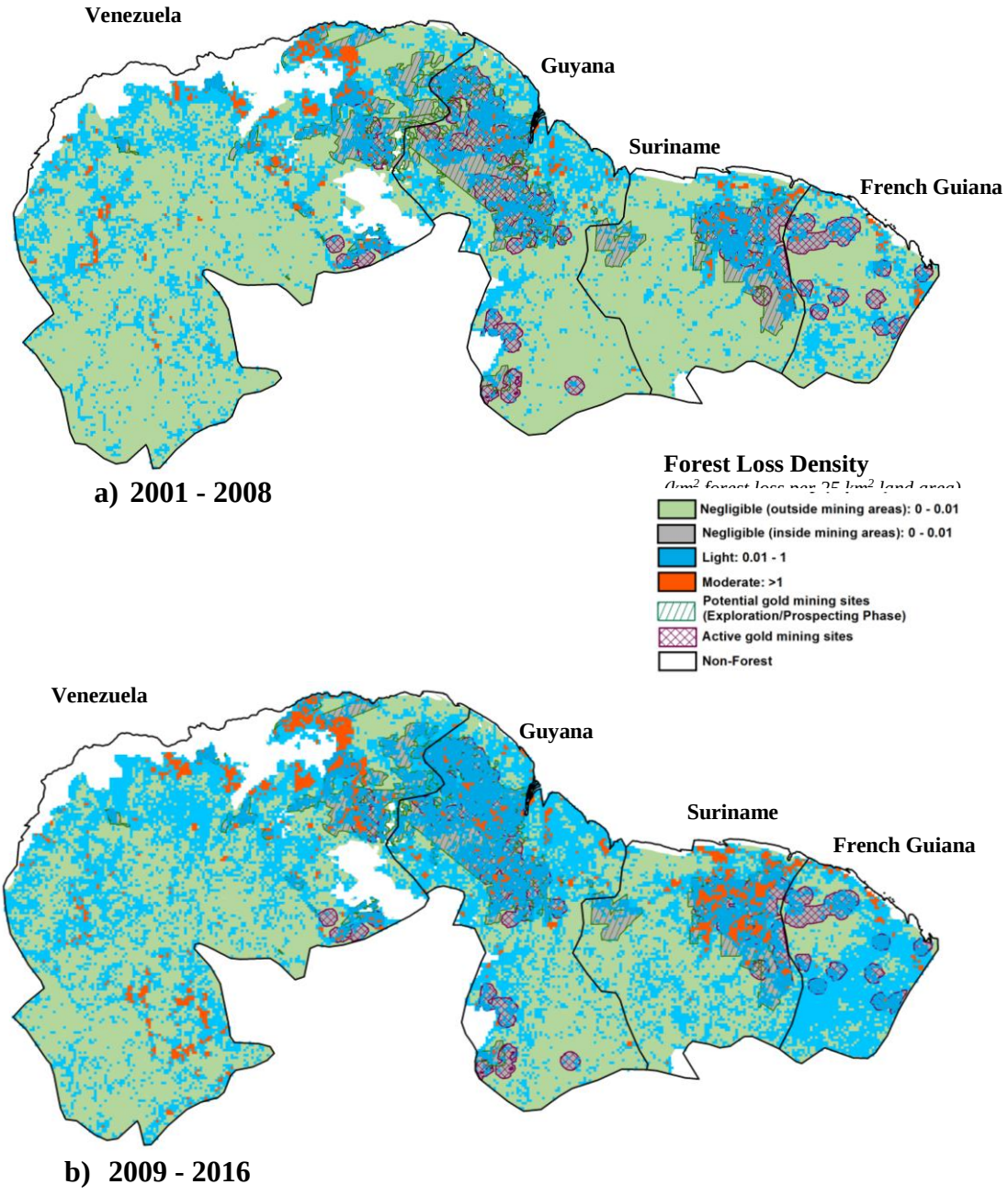

Appendix 3.3 Forest Loss Density (km^2 forest loss per 25km^2 land area) inside protected areas indicating gold mining activities and associated buffer zones across northern Amazonia, as calculated using the GFC product for: (a) 2001-2008 and (b) 2009-2016.

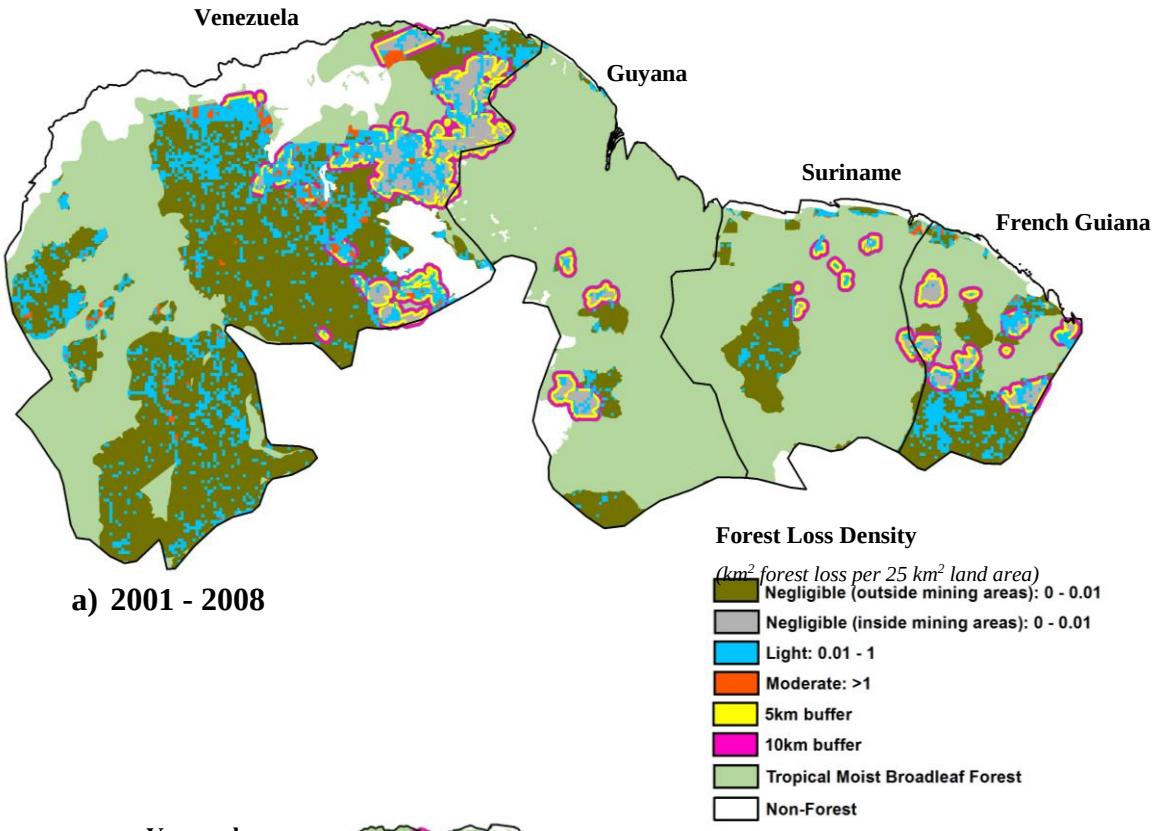

a) 2001 - 2008

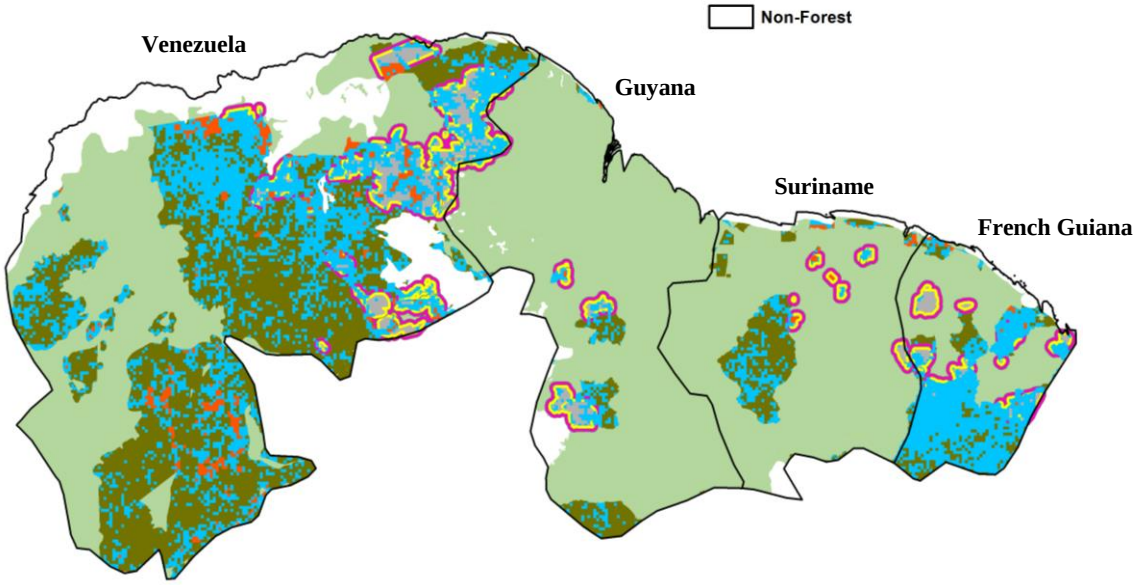

b) 2009 - 2016

Appendix 5.2 Comparison of field plots in Censuses I and II.

Plot at Mahdia in (a) Census I and (b) Census II

Tailing Pond at Puruni in (a) Census I and (b) Census II. Overburden in left top corner

Overburden and tailing pond at Mahdia in (a) Census I and (b) Census II

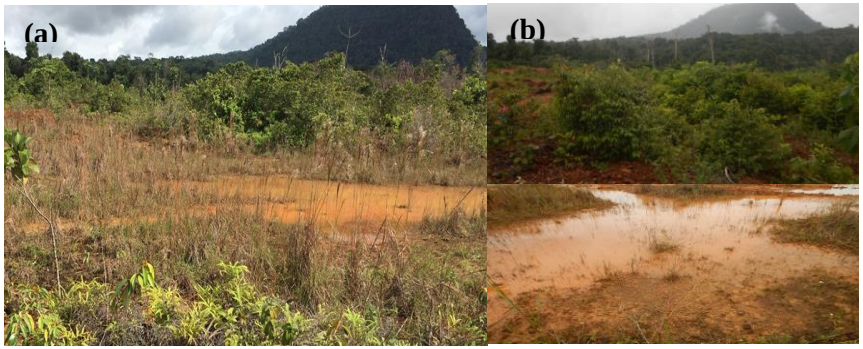

Mining Pit at Puruni in (a) Census I and (b) Census

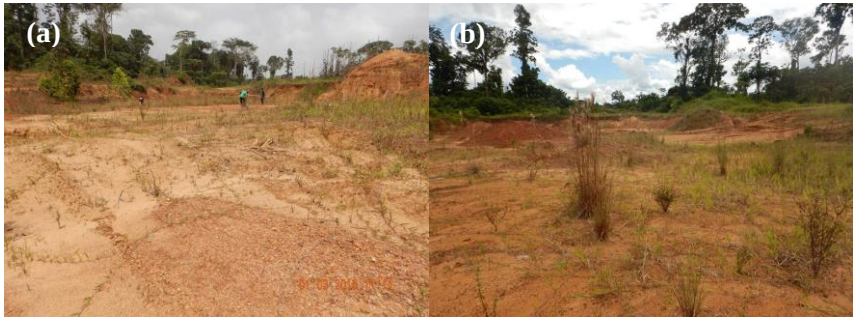

Appendix 5.2 The relationship of distance to annual biomass change (ΔAGB) at Mahdia and Puruni.